A STUDY OF CHIRAL PENTACYCLO-UNDECANE DERIVED MACROCYCLES AND LIGANDS

Thavendran Govender

A thesis submitted to the School of Chemistry, Faculty of Science, University of KwaZulu-Natal, Durban, for the degree of Doctor of Philosophy.

DECLARATION

I HEREBY DECLARE THAT THE WORK PRESENTED IN THIS THESIS IS MY OWN, UNAIDED WORK AND HAS NEVER BEFORE BEEN SUBMITTED FOR ANY DEGREE AT THIS OR ANY OTHER UNIVERSITY.

T. GOVENDER

1st day of September 2004

ABSTRACT

Several chiral macrocyclic crown ethers and related analogues have shown to be capable of enantioselectively complexing chiral organic ammonium salts. The design and synthesis of chiral host macrocycles which are able to distinguish between the enantiomers of guest organic ammonium salts is of interest in the areas that include synthesis of enzymes, electrodes for specific ions or molecules, drugs targeted for specific sites, and enantiomer separation. A synthetic procedure has been established for the preparation of cage annulated chiral host systems (**1**) derived from amino acids. The enantioselectivity of a series of hosts was studied *via* extraction (**chapter 2**) and computational methods (**chapter 3**). The advantage of using cage compounds in macrocycles is due to increased rigidity, increased solubility in non-polar solvents and increased chirality.

The search for new chiral ligands used in asymmetric catalysis is of great interest in the field of synthetic chemistry. Carbon-carbon bond forming reactions is a very active research area. The synthesis of a new class of chiral cage annulated ligands is reported. The ability of the chiral amino alcohols to catalyse enantioselective addition of diethyl zinc to benzaldehyde was investigated (**chapter 4**). The cage annulated amino alcohols showed poor to good enantioselectivity but consistently high chemical yields. The synthesis of ligands such as **2** as well as their chiral catalytic influence in diethyl zinc addition to aldehydes is presented.

Catalytic asymmetric Michael additions have been studied using various catalysts and one of the most recent techniques has been the use of chiral crown ethers as phase transfer catalysts. Many chiral crown ethers have been synthesised and tested in asymmetric catalysis but there is still a need for a better understanding of the design of these systems. The synthesis of macrocycles such as **3** and its application in asymmetric Michael addition reactions are described (**chapter 5**).

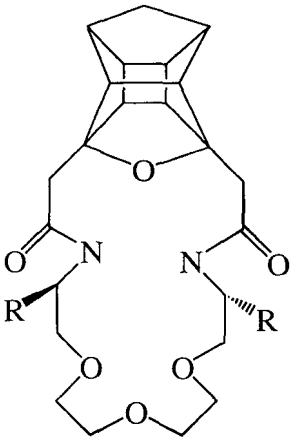

1

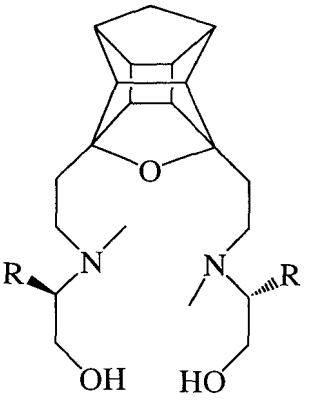

2

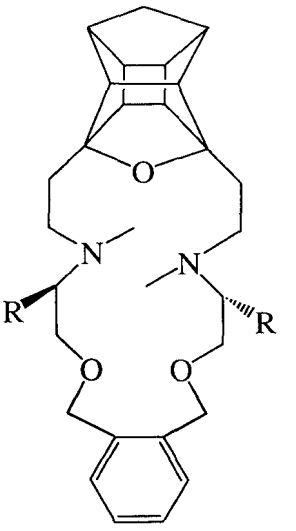

3

ACKNOWLEDGEMENTS

I sincerely thank all my mentors for contributing to my growth as a scientist:

Dr. H.G. Kruger	University of KwaZulu-Natal, South Africa
Dr. G.E. Maguire	University of KwaZulu-Natal, South Africa
Prof. K. Majerski	Ruđjer Bosković Institute, Croatia
Dr. T.D. Power	University of Texas Medical Branch, Galveston USA

I also thank all the technical staff at the University of Kwa-Zulu Natal especially:

Gregory Moodley	Stores
Saroj Naidoo	Technician
Jay Govender	Finance
Dilip Jagjivan	NMR
Anita Naidoo	Technician
Zarina Ali	Technician

I thank the NRF and the University of Natal for their generous financial support.

I dedicate this work to my wife (Ashmeetha), family, friends and my late beloved father.

CONTENTS

SUPPLEMENTARY MATERIAL:

A CD accompanying this thesis includes the following:

Text containing Chapters 1-6

Appendices 1 and 2

The Cartesian coordinates of all the 3D structures presented in chapters 3 and 5.

LIST OF TABLES

LIST OF FIGURES

LIST OF SCHEMES

CHAPTER 1

INTRODUCTION

CROWN ETHERS

Pedersen published the first account of crown compounds in 1967.[1] He discovered (Scheme 1) the macrocyclic polyether **1** as a minor product while synthesising bis-[(2,2`-o-hydroxyphenoxy)-ethyl]-ether (**2**).

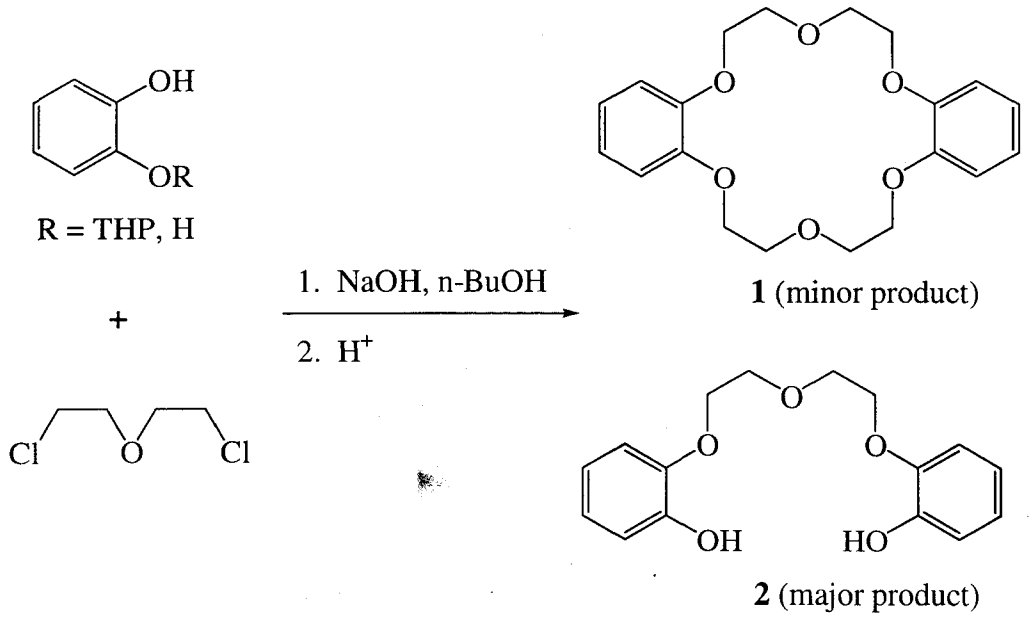

Scheme 1: Serendipity of Pedersen[1]

He observed that these compounds formed stable complexes with salts of alkali metals and the complexes were soluble in organic solvents including non-polar solvents such as carbon tetrachloride and benzene. Even more impressive was that the stability of the complexes depended on the relative size between ionic radius of the cation and the cavity in the macrocyclic polyether.[2] This groundbreaking research stimulated the interest of many chemists. Christensen *et al.* published a review[3] listing 221 kinds of macrocyclic compounds only seven years after Pederson's initial report.

Synthesis of crown ethers[7,4,5,6]

Crown compounds are generally synthesised by reactions used for the formation of ethers, secondary amines and thioethers. High dilution, two-step condensation and the template effect are techniques used to depress the formation of linear polymeric by-products. High dilution technique favours the intramolecular (S_N2) reaction over the intermolecular (S_N2)

reaction after the condensation of one of the terminal groups on both bifunctional compounds. The intermolecular reaction would lead to chain extension and the intramolecular reaction would lead to ring closure. In the two-step condensation technique (Scheme 2), one of the terminal groups on both bifunctional compounds is protected (p), while the other is condensed. The protecting group is removed, the intermediate purified and the remaining functional group is condensed.

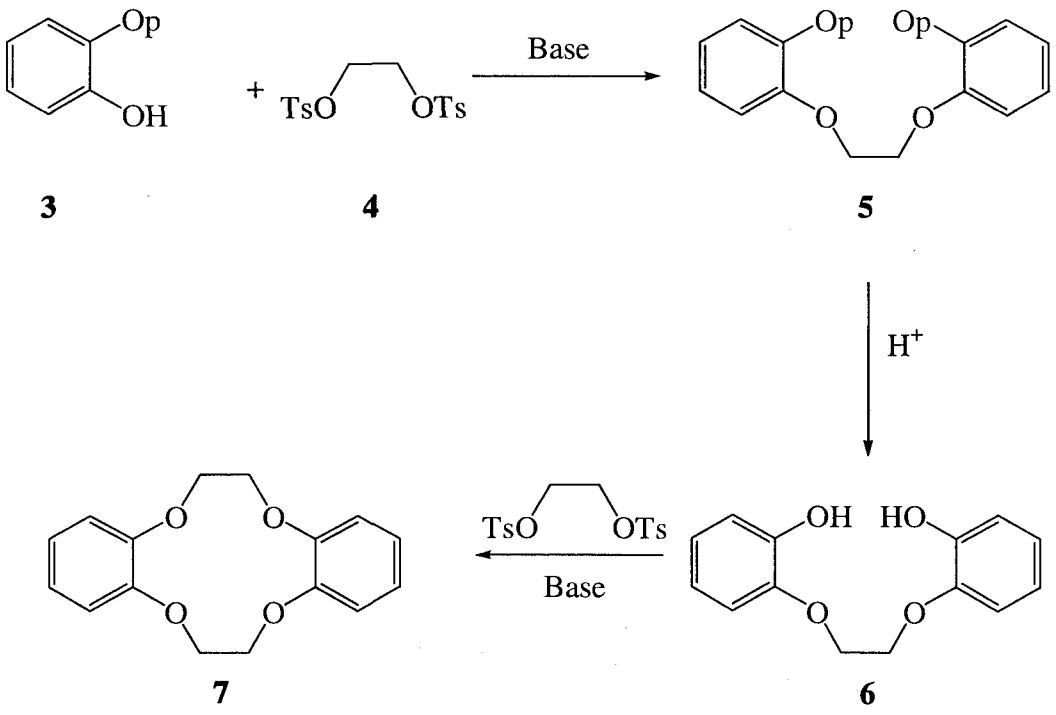

Scheme 2: An example of a two-step condensation technique

The template effect (Scheme 3) involves the use of a metal ion chosen on the basis of its ionic diameter. It uses the ionic dipole interaction between the metal ion and the intermediates to promote ring closure.

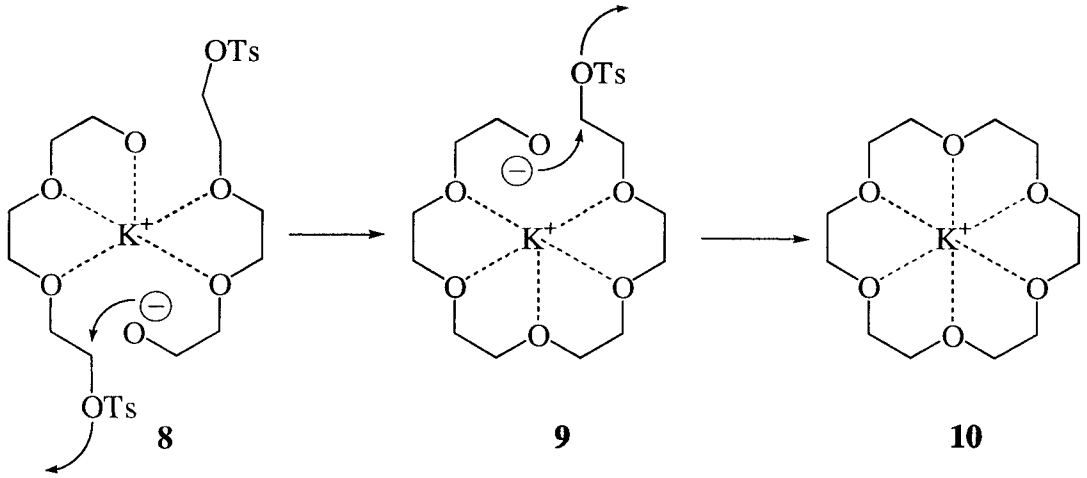

Scheme 3: An example of the template effect technique[4]

Types of crown ethers

Crown compounds are described[7] as "macrocyclic compounds having heteroatoms such as O, N, or S as the electron donor atoms in their structures and the property of incorporating cations into their cavity." Nomenclature of these types of compounds is described in early reviews.[6,7] Crown ethers are macrocyclic polyethers containing only O donor atoms, azacrown ethers have at least one N donor atom and thiacrown ethers have at lease one S donor atom. Cryptands are multicyclic crown compounds and bind metal ions more tightly and more selectively.[8] Below are examples of the different types of crown ethers.

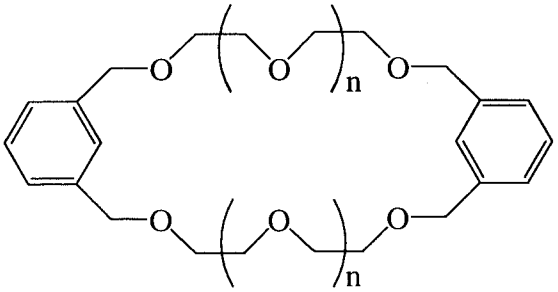

11

aromatic[9]

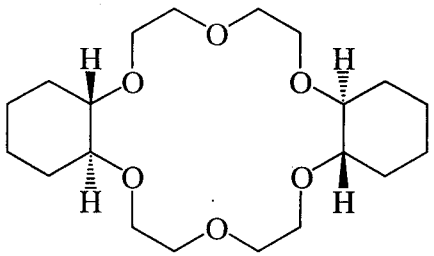

12

alicyclic[10]

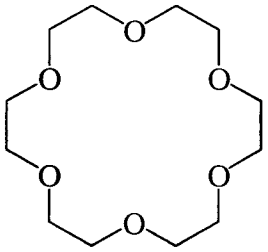

13

alkylene oxides[11]

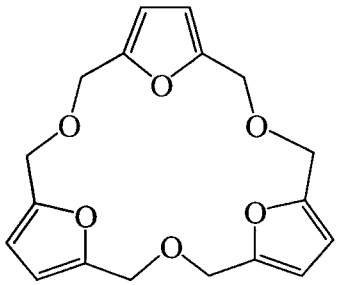

14

heterocyclic[12]

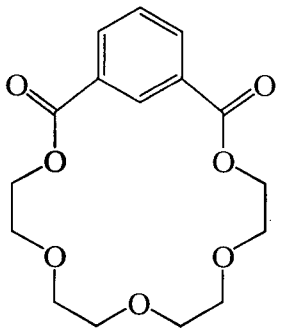

15

cyclic polyether esters[13]

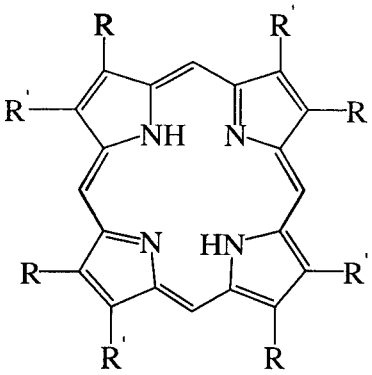

16

cyclic polyamines[14]

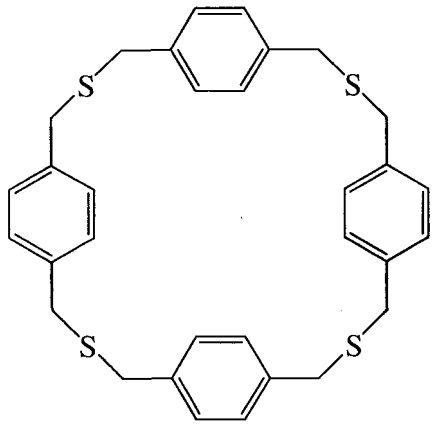

17

cyclic polythiaethers[15]

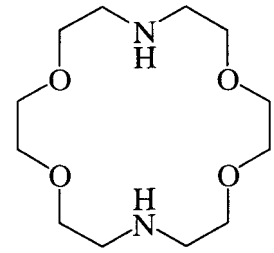

18

azacrown ethers[8]

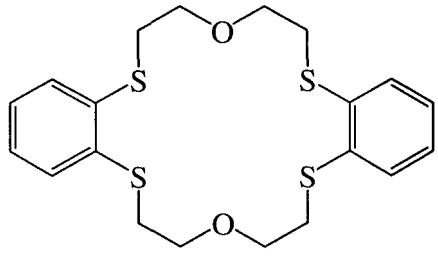

19

thiacrown ethers[16]

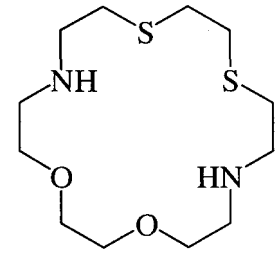

20

azathiacrown ethers[17]

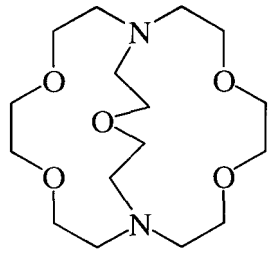

21

cryptand[18]

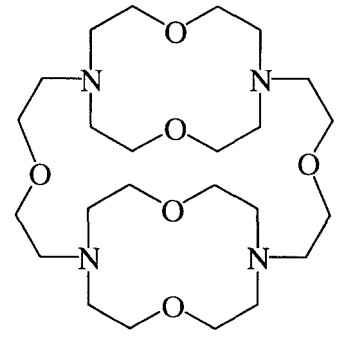

22

bicyclic cryptand[19]

Functional groups on crowns are important because they affect complexation and they could be used to prepare "immobilised" crown compounds. Lariat crown ethers (*eg.* **23**)[20]usually form more stable complexes relative to the simple crowns, especially if the flexible chains have additional binding sites. In some cases the side chain is utilised to supply the counter ion, improving the solubility of metal ion complexes.

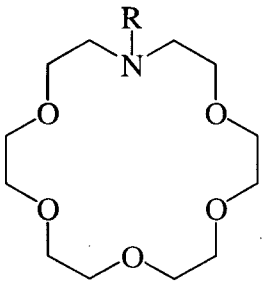

R = -$(CH_2CH_2O)_nH$

23

Immobilised crown ethers are synthesised either by copolymerisation of suitably functionalised macrocycles (*eg.* **24**) or by appending functional macrocycles to existing polymeric substrates (*eg.* **25**). These systems can be used for ion selective membranes, chromatographic stationary phase and even trace element enrichment of radionuclides.[21]

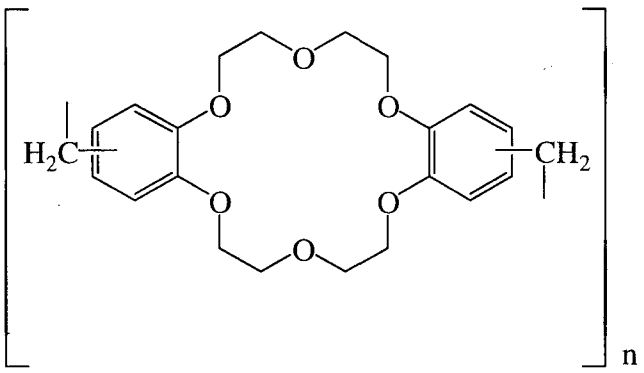

24

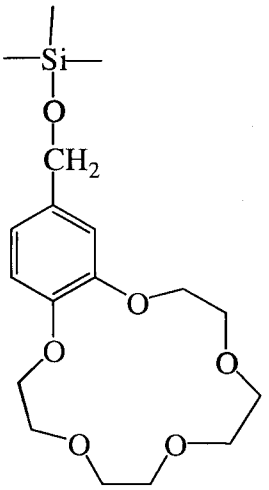

25

Chromogenic crown ethers (*eg.* **26**)[22] have colour inducing functional groups designed to give specific colour changes when complexed with certain alkali and alkali earth metals.

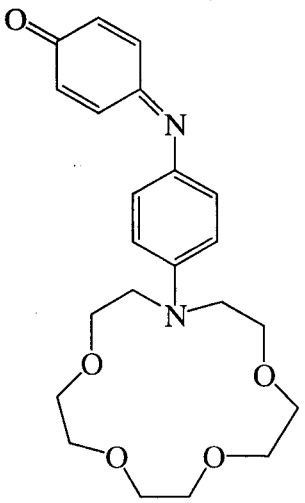

26

Photo-responsive crown ethers (*eg.* **27** and **28**)[23] contain a functional group that is able to induce structural change upon irradiation with a suitable source. A requirement for a photoresponsive crown is that it exhibits high quantum yield, high reversibility and significant structural change upon irradiation.

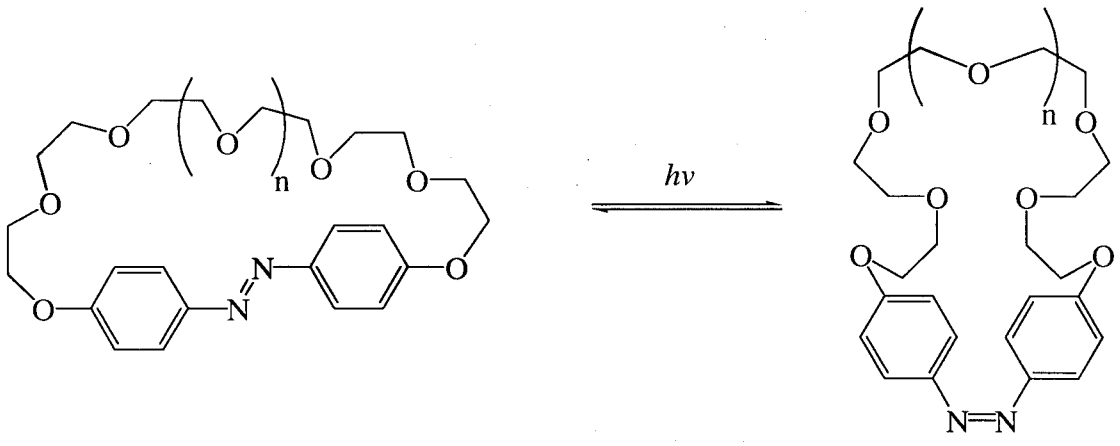

27 **28**

Applications of Crown Compounds

Crown compounds are found to be useful in the separation of metal ions. They are able to form selective complexes with cations with specific ionic diameter. Organic solvents containing the crown ether are used to selectively extract inorganic salts from aqueous solutions. Crown compounds are applied in many fields, but most progress has been made in applications in organic synthesis. They are useful in synthesis because they solubilise inorganic salts or alkali metals even in non-polar solvents and are also useful because the

counter ion is present in solution as a naked, highly active, non-solvated anion.[4] The following are examples of reactions involving crown ethers.

Neutralisation and Saponification:[2] Saponification of 2,4,6-trimethylbenzoic acid ester (**29**) could not be achieved under conventional conditions but was achieved with the use of dicyclohexyl-18-crown-6 complex with KOH in toluene. This demonstrates that the HO^- is highly activated and sterically less hindered since it is not solvated.

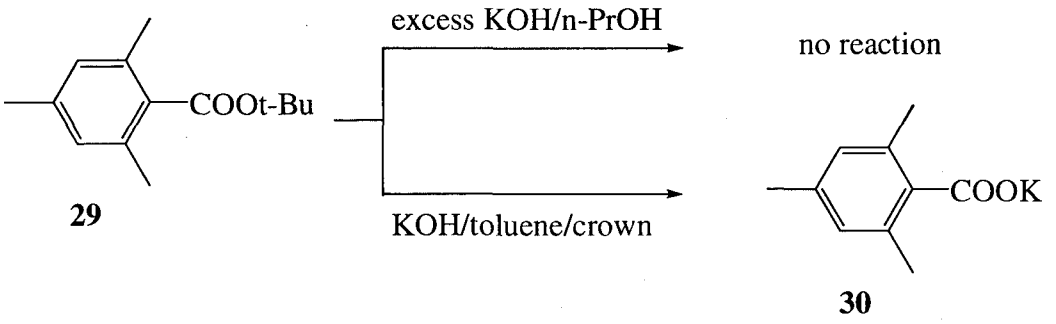

29 **30**

Scheme 4: Saponification of 2,4,6-trimethylbenzoic acid ester using dicyclohexyl-18-crown-6

Oxidation:[24] $KmnO_4$ is a strong oxidising agent and is insoluble in organic solvents except in the presence of crown ethers. This reaction cannot be performed in apolar organic solvents with the same success without the aid of a solubilising agent.

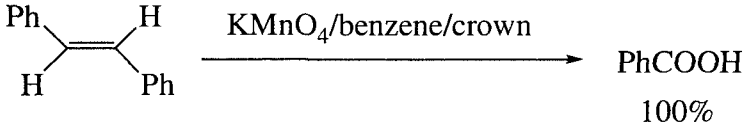

31 **32**

Scheme 5: Oxidation of stilbene with $KMnO_4$ in the presence of crown ether

Reduction:[25] The use of crown ethers in reduction showed an increase in yield and selectivity. Reduction of 4-methyl-cyclohexanone can result in a *cis* or *trans* alcohol but can be favoured to form the *trans* isomer with the use of crown ethers.

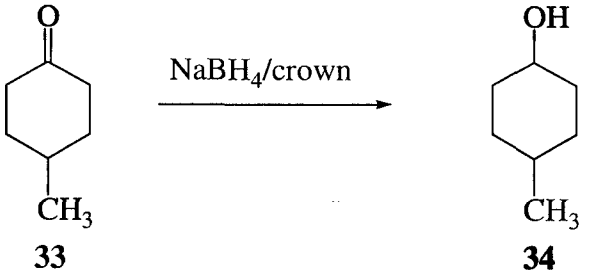

33 **34**

Scheme 6: Reduction of cyclohexanone with $NaBH_4$ in the presence of crown ether

Substitution:[26] The reaction was carried out in liquid-liquid phase system. The crown ether/KI complex was found to be more nucleophilic than $Bu_4N^+I^-$ and therefore increased the reaction rate.

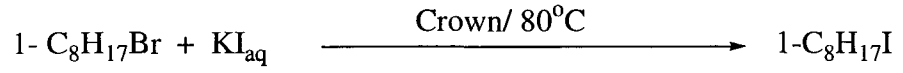

35 **36**

Scheme 7: Halogen substitution of octyl bromide using catalytic amounts of crown ether

Elimination:[27] Certain decarboxylation reaction rates increased up to 10^5 times in the presence of crown ethers.

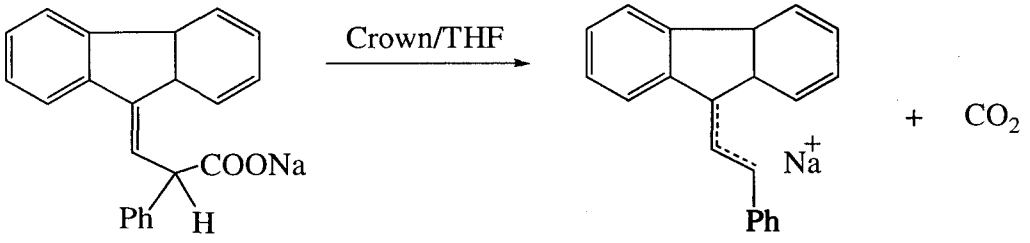

37 **38**

Scheme 8: Decarboxylation in presence of crown ether

Condensation:[26] Reaction rates of condensation reactions in which carbanions were generated were increased up to 10^2~10^5 times.

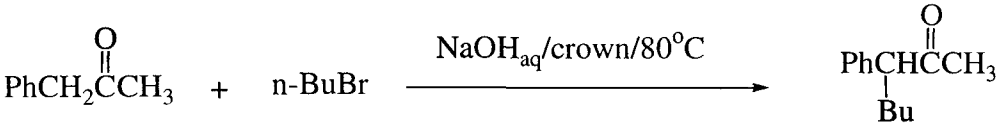

39 **40**

Scheme 9: Alkylation of benzyl methyl ketone using crown ethers as phase transfer catalysts

Isomerisation and Rearrangement:[28] Crown ethers increased the rate of isomerisation reactions in cases where the addition of tetraglyme (increases solubility of potassium salt in polar solvents such as DMSO) had no effect.

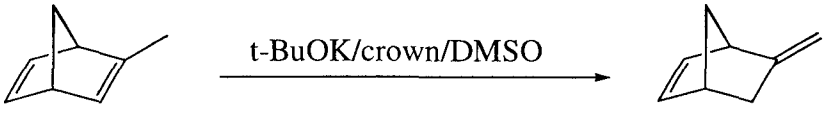

41 **42**

Scheme 10: A rearrangement reaction in the presence of a crown ether

CHIRALITY

Three-dimensional objects could potentially be chiral. A chiral object cannot be superimposed upon its mirror image. Some categories of optically active compounds are: [29]

- A carbon atom attached to four different groups is chiral e.g. the amino acid valine.

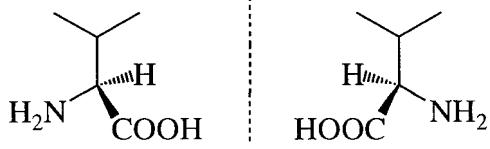

S-(-)-valine *R*-(+)-valine

43

- A molecule containing an atom that has four bonds in tetrahedral symmetry will be optically active if the four groups are different.

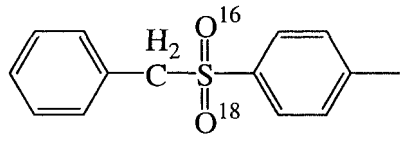

44

- A nitrogen atom that is attached to 3 different groups might be expected to give rise to optical activity since the lone pair of electrons is analogous to a fourth group. The following is an example where the nitrogen is sufficiently immobilised (inversion does not occur at room temperature as with ammonia) to produce chiral amines.[30,31]

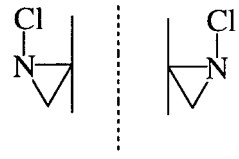

45

- Adamantane molecules with four different substituents at the bridgehead positions.[32]

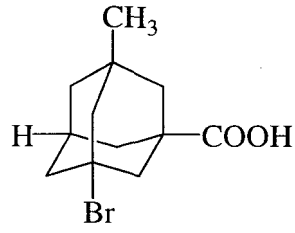

46

- Compounds that have restricted rotation do not need asymmetric atoms to be chiral *eg.* binaphthol (**47**)

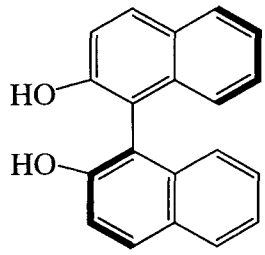

47

- Several compounds are chiral due to their helical shape. The helix can either be left- or right-handed *eg*. trans-cyclooctene (**48**).

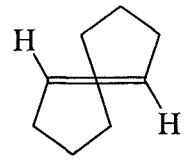

48

- Some molecules have neither chiral carbons nor a rigid shape but have been found to be chiral since it has the form of a Möbius strip. In structure **49** there is a -CH_2CH_2- between every two oxygen atoms.

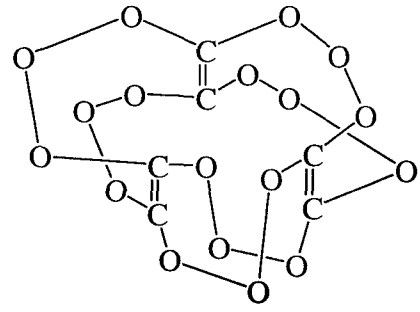

49

In the absence of an external chiral influence, enantiomers have identical chemical and physical properties except that they rotate plane-polarised light in opposite directions.[33] Molecular symmetry plays a crucial role in science and technology and this is mainly due to chirality being a major phenomenon in nature. Strict matching of chirality is essential since a variety of significant biological functions emerge through molecular recognition. Most of the important building blocks which make up the biological macromolecules of living systems do so largely in one enantiomeric form, namely only L-form.[34,35] Different biochemical effects should be expected when the two enantiomers of a biologically active chiral compound, such as a drug, interact with a receptor site which is chiral.[33]

Both enantiomers of thalidomide (**50**) have the same sedative effect (calming or tranquillising) but only the (-)-enantiomer causes foetal deformities. In the 1960's, a high incidence of foetal deaths and malformations occurred due to its use by pregnant women.[33]

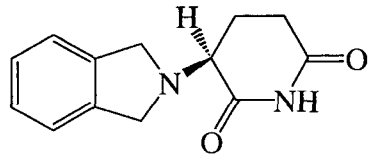

(-)-**50**

This discovery sparked an enormous scientific drive to synthesise chiral molecules in optically active form.[29,33,34,35,36] However, due to the lack of chiral synthetic routes or the high cost of chiral synthesis, a large number of biologically active compounds and pharmaceutical drugs are still synthesised as racemates.[33,35,37,38] Resolution of these mixtures would involve enzymatic methods,[39,40] chiral chromatography and in some cases fractional crystallisation with a co-chiral molecule.[33] It was recently predicted that chiral crown ethers will play a major role in future enantiomeric separations.[41]

CHIRAL CROWN COMPOUNDS

Pedersen, Lehn and Cram won the 1987 Nobel Prize in chemistry for their contribution to the field of host-guest chemistry. Pedersen was mainly responsible for the initial synthesis of crown ethers, Lehn's contribution was the bicyclic and tricyclic compounds called cryptands and Cram's main contribution was his pioneering work on chiral crown ethers.

Enantiomeric recognition of chiral ammonium compounds

The first chiral crown ether (**51**) was synthesised by Cram in 1972,[42,43] and since then many other chiral crown ethers and macrocycles have been synthesised[44,45,46,47,48,49,50,51] and have shown to form enantioselective complexes with chiral organic ammonium salts.[52,53,54,55]

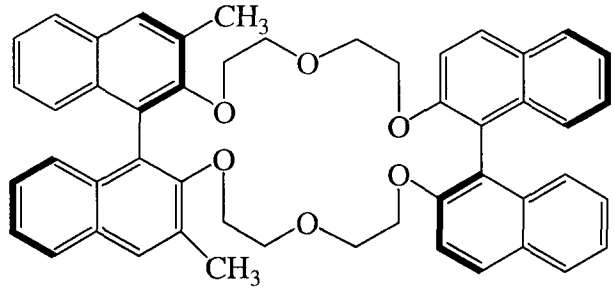

(*R,R*)-**51**

Pedersen proposed that these complexes formed via ion-dipole interactions.[2] Cram and his co-workers demonstrated that the binding interaction between crown ethers and primary ammonium salts were formed by three hydrogen bonds together with three ion-dipole interactions.[5]

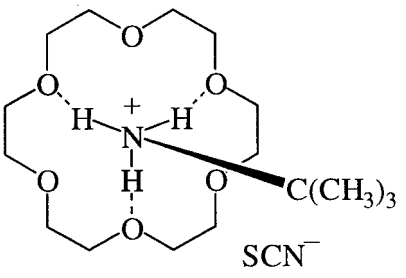

52

Cram *et al.* used the binaphthyl crowns as hosts and succeeded in optical resolution of racemic primary ammonium and amino acid ester salts. The extent of selectivity depends on the relative stability of the diastereomeric complexes formed.

Cram and co-workers developed a unique method (U- and W-tube)[43] for resolving enantiomers in 1973 and although many hosts were synthesised since then by various people no reports on the use of the U- and W-tube appeared until 1999. Enantiomeric resolutions were demonstrated by chromatographic methods[56] and capillary zone electrophoresis.[57] Enantiomeric recognition of crown ethers was thermodynamically quantified by calorimetry,[58] mass spectrometry[59] and fluorescence spectroscopy.[60] Kinetic quantification of the chiral preference of crown compounds was done using ^{1}H NMR.[61,62] Computational chemistry is a theoretical method, which has been applied to a limited extent[63,64,65] in order to calculate the stability of chiral host-guest complexes. It is important to note that a literature survey showed application of mostly one of the analytical techniques combined with computational methods. A few examples of chiral macrocycles tested with various methods are illustrated below.

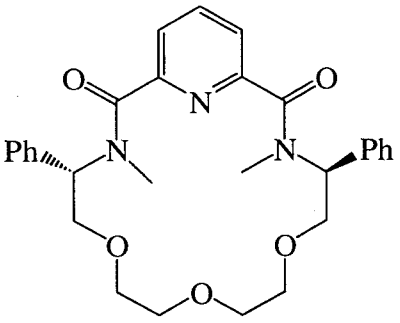

53 (NMR)

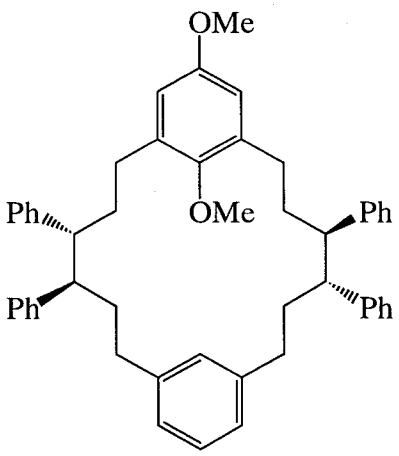

54 (mass spectrometry)

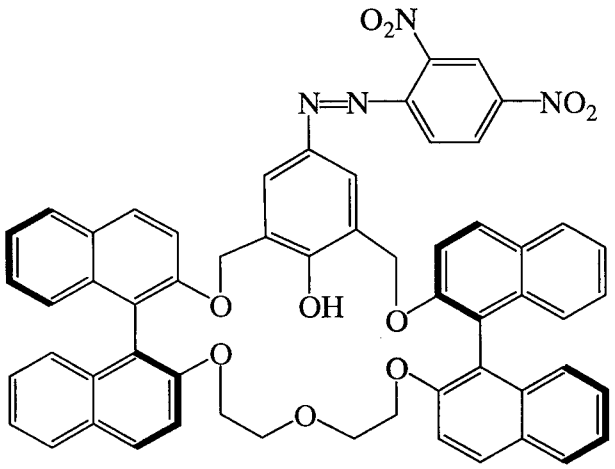

55 (visible spectrometry)

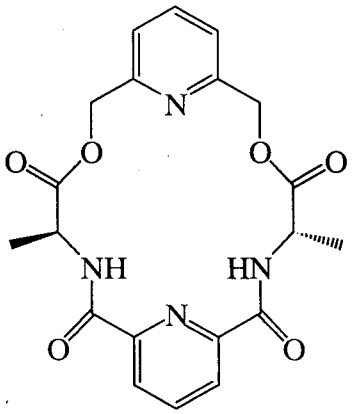

56 (fluorescence spectroscopy)

Cram's method involved the use of a U- or W-tube as mentioned above.[5,42] A racemic solution of guests in an aqueous phase (source or α-arm) forms a complex with the host in an organic phase ($CHCl_3$) at the solvent interface and is transferred into the organic phase. Subsequent transport to the other side of the U- or W-tube enables releasing of the guest to the second water phase (receiving or β-arm). If the rate (k_1) of transport of (*R*)-guest is larger than that of (*S*)-guest, then after some time, the optical activity of the second aqueous phase will indicate enantiomeric excess for (*R*)-guest. In a U-tube the enantiomeric excess will decrease with time since equilibrium will ultimately be obtained. In a W-tube with (*R*)-host in one side of the W-tube and (*S*)-host on the other side, a racemic mixture of guest in the centre (α-arm), complete resolution of the guest can be achieved after infinite time.[66]

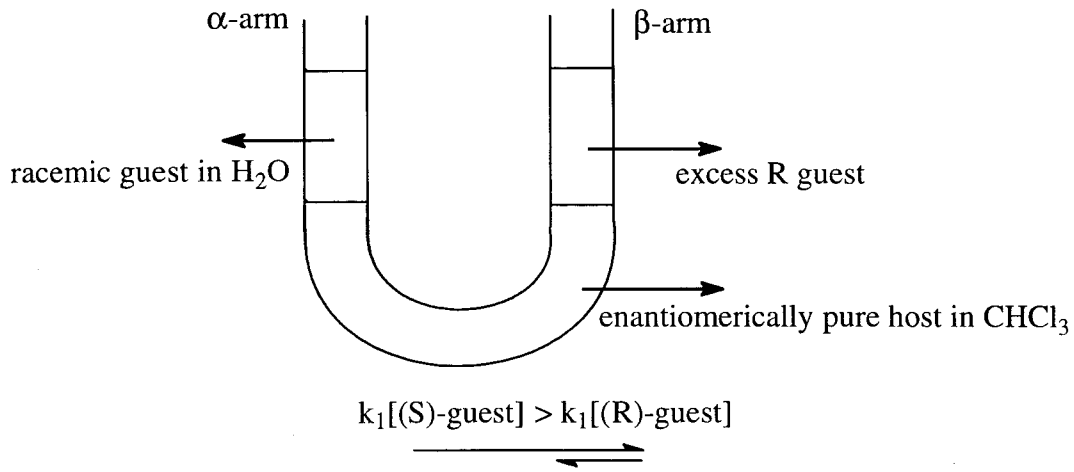

Figure 1: U-tube[5]

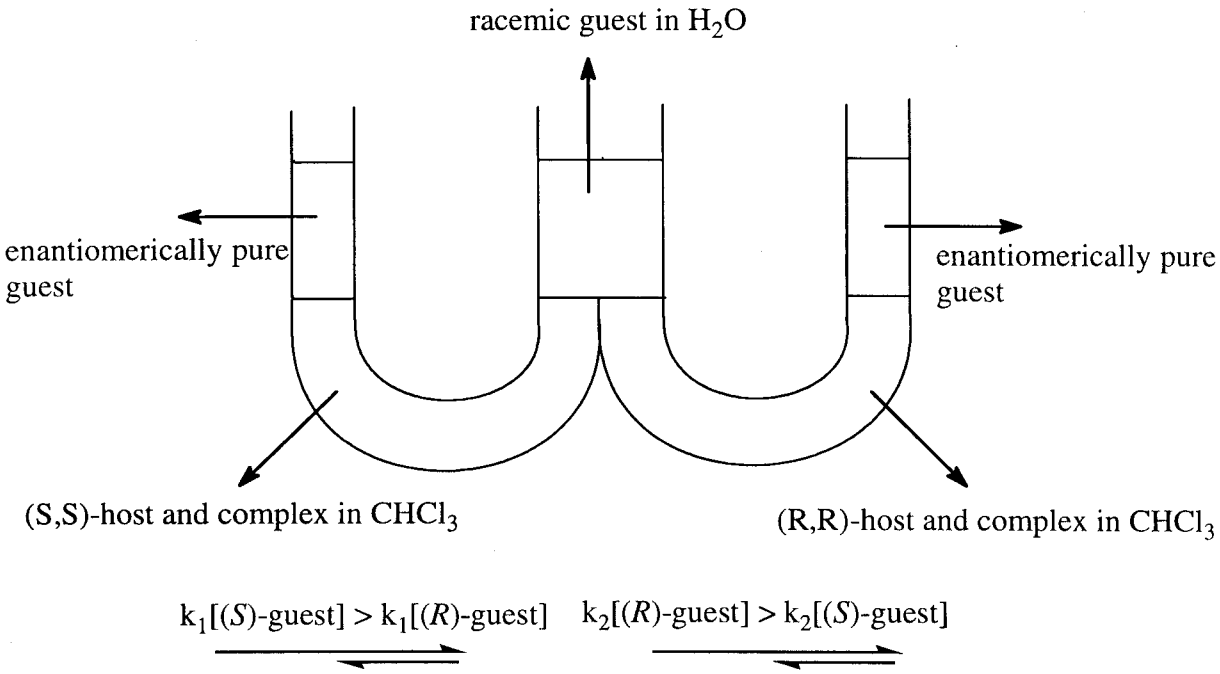

Figure 2: W-tube[5]

NMR line-shape methods are a valuable tool for studying a variety of processes that become slow on the NMR time scale at temperatures between room temperature and -90°C.[67,68] Reinhoudt and de Jong[62] have discussed the specific application of NMR line-shape methods to determine rate constants and activation energies for the dissociation of crown ether complexes. The concept can be explained using Figure 3. In the absence of complex formation, protons H_a and H_b are indistinguishable on a NMR spectrum. When complex formation occurs, the proton on the same side of the crown as the alkyl group of the alkyl ammonium salt experiences a different magnetic environment than the proton on the opposite side. At ambient temperatures, the rate of complexation and dissociation of the host guest system is so rapid on the NMR time scale that only an average chemical shift of the protons is observed. Lowering the temperature of the NMR probe "freezes" complexes that have high

activation energies for dissociation (i.e. more stable complexes). This slows down the exchange rate on the NMR time scale resulting in the observation of different signals for H_a and H_b.[62]

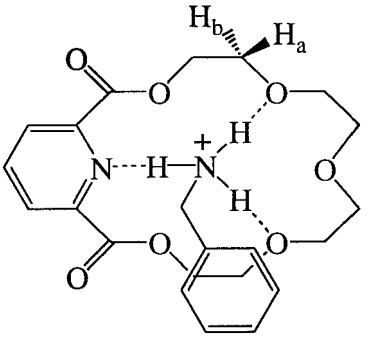

Figure 3: A typical complex formation of a macrocycle with and ammonium ion[62]

Recently, Hua (2000), reported the use of fluorescence spectroscopy in determining enantiomeric recognition.[69] With this technique, fluorescence emissions were measured for hosts and for mixtures of hosts and guests, and the difference in wavelength at maximum intensity ($\Delta\lambda$) between the two diastereoisomers was taken as a thermodynamic measure of enantiomeric discrimination. Stronger complexation between host and guest would result in greater significant change in configuration of the molecules and therefore a larger change in the wavelength (50 nm) at maximum intensity (λ_{max}).

Computational chemistry, due to spectacular advances in both hard and software,[70] has become a valuable tool to enhance our understanding about many complex chemical systems. There are three areas of computational tools available. Molecular mechanics or force field derived calculations, semi-empirical methods and *ab initio* and density functional theory (DFT) calculations. Molecular mechanics are typically used for very large biochemical systems such as proteins and although it is the cheapest method with respect to computer time and resources, good force fields for macrocyclic hosts with ammonium ion guest interactions have not yet explicitly been developed. In general molecular mechanics also give the least accurate results.[71]

Marchand *et al* reported the first chiral crown ethers (**57**) to incorporate the pentacyclo-undecane (PCU) unit in 1999 and used Cram's U-tube method to determine its enantioselectivity towards chiral ammonium salts.[72]

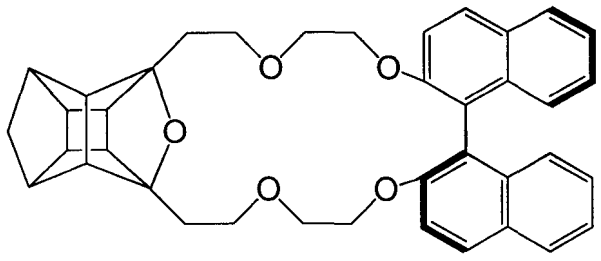

(R)-**57**

It was predicted[72] that chiral crown ethers with the PCU moiety will enhance their enantioselectivity by providing:

- a high degree of rigidity
- ten extra chiral centres
- clear differentiation between the two faces of the ligand and
- increased solubility in non-polar solvents.

Applications in Asymmetric Synthesis

Crown ethers are used as phase transfer catalysts (PTC) in a large number of reactions. The field of chiral phase transfer catalysis is becoming an important area of research. The most commonly used PTC's are chiral quaternary ammonium salts like the cinchona ligand (*eg.* **58**)[73]. PTC can work in a liquid-liquid system or in a solid-liquid system by transporting reactants from one phase to another.

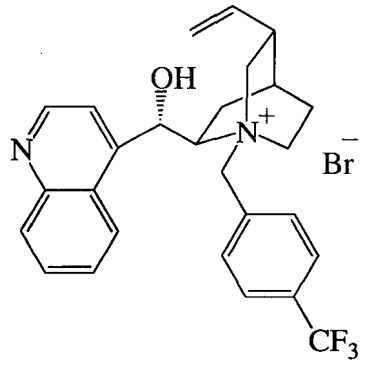

58

Chiral macrocycles have limited use due to the high cost of synthesis, although they are less prone to degradation and therefore have higher turnover numbers than quaternary ammonium salts.[73] Examples of reactions catalysed by chiral crown ethers are described below.

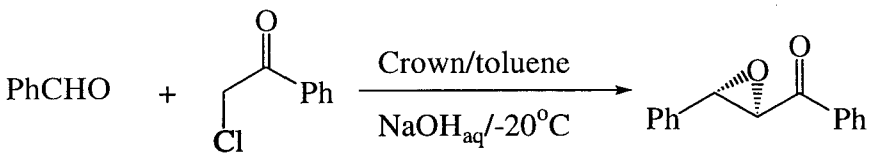

59 **60** **61**

Scheme 11: Chiral crown catalysed Darzens reaction[74]

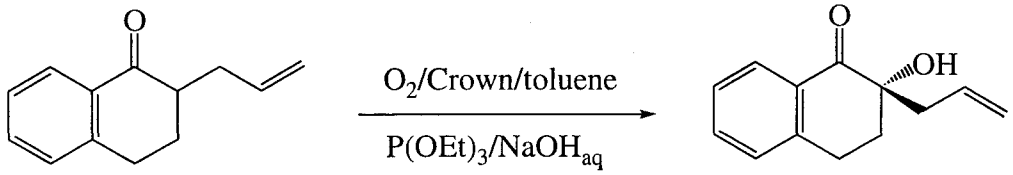

62 **63**

Scheme 12: Chiral crown catalysed oxidation reaction[75]

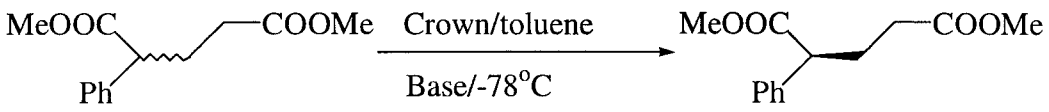

64 **65**

Scheme 13: Chiral crown catalysed deracemisation reaction[76]

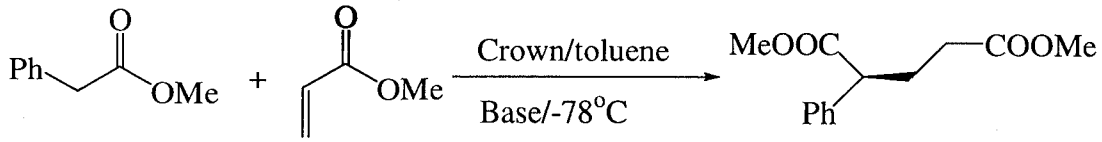

66 **67** **65**

Scheme 14: Chiral crown catalysed Michael addition reaction[76]

This thesis will describe the synthesis of new classes of chiral PCU annulated ligands and macrocycles. Various use of these systems in enantioselective transport of chiral ammonium salts, and their ability to catalyse Michael addition reactions will be investigated. A computational model for predicting the enantioselectivity of chiral hosts in transport experiments is also proposed.

REFERENCES

1. Pederson, C.J. *J. Amer. Chem. Soc.* **1967**, *89*, 2495.
2. Pederson, C.J. *J. Amer. Chem. Soc.* **1967**, *89*, 7017.
3. Christensen, J.J.; Eatogh, D.J.; Izatt, R.M. *Chem. Rev.* **1974**, *74*, 351.
4. Weber, E; Toner, J. L.; Goldberg, I.; Vogtle, F.; Laidler, D.A.; Stoddart, J.F.; Bartsch, R.A.; Liotta, C.L. in *Crown ethers and analogs*, Patai, S. Ed., John Wiley and Sons, New York, **1989**.
5. Cram, D.J. and Cram, J.M. in *Container molecules and their guests*, Stoddart, J.F. Ed., Royal Society of Chemistry, Cambridge, **1994**.
6. Lindoy, L.F. in *The chemistry of macrocyclic complexes*, Cambridge University Press, Cambridge, **1989**.
7. Hiraoka, M. in *Crown compounds: Their characteristics and applications*, Elsevier Scientific publishing company, New York, **1982**.
8. Dietrich, B.; Lehn, J.M.; Sauvage, J.P. *Tetrahedron Lett.* **1969**, 2885; Lehn, J.M.; Sauvage, J.P. *Chem. Commun.* **1971**, 440; Cheney, J.; Lehn, J.M. *ibid.* **1972**, 487.
9. Timko, J.M.; Moore, S.S.; Walba, D.M.; Hibery, P.C.; Cram, D.J. *J. Am. Chem. Soc.* **1977**, *99*, 4207.
10. Stoddart, J.F.; Wheatley, C.M. *Chem. Comm.* **1974**, 390.
11. Gokel, G.W.; Cram, D.J.; Liotta, C.L.; Harris, H.P.; Cook, F.L. *J. Org. Chem.* **1974**, *39*, 2445.
12. Timko, J.M.; Cram, D.J. *J. Am. Chem. Soc.* **1974**, *96*, 7159.
13. Frensch, K.; Vogtle, F. *Tetrahedron Lett.* **1975**, 2109.
14. Fleisher, E.B. *Inorg. Chem.* **1962**, *1*, 493.
15. Tabushi, I.; Sasaki, H.; Kuroda, Y. *J. Am. Chem. Soc.* **1976**, *98*, 5727.
16. Pederson, C.J. *J. Org. Chem.* **1971**, *39*, 2351.
17. Dietrich, B.; Lehn, J.M.; Sauvage, J.P. *Chem. Commun.* **1970**, 1055.
18. Graf, E.; Lehn, J.M. *J. Am. Chem. Soc.* **1975**, *97*, 5022.
19. Lehn, J.M.; Simon, J.; Wagner, J. *Angew. Chem. Intern. Ed.* **1973**, *12*, 578.
20. Masuyama, A.; Nakatsuji, Y.; Ikeda, I.; Okahara, M. *Tetrahedron Lett.* **1981**, *22*, 4665.
21. Blasius, E.; Janzen, K.P. *Pure and Applied Chemistry*, **1982**, *54*, 2115.
22. Dix, J.P.; Vogtle, F. *Chemische Berichte* **1981**, *114*, 638.
23. Shinkai, S.; Minami, T.; Kusano, Y.; Manabe, O. *J. Am. Chem. Soc.* **1983**, *105*, 1851.
24. Sam, D.J.; Simmons, H.F. *J. Am. Chem. Soc.* **1972**, *94*, 4024.
25. Matsuda, T.; Koida, K. *Bull. Chem. Soc. Japan* **1973**, *46*, 2259.
26. Landini, D.; Montanari, F.; Pirisi, F.M. *Chem. Commun.* **1974**, 879.

27. Hunter, D.H.; Lee, W.; Sim, S.K. *Chem. Commun.* **1974**, 1018.
28. Maskornick, M.J. *Tetrahedron letters* **1972**, 1797.
29. March, J. in *Advanced Organic Chemistry*, 4th Ed,John Wiley and Sons, New York, **1992**.
30. Schurig, V.; Leyrer, U. *Tetrahedron: Asymmetry* **1990**, *12*, 865.
31. Gassman, P.G.; Dygos, D.K.; Trent, J.E. *J.Am.Chem.Soc.* **1970**, *92*, 2084
32. Hamill, M. *Chem. Commun.* **1969**, 864.
33. Aitken, R.A.; Kilényi, S.N. Editors of *Asymmetric Synthesis*, Blackie Academic & Professional, London, **1992**.
34. Coppola, G.M.; Schuster, H.F. in *Asymmetric Synthesis, Construction of Achiral Molecules Using Amino Acids*, John Wiley and Sons, New York, **1987**.
35. Williams, R.M. in *Synthesis of Optically Pure α-Amino Acids*, Permagon Press, Oxford, **1989**.
36. *α-Amino Acid Synthesis*, Tetrahedron Symposium in Print, 33; O'Donnell, M.J. Ed.; *Tetrahedron*, **1988**, *44*, 5253.
37. Walbroel, Y.; Wagner J. *J. Chromatogr.*, A **1994**, *680*, 253.
38. Walbroel Y., Wagner J. *J. Chromatogr.*, A **1994**, *685*, 321.
39. Palmer, T. in *Understanding Enzymes*, 4th Ed, Prentice Hall, London, **1991**.
40. Halgas, J. in Biocatalysts in Organic Synthesis. Studies in Organic Chemistry 46, Elsevier, Amsterdam, **1992**.
41. Armstrong, D.W.; Zhou, Y.W. *.J.Liq.Chromatogr., A* **1995**, *715*, 143.
42. Kyba, E.P.; Koga, K.; Sousa, L.R.; Siegel, M.G.; Cram, D.J. *J.Am.Chem.Soc.* **1973**, *95*, 2692.
43. Sogah, G.D.Y.; Cram, D.J. *J.Am.Chem.Soc.* **1979**, *101*, 3035.
44. Stoddart, J.F. *Chem.Soc.Review* **1979**, *8*, 85.
45. Izatt, R.M.; Zhu, C.Y.; Huszthy, P.; Bradshaw, J.S. in *Crown Compounds: Towards Future Applications*, Cooper S.R., Ed., VCH Publishers: New York, **1992**, chapter 12.
46. Kaneda, T. in *Crown ethers and Analoguous Compounds,* Hiraoka M., Ed., Elsevier: Amsterdam, **1992**, chapter 6.
47. Still, W.C. *Acc. Chem.Res.* **1996**, *29*, 155.
48. Webb, T.H.; Wilcox, C.S. *Chem.Soc.Rev.* **1993**, *22*, 383.
49. Yokota, K.; Haba, O.; Satoh, T. *Macromol.Chem.Phys.* **1995**, *196*, 2383.
50. Naemura, K.; Tobe, Y.; Kaneda, T. *Coord.Chem.Rev.* **1996**, *148*, 199.
51. Sawada, M.J. *Mass.Spectrom.Soc.Jpn.* **1997**, *45*, 439.
52. Cram, D.J. *Angew.Chem.Int.Ed.Engl.* **1988**, *27*, 1009.

53. Cram, D.J. *J.Incl.Phenom.Mol.Recogn.Chem.* **1988**, *6*, 397 and references cited therein.
54. Zhang, X.X.; Bradshaw, J.S.; Izatt, R.M. *Chem.Rev.* **1997**, *97*, 3313.
55. Armstrong, D.W.; Tang, Y.; Chen, S.; Zhou, Y.W.; Bagwill, C.; Chen, J.R. *Anal.Chem.* **1994**, *66*, 1473.
56. Gasparrini, F.; Misiti, D.; Villani, C.; Borchardt, A.; Burger, M.T.; Still, W.C. *J. Org. Chem.* **1995**, *60*, 4314.
57. Kuhn, R.; Riester, D.; Fleckenstein, B.; Wiesmuller, K.H. *J. Chromatogr. A* **1995**, 716, 371.
58. Izatt, R.M.; Zhang, X.X.; Huszthy, P.; Zhu, C.Y.; Hathaway, J.K.; Wang, T.M.; Bradshaw, J.S. *J. Inclusion Phenom. Mol. Recognit. Chem.* **1994**, *17*, 157.
59. Chu, I.-H.; Dearden, D.V.; Bradshaw, J.S.; Huszthy, P.; Izatt, R.M. *J. Am. Chem. Soc.* **1993**, *115*, 4318.
60. Zhao, H.; Hua, W. *J. Org. Chem.* **2000**, *65*, 2933.
61. Baxter, S.L.; Bradshaw, J.S. *J. Heterocyclic Chem.* **1981**, *18*, 233.
62. Reinhoudt, D.N.; de Jong, F. in *Progress in Macrocyclic Chemistry*, Izatt R.M. and Christensen J.J. Eds, Wiley, Vol. 1, New York, N.Y., **1979**, pp157-217.
63. Marchand, A.P.; Chong, H.S.; Ganguly, B. *Tetrahedron Asymmetry* **1999**, *10*, 4965.
64. Wang, T.; Bradshaw, J.S.; Izatt, R.M. *J.Heterocyclic.Chem.* **1994**, *31*, 1097.
65. Bradshaw, J.S.; Huszthy, P.; McDaniel, C.W.; Zhu, C.Y.; Dalley, N.K.; Izatt, R.M. *J.Org.Chem.* **1990**, *55*, 3129.
66. Newcomb, M.; Toner, J.L.; Helgeson, R.C.; Cram, D.J. *J.Am.Chem.Soc.* **1979**, *101*, 4941.
67. Baxter, S.L.; Bradshaw, J.S. *J. Heterocyclic Chem.* **1981**, *18*, 233.
68. Johnson, C.S. Jr. *Advan. Magn. Reson.* **1965**, *1*, 33.
69. Zhao, H.; Hua, W. *J. Org. Chem.* **2000**, *65*, 2933.
70. Pople, J.A.; Gast, A.P.; Trollsas, M.; Claesson, H.; Hedrick, J.L. *Polym. Prepr.* **1999**, *40*, 462.
71. Jensen, F. in *Introduction to Computational Chemistry*, **1999**, John Wiley and Sons, Chichester.
72. Marchand, A.P.; Chong, H.S.; Ganguly, B. *Tetrahedron Asymmetry* **1999**, *10*, 4965.
73. Dolling, U.H.; Davis, P.; Gabrowski, E.J.J. *J. Am. Chem. Soc.* **1984**, *106*, 446.
74. Bakó, P.; Szöllõsy, A.; Bombicz, P.; Tõke L. *Synlett.* **1997**, 291.
75. De Vries, E.F.J.; Ploeg, L.; Colao, M.; Brussee, J.; van der Gen, A. *Tetrahedron: Asymmetry* **1995**, *6*, 1123.
76. Tõke L.; Bakó, P.; Keseru, G.M.; Albert, M.; Fenichel, L. *Tetrahedron* **1998**, *54*, 213.

CHAPTER 2

SYNTHESIS AND TRANSPORT STUDIES OF A NEW CLASS OF CAGE ANNULATED CHIRAL MACROCYCLES

INTRODUCTION

Relatively few crown ethers containing a "cage" moiety as part of its "backbone" have been reported.[1] Compounds **68**[2] and **69**[3] are examples of cage containing crown ethers but the cage in either case simply functions as a lipophilic "spacer".

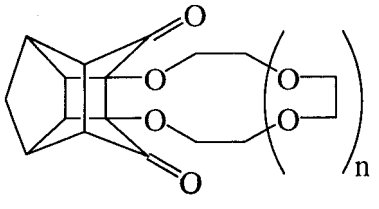

68

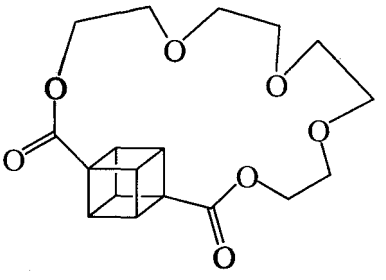

69

Marchand *et al.* developed an improved system of incorporating cage moieties into crown ethers using the PCU cage dione **70**.[1] The synthesis of the cage annulated crown ether **74**[1] is illustrated in Scheme 15. The cage is now serving as a rigidifying moiety and the ether oxygen atom can participate, with the other donating atoms, in complexation of a guest. In addition, the PCU derived crown ethers are inherently not C_2 symmetric since the pentacyclo-undecane (PCU) cage renders the "faces" diastereotopically non-equivalent. Alkali metal picrate extraction experiments on this type of crown ethers have shown[1] that they are better as transport hosts than their corresponding non-cage annulated systems.

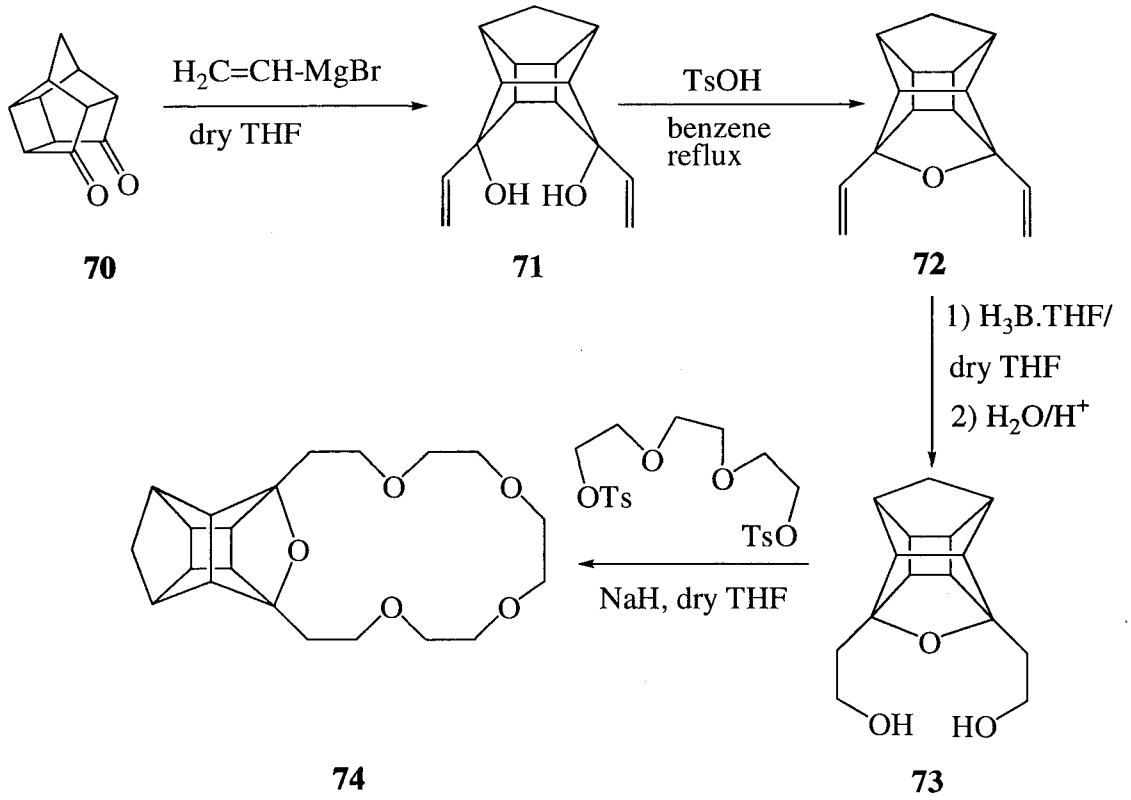

Scheme 15: Improved PCU cage annulated crown ether[1]

Cram's bis-binaphtol derived crown ether, **75**,[4] transported α-methylbenzylammonium ions with good enantioselectivity (*ca.* 82% *ee*) and at a moderate transport rate (0.6% h^{-1} with PF_6^- as counter ion). A closely related, cage annulated crown ether (**57**)[5] showed a much higher rate of transport (approx. 3% h^{-1} with PF_6^- as the counter ion) and exhibited good enantioselectivity (*ca.* 79% *ee*) with the same guest and counter ion.

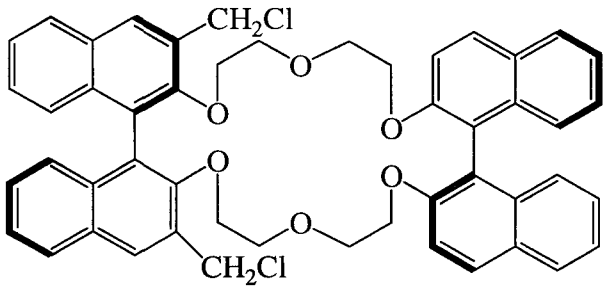

(*R,R*)-**75**

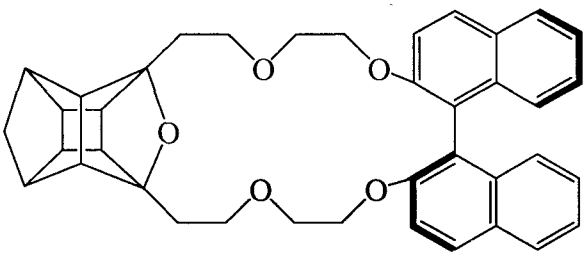

(*R*)-**57**

Bradshaw[6] synthesised a series of host-guest systems that displayed moderate to good chiral recognition. However, due to their low lipophilicity, it is unlikely that these systems would function effectively as transport agents. It was reported both with a chiral ammonium guests[5] as well as with metal ion transport experiments[7] that the cage annulation enhances the lipophilicity and consequent transport ability of host systems. The purpose of this study was to combine cage annulation with Bradshaw's macrocycle, **76**,[6] in order to investigate enantioselectivity and transport ability of the resulting host-guest system. It was therefore decided to use a similar route to that described by Bradshaw in order to synthesise macrocycle **76** and the novel macrocycles **77**,**78** and **79**.[8]

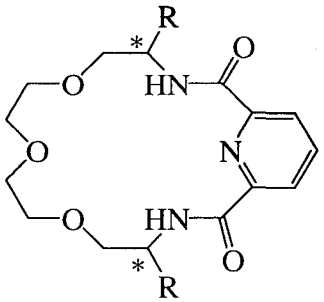

(*S,S*)-**76**: R=Ph
(*S,S*)-**77**: R=$CH(CH_3)_2$

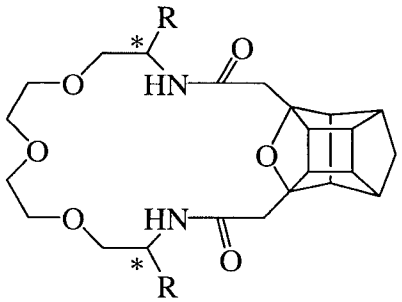

(*S,S*)-**78**: R=Ph
(*S,S*)-**79**: R=$CH(CH_3)_2$

RESULTS AND DISCUSSION

The reaction of pentacyclo[5.4.0.0^{2,6}.0^{3,10}.0^{5,9}]undecane-8,11-dione (PCU dione, **70**) with excess allylmagnesium bromide afforded the corresponding endo-8-endo-11-diol (**80**) [9] (91% yield). The ^{13}C NMR showed a triplet at 117.5 ppm and a doublet at 133.8 ppm indicating the presence of the allyl group and a singlet at 77.2 ppm for the quaternary carbon on the PCU unit. Subsequent dehydration of the diol (**80**) produced the corresponding hexacyclic ether, (**81**)[9] and confirmed by the downfield shift of the singlet carbon to 95.1 ppm on ^{13}C NMR.

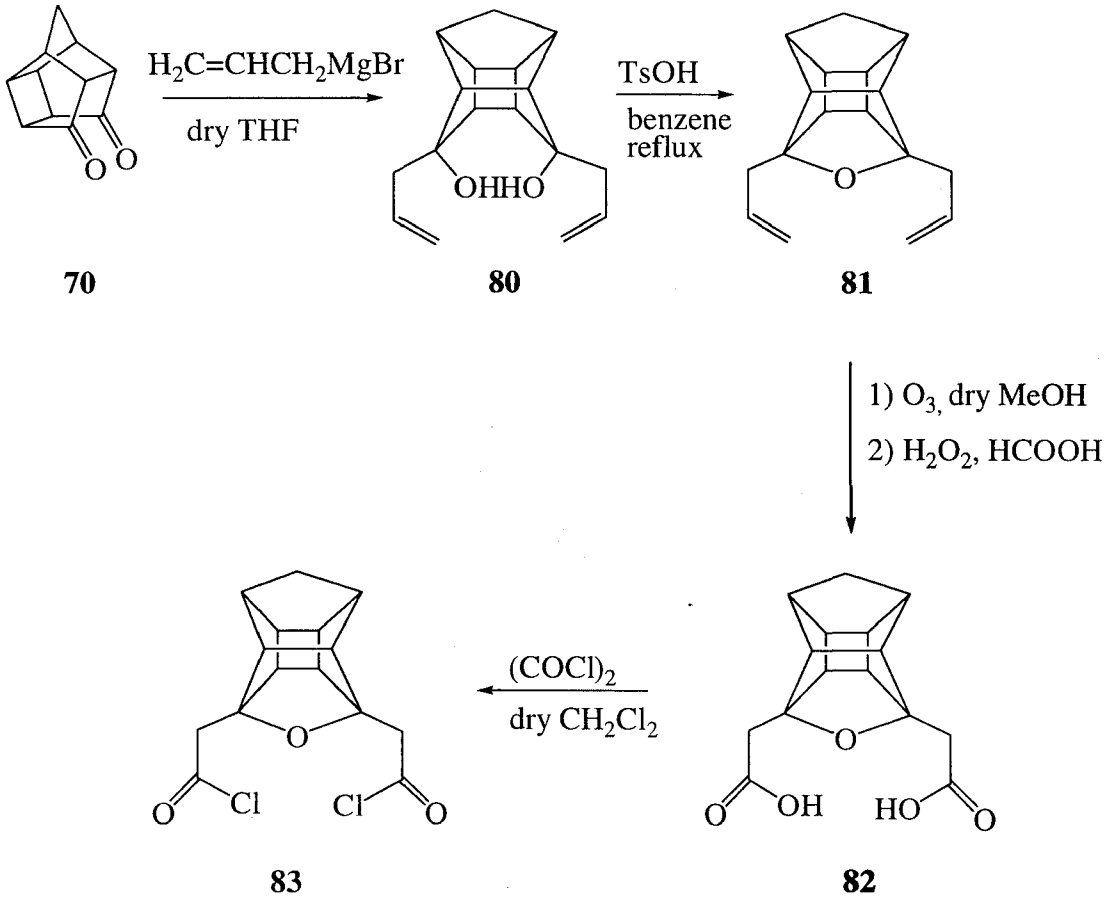

Scheme 16: Synthesis of PCU diacyl chloride **83**

Ozonolysis of **81** followed by oxidative work-up afforded the corresponding novel diacid, **82** (76% yield).[8] The ^{1}H NMR showed an AB pattern at 1.45 and 1.83 ppm with a coupling constant of 10 Hz indicating the presence of the methylene bridge of the PCU cage. The ^{13}C NMR showed a triplet at 42.8 ppm, which is characteristic of the methylene on the cage. A triplet at 37.9 ppm represents the sidechain methylene joining the carboxylic acid to the cage and a singlet at 171.4 ppm for the carbon of the carboxylic acid. Subsequent reaction of **82** with oxalyl chloride produced the corresponding novel diacyl chloride, **83**,[8] which was directly used to form macrocycles **78** and **79**, respectively (see Scheme 17).

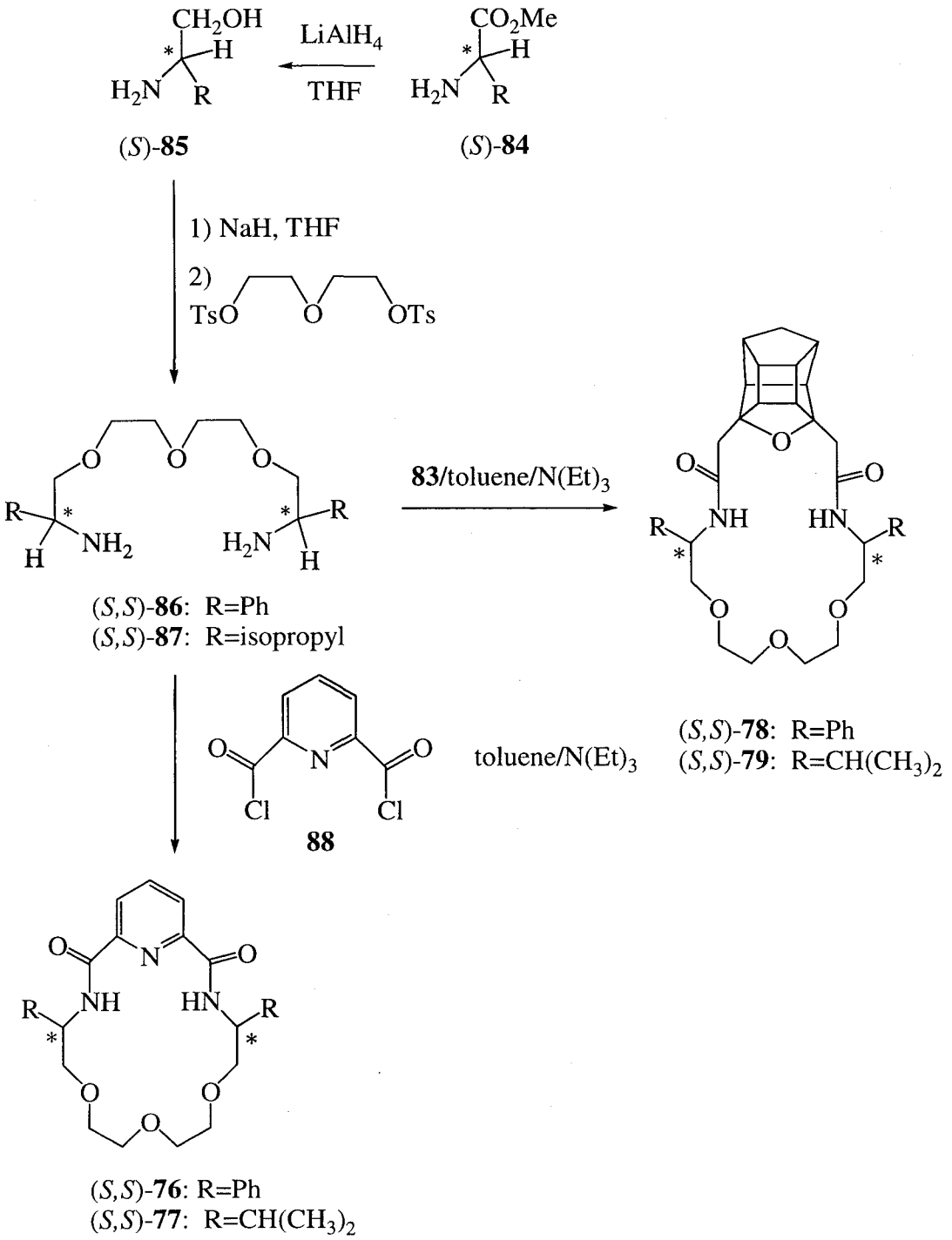

Scheme 17: Synthesis of macrocycles **76-79**

The infrared spectrum of **78** showed multiple peaks from 3307 - 3343 cm^{-1} representative of secondary amide NH stretching and a peak at 1517 cm^{-1} representing secondary amide NH bending. A characteristic CO stretching vibration peak at 1674 cm^{-1} confirmed the amide group. ^1H NMR showed an AB pattern at 1.49 and 1.82 ppm with a coupling constant of 10 Hz and a complex multiplet from 2.15 to 2.80 ppm representing the methylene bridge on the

PCU cage. Another complex multiplet from 3.45 to 3.95 ppm indicated the presence of the OCH_2 protons. The aromatic protons exhibited a multiplet from 7.12 to 7.53 ppm. ^{13}C NMR of **78** showed eleven signals for the cage carbons (unlike in the regular achiral cage annulated crowns and the chiral crown **57** reported by Marchand *et al.*, which showed only six signals for the cage carbons). Positioning of the chiral agents should be closer to the cage to induce chirality in the otherwise symmetric PCU unit. The incorporation of the chiral agent (phenylglycinol) successfully induced chirality on all ten of the inducible carbons of the cage and is observed in **78**. Mass spectrometry confirmed the [1:1] cyclisation product with a m/z peak at 585 and supports a formula of $C_{35}H_{41}N_2O_6$. **79** was characterised in a similar way to that of **78**. IR spectroscopy displayed evidence of the secondary amide bonds and ^1H NMR showed the presence of the isopropyl groups with a multiplet between 0.78 and 0.96 ppm integrating for twelve protons. One part of the AB pattern characteristic of the methylene bridge of the cage is present at 1.53 ppm. Mass spectrometry confirmed the [1:1] cyclisation product with a m/z peak at 518 and supports a formula of $C_{29}H_{44}N_2O_6$. Macrocycles **76** and **77** were synthesised in similar fashion, although thionyl chloride was used to form the pyridine diacyl chloride (**88**) as reported in literature.[6] Diamines **86** and **87** were synthesised via established procedures.[6,10] The coupling reactions were performed at relatively high dilution ([diamine] = 2 mmol dm^{-3} of solvent) and produced the desired products in yields of 25-43% (see Scheme 17). Macrocycle **77** was characterised in a similar way to that of **79** except for the presence of a pyridine unit in place of the cage moiety. A triplet at 8.00 ppm and a doublet at 8.33 ppm were evidence for the presence of pyridine.

TRANSPORT STUDIES

U-tube transport studies using observed optical rotations is a rapid, time dependent method that can be used to determine the enantioselectivity of a host-guest system. When promising enantioselectivity of a host is observed it would then be appropriate to pursue more precise methods, *eg.* W-tube experiments,[4] to determine a more accurate enantioselectivity. In order to permit direct comparison of the complexation properties of the new macrocycles with those already published,[4,5] methyl-2-phenylglycinate hydrochloride (**90**) was employed as the guest molecule. Complexation and transport of α-methylbenzylamine hydrochloride (**89**) was also studied; however, this hydrochloride salt proved to be readily soluble in chloroform. In a control run, as much as 30% dissolved into the organic phase within 4 hours,[8] thereby disqualifying **89** as guest in transport studies.

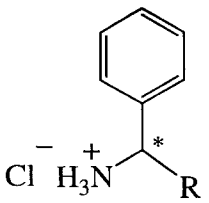

(*R*)/(*S*)-**89**: R=CH_3
(*R*)/(*S*)-**90**: R=COOMe

Table 1: Transport of enantiomers of (±)-methyl-2-phenylglycinate hydrochloride (**90**) by 0.027 M hosts **78** and **79** in $CHCl_3$ and PF_6^- as counter ion.

Run no.	Time (hr)[a]	host	% transported[b]	Dominant enantiomer	% *ee*[c]
1	24	none	3 ± 0.5		
4	1.5	**78**	18	***R***	27
5	2	**78**	24	***R***	20
6	4	**79**	24.5	***R***	25
7	8	**79**	29.7	***R***	22

a. Approximate time at which a maximum *ee* was observed.
b. Confidence limit was ± 3 %
c. Confidence limit was ± 1 %

Table 1 shows the results for the transport studies of macrocycles **78** and **79** with (±)-methyl-2-phenylglycinate hydrochloride with lithium hexafluorophosphate ($LiPF_6$) in the source phase (α-arm). Cram used PF_6^- since it is a relatively soft counter ion and would promote salting-out of the guest into the organic phase.[4] The receiving phase (β-arm) was analyzed every 30 minutes until maximum optical rotation had been attained. Cage macrocycle **78** showed a very high rate of transport (12% h^{-1}) and poor preference for the (*R*)-enantiomer. Macrocycle **79** had a lower rate of transport and only weak selectivity for the (*R*)-enantiomer. Very rapid transport by macrocycles **78** and **79** made it difficult to determine when the observed optical rotation reached a maximum, since at some stage the concentration gradient worked against enantioselectivity, after which time the *ee* began to decrease. Thus, rapid transport of the guest by the macrocyclic host rendered determination of the observed optical rotation difficult and increased the error in measurement of optical rotation. This was not a complication in previous reports,[4,5] wherein the rate of transport was considerably slower. A possible solution to this problem would be to measure the optical activity at shorter intervals. This was difficult to achieve with the apparatus at our disposal. To overcome this problem when macrocycles **78** and **79** were employed as hosts, PF_6^- was replaced as the counter ion with Cl^- to slow the rate of transport.[8]

Table 2: Transport of enantiomers of (±)-methyl-2-phenylglycinate hydrochloride (**90**) by 0.027 M hosts **78** and **79** in $CHCl_3$ and Cl^- as counter ion.

Run no.	Time (hr)[a]	host	% transported[b]	Dominant enantiomer	% *ee*[c]
1	24	none	1 ± 0.5		
2	12	**78**	16	***R***	**29**
3	19	**78**	22	***R***	**22**
4	12	**79**	6.8	***R***	**48**
5	18	**79**	13.2	***R***	**68**

a. Approximate time at which a maximum *ee* was observed.
b. Confidence limit was ± 1 %
c. Confidence limit was ± 1 %

Table 2 shows the results obtained for the same host-guest systems by using HCl in the source phase. The receiving phase was analyzed every sixty minutes until maximum enantiomeric excess had been attained. Comparison of the enantioselectivities in Tables 1 and 2 confirms that a more precise measurement of the enantioselectivity is possible with slower rates of transport since this measurement is time dependant. Macrocycle **79** showed moderate enantioselectivity for the (*R*)-methyl-2-phenylglycinate (68% *ee*). Host **78** still showed weak preference for the (*R*)-enantiomer (29% *ee*).

The pyridine macrocycles **76** and **77** displayed poor transport ability with both counter ions. The presence of host could be detected in both the source and receiving phases after 24 h, thereby disqualifying hosts **76** and **77** as candidates for transport studies. This observation indicated that they are capable of forming a relatively strong host-guest complex, but are unable to transport the guest into the organic phase due to their low lipophilicity.

CONCLUSION

A new class of chiral macrocycles had been synthesised. Compared to the previous two reports on this type of enantiomeric recognition studies, these hosts exhibited the highest rate of transport (12% h^{-1} with PF_6^- as counter ion) to date, but with moderate to poor enantioselectivity. Marchand's PCU annulated binaphthyl crown transported the guest at a rate of 3% h^{-1} whereas Cram's binaphthyl crown had a rate of 0.67% h^{-1} with PF_6^- as the counter ion. It is clear from the above results that incorporation of the cage into macrocycles increased the lipophilicity and transport ability of the host systems. Although transport rate is secondary in importance to enantioselectivity in these experiments, an ideal system is one that exhibits both high enantioselectivity as well as a high rate of guest transport. Higher enantioselectivity was achieved by slowing the transport rate by the use of a harder counter

ion. With only three reports on this type of transport experiments, it is clear that this field warrants further investigation.

REFERENCES

1. Marchand, A.P.; Kumar, K.A.; Mckim, A.S. *Tetrahedron* **1997**, *53*, 3467.
2. Moriarty, R.M.; Rao, M.S.C.; Tuladhar, S.M.; D'Silva, C.; Williams, G.; Gilardi, R. *J.Am.Chem.Soc.* **1993**, *115*, 1194.
3. Hayakawa, K.; Kido, K.; Kanematsu, K. *J.Chem.Soc.Commun.* **1986**, 268.
4. Sogah, G.D.Y.; Cram, D.J. *J.Am.Chem.Soc.* **1979**, *101*, 3035.
5. Marchand, A.P.; Chong, H.S.; Ganguly, B. *Tetrahedron Asymmetry* **1999**, *10*, 4965.
6. Huszthy, P.; Oue, M.; Bradshaw, J.S.; Zhu, C.Y.; Wang, T.; Dalley, N.K.; Curtis, J.C.; Izatt, R.M. *J.Org.Chem.* **1992**, *57*, 5383.
7. Marchand, A.P.; Alihodzic, S.; McKim, A.S.; Kumar, K.A.;Mlinaric-Majerski, K.; Kragol, G. *Tetrahedron Lett.* **1998**, *39*, 1861.
8. Govender, T.; Hariprakasha, H.K.; Kruger, H.G.; Marchand, A.P. *Tetrahedron: Asymmetry* **2003**, *14*, 1553-1557.
9. Marchand, A. P.; Huang, Z.; Chen, Z.; Hariprakasha, H. K.; Namboothiri, I. N. N.; Brodbelt, J. S.; Reyzer, M. L. *J. Heterocyclic Chem.* **2001**, *38*, 1361.
10. Chadwick, D.J.; Cliffe, I.A.; Sutherland, I.O. *J.Chem.Soc., Chem. Commun.*, **1981**, *19*, 992.

CHAPTER 3

USE OF MM3 IN PREDICTING THE ENANTIOSELECTIVITY OF CHIRAL MACROCYCLES FOR CHIRAL AMMONIUM COMPOUNDS

INTRODUCTION

Chiral host-guest chemistry has been of interest for many research groups over the past three decades.[1] A computational model could assist with the rational design of enantioselective host-guest systems.

A fast and reliable computational methodology is likely to advance the field as a whole since the synthetic approach[2] is intensive with respect to cost of chiral starting material and time; not to mention riddled with a relatively high degree of difficulty in both the synthetic and purification stages. It was therefore decided to investigate the possibility of calibrating existing experimental chiral recognition studies against a computational method with regard to approximate binding energy (see Equation 1 below) as well as enantioselectivity.

It was shown by Hay and co-workers that MM3 is a valuable method for optimisation of crown ethers with alkali metal guests[3,4] which prompted our laboratory to investigate the use of a MM3 model to investigate chiral host-guest interactions.

COMPUTATIONAL METHODOLOGY

A practical limit is placed on the computational model to be used in view of the number of calculations to be performed as well as the computational resources required. Density Functional Theory (DFT) methods are the most accepted and recognised method for computational chemistry since it calculates from first principals. However, these calculations require huge computational time and this is proportional to the number of atoms in the system studied. A DFT calculation of a typical host-guest complex took approximately 2 weeks of computer time on a super computer using four CPU's and four gigabytes of memory. For this reason DFT calculations were used as benchmark to determine the quality of a molecular mechanical and a semi-empirical computational model.

Verification of the computational model

On the advice of Hay[3] and with the initial assistance[5] of Allinger[3] we calculated the geometry and approximate binding energy of the two host-guest complexes synthesised by Bradshaw *et al.* (**89** and **90**) using the coordinates from their X-ray structures.[6] The complex structures were optimised with DFT, MM3, AM1 and PM3 respectively. Calculations with molecular mechanics were performed using the MM3 force field[7] with the default parameters presented

in Alchemy.[8] Semi-empirical (AM1 and PM3) and DFT calculations were performed using Gaussian.[9] All calculations excluded solvent effects in order to simplify the computational model. The three methods (MM3, AM1 and PM3) were calibrated against a high level DFT result in terms of RMS overlay and approximate binding energy (BE, see Equation 1). The DFT calculation used B3LYP[10,11,12] with the 6-31G(d) basis set.

$$BE = E_{complex} - (E_{host} + E_{guest}) \qquad (1)$$

The MM3 results compared well with the DFT optimised structures both in terms of RMS overlay and relative energies (see the results in Table 3). As MM3 gave very promising results (see Table 3), the host-guest interactions of all other systems was calculated using MM3 exclusively.

Determining low energy structures of the free host and guest

A molecular dynamics (MD) procedure was utilised to determine a number of low energy host and guest structures separately. The procedure is described in Appendix 2. Each of the low energy host structures obtained with the MD procedure were optimised using MM3 as well as DFT. The order of energy stayed the same for both MM3 and DFT, indicating that MM3 is a suitable method to determine low energy structures of the free host. The lowest structure/energy (E_{host} and E_{guest}) was used in Equation 1.

Determining low energy structures of the host-guest complex

The model developed involves the use of a MD calculation of the guest from which a number of "flat" host structures were manually chosen to ensure optimum interaction between the guest ammonium ion and the heavy atoms of the host system. The required degree of "flatness" for the host system is described in Appendix 2.

- **Docking procedure to find the host-guest starting structures**

A MM3 MD docking procedure was applied in an attempt to obtain a complex structure with a high degree of interaction between the host and guest and is described in Appendix 2.

- **Conformational search to find the lowest energy host-guest complex**

Despite the huge rotations/movement observed for the host-guest system during the initial MD docking procedure as described above, it is still possible that energy barriers prevent rotation/movement of the guest with respect to the host, with the result that existing lower energy complexes are not found. In order to ensure a reasonable chance to obtain the lowest energy host-guest structure, a conformational search also utilising a MD procedure was performed. The procedure is described in Appendix 2.

At least ten host-guest structures [five with (*R*)- and five with (*S*)-guest] are obtained from this conformational search; each of the minimum host-guest structures is then optimised using MM3. The ten complex structures are ranked by energy and the lowest energy ($E_{complex}$) is

used to determine the approximate binding energy as described in Equation 1. The lowest energy structure for each system (host with (*S*)- or (*R*)-guest) is determined and the chiral preference (E_{CP}) determined in kcal mol^{-1} ($E_{CP} = | E_{(R)\text{-complex}} - E_{(S)\text{-complex}} |$). The cartesian coordinates of the host-guest systems with lowest energy are provided on attached CD.

Computational results and considerations

It is important to realise that the counter ion plays an important role in the stability of host-guest complexes.[13] In order to simplify the computational model, the contributions of the counter ion and solvent effects to the binding energy are neglected. The "binding energy" reported is therefore only an approximate thermodynamic quantity (see Equation 1). Since the counter ion factor is neglected for all systems studied and the energies reported as relative energies, the error should cancel out. Neglecting packing forces in crystals (including forces exerted by the counter ion) has a profound effect on the structure of the computed structure. Nevertheless, the RMS overlay (0.4Å) of the DFT calculated structure with the X-ray structure[14] produces in principle the same conformation, as can be seen in Figure 4.

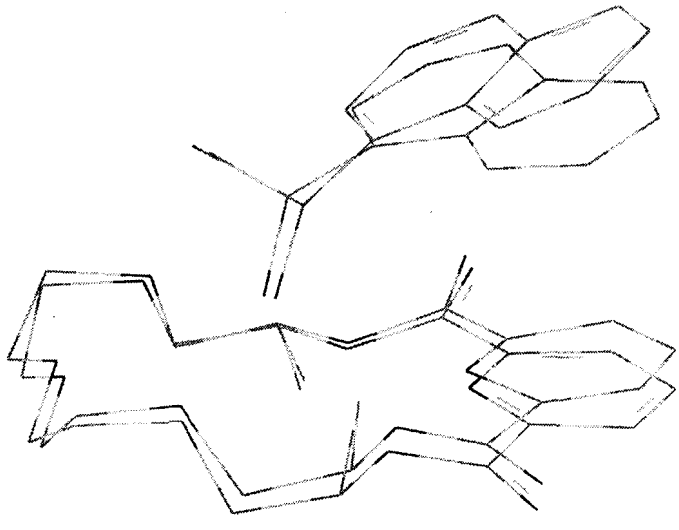

Figure 4: RMS overlay of the X-ray and DFT computed structures of **89**. Hydrogen atoms were omitted to allow for a clearer view of deviations between the two frameworks.

Based on the initial positive results the computational model was expanded to include host-guest systems where experimental results are available; such as NMR experiments,[15] fluorescence studies[16] and extraction studies.[17,18,19]

COMPARISON OF THE MM3 AND SEMI-EMPIRICAL RESULTS WITH A DFT CALCULATION

The precision of the MM3 and Semi-Empirical models was determined upon comparison with DFT results. The method applied was discussed above (see Appendix 2) and the results presented in Table 3.

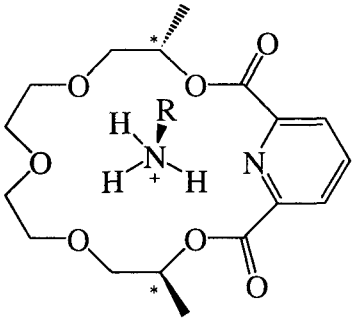

91: R =1-naphthylethyl
92: R = $CHPhCH_2OH$

Figure 5: Structures of host-guest systems **91** and **92** obtained from X-ray results[6]

Table 3: Comparison of PM3, AM1 and MM3 results with the DFT[a] result

Method	RMS overlay/Å		Energy[c]/ kcal/mol		CPU time/min[d]
Complex	**91**	**92**	**91**	**92**	
PM3[b]	0.476	0.758	+17.9	+19.9	120-300
AM1[b]	0.473	0.567	+15.6	+15.35	120-300
MM3[b]	0.035	0.082	+7.7	+11.5	1-5

[a] X-ray coordinates optimised with B3LYP/6-31G(d).

[b] X-ray coordinates optimised with PM3, AM1 and MM3 respectively. Cartesian coordinates of each optimised complex are reported on attached CD.

[c] Energies relative to the DFT binding energy calculated as -53 kcal mol^{-1} for both complexes **91** and **92**. Approximate binding energy: $BE = E_{complex} - (E_{host} + E_{guest})$.

[d] CPU time on the same computer (1.5 GHz PC).

The MM3 results compared favourably with a high level DFT calculation and found to be excellent regarding RMS overlay (0.04-0.08Å) and reasonable with respect to binding energy (+8 to +12 kcal mol^{-1}). The approximate DFT calculated binding energy of both complexes **91** and **92** was approximately -53 kcal mol^{-1}. The semi-empirical results were less accurate both in terms of geometry and energy (see Table 3). Note that the MM3 conformational search procedure described above (also see Appendix 2) produces a complex of lower energy

compared to the MM3 optimised crystal structure. This was expected since strong packing forces exist in crystals, which could enforce a conformation of higher energy.

APPLYING THE MM3 COMPUTATIONAL MODEL ON EXPERIMENTAL NMR TITRATION RESULTS

The experimental work on pyridine-derived macrocycles was done by Bradshaw *et al.* [14,20] Unfortunately these experimental results reported kinetic data, which should not automatically match the thermodynamic data calculated using the MM3 model. Comparing the approximate binding energies of these complexes (NMR) with those complexes used for other experimental results should, however, shed some light on the magnitude of the different host-guest interactions. The authors[14,20] reported the Gibbs energy of activation $(\Delta\Delta G_c)^{\ddagger}$ measured by NMR as a function of temperature. Optically pure host was mixed with either (*R*)- or (*S*)-guest, and the proton NMR spectrum taken at low temperature after complex formation had occurred. The temperature of the probe was increased and the kinetics of the decomplexation followed, which allowed them to calculate the Gibbs energy of activation.

Macrocycles **93-97** were chosen since they exhibit a wide range of kinetic enantioselectivities. Starting geometries of the hosts and complexes were obtained as described above (also see Appendix 2) with (*R*) and (*S*) forms of [α-(1-naphthyl)ethyl ammonium] ion (**98**) as guest.

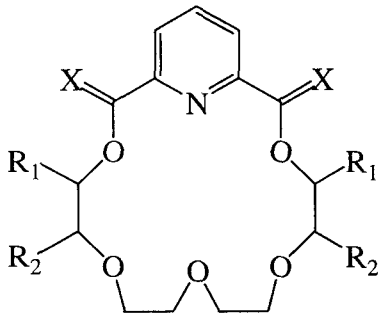

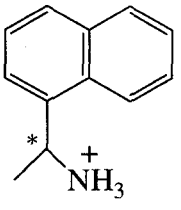

(*S,S*)-**93**: X=O; R_1=2H; R_2=phenyl
(*S,S*)-**94**: X=O; R_1=phenyl; R_2=2H
(*R,R*)-**95**: X=2H; R_1=phenyl; R_2=2H
(*S,S*)-**96**: X=O; R_1=t-butyl; R_2=2H
(*S,S*)-**97**: X=2H; R_1=t-butyl; R_2=2H

(*R*)/(*S*)- **98**

Figure 6: Structures of hosts **93-97** and guest **98** used in NMR techniques to determine the extent of enantioselectivity

The approximate binding energies of the complexes were calculated using the MM3 model described above (also see Appendix 2) and is reported in Table 4.

Table 4: Approximate binding energies calculated with MM3 for different host-guest complexes and reported $\Delta\Delta G^{\ddagger}$ values obtained via NMR techniques.

Host-guest complex[a]	BE[b]/ kcal.mol^{-1}	Calculated thermodynamic preference[c]/ kcal.mol^{-1}	Reported $\Delta\Delta G^{\ddagger}$ value/ kcal.mol^{-1}
(*S,S*)-**93** and (*S*)-**98**	-36.38	2.65	
(*S,S*)-**93** and (*R*)-**98**	-33.73		0.1[d]
(*S,S*)-**94** and (*S*)-**98**	-36.10	0.1	
(*S,S*)-**94** and (*R*)-**98**	-36.01		1.3[e]
(*R,R*)-**95** and (*S*)-**98**	-41.00		
(*R,R*)-**95** and (*R*)-**98**	-42.67	1.67	2.8[e]
(*S,S*)-**96** and (*S*)-**98**	-39.65	0.46	
(*S,S*)-**96** and (*R*)-**98**	-39.19		1.8[e]
(*S,S*)-**97** and (*S*)-**98**	-34.43	2.28	
(*S,S*)-**97** and (*R*)-**98**	-32.15		2.5[e]

[a] Cartesian coordinates of each calculated complex available on CD attached.

[b] See equation 1: Approximate BE = $E_{complex} - (E_{host} + E_{Guest})$.

[c] Relative energy of the complex with (*R*)-guest vs complex with (*S*)-guest.

[d] Experimental data.[14]

[e] Experimental data.[20]

As expected from the results presented in Table 4, the calculated MM3 thermodynamic preferences do not coincide with the most of the experimental kinetic preferences $(\Delta\Delta G_c)^{\ddagger}$ of the host-guest systems. It is interesting to note that the calculated thermodynamic enantioselectivity of host **95** displayed towards guest **98** was the only thermodynamic result that agrees with the experimental kinetic enantioselectivity. The authors[20] mentioned that the kinetic result obtained for host **95** was a surprise since it was the first time that a (*R,R*)-host had formed a kinetically more stable complex with guest (*R*)-**98** of the same configuration.

The calculated thermodynamic data in Table 4 suggests that hosts **93** and **97** should demonstrate the highest enantioselectivity for host **98**, of opposite chirality, under thermodynamically controlled conditions. Note that setting up a competing NMR experiment to show which enantiomer of guest **98** would preferentially form a host-guest complex with **95** or **97** is in principle possible since it is expected that a thermodynamically more stable complex would induce as larger shift for certain protons on the macrocycle.

APPLYING THE MM3 COMPUTATIONAL MODEL ON EXPERIMENTAL FLUORESCENCE RESULTS

Recent complexation studies[16] reported fluorescence as a tool to determine the enantiomeric recognition properties of chiral macrocycles. The (*S,S*)-form of macrocycles **99** and **100** were shown to bind preferentially to (*R*)- and (*S*)-alanine methyl ester hydrochloride (**101**), respectively. A literature survey reveals that a non-aromatic guest such as **101** was rarely reported in enantiomeric recognition studies.

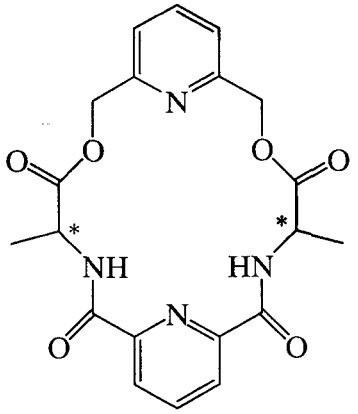

(*S,S*)-**99**

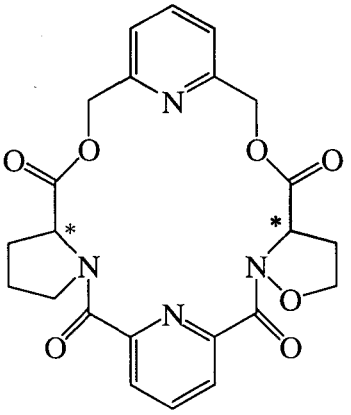

(*S,S*)-**100**

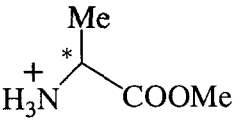

(*R*)/(*S*)-**101**

Figure 7: Structures of host systems **99** and **100** and guest **101** used in fluorescence experiments to determine enantioselectivities

The approximate binding energy of the complexes was calculated as before and the results are presented in Table 5.

Table 5: MM3 calculated binding energies for the different complexes and Δλ (nm) values obtained via experimental fluorescence experiments.

Complex[a]	BE[b]/ kcal.mol^{-1}	Calculated enantiomeric preference[c]/ kcal.mol^{-1}	Observed[d] Δλ (nm)
(*S,S*)-**99** and (*R*)-**101**	-22.46	0.28	8
(*S,S*)-**99** and (*S*)-**101**	-22.18		
(*S,S*)-**100** and (*R*)-**101**	-29.45		
(*S,S*)-**100** and (*S*)-**101**	-30.77	1.32	50

a Cartesian coordinates of each calculated complex available on CD attached.

b See equation 1: Binding Energy = $E_{complex} - (E_{host} + E_{Guest})$

c Relative energy of complex with (*R*)-guest vs complex with (*S*)-guest.

d Relative shift in fluorescence emission spectra.[12]

The results in Table 5 indicate that the MM3 model correctly predicts the enantiomeric preference for non-aromatic guests. The ratio of the magnitude of the experimental enantiomeric preference between hosts (*S,S*)-**99** and (*S,S*)-**100** was approximately ~1:6 (8:50) while the calculated ratio was ~1:5 (0.28:1.32) which was essentially of the same order.
The calculated thermodynamic preference exhibited by (*S,S*)-**100** for (*R*)-**101** was lower (~1.3 kcal mol^{-1}) than those found for the NMR model systems, i.e. that of (*R,R*)-**93** for (*R*)-**98** (~2.7 kcal mol^{-1}) reported in Table 4. The calculated binding energies were higher (-22 to -30 kcal mol^{-1}) than for the NMR model systems, which were between -32 to -41 kcal mol^{-1}.
These results suggest that the hosts systems used for NMR studies (**93** and **97**) exhibit better chiral preference as well as stronger binding energies than systems (*S,S*)-**99** and (*S,S*)-**100**.

APPLYING THE MM3 COMPUTATIONAL MODEL ON EXPERIMENTAL TRANSPORT RESULTS

Two 1,1'-bi-2-naphtol crown ethers (**51** and **75**)[17,21] a cage annulated naphtol crown (**57**)[17] and a new class of cage annulated macrocycles (**78** and **79**) recently reported[19] were chosen since experimental U-tube transport results are available for each system (see Figure 8).
Although it was known[19] that hosts **76** and **77** display no transport ability, it was decided to include these compounds in this study since **76** showed[14] promising enantioselectivity using the same NMR techniques discussed above. Furthermore, host **76** served as a model compound for the new class of cage annulated macrocycles (**78** and **79**).[19] Comparison of this class of hosts (**76** and **77**) with the hosts traditionally used for transport studies might shed additional light on the nature of the different host-guest interactions.

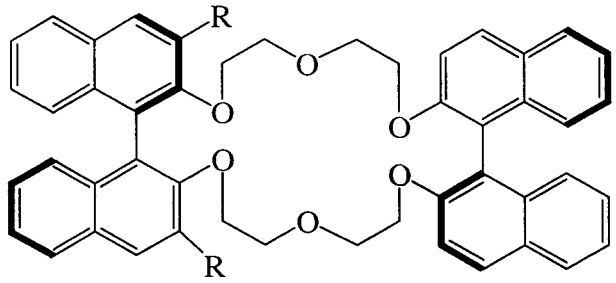

(*R*,*R*)-**51**: R = CH_3
(*R*,*R*)-**75**: R = CH_2Cl

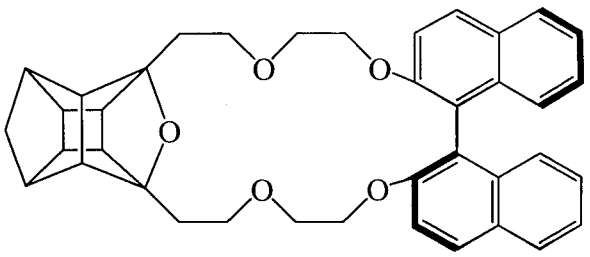

(*R*)-**57**

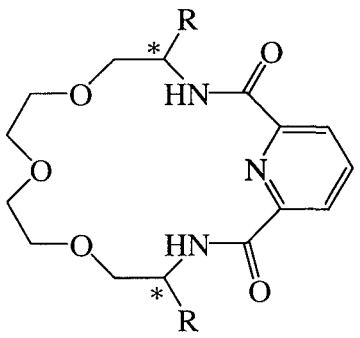

(*S*,*S*)-**76**: R=Ph
(*S*,*S*)-**77**: R=$CH(CH_3)_2$

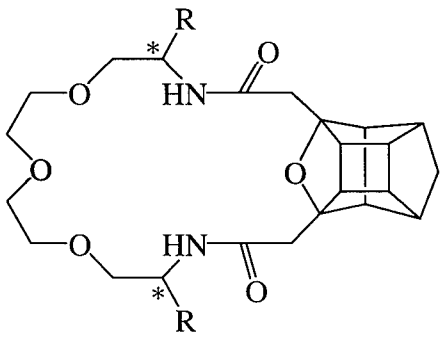

(*S*,*S*)-**78**: R=Ph
(*S*,*S*)-**79**: R=$CH(CH_3)_2$

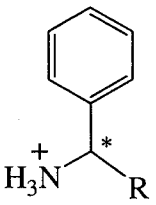

(*R*)/(*S*)-**89**: R=CH_3
(*R*)/(*S*)-**90**: R=COOMe

Figure 8: Structures of host systems and guests used in U-tube transport experiments

Starting geometries of the hosts and complexes were obtained with guests phenylglycine methylester (**90**) and α-methylbenzylamine (**89**) and the approximate binding energies calculated as described above. The results are presented in Table 6.

Host molecules containing the PCU cage present two potential complexation "faces" to an approaching guest molecule.[17] The guest can pursue either a "topside" approach i.e., along a trajectory proximal to the methylene carbon of the cage moiety, or a "bottomside" approach in which the approaching guest follows a trajectory that lies distal to the methylene carbon atom in this moiety (see Figure 9).[17] In order to determine the calculated enantioselectivity of the cage annulated hosts (**57**, **78** and **79**) the thermodynamic stability of both the "topside" and "bottomside" complexes should be determined.

"topside" approach

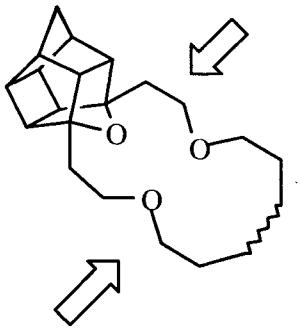

"bottomside" approach

Figure 9: Designation of orientation in PCU crown ethers

Table 6: MM3 calculated binding energies for the different complexes and reported enantiomeric preferences obtained with U-tube transport experiments.

Complex	BE[a]/ kcal.mol^{-1}	Calculated[b] enantiomeric preference/ kcal.mol^{-1}	*ee*	Rate of transport/ %mass.h^{-1}
(*R*,*R*)-**51** and (*S*)-**90**	-38.53			
(*R*,*R*)-**51** and (*R*)-**90**	-39.63	1.1	78%[c]	0.63[c]
(*R*,*R*)-**75** and (S)-**90**	-35.93			
(*R*,*R*)-**75** and (*R*)-**90**	-37.33	1.4	82%[c]	0.67[c]
(*R*)-**57** and (*S*)-**90**	-41.68			
(*R*)-**57** and (*R*)-**90**	-41.79	0.11	15%[d]	3.0[d]
(*R*)-**57** and (*S*)-**89**	-42.20	0.19	79%[d]	2.5[d]
(*R*)-**57** and (*R*)-**89**	-42.01			
(*S*,*S*)-**76** and (*S*)-**90**	-29.22		[e]	
(*S*,*S*)-**76** and (*R*)-**90**	-31.18	1.96	[e]	[e]
(*S*,*S*)-**77** and (*S*)-**90**	-31.38		[e]	[e]
(*S*,*S*)-**77** and (*R*)-**90**	-32.82	1.44	[e]	[e]
(*S*,*S*)-**78** and (*S*)-**90**	-49.08			
(*S*,*S*)-**78** and (*R*)-**90**	-49.21	0.13	29%[f]	1.3[f]
(*S*,*S*)-**79** and (*S*)-**90**	-44.03			
(*S*,*S*)-**79** and (*R*)-**90**	-44.75	0.72	68%[f]	0.72[f]

[a] See equation 1: Binding Energy = $E_{complex} - (E_{host} + E_{guest})$

[b] Relative energy (*R*)-complex vs (*S*)-complex .

[c] Experimental Data[17].

[d] Experimental Data[18].

[e] Experimental transport results not available.[19]

[f] Note that a different counter ion was used to slow the rate of transport down.[19]

These results indicate that the MM3 computational model was able to correctly predict the enantiomeric preference of chiral hosts towards chiral ammonium guests. In general higher calculated binding energies results in higher rates of transport. The computational model suggests that if the results by Cram *et al*[17] are taken as a benchmark (calculated enantiomeric preference of 1.4 kcal mol^{-1} results in a 80% experimental *ee*), then a system with a calculated chiral preference higher than 1.4 kcal mol^{-1} should exhibit exceptional chiral separation using W-tube experiments.

Macrocycle **76** indeed showed promising enantioselectivity (~2.0 kcal mol^{-1}) according to the computational model, which was better than those calculated for the cage annulated macrocycles **78** and **79** (0.1 and 0.7 kcal mol^{-1} respectively). Macrocycle **76** was the equivalent of a 18-crown-6 while macrocycles **78** and **79** are equivalent to a 20-crown-6. The calculated enantioselectivity was lower [~2.0 kcal mol^{-1} for host (*S,S*)-**76** with (*R*)-**89**] than the best host used for the NMR studies [~2.7 kcal mol^{-1} for host (*S,S*)-**93** with guest (*R*)-**89**] and higher than the systems used for fluorescence studies [~1.3 kcal mol^{-1} for host (*S,S*)-**100** with (*S*)-**101**].

Using the benchmark by Cram *et al*[17] (calculated enantiomeric preference of 1.4 kcal mol^{-1} results in a 80% experimental *ee*), then host **57** with guest **89** should theoretically exhibit an experimental preference of about 11% *ee* and not 79% as reported.[18] It should be noted that subsequent studies[19] indicated that the guest **89** was unsuitable for transport experiments, which should clarify the discrepancy between the calculated and the experimentally observed data.

CONCLUSION

MM3 is a crude but acceptable computational tool to calculate host-guest interactions between chiral macrocycles and chiral ammonium ions. The model closely reproduced a high level DFT result with a RMS overlay of between 0.04 – 0.08Å with respect to the DFT optimised structure and an approximate binding energy of between +8 to +12 kcal mol^{-1} higher than the DFT calculated binding energy which was better than semi-empirical methods (PM3 and AM1). The model correctly determined the thermodynamic/enantiomeric preferences of chiral hosts towards chiral hosts. The calculated relative binding energies also coincide with the magnitude of the experimentally observed chiral preference. The MM3 model calculates crude relative binding energies, which correspond in most cases to a reasonable extent with the magnitude of the reported experimental chiral preferences. The model has promising potential to assist researchers in the field with the rational design of better chiral host-guest systems. Since no other reports on a computational approach of this kind have appeared to date, it is difficult to assess its validity fully at this stage. The ultimate test of this computational model would be to design a theoretical chiral host-guest system that

would be better than Cram's binaphthyl host (calculated enantioselectivity > 1.4 kcal mol^{-1}). The theoretical host should then be synthesised and tested using a U-tube and/or W-tube transport experiment.

Supporting information

Cartesian coordinates of all calculated low energy complexes reported are available on attached CD as supplementary material.

REFERENCES

1. Zhang, X.X.; Bradshaw, J.S.; Izatt, R.M. *Chem.Rev.* **1997**, *97*, 3313.
2. (a) Stoddart, J.F. *Chem. Soc. Rev.* **1979**, *8*, 85. (b) Izatt, R.M.; Zhu, C.Y.; Huszthy, P.; Bradshaw, J.S. in *Crown Compounds: Towards Future Applications*, Cooper S.R., Ed., VCH Publishers: New York, **1992**, chapter 12. (c) Kaneda, T. in *Crown ethers and Analogous Compounds,* Hiraoka M., Ed., Elsevier: Amsterdam, **1992**, chapter 6. (d) Still, W.C. *Acc. Chem. Res.* **1996**, *29*, 155. (e) Webb, T.H.; Wilcox, C.S. *Chem. Soc. Rev.* **1993**, *22*, 383. (f) Yokota, K.; Haba, O.; Satoh, T. *Macromol. Chem. Phys.* **1995**, *196*, 2383. (g) Naemura, K.; Tobe, Y.; Kaneda, T. *Coord. Chem. Rev.* **1996**, *148*, 199.
3. Hay, B.P.; Yang, L.; Allinger, N.L.; Lii, J.H. *J.Mol.Struct. (THEOCHEM)* **1998** *428*, 203.
4. Hay, B.P.; Rustad, J.R.; Hostetler, C.J. *J.Am.Chem.Soc.* **1993**, *115*, 11158.
5. Prof. Allinger kindly performed the MM3 calculations required for the validation of the MM3 model. Thereafter a copy of Alchemy was purchased and used for the remainder of the project.
6. Davidson, R.B.; Bradshaw, J.S.; Jones, B.A.; Dalley, N.K.; Christensen, J.J.; Izatt. R.M. *J.Org.Chem.*, **1994**, *49*, 353.
7. (a) Allinger, N. L.; Yuh, Y. H. and Lii, J. H. *J. Amer. Chem. Soc.* **1989**, *111*, 8551 (b) Lii, J. H. and Allinger, N. L. *J. Amer. Chem. Soc.*, **1989**, *111*, 8566. (c) Lii, J. H. and Allinger, N. L. *J. Amer. Chem. Soc.*, **1989**, *111*, 8576.
8. Alchemy is a registered product of Tripos, Inc., Louis, MO, USA.
9. Gaussian 98, Revision A.9, Frisch M. J.; Trucks G. W.; Schlegel H. B.; Scuseria G. E.; Robb M. A.; Cheeseman J. R.; Zakrzewski V. G.; Montgomery Jr. J. A.; Stratmann R. E.; Burant J. C., Dapprich S.; Millam J. M.; Daniels A. D.; Kudin K. N., Strain M. C.; Farkas O.; Tomasi J.; Barone V.; Cossi M.; Cammi R.; Mennucci B.; Pomelli C.; Adamo C.; Clifford S.; Ochterski J.; Petersson G. A.; Ayala P.Y.; Cui Q.; Morokuma K.; Malick D.K.; Rabuck A. D.; Raghavachari K.; Foresman J. B.; Cioslowski J.; Ortiz J. V.; Baboul A. G.; Stefanov B. B.; Liu G.; Liashenko A.; Piskorz P.; Komaromi I.;Gomperts R.; Martin R. L.; Fox D. J.; Keith T.; Al-Laham M. A.; Peng C. Y.; Nanayakkara A.; Challacombe M.; Gill P.M.W.; Johnson B.; Chen W.; Wong M.W.; Andres J.L.; Gonzalez C.; Head-Gordon M.; Replogle E.S.; and Pople J.A.; Gaussian, Inc., Pittsburgh PA, **1998.**
10. Becke, A. D. *J. Chem. Phys.* **1993**, *98*, 5648.
11. Lee, C.; Yang, W.; Parr, R. G. *Phys. Rev.*, **1988**, *B37*, 785.
12. Mielich, B.; Savin. A.; Stoll, H.; Peus, H. *Chem. Phys. Lett.*, **1989**, *157*, 200.

13. Marchand, A. P.; Hazlewood, A.; Huang, Z.; Vadlakonda, S. K.; Rocha, J.-D. R.; Power, T. D.; Mlinaric-Majerski, K.; Klaic, L.; Kragol, G. and Bryan, J. C., *Struct. Chem.* **2003**, *14*, 279-288.

14. Huszthy, P.; Oue, M.; Bradshaw, J.S.; Zhu, C.Y.; Wang, T.; Dalley, N.K.; Curtis, J.C.; Izatt, R.M. *J. Org. Chem.* **1992**, 57, 5383.

15. Reinhoudt, D.N.; de Jong, F. in *Progress in Macrocyclic Chemistry*, Izatt R.M. and Christensen J.J. Eds, Wiley, Vol. 1, New York, N.Y., **1979**, pp157-217.

16. Zhao, H.; Hua, W. *J. Org. Chem.* **2000**, *65*, 2933.

17. Sogah, G.D.Y.; Cram, D.J. *J. Am. Chem. Soc.* **1979**, *101*, 3035.

18. Marchand, A.P.; Chong, H.S.; Ganguly, B., *Tetrahedron Asymmetry* **1999**, *10*, 4965.

19. Govender, T.; Hariprakasha, H.; Kruger H.G.; Marchand, A.P. *Tetrahedron Asym.* **2003**, *14(11)*, 1553.

20. Huszthy, P.; Bradshaw, J.S.; Zhu, Y.Z. and Izatt, R.M., J. Org. Chem,., **1991**, *56*, 3330.

21. Kyba, E.P.; Koga, K.; Sousa, L.R.; Siegel, M.G.; Cram, D.J. *J. Am. Chem. Soc.* **1973**, *95*, 2692.

CHAPTER 4

SYNTHESIS OF NOVEL CHIRAL CAGE ANNULATED CROWN ETHERS AND LIGANDS

SYNTHESIS OF CHIRAL CROWN ETHERS

As mentioned in Chapter 1, one of the most recent techniques of asymmetric synthesis is the use of chiral crown compounds in phase transfer catalysis.[1,2] The aim of this project was to synthesise crown ethers that complex sodium and potassium bases, and to test their ability towards asymmetric synthesis involving reactions catalysed by these systems. Since the cavity of the macrocyclic polyether depends on the size of the ionic radius of the cation,[3] it is imperative to design a host for that specific ion. Crown ether **102**, was shown to complex sodium and potassium picrate, with no preference, in extraction studies.[4] This is one of the reasons for the design of crown ethers **103** and **104**, and the other reason is due to the higher yields of product obtained by use of the gauche effect discussed below.

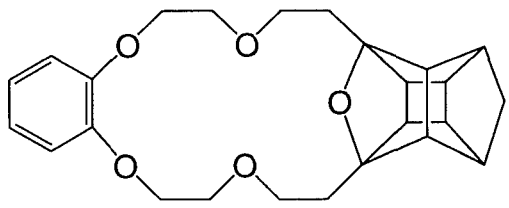

102

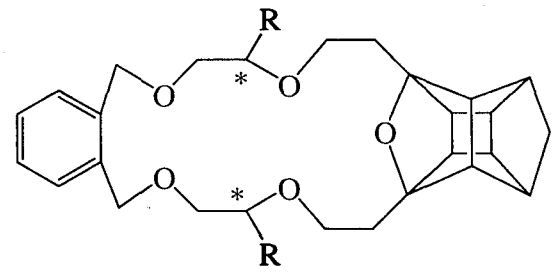

103: R = C_6H_5
104: R = CH_3

It is well documented that the C-C bond in $-OCH_2CH_2O-$ units prefer to adopt the *gauche* conformation.[5] *Gauche* conformations about the C-C bonds with *anti* preferences for the C-O bonds normally leads to crown ethers with higher association constants for the desired metal.[6] Crown ethers **103** and **104** have two additional carbons and this is designed to make the cavity of the host more accessible.

A discussed in Chapter 2, the design of cage macrocycles with the chiral substituents closer to the cage is essential to induce chirality on the otherwise symmetric cage.

The Williamson ether synthesis is the general method to prepare macrocyclic polyethers. It involves the displacement of halide ions from a dihaloalkane by a dianion derived from a diol. The synthesis of **101** (Scheme 18) utilised a slight modification in that the leaving group is a *p*-toluenesulphonyl salt rather than a halide salt.[4]

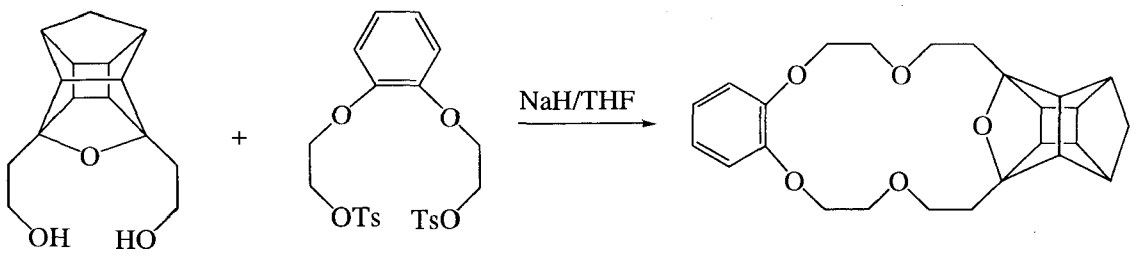

73 105 102

Scheme 18: Synthetic route employed by Marchand[4] to synthesise non chiral crown **102**

A similar synthetic pathway was attempted for **103** and **104** as described below.

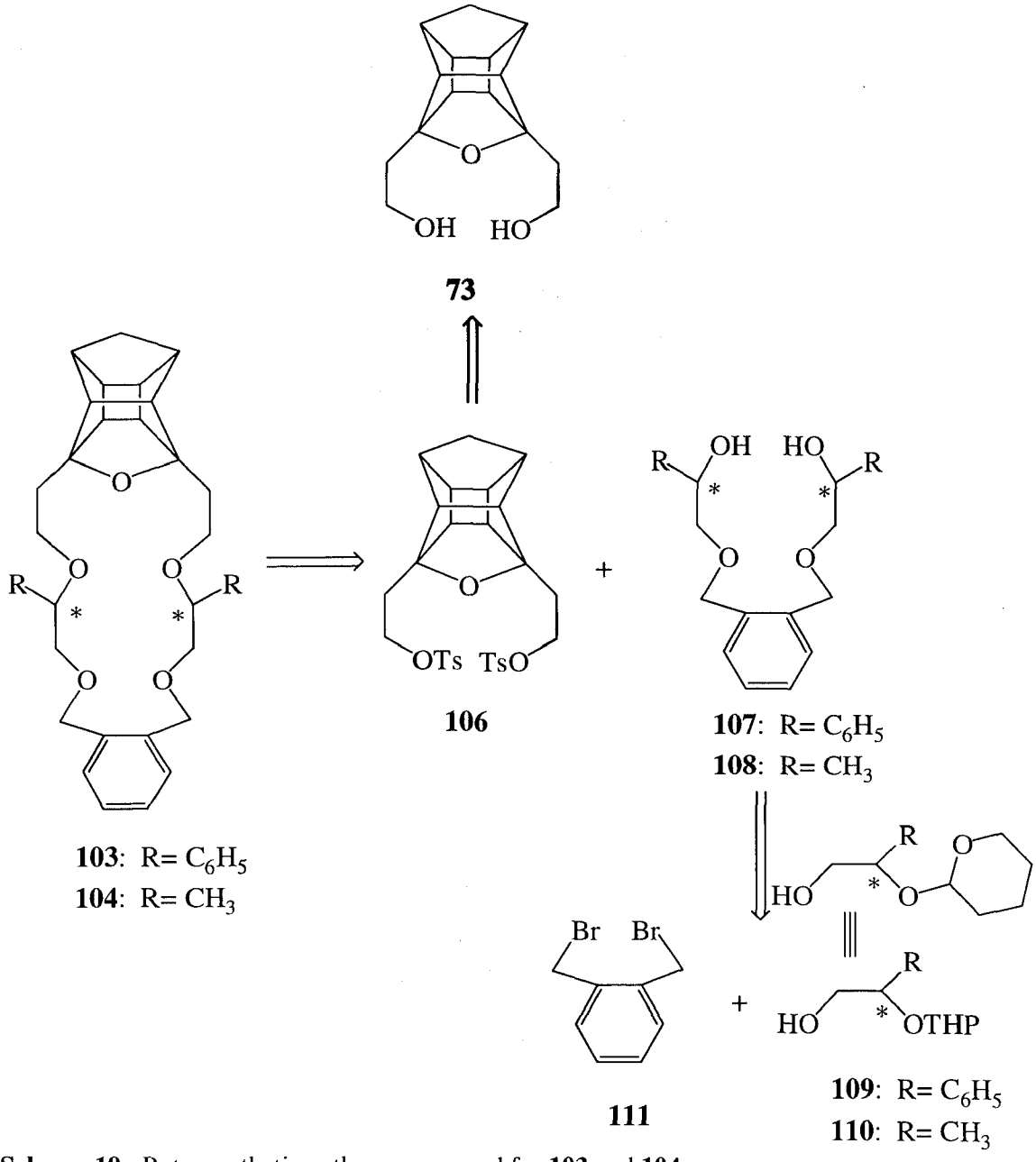

Scheme 19: Retrosynthetic pathway proposed for **103** and **104**

Synthesis of PCU diene **81** was described in chapter 2. Ozonolysis of **81** followed by a reductive workup using $NaBH_4$ afforded the 3,5-(2',2"-bis(hydroxyethyl))-4-oxahexacyclo[5.4.1.$0^{2,6}$.$0^{3,10}$.$0^{5,9}$.$0^{8,11}$]dodecane (**73**, PCU diol, 90%). **73** had been characterised by Marchand *et al.* but synthesised via a different method.[7] The diol (**73**) was treated with *p*-toluenesulphonyl chloride and solid potassium hydroxide in tetrahydrofuran to yield the PCU-ditosylate (**106**,[8] 62%).

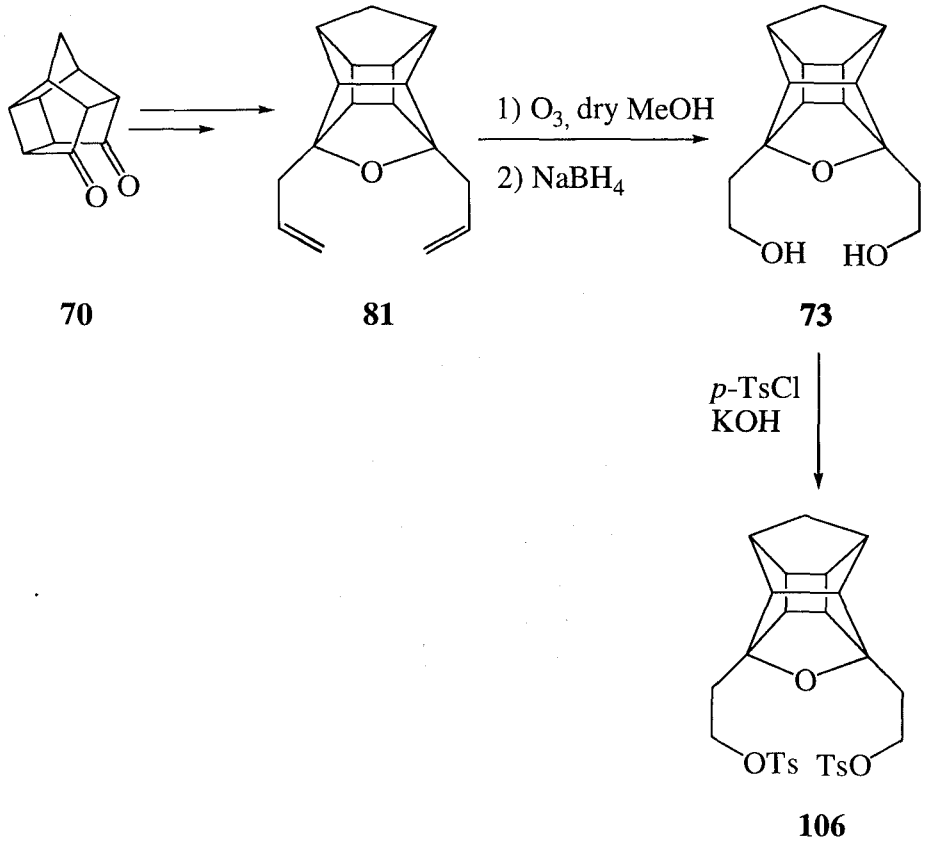

70 **81** **73** **106**

Scheme 20: Synthesis of PCU ditosylate **106**

In the synthesis of macrocycle **103**, (*S*)-(+)-mandelic acid (**112**) was used as the chiral starting material.

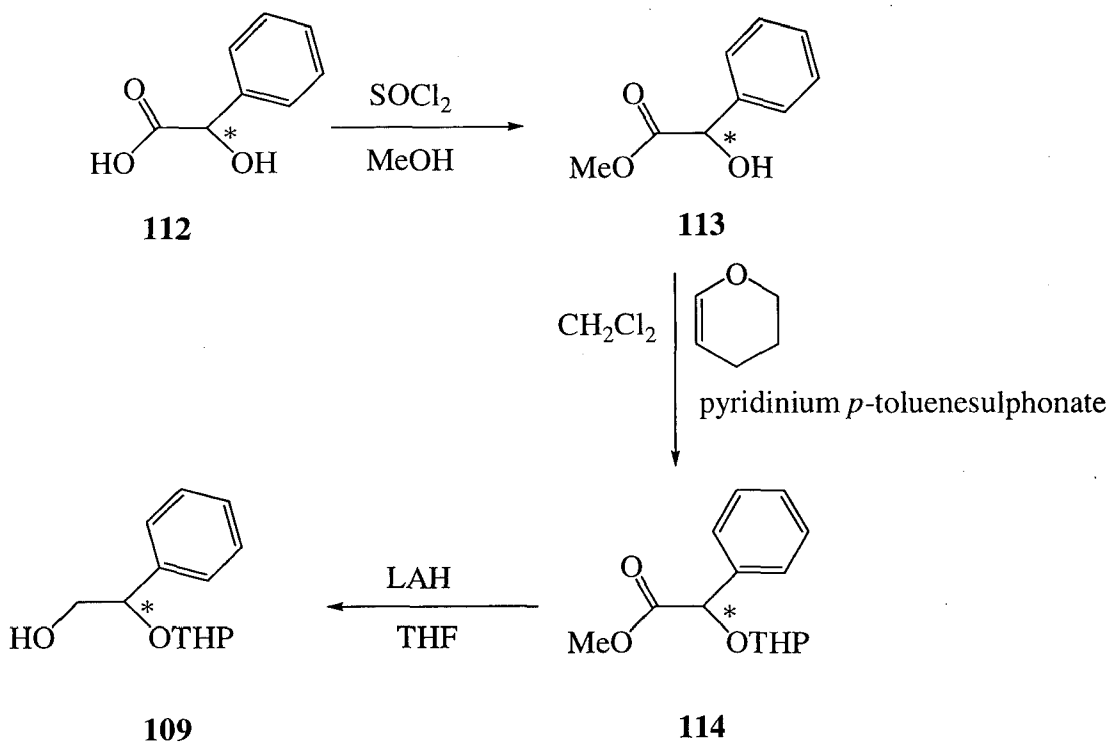

112 **113** **114** **109**

Scheme 21: Synthesis of (S)-(+)-2-phenyl-2(tetrahydropyranyloxy)ethanol (**109**)

Mandelic acid (**112**) was reacted with thionyl chloride in methanol to yield the (S)-(+)-methyl mandelate (**113**).[9] The alcohol group on **113** was protected by reacting it with 3,4-dihydro-2H-pyran (DHP) in the presence of a catalyst (pyridinium *p*-toluenesulphonate) in dichloromethane.[9] This reaction involves a Markovnikov addition of an alcohol across a double bond to yield the (S)-(+)-methyl-2-phenyl-2-(tetrahydopyranyloxy)acetate (**114**) which was subsequently reduced via lithium aluminium hydride to yield (S)-(+)-2-phenyl-2-(tetrahydropyranyloxy)ethanol (**109**).[9]

For the synthesis of macrocycle **104** the starting material, (S)-ethyl lactate (**115**) was purchased as the ester. Beyond this difference the reactions carried out are exactly as described above to yield the (S)-2-methyl-2-(tetrahydropyranyloxy)ethanol[10] (**110**).

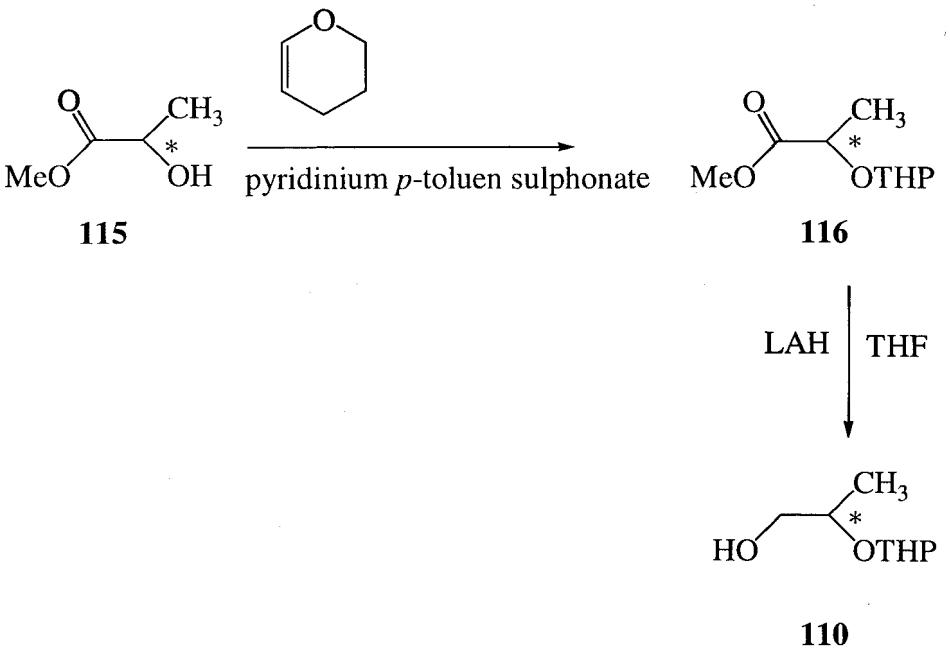

115 **116** **110**

Scheme 22: Synthesis of (S)-2-methyl-2-(tetrahydropyranyloxy) ethanol (**110**)

The protected alcohols **109** and **110** were reacted with α,α-dibromo-*o*-xylene (**111**) in the presence of sodium hydride in THF and the THP protecting groups were removed via acid hydrolysis to give the resulting chiral diols **107** and **108**, respectively. These diols were subsequently reacted with the 'cage ditosyl' **106** in the presence of sodium hydride. Workup and isolation of the products revealed the presence of mostly starting materials and some elimination product **117**.

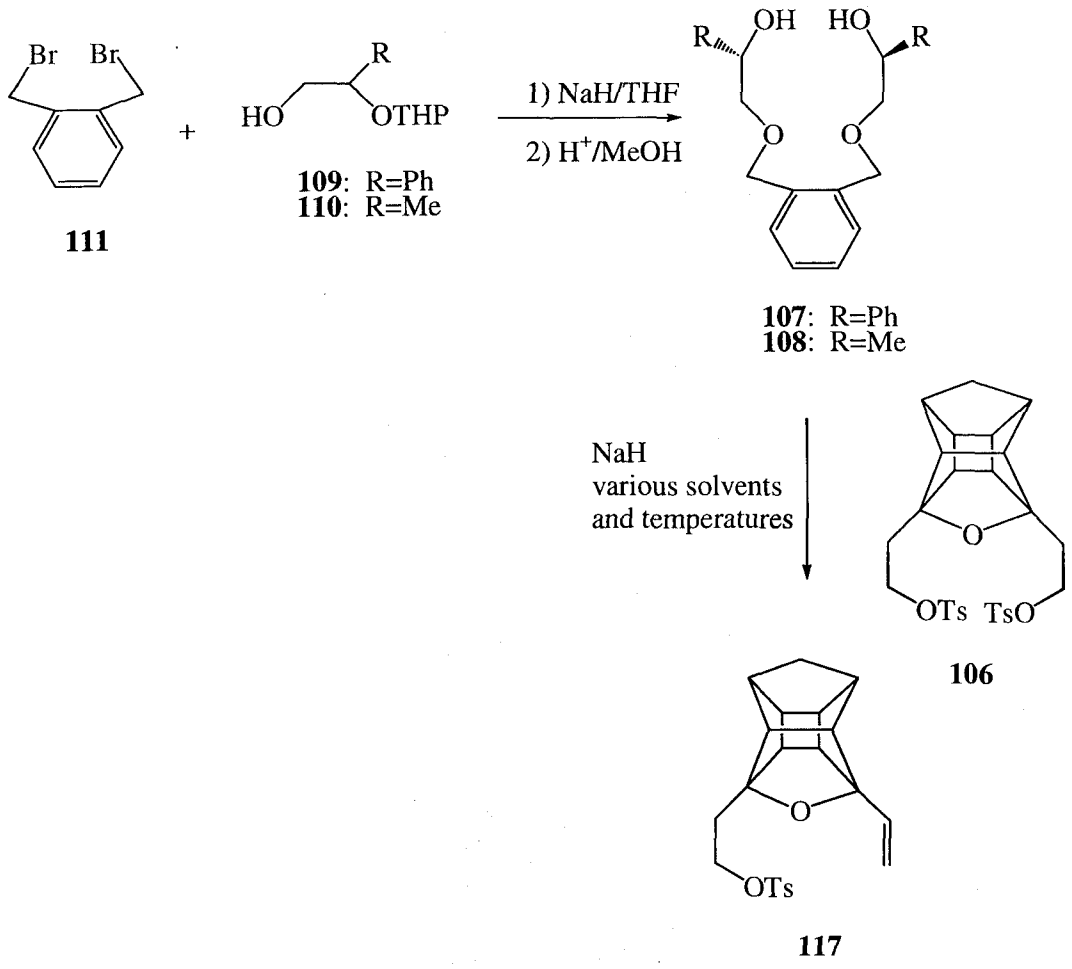

Scheme 23: Attempted synthesis of macrocycles **103** and **104**

In light of the above results, it was decided to synthesise chiral cage annulated crown ethers **118** and **119** (Scheme 24). These crown ethers are slightly different from **103** and **104** in that the chiral centres are now one carbon further away from the PCU unit. This might help the substitution reaction by decreasing the steric bulk at the reactive carbons. This new design would also help in increasing the yield on the cyclisation step. When using the high dilution technique to increase yield in cyclisation, it is important that the bonds form quickly and alkyl-benzyl ether synthesis is a faster reaction than alkyl-alkyl ether synthesis.

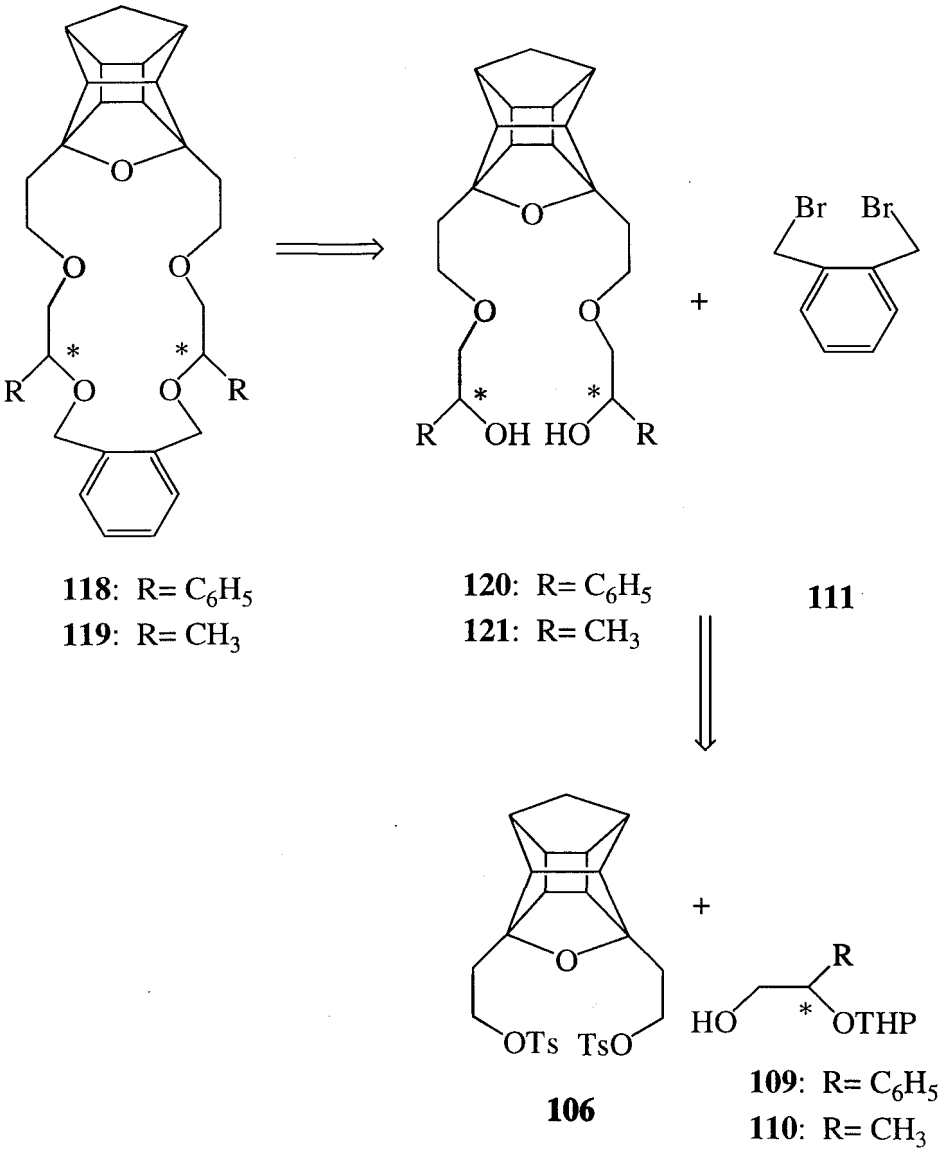

Scheme 24: Retrosynthetic pathway proposed for chiral crown ethers **118** and **119**

The protected alcohols **109** and **110** were reacted with the 'cage ditosyl' **106** in the presence of sodium hydride in the hope of synthesising chiral diols **120** and **121**, respectively (Scheme 25). However on analysis of the isolated product, it was found that the 'cage ditosyl' was undergoing an elimination reaction to form compound **117**. This reaction was carried out at ambient temperature and under reflux conditions. In both instances the result was the same except that at lower temperatures, the elimination reaction was slower.

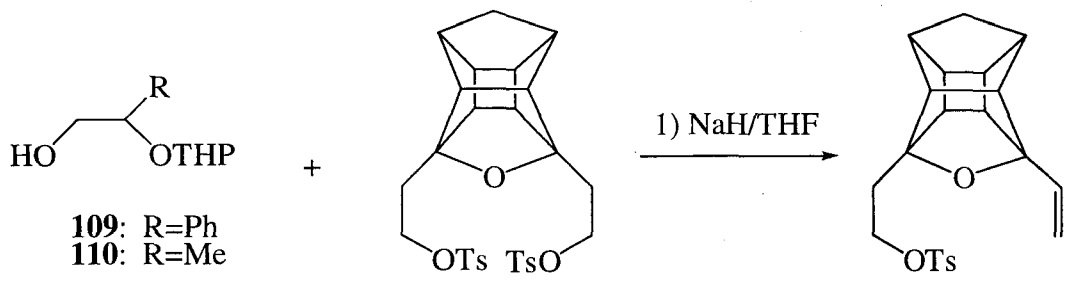

109: R=Ph
110: R=Me

106 **117**

Scheme 25: Attempted synthesis of ligands **120** and **121**

At this stage it was decided to use the PCU as the source of the nucleophile for the substitution reaction. The two alcohol products **109** and **110** were reacted with *p*-toluenesulphonyl chloride and triethylamine in dichloromethane (Scheme 26) to form **120** and **121** respectively.

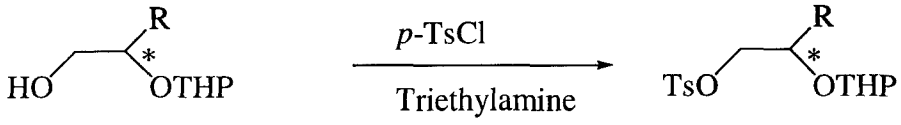

109: R=C_6H_5
110: R=CH_3

122: R=C_6H_5
123: R=CH_3

Scheme 26: Tosylation of (*S*)-(+)-2-phenyl-2-(tetrahydropyranyloxy)ethanol (**109**) and (*S*)-2-methyl-2-(tetrahydropyranyloxy)ethanol (**110**)

The resultant tosylated products **122** and **123** were reacted with the cage diol **73** in the presence of sodium hydride. On thin layer chromatography (TLC) analysis of the reaction mixture, the presence of only the two starting materials was evident. The reaction was monitored for several days while under reflux and even though TLC showed no sign of products, the reaction was worked up. On isolation and analysis it was found that no reaction had occurred between the cage diol **73** and the tosylated reactants **122** and **123**.

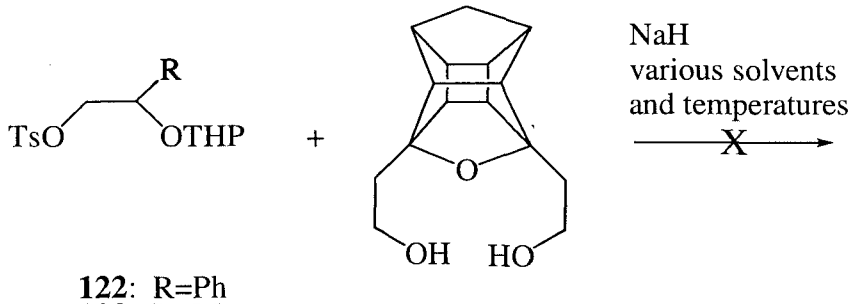

122: R=Ph
123: R=Me

73

Scheme 27: Attempted synthesis of ligands **120** and **121**

From the above results, it was clear that the undesired elimination reaction dominated the desired substitution reaction when the leaving group was on the PCU moiety. Even at ambient temperature **117** was the only product formed. In order to suppress the elimination reaction, it is necessary to either use lower temperatures or a weaker base. Since a change in temperature did not affect the outcome of the reaction, the only alternative would be the use of a milder base.

SYNTHESIS OF CHIRAL AMINO ALCOHOLS

As the strategies above proved to be unsuccessful, a different strategy was investigated. Marchand *et al.* reported[11] the synthesis of azacrown compounds starting from the PCU ditosylate (**106**) and a mild base (potassium carbonate). Two equivalents of a secondary amine were added to both arms of **106** (Scheme 28).

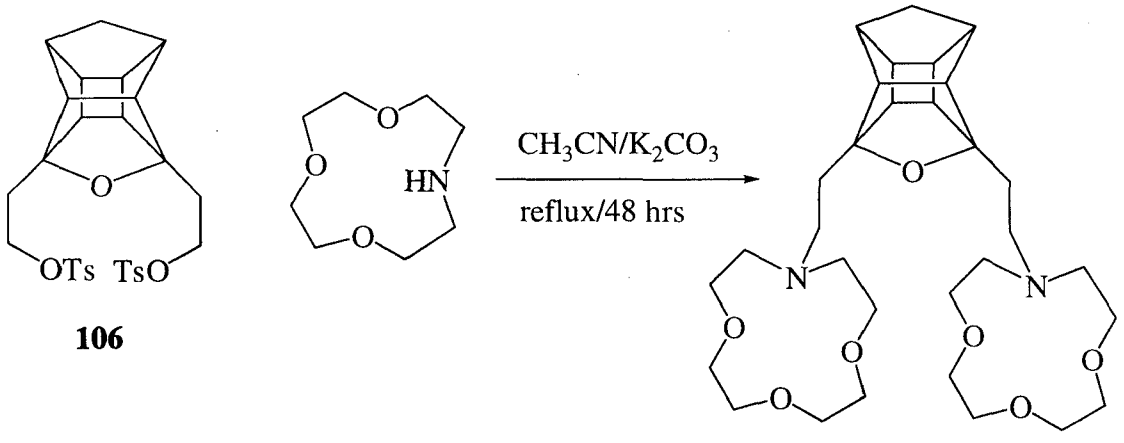

106

Scheme 28: Synthesis of PCU annulated azacrown ethers

With this in mind, a synthetic route towards chiral cage annulated macrocycles of type **124** was designed. Hosts with nitrogen donor atoms were not part of the original design since the use of chiral diazacrown ethers as catalysts in asymmetric synthesis has not been reported although the use of monoazacrown ethers has been reported for this purpose.[1] An interesting aspect of this design is that chiral amino alcohols of the type **125** could also be used in asymmetric catalysis. The rest of chapter 4 will focus on the synthesis and use of these amino alcohols and the synthesis and use of its macrocyclic analogues will be presented in chapter 5.

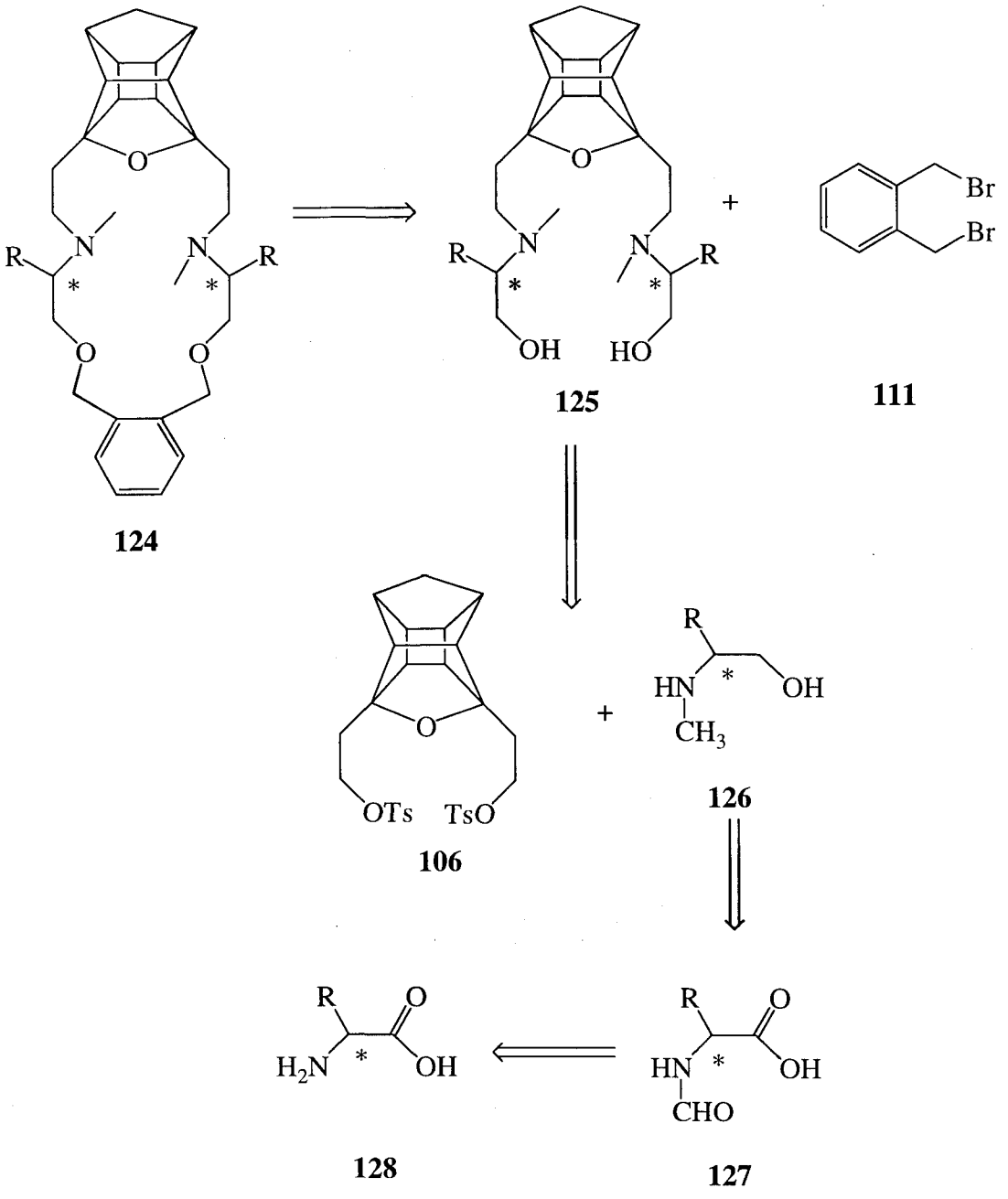

Scheme 29: Retrosynthetic route towards novel chiral PCU annulated diazacrown ethers

One of the fundamental tools employed in the synthesis of chiral organic compounds are chiral metal complexes.[12] Important organic reactions include carbon-carbon bond formation, oxidation, reduction and functional group transformation. One of the most common reactions for carbon-carbon bond formations is the addition of organometallic reagents to carbonyl compounds. Frankland pioneered organometallic chemistry in 1849 when he discovered the first organozinc compounds but this work remained underexploited in terms of synthetic applications.[13] Some of the early uses came in the form of the Reformatsky[14] and Simmons-Smith[15] reactions, which involve the use of zinc metal in alkylation of carbonyl compounds. Grignard reagents[16] and organolithium compounds[17,18] superseded organozinc compounds due

to their higher generality, reactivity and ease of manipulation. If the organometallic reagent is subject to a chiral environment and reacted with a carbonyl group, it can lead to synthetically important alcohols in high enantiomeric excess.[12] Chirality can be imposed onto the organometallic reagent either by the use of chiral "solvents" or complexing agents, or by the use of chiral ligands such as alcohols or amines. Examples of a chiral ligands for Grignard and lithium reagents are represented by the structures below.[19,20]

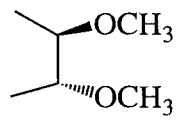

Grignard

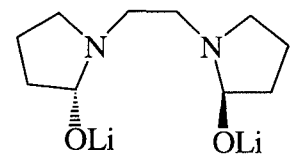

lithium

Investigations into the asymmetric organozinc addition to carbonyl compounds has grown drastically since the initial report of diethylzinc with benzaldehyde in the presence of a catalytic amount of amino alcohol in 1984.[21] Noyori and co-workers discovered the first highly enantioselective ligand, (-)-3-exo-dimethylaminoisobornenol [(-)-DAIB, **129**], for the dialkylzinc addition to aldehydes.[22]

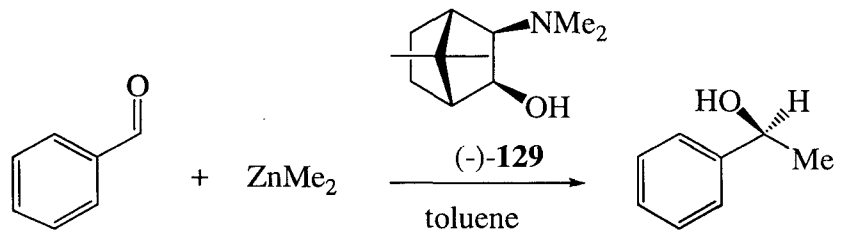

130

(S)-**131** 95% ee

Scheme 30: Dimethylzinc addition to benzaldehyde catalysed by DAIB

At 25-40°C, in toluene 2 mol % of (-)-**129** catalysed the addition of dimethylzinc to benzaldehyde and gave the (S)-1-phenylethanol (**131**) with up to 95% *ee*. Since then a large number of chiral catalysts have been synthesised and high enantioselectivities (up to 99%) have been achieved.[12,23,24,25]

Chiral pentacyclo-undecane (PCU) cage moieties has been used as hosts for chiral ammonium ions,[26,27] but applications of the PCU unit as an integral part of chiral ligands for asymmetric synthesis have not been reported. The synthesis of ligands **132-136** was accomplished in respectable yields starting from the pentacyclo(5.4.0.$0^{2,6}$.$0^{3,10}$.$0^{5,9}$)-undecane-8,11-dione (PCU-dione, **70**)[28,29] and with commercially available amino acids as the source of chirality.

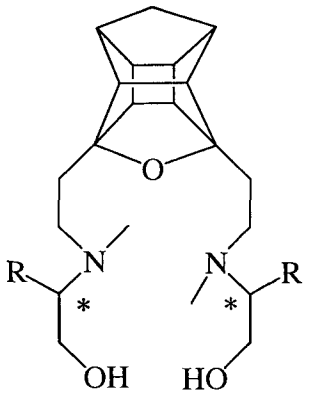

(*R,R*)-**132**: R = CH_2CH_3
(*S,S*)-**133**: R = $CH(CH_3)_2$
(*S,S*)-**134**: R = $CH_2CH(CH_3)_2$
(*S,S*)-**135**: R = C_6H_5

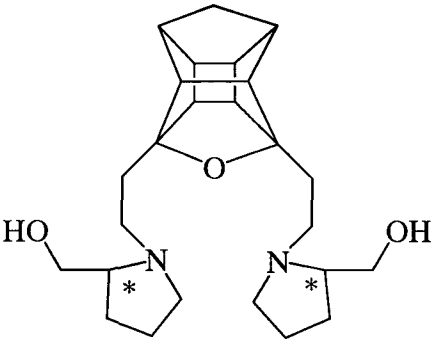

(*S,S*)-**136**

The *N*-methyl amino alcohols were synthesised from their respective amino acids (Scheme 31) by treating the amino acids **137-140** with formic acid and acetic anhydride to give the formamides **141-144** respectively.[30,31,32] The formamides were reduced to the corresponding N-methyl amino alcohols (**145-148**) via $LiAlH_4$ at ambient temperature. *N*-methyl amino alcohols were chosen over amino alcohols since the macrocycles were designed to catalyse reactions with strong base. Any exchangeable protons may interfere with the reaction by quenching the base. An additional advantage of using the *N*-methyl amino alcohols is that purification of the resulting products (**132-135**) is much easier than the corresponding products without the *N*-substituted amino alcohol.

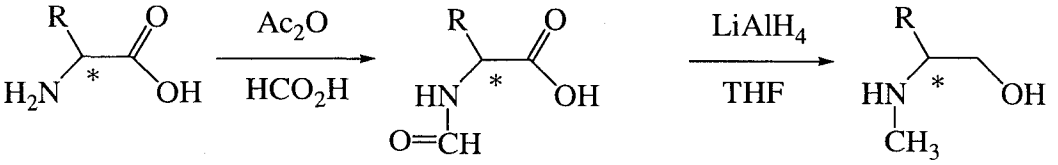

(*R*)-**137**: R = CH_2CH_3
(*S*)-**138**: R = $CH(CH_3)_2$
(*S*)-**139**: R = $CH_2CH(CH_3)_2$
(*S*)-**140**: R = C_6H_5

(*R*)-**141**: R = CH_2CH_3
(*S*)-**142**: R = $CH(CH_3)_2$
(*S*)-**143**: R = $CH_2CH(CH_3)_2$
(*S*)-**144**: R = C_6H_5

(*R*)-**145**: R = CH_2CH_3
(*S*)-**146**: R = $CH(CH_3)_2$
(*S*)-**147**: R = $CH_2CH(CH_3)_2$
(*S*)-**148**: R = C_6H_5

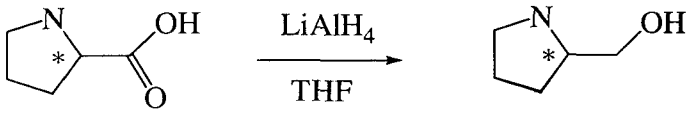

(*S*)-**149** (*S*)-**150**

Scheme 31: Synthesis the amino alcohols **145-148** and **150**

The reduction of (*S*)-(+)-proline (**149**) to (*S*)-(+)-prolinol (**150**) does not require the additional step. Ligands **132-135** were formed by reacting the PCU-ditosylate (**104**) with the corresponding amino alcohols (see Scheme 32). IR spectra for all five ligands showed a strong, broad peak at ~3400 cm^{-1} and peaks at ~1200 cm^{-1} that is characteristic of O-H and N-C stretching vibrations, respectively. ^{1}H NMR showed AB patterns at 1.49 and 1.85 ppm with a coupling constant of 10 Hz and a complex multiplet from 2.15 to 2.70 ppm representative of the methylene bridge of the PCU cage for **135** and **136**. The shift of the protons of the R-groups for **132-134** masks the distinctive AB pattern. The complex multiplet between 2.10 to 2.90 ppm also implied that the cage was present. ^{13}C NMR confirmed the structures with a triplet at ~43 ppm for the methylene bridge carbon and two peaks at ~90 ppm for the non-symmetric quaternary carbon of the cage. Mass spectrometry confirmed the [2:1] addition products.

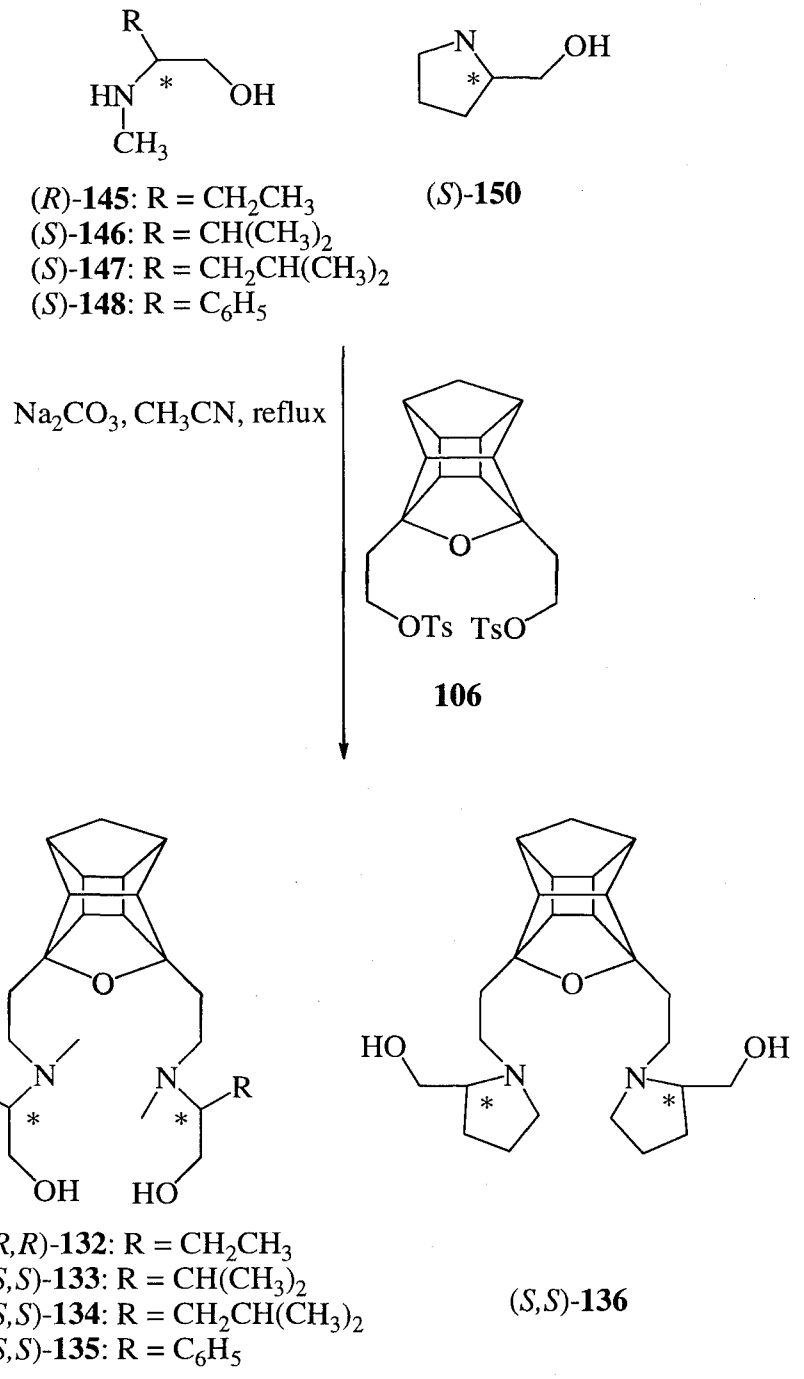

Scheme 32: Synthesis of the PCU-ligands **132-136**

CATALYTIC ABILITY OF CHIRAL AMINO ALCOHOLS

The catalytic activity of these ligands was investigated using the classical reaction of diethylzinc and benzaldehyde (**130**). Reactions were carried out in dry toluene at ambient temperature in the presence of 10 mol% chiral ligand and monitored[33] by chiral GC. When complete conversion of the aldehyde was detected (approximately 5hrs) the reaction was stirred for a further 48 hours. Previous reports[34,35] indicated that the reaction was quenched when all aldehyde was consumed, but with the PCU-ligands, this early workup resulted in

lower yield of the desired product (**151**) and the formation of benzyl alcohol (**152**) as the major by-product. After the prolonged reaction time, the reaction was quenched with 10% HCl and extracted with diethyl ether.

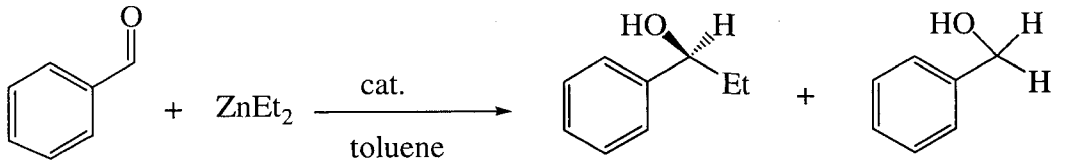

130

151
1-phenyl-1-propanol
desired product

152
benzyl alcohol
undesired product

Scheme 33: Addition of diethylzinc to benzaldehyde catalysed by PCU amino alcohols **132-136**

The organic phase was dried, solvent evaporated and the product purified via preparative TLC. All reactions were repeated and an average of the yields are reported. The reaction was also carried out at 0°C and this required reaction times in excess of 90 hours with no appreciable increase in the *ee* values.

Table 7: Results from the addition of diethylzinc to benzaldehyde catalysed by ligands **132-136**

Ligand	Time (h)[a]	Yield[b] %	*ee*[c]	Configuration[d]
132	30	92	-	-
133	30	**90**	15	S
134	30	**84**	**90**	S
135	30	**60**	10	S
136	30	**92**	-	-

a Quenching the reaction as soon as benzaldehyde was no longer detectable, resulted in benzylalcohol as the major product.
b Product was isolated by preparative TLC and the confidence limit was ±5 %.
c Determined by chiral GC as described in the experimental section and the confidences limit was ±1 %.
d Determined by optical rotation.

The results in Table 7 show that in the presence of the ligands **132-136**, diethylzinc reacts with benzaldehyde providing 1-phenyl-1-propanol (**151**) in high yields. Ligand **134** gave the best *ee* values. The source of chirality in **134** is leucinol which on its own catalysed this reaction with an *ee* of only 48%.[36] The only explanation that can be offered for this observation is that of the influence of the iso-butyl group. In the case of leucinol, the iso-

butyl group can adopt positions towards or away from the OH group. In the case of ligand **134**, the iso-butyl group is expected to be directed mainly towards the OH group since the steric hinderance exerted by the PCU moiety will induce the iso-butyl group to be positioned closer the OH group. This will enhance the chiral influence of the chiral centre upon complexation.

CONCLUSION

All attempts to synthesise new classes of cage annulated chiral crown ethers failed. Considerable time and effort was invested into this project and although the desired results were not achieved, substantial knowledge was gained by attempting new reactions and conditions. A positive aspect to the negative results obtained was that a new class of chiral PCU annulated amino alcohols were synthesised. These ligands are useful as precursors for preparing chiral macrocycles (see Chapter 5) and reactions that are catalysed by amino alcohols. Compared to other amino alcohols tested for the addition of diethylzinc to benzaldehyde, the new ligands catalysed the reaction with competitive turnover numbers, but with poor to good enantioselectivity. Amino alcohols that catalysed the reaction with higher *ee* values have more substituents on the carbon with the alcohol group and the carbon with the nitrogen group thereby favouring steric hinderance and higher selectivity. It is clear that incorporation of the PCU cage into such ligands warrants further investigation as it enhances the enantioselectivity of simpler/less sterically hindered amino alcohols (eg. leucinol). These chiral ligands can in future be tested for reactions that are catalysed by copper, lithium and Grignard reactions.

REFERENCES

1. Bakó, P.; Bajor, Z.; Tõke L. *J. Chem. Soc., Perking Trans 1* **1999**, 3651.
2. Bakó, P.; Czinge, E.; Bakó, T.; Czugler, M.; Tõke L. *Tetrahedron: Asymmetry* **1999**, *10*, 4539.
3. Pederson C.J. *J. Amer. Chem. Soc.* **1967**, *89*, 7017.
4. Marchand, A. P.; Kumar, K. A.; McKim, A. S. *Tetrahedron* **1997**, 3467.
5. Stoddart, J.F. *Chem.Soc.Review* **1979**, *8*, 85.
6. Weber, E; Toner, J. L.; Goldberg, I.; Vogtle, F.; Laidler, D.A.; Stoddart, J.F.; Bartsch, R.A.; Liotta, C.L. in *Crown ethers and analogs*, Patai, S. Ed., John Wiley and Sons, New York, **1989.**
7. Marchand, A. P.; Kumar, K. A.; McKim, A. S.; Majerski, K.M.; Kragol, G. *Tetrahedron* **1997**, *10*, 3467-3474.
8. Marchand, A. P.; Cal, D.; Majerski, M.K.; Ejsmont, K.; Watson, W. H. *J.Chem.Crystallogr.* **2002**; *11*, 447.
9. Huszuthy, P.; Bradshaw, J.S.; Zhu, C.Y.; Izatt, R.M. *J. Org Chem.***1991,** *56*, 3330.
10. Naemura, K.; Asada, M.; Hirose, K.; Tobe, Y. *Tetrahedron: Asymmetry* **1995**, *6*, 1873.
11. Marchand, A. P.; McKim, A. S.; Kumar, K. A.*Tetrahedron* **1998**, 13421.
12. Noyori, R.; Kitamura, M. *Angew. Chem., Intl. Ed. Engl.* **1991**, *30*, 49.
13. Frankland, E. *Ann. Chem. Pharm.* **1849**, *71*, 171.
14. Rathke, M.W. *Org. React.* **1975**, *22*, 423.
15. Simmons, H.E.; Cairns, T.L.; Vladuchick, S.A. *Organic Reactions* **1973**, *20*, 1.
16. Grignard, V. *C. R. Hebd. Sceances Acad. Sci.* **1900**, *130*, 1322.
17. Wittig, G.; Pockels, U.; Droge, H. *Chem. Ber.* **1938**, *71*, 1903.
18. Gilman, H.; Langham, W.; Jacoby, A.L. *J. Am. Chem. Soc.* **1939**, *61*, 106.
19 Cohen, H.L.; Wright, G.F. *J. Org. Chem.* **1953**, *18*, 432.
20 Colombo, L.; Gennari, C.; Poli, G.; Scolastico, C. *Tetrahedron* **1982**, *38*, 2725.
21. Oguni, N.; Omi, T. *Tetrahedron Lett.* **1984**, *25*, 2823.
22. Kitamura, M.; Suga, S.; Kawai, K.; Noyori, R. *J. Am. Chem. Soc.* **1986**, *108*, 6071.
23. Soai, K.; Niwa, S. *Chem. Rev.* **1992**, *92*, 833.
24. Knochel, P.; Singer, R.D. *Angew. Chem.Rev.* **1993**, *93*, 2117.
25. Soai, K.; Shibata, T. in *Comprehensive Asymmetric Catalysis*; Jacobsen, E.N., Pfaltz, A., Yamamoto, H., Eds.; Springer-Verlag: Berlin, **1999**; Vol.2, pp 911.
26. Marchand, A.P.; Chong, H.-S.; Ganguly, B., *Tetrahedron: Asymmetry* **1999**, *10,* 4695.

27. Govender, T.; Hariprakasha, H.K.; Kruger, H.G.; Marchand, A.P. *Tetrahedron: Asymmetry* **2003**, *14*, 1553.

28. R.C.Cookson; E. Crundwell; R.R.Hill, and J. Hudec, J. Chem. Soc. **1964** 3062.

29. A.P. Marchand and R.W. Allen, J. Org. Chem. **1974** 1596.

30. Muramatsu, I. Et al. *Bull.Chem.Soc.Jap.* **1965**; 244.

31. Aitali, M.; Allaoud, S.; Karim, A.; Meliet, C.; Mortreux, A. *Tetrahedron:Asymmetry* **2000**, **11**, 1367.

32. Huszthy, P.; Oue, M.; Bradshaw, J.S.; Zhu, C.Y.; Wang, T. *J.Org.Chem.* **1992**, *57*, 5383.

33. See experimental section for GC conditions.

34. Vilaplana, M.J.; Molina, P.; Arques, A.; Andres, C.; Pedrosa, R. *Tetrahedron: Asymmetry* **2002**, *13*, 5.

35. Superchi, S.; Giorgio, E.; Scafato, P.; Rosini, C. *Tetrahedron: Asymmetry* **2002**, *13*, 1385.

36. Oguni, N.; Omi, T. *Tetrahedron Lett.* **1984**, *25*, 2823.

CHAPTER 5

SYNTHESIS OF NOVEL CHIRAL CAGE ANNULATED MACROCYCLES AND THEIR EFFICIENCY IN STEREOSELECTIVE MICHAEL ADDITIONS

INTRODUCTION

Another classical carbon-carbon bond forming reaction is the Michael addition.[1,2,3,4] A considerable amount of effort has been devoted to the development of stereoselective methods, since this reaction often leads to the formation of a stereogenic centre.[4]

There are three possible strategies (Scheme 34) *i.e.* diastereoselective, enantioselective and catalytic enantioselective Michael additions. The use of chiral auxiliaries like Oppolzer's[5] chiral bornane sultams have led to diastereoselective additions being firmly established and frequently employed.[3,4] Enantioselective additions are more challenging and require the use of chirally modified nucleophiles to prochiral substrates. Organometallic reagents are used and the transfer of the R-group to the Michael acceptor is stereochemically controlled by a chiral ligand. A good example of this is the use of 'chiral cuprates' of the general formula $RCu(L^*)Li$ wherein L^* is the chiral ligand (*eg.* ephedrine and proline derivatives).[3,6] This strategy has proven to be successful with respect to high enantioselectivities, but the downside is that stoichiometric amounts of metal and chiral ligand are required and the chiral ligand can usually not be recovered. Another limitation of this strategy is the high substrate specificity *i.e.* certain chirally modified ligands give high *ee* values with only a few Michael acceptors.[4]

Diastereoselective Michael Addition:

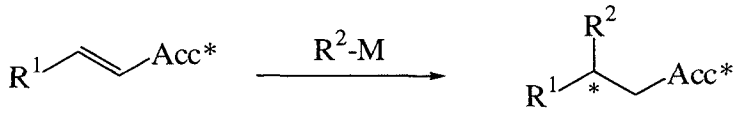

Enantioselective Michael Addition:

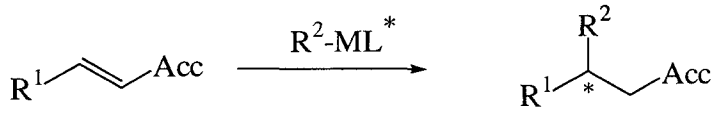

Catalytic Enantioselective Michael Addition:

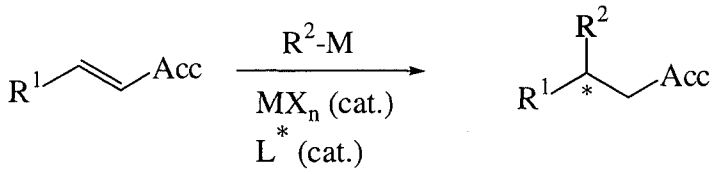

Scheme 34: Strategies for stereoselective Michael additions

With this in mind, the most elegant strategy would be a catalytic enantioselective Michael addition *i.e.* where only catalytic amounts of both the metal and the chiral ligand are required. There have been many developments on this method, making use of organolithium,[7] Grignard[8] or organozinc[9] reagents.

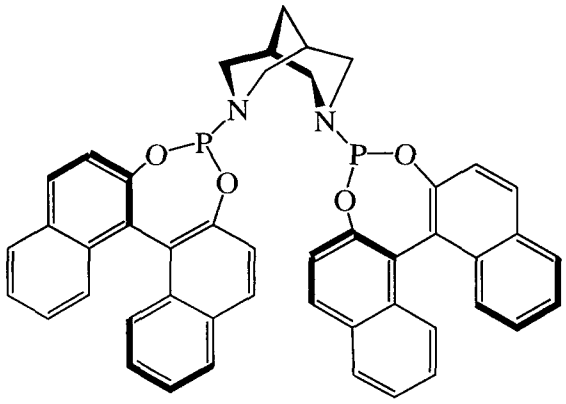

(*R,R*)-**153**

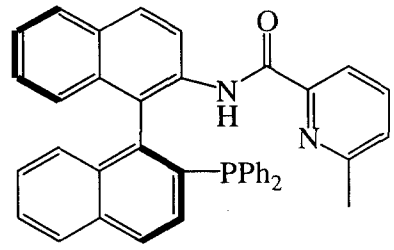

(*S*)-**154**

Ligands **153**[10] and **154**[11] are examples of binaphthalene derived ligands used for copper catalysed enantioselective Michael additions. Crown ethers have also been found to be useful as chiral phase transfer catalyst in carbon-carbon bond forming reactions.[12,13] Below is a list of the various crown compounds used to catalyse Michael addition reactions.

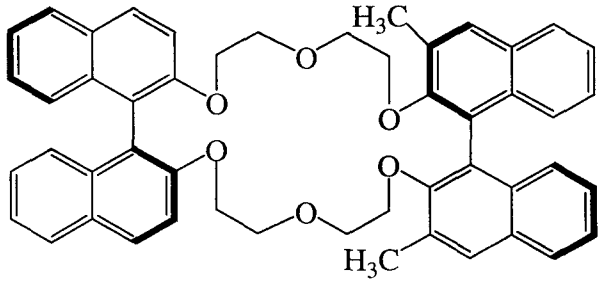

(*S,S*)-**155** (99% ee)

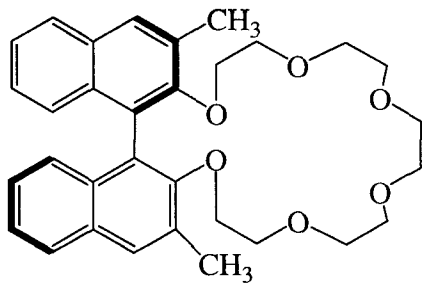

(*R*)-**156** (83% ee)

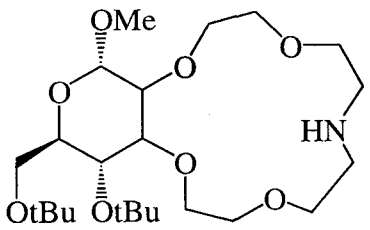

157 (90% *ee*)

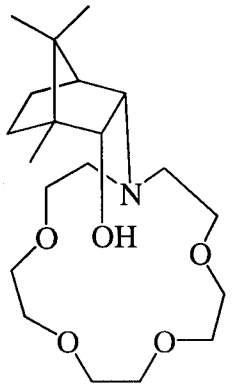

158 (83% *ee*)

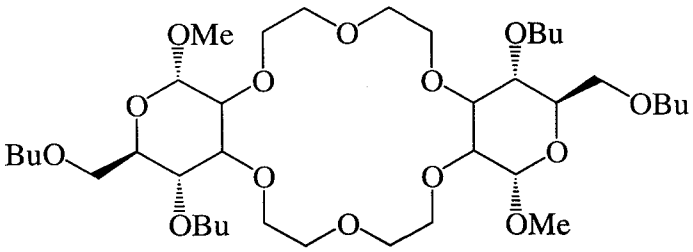

159 (84% *ee*)

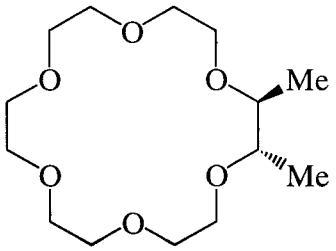

160 (79% *ee*)

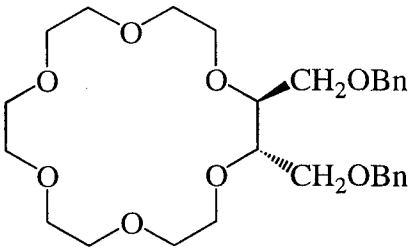

161 (71% *ee*)

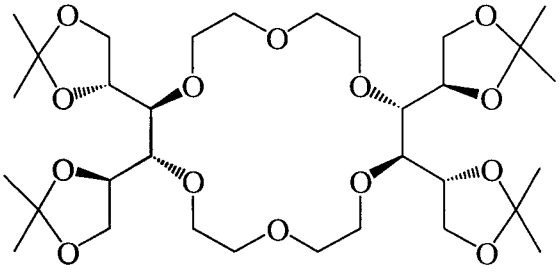

162 (71% *ee*)

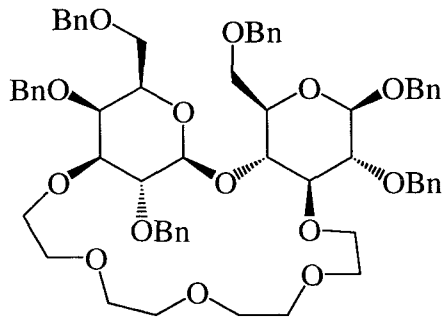

163 (70% *ee*)

Scheme 35 attempts to illustrate how enantioselectivity arises in the Michael addition of methyl phenylacetate and methyl acrylate. When the sodium base is added to the reaction, it extracts a proton from the methyl phenylacetate to yield the carbanions (**164**). The sodium cation that is complexed to the macrocycle to form the chiral host guest complex (**165**) then acts as a counter-ion to this carbanion.

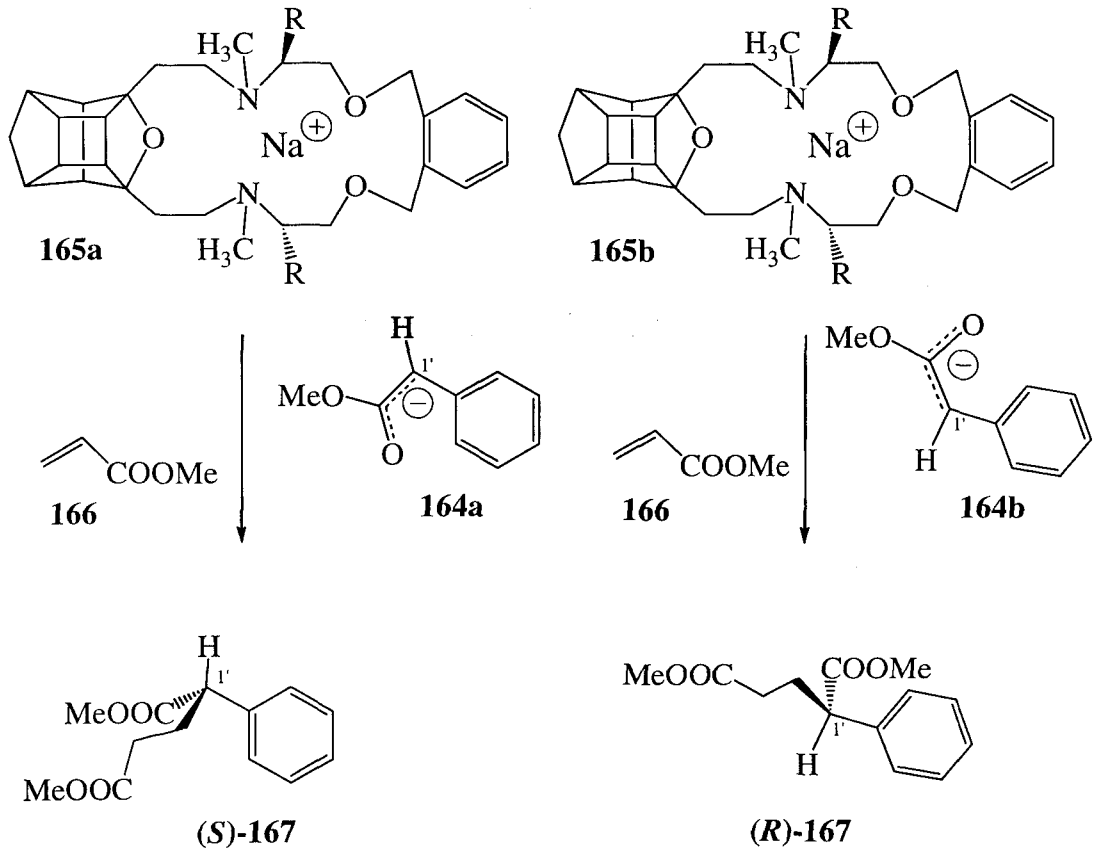

Scheme 35: Michael Addition of methyl phenylacetate to methyl acrylate

In Scheme 35, the convention used is that the anion is complexed above the macrocyle (*i.e.* pointing out of the plane of the page). Attack from C-1′ to the methyl acrylate also occurs towards above the plane of the page as the acrylate is approaching from above the plane of the complex, resulting in the two possible enantiomers forming. The energies of the possible

initial complexes formed, between the host, metal and carbanion are related to the steric influence of the R-groups of the host. As a result of this, an enantiomeric excess of one enantiomer over the other will result upon collision of the complex with methylacrylate.

RESULTS AND DISCUSSION

In Chapter 4 the synthesis of cage annulated amino alcohols **132-135** were reported. These amino alcohols were reacted with α,α'-dibromo-o-xylene (**111**) and sodium hydride in tetrahydrofuran to afford the corresponding macrocycles (**168-171**). Macrocycle **168** could not be isolated as the free amine because it co-migrated with another compound on column chromatography. Macrocycles **169-171** were isolated via column chromatography on silica gel using methanol, chloroform and ammonium hydroxide. The ammonium hydroxide was essential in order to prevent streaking of the product on the column. Infrared spectra of the macrocycles clearly indicated the absence of the O-H stretching vibration peak at approximately 3300 cm^{-1} and the presence of C-O-C asymmetric stretching vibrations at ~1080 cm^{-1}. C-C stretching vibration peaks (skeletal bands) of the aromatic ring was present at ~1460 cm^{-1}. The ^{1}H NMR spectrum indicated the presence of the benzyl group with a peak at approximately 4.5ppm. The ^{13}C spectrum showed peaks at ~70-71 ppm (CH_2 of the benzylic group) confirming the presence of the xylene substituent. A triplet peak at ~43 ppm represented the methylene bridge carbon of the cage substituent and two non-equivalent quartets at ~38.6 ppm for the methyl groups attached to the nitrogen atoms. Mass spectrometry confirmed the [1:1] cyclisation products with m/z peaks that support the respective formulae.

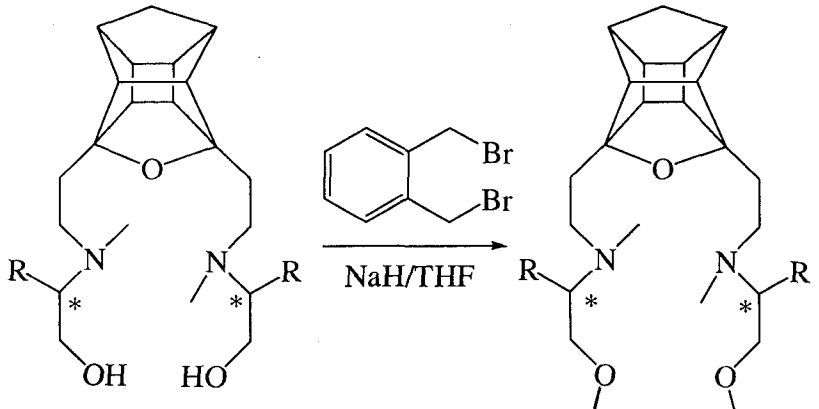

(*R,R*)-**132**: R = CH_2CH_3
(*S,S*)-**133**: R = $CH(CH_3)_2$
(*S,S*)-**134**: R = $CH_2CH(CH_3)_2$
(*S,S*)-**135**: R = C_6H_5

(*R,R*)-**168**: R = CH_2CH_3
(*S,S*)-**169**: R = $CH(CH_3)_2$
(*S,S*)-**170**: R = $CH_2CH(CH_3)_2$
(*S,S*)-**171**: R = C_6H_5

Scheme 36: Synthesis of novel cage annulated macrocycles **168-171**

It was decided to test the asymmetric catalytic abilities of theses macrocycles with the classical Michael addition reaction of methyl phenylacetate (**172**) and methyl acrylate (**173**) in the presence of base. These substrates were common to most of the reports dealing with chiral host catalysed Michael additions. Finding a suitable procedure for carrying out the experiments was crucial since different investigators reported different methods with respect to the amount of base used and the sequence in which the reactants were introduced into the reaction vessel. Cram *et al.*[14] used mainly an equal amount of host to base. In their procedures the base and substrate **172** were mixed together, followed by the host and then the methyl acrylate (**173**). Penadès *et al.*[15] reported using 5 times excess of base with respect to host. Koga *et al.*[16] carried out the procedure according to Cram. Pandit *et al.*[17] used the same ratios as Cram and Koga but mixed the base and host at room temperature before cooling and adding substrates **172** and **173**. Bakó *et al.*[18] reported using five to ten molar excess of base to host. It was decided not to use excess base since all investigators reported the reaction proceeding in the absence of a chiral influence and it therefore might have a negative influence on the enantiomeric excess. "Clearly, high enantioselectivities can only be reached if any uncatalysed background reaction of the nucleophile with the substrate is negligible."[4]

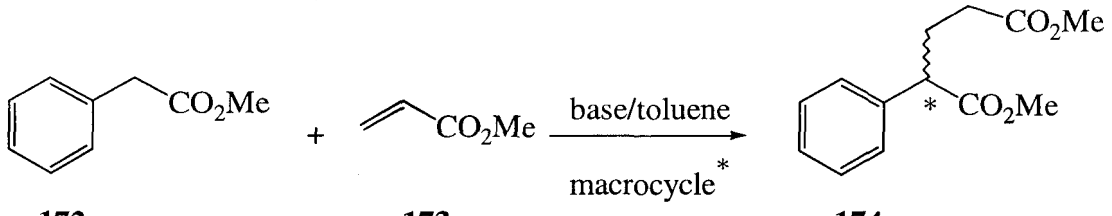

172 **173** **174**

Scheme 37: Macrocycle catalysed Michael addition reaction of methyl phenylacetate to methyl acrylate

The experimental procedure reported by Pandit *et al.*[17] was initially employed, wherein the nucleophile was first complexed to the crown and then reacted with the substrate thereby eliminating any chance of the reaction proceeding in the absence of a chiral influence. The procedure used by Pandit *et al.* (Tables 8 and 9) was adopted in the subsequent experiments with very little success and therefore, the procedure used by Cram and Koga (Table 10) was also investigated. Changing the reaction conditions did not make any difference to the results since the reaction did not yield any product until excess base was used. Excess base resulted in high chemical yields but negligible enantiomeric excess.

Table 8: Michael reaction of methyl phenylacetate (**172**) and methyl acrylate (**173**) at -70°C catalysed by sodium *t*-butoxide and different macrocycles

	Host							
	None	**18-C-6**	**169**	**170**	**171**	**169**	**170**	**171**
Base	$NaOBu^t$	$NaOBu^t$	$NaOBu^t$	$NaOBu^t$	$NaOBu^t$	$NaOBu^t$	$NaOBu^t$	$NaOBu^t$
[host][a]	None	0.05	0.05	0.05	0.05	0.05	0.05	0.05
[base][a]	0.05	0.05	0.05	0.05	0.05	0.1	0.1	0.1
Temp./°C	-70	-70	-70	-70	-70	-70	-70	-70
Time/hrs	1	1	3	3	3	1	1	1
Yield/%[b]	48	90	0	0	0	28	31	29
ee/%[c]	0	0	0	0	0	11.3	6.3	2.1

a Amount of host/base in mmol
b Confidence limit was ±2 %.
c Confidence limit was ±2 %.

From the control run with no host it was evident that the reaction was catalysed in the absence of host, which meant that an excess of base would result in the formation or racemic product. The amount of racemic product was directly proportional to the amount of base in excess. From the control run with a non-chiral host, it was evident that the reaction rate was increased in comparison to when a host was absent. Addition of chiral hosts **169-171** to the reaction vessel prevented any catalysis from occurring. From this data it was clear that the host had complexed the sodium of the catalyst. As mentioned earlier in the chapter, the initial step is for the *t*-butoxide anion to abstract the acidic proton from methyl phenylacetate to yield a carbanion (**165**) which then complexes with the sodium cation. The next step is the condensation of the electrophile (methyl acrylate) to complexed carbanion **165**. It was suspected that the initial reaction (formation of the anion **165** from Scheme 35) was not occurring; due to either steric hindrance or very stable complexation of the base by the complex. At this stage it was decided to try elevated temperatures to destabilise the complex and to overcome any rotational barriers that might be contributing to the steric hindrance. A larger metal *eg.* potassium might lead to a less stable complex since it would prefer a larger cavity size.

Table 9: Michael reaction of methyl phenylacetate and methyl acrylate at various temperatures catalysed by sodium *t*-butoxide and potassium *t*-butoxide

	Host					
	None	**18-C-6**	**170**	**170**	**171**	**171**
Base	$NaOBu^t$	$NaOBu^t$	$NaOBu^t$	$NaOBu^t$	$KOBu^t$	$KOBu^t$
[host][a]	None	0.05	0.05	0.05	0.05	0.05
[base][a]	0.05	0.05	0.05	0.05	0.05	0.05
Temp./°C	25	25	25	60	-70	60
Time/hrs	1	1	5	24	3	24
Yield/%[b]	62	76	0	0	0	0
ee/%	0	0	0	0	0	0

a Aamount of host/base in mmol
b Confidence limit was ±2 %.

It was decided to use host **171** to investigate the effect of changing from a potassium base to a sodium base since **171** is less sterically hindered than **169** and **170**, and would therefore complex the larger metal ion better. Hosts **169** and **170** were to be tested if there was any evidence of product formation with the use of **171**. The reaction could not be catalysed with the use of chiral crown ethers **170** and **171** even at temperatures as high as 60 °C. Also the use of a potassium ion did not result in any product formation. From this evidence, steric hindrance was suspected as the major cause for the negative results. Since it was not practical at that stage of the project to decrease the steric bulk on the host, a decrease in the bulk of the base was investigated. Sodium methoxide is a weaker base than sodium *t*-butoxide but is much less bulky.

Table 10: Michael reaction of methyl phenylacetate and methyl acrylate at various temperatures catalysed by sodium methoxide

	Host				
	None	**18-C-6**	**171**	**171**	**171**
Base	NaOMe	NaOMe	NaOMe	NaOMe	NaOMe
[host][a]	None	0.05	0.05	0.05	0.05
[base][a]	0.05	0.05	0.05	0.05	0.05
Temp./°C	-70	-70	-70	25	60
Time/hrs	3	3	3	24	24
Yield/%[b]	0	60	0	0	0
ee/%	0	0	0	0	0

a Amount of host/base in mmol
b Confidence limit was ±2 %.

The results in table 10 indicated that no products were observed in the control run with no host but product did form in the control run in the presence of non-chiral host. This showed that the use of sodium methoxide would result in a true catalytic reaction and yield product with optimum *ee*. There was no evidence of product formation in the presence of chiral macrocycle **171** even at elevated temperatures.

Motivation why deprotonation of methyl phenylacetate (to form the anion **165**) possibly never occurred when the PCU macrocycles were added to the reaction:

The Michael addition reaction occurred without the presence of a macrocycle.

The reaction occurred with host 18-crown-6.

The reaction gave no product in the presence of PCU macrocycles, even at with temperatures up to 60°C.

If the anion (**165**) had formed, the reaction should have proceeded since the species is reactive.

As can be seen from Scheme 35, attack should result from an effective collision between the anion and methylacrylate.

Since attack occurs from the "outside", steric hindrance is not expected to play such an important inhibiting role in the subsequent step.

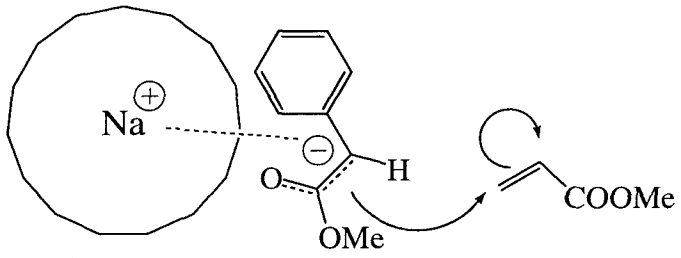

Na^+-host complex

Figure 10: An illustration of the nucleophilic attack of the complex to the electrophile

In order to verify the degree of steric hindrance involved upon complexation of Na-*t*-butoxide by the cage macrocycle, a number of calculations were performed to determine the low energy structure of the complex. As the MM3 forcefield[19] available in Alchemy[20] is not parameterised for sodium, it was decided to use the Oniom function[21] in Gaussian[22] to obtain the structure of the complex. Oniom provides the possibility to calculate the structure of a molecule at three different levels/basis sets. In this case sodium was calculated using UB3LYP/6-31+g(d), the donor atoms with B3LYP/6-31+g(d) and the remainder of the macrocycle and base with AM1 (semi-empirical).

The optimised structure for the complexes of cage macrocycle and 18-crown-6 with Na-*t*-butoxide respectively is provided in Figure 11.

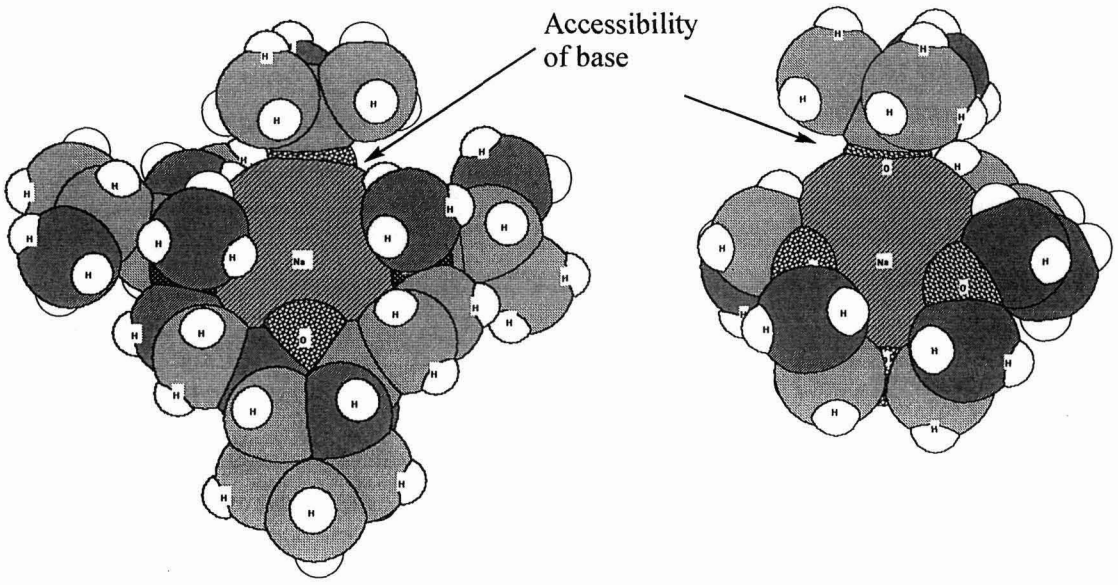

Figure 11: Optimised complexes of host **169** and 18-crown-6 with sodium tert-butoxide (cartesian coordinates on CD)

Figure 11 clearly illustrates the magnitude of the steric hindrance of the cage-annulated macrocycle as compared to very little steric hindrance of the 18-crown-6 complex. The butoxide oxygen of the cage complex is almost completely shielded from nucleophilic attack by the two methyl groups on the nitrogen donor atoms. As the butoxide is tilted toward the benzene ring of **169**, nucleophilic attack from the backside of the complex is also prevented. The sodium in the cage complex is positioned in the centre of the donor atoms while with the 18-crown-6 it has to bend to ensure maximum interaction of the donor atoms to Na, causing the base to be more accessible to nucleophilic attack.

In order to investigate the role of steric hindrance in the macrocycle/sodium-*t*-butoxide complex, it was decided to calculate the geometry and stability of the complex using Gaussian. It is clear from the computed results that the oxygen of the sodium-*t*-butoxide is completely shielded by the two methyl groups of the nitrogen donor atoms of the macrocycle. It may be possible that a smaller electrophile (smaller substitute for methyl phenylacetate **172**) may change the course of the reaction.

A comparison of hosts **169-171** with hosts[14,15,16,17] that worked successively for this reaction suggested that the size of the PCU macrocycles may be too small. All the successful hosts had at least 6 donor atoms whereas **169-171** have only 5 donor atoms. The use of hosts (*eg.* **175**) with 5 donor atoms has been reported by Bakó *et al.*[18,23,24]

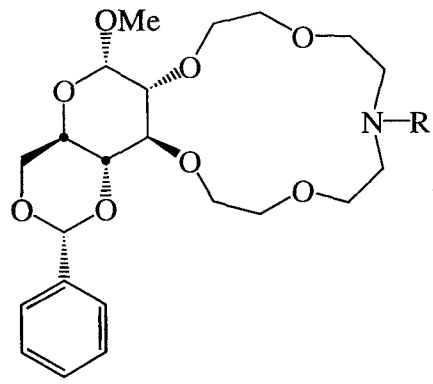

175

These macrocycles were tested with the Michael addition reaction of 2-nitropropane (**176**) and chalcone (**177**) in the presence of base. In this case, 2-nitropropane reacts with base to form the nucleophile.

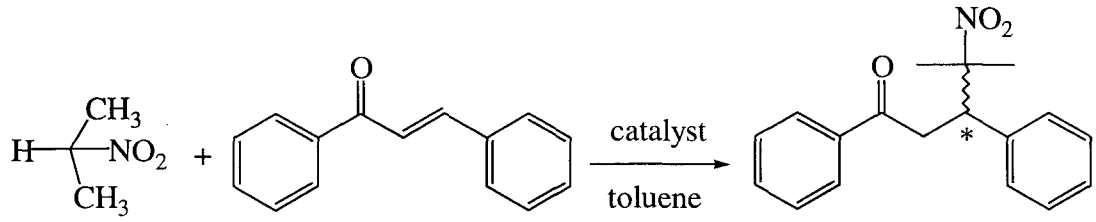

176 **177** **178**

Scheme 38: Michael addition reaction of 2-nitropropane and chalcone

It should be pointed out that the change of electrophile unfortunately also induces an electronic factor to the problem as 2-nitropropane is much more acidic compared to methyl phenylacetate [methyl phenylacetate (**172** - pK_a = 22.6)[25] and 2-nitropropane (**176** – pK_a = 7.7)[26]. This complication would make it almost impossible to prove beyond doubt that the difficulties before were due to steric factors alone.

This approach seemed to be much more profitable since the Michael addition reaction with cage macrocycles indeed gave product as well as a reasonable *ee* in one case (see Table 11).

Table 11: Michael reaction of 2-nitropropane (**176**) and chalcone (**177**) catalysed by sodium methoxide and **169-171** at 25°C

	Host					
	None	**None**	**18-C-6**	**169**	**170**	**171**
Base	$NaOBu^t$	NaOMe	NaOMe	NaOMe	NaOMe	NaOMe
[host][a]	none	None	0.05	0.05	0.05	0.05
[base][a]	0.05	0.05	0.05	0.05	0.05	0.05
Time/hrs	48	48	48	120	120	120
Yield %[b]	24	0	54	12	12	20
ee/%[c]	0	0	0	92	92	80

a Amount of host/base in mmol
b Confidence limit was ±2 %.
c Confidence limit was ±2 %.

A control run using sodium *t*-butoxide resulted in 24% product formation in the absence of host. The use of sodium methoxide would represent a better example of a solid-liquid phase transfer reaction since in the absence of host, there is no product formation. Use of control host 18-crown-6 catalysed the reaction with 54% yield in 48 hours and the use of hosts **169-171** resulted in decreased rate of the reaction with only 12%, 12% and 20% respectively after 120 hours.

Results in Tables 10 and 11 imply that the Michael addition reaction with methyl phenylacetate (**172**, Scheme 37) proceeds at a much higher rate than the reaction with 2-nitropropane (**176**, Scheme 38) with the use of sodium methoxide and 18-crown-6 as catalyst. It is important to note that the reaction carried out in Scheme 37 did not yield any by-products, only starting materials and product were isolated after workup. The reaction carried out in Scheme 38 yielded many by-products, product and no starting material. The formation of by-products is the main reason for the lower yields. The decrease in the yields of this reaction with the use of chiral hosts **169-171** can also be attributed to steric factors. The nucleophile formed from 2-nitropropane (**176**) would be sterically hindered from attacking the bulky electrophile, chalcone. This slows down the reaction resulting in an increase of by-products and therefore lower yields. A positive side to this reaction is that the product is formed with high enantioselectivity. Results in Table 10 can also be attributed to steric effects. In this case it is believed that the reaction was stalling at the step required to form the nucleophile of methyl phenylacetate (**172**) since the electrophile, methyl acrylate, is not bulky and should therefore not pose any steric opposition to the reaction.

CONCLUSION

A procedure for synthesising a new class of cage annulated chiral macrocycles has been established. Macrocycles of this type were tested as chiral phase transfer catalysts for the first time. These hosts could not catalyse the Michael addition reaction between methyl phenylacetate and methyl acrylate in the presence of base. It was successful in catalysing the reaction between 2-nitropropane and chalcone with a low turnover rate (12%), but high enantioselectivity (92%). These results are comparable to some of the best results reported elsewhere with respect to *ee*'s. Cram's binaphthyl crown ether catalysed a Michael addition reaction with 48% yield and 99% *ee* in 120 hours at –78°C. When the reaction was performed at 25°C, the reaction was catalysed to give 75% yield and 67% *ee* in 96 hours. It is possible that a decrease in temperature could result in an increase in *ee* (~99%) values, but this was not investigated since the reaction proceeded at a relatively low rate. Other reports on the use of chiral crown compounds to catalyse the Michael addition of 2-nitropropane and chalcone resulted in yields ranging from 20-80% with *ee* values of 2-94% with the bulk at 40-50%. In context of these results, chiral hosts containing the PCU framework deserve further investigation.

REFERENCES

1. Bergmann, E.D.; Ginsburg, D.; Pappo, R. *Org. React.* **1959**, *10*, 179.
2. Ihara, M.; Fukumoto, K. *Angew. Chem., Int. Ed. Engl.* **1993**, *32* 1010.
3. Krause, N.; Gerold, A. *Angew. Chem., Int. Ed. Engl.* **1997**, *36*, 186.
4. Krause, N.; Röder, A.H. *Synthesis* **2001**, *2*, 171.
5. Oppolzer, W. *Tetrahedron* **1987**, *43*, 1969.
6. Rossiter, B.E.; Swingle, N.M. *Chem. Rev.* **1992**, *92*, 771.
7. Cohen, H.L.; Wright, G.F. *J. Org. Chem.* **1953**, *18*, 432.
8. Colombo, L.; Gennari, C.; Poli, G.; Scolastico, C. *Tetrahedron* **1982**, *38*, 2725.
9. Oguni, N.; Omi, T. *Tetrahedron Lett.* **1984**, *25*, 2823.
10. Huttenloch, O.; Speiler, J.; Waldmann, H. *Chem. Eur. J.* in press.
11. Hu, X.; Chen, H.; Zhang, X. *Angew. Chem., Int. Ed. Engl.* **1998**, *38*, 3518.
12. Bakó, P.; Bajor, Z.; Tõke L. *J. Chem. Soc., Perking Trans 1* **1999**, 3651.
13. Bakó, P.; Czinge, E.; Bakó, T.; Czugler, M.; Tõke L. *Tetrahedron: Asymmetry* **1999**, *10*, 4539.
14. Cram, D.J.; Sogah, G.D.Y. *J.Chem.Soc., Chem. Commun.* **1981**, 625.
15. Vicent, C.; Martin-Lomas, M.; Penadés, S. *Tetrahedron* **1989**, *45*, 3605.
16. Aoki, S.; Sasaki, S.; Koga, K. *Tetrahedron Letters* **1989**, *30*, 7229.
17. Maarschalkerwart, D.A.H.; Willard, N.P.; Pandit, U.K. *Tetrahedron* **1992**, *48*,8825.
18. Bakó, P.; Bajor, Z.; Tõke L. *J. Chem. Soc., Perking Trans 1* **1999**, 3651.
19. (a) Allinger, N. L.; Yuh, Y. H. and Lii, J. H. *J. Amer. Chem. Soc.* **1989**, *111*, 8551 (b) Lii, J. H. and Allinger, N. L. *J. Amer. Chem. Soc.*, **1989**, *111*, 8566. (c) Lii, J. H. and Allinger, N. L. *J. Amer. Chem. Soc.*, **1989**, *111*, 8576.
20. Alchemy is a registered product of Tripos, Inc., Louis, MO, USA.
21. T. Vreven, K. Morokuma, Ö. Farkas, H. B. Schlegel, and M. J. Frisch, J. Comp. Chem. in press (**2003**). T. Vreven, I. Komáromi, S. Dapprich, K. S. Byun, J. A. Montgomery Jr., K. Morokuma, and M. J. Frisch, in prep. (**2003**)
22. Gaussian 98, Revision A.9, Frisch M. J.; Trucks G. W.; Schlegel H. B.; Scuseria G. E.; Robb M. A.; Cheeseman J. R.; Zakrzewski V. G.; Montgomery Jr. J. A.; Stratmann R. E.; Burant J. C., Dapprich S.; Millam J. M.; Daniels A. D.; Kudin K. N., Strain M. C.; Farkas O.; Tomasi J.; Barone V.; Cossi M.; Cammi R.; Mennucci B.; Pomelli C.; Adamo C.; Clifford S.; Ochterski J.; Petersson G. A.; Ayala P.Y.; Cui Q.; Morokuma K.; Malick D.K.; Rabuck A. D.; Raghavachari K.; Foresman J. B.; Cioslowski J.; Ortiz J. V.; Baboul A. G.; Stefanov B. B.; Liu G.; Liashenko A.; Piskorz P.; Komaromi I.;Gomperts R.; Martin R. L.; Fox D. J.; Keith T.; Al-Laham M. A.; Peng C. Y.; Nanayakkara A.; Challacombe M.; Gill P.M.W.; Johnson B.;

Chen W.; Wong M.W.; Andres J.L.; Gonzalez C.; Head-Gordon M.; Replogle E.S.; and Pople J.A.; Gaussian, Inc., Pittsburgh PA, **1998.**

23. Bakó, P.; Novák, T.; Ludányi, K.; Pete, B.; Tõke L.; Keglevich, G. *Tetrahedron: Asymmetry* **1999**, *10,* 2373.
24. Bakó, P.; Vizvárdi, K.; Toppet, S.; Van der Eycken, E.; Hooernaert, G.J.; Tõke L. *Tetrahedron* **1998**, *54*; 14975.
25. Bordwell, F.G.; Fried, H.E. *J. Org. Chem.* **1981**, *46*, 4327.
26. Gilbert, H.F. *J. Am. Chem. Soc.* **1980**, *102*, 7059.

CHAPTER 6

EXPERIMENTAL

Melting points are uncorrected. All UV readings were recorded by using a Varian Carey 1E UV-vis spectrophotometer. Optical rotations were taken on a Perkin Elmer 341 polarimeter. All mass spectrometric analyses were carried out on a VG70-70E mass spectrometer. FAB mass spectra were obtained by bombardment of samples with xenon atoms (1 mA at 8 keV). *m*-Nitrobenzyl alcohol was used as matrix. NMR spectra were recorded on a Varian Unity Inova-300 MHz spectrometer. Elemental microanalyses were obtained at the University of KwaZulu-Natal using a LECO CHNS-932 for carbon, hydrogen and nitrogen, and LECO VTF-900 for oxygen. The enantiomeric excess of the product was determined by GC (SGE Cydex-B chiral column, 25m x 0.22mm, inlet pressure 12psi, injection volume 0.1 µl, isothermal 110°C, T_1 = 25.4, T_2 = 26.2). Toluene was freshly distilled prior to its use on sodium benzophenone ketyl under nitrogen atmosphere. Diethylzinc was used as 1.0M solutions in hexane (Aldrich) and was used as purchased. All amino acids were bought from Novabiochem.

EXPERIMENTAL FOR CHAPTER 2

Pentacyclo[5.4.0.0^{2,6}.0^{3,10}.0^{5,9}]undecane-8,11-dione (**70**)

p-Benzoquinone (240 g, 2.22 mol) in methanol (1L) was cooled to -70°C via application of an external dry ice-acetone bath. To this was added, over 8 hours, with stirring a solution of freshly cracked cyclopentadiene (171.6 g, 2.6 mol) in cold methanol (200 ml). The reaction mixture was allowed to warm gradually to room temperature with stirring. The product was filtered and recrystallised from *n*-hexane to yield the adduct as yellowish-green crystals 30 (280 g, 68 %).

The above adduct (**30**, 60 g) was dissolved in 600 ml acetone and irradiated with a 500 W mercury lamp until the TLC (4:1 hexane:ethyl acetate) indicated the absence of starting material (6-8 hours). The solvent was evaporated to give the product as a colourless microcrystalline solid **70** (52g, 86%), m.p. 233 °C.

exo-8-*exo*-11-Diallylpentacyclo[5.4.0.0^{2,6}.0^{3,10}.0^{5,9}]undecane-*endo*-8-*endo*-11-diol (**80**)

A solution of dione **70** (58.47 g, 336 mmol) in dry THF (500 mL) was added dropwise over 2 hours to a mechanically stirred suspension of freshly prepared allylmagnesium bromide (2.2 L

of 0.392 M in dry THF; excess) under argon at 0 °C. After the addition had been completed, the external ice-water bath was removed, and the reaction mixture was allowed to warm gradually to ambient temperature while stirring under argon during 24 hours. The reaction was quenched via addition of saturated aqueous NH_4Cl (until pH is 6~7), the layers were separated, and the aqueous layer was extracted with EtOAc (2 x 500 mL). The combined organic extracts were dried ($MgSO_4$) and filtered, and the filtrate was concentrated *in vacuo*. The residue was recrystallised from hexane, thereby affording pure **80** (78.89 g, 91 %) as a colourless microcrystalline solid: m.p. 82-83 °C; IR (KBr): ν_{max} 3169, 2976, 1639 cm^{-1} ; ^1H NMR [$CDCl_3$, 200 MHz]: δ_H 1.05 (*AB*, J_{AB} = 10.8 Hz, 1 H), 1.49 (A*B*, J_{AB} = 10.8 Hz, 1 H), 1.97-2.24 (m, 6 H), 2.30-2.61 (m, 6 H), 5.01 (dd, J = 8.0 & 2.6 Hz, 2 H), 5.04 (dd, J = 16.85 & 2.6 Hz, 2 H), 5.90 (m, 2 H), 6.52 (br s, 2 H); ^{13}C NMR [$CDCl_3$, 50 MHz]: δ_C 33.9 (t), 40.0 (d), 42.8 (d), 44.0 (d), 44.1 (t), 49.1 (d), 77.2 (s), 117.5 (t), 133.8 (d). CI MS: Calc. for $C_{17}H_{22}O_2$: $[M + H]^+$ *m/z* 259.16981. Found: $[M + H]^+$ *m/z* 259.16994. Anal. Calc. for $C_{17}H_{22}O_2$: C, 79.03; H, 8.58. Found: C, 79.14; H, 8.42 %

3,5-Diallyl-4-oxahexacyclo[5.4.1.$0^{2,6}$.$0^{3,10}$.$0^{5,9}$.$0^{8,11}$] dodecane (**81**)

A solution of **80** (61 g, 0.236 mol) and *p*-toluenesulphonic acid (1.5 g, 0.79 mmol, catalytic amount) in benzene (1.2 L) was refluxed in a Dean-Stark apparatus and the resulting water was removed azeotropically. After every 12 hours, additional *p*-toluenesulphonic acid (500 mg) was added. When TLC indicated the absence of **80** (72 hours), the reaction mixture was allowed to cool gradually to ambient temperature and washed sequentially with 10% aqueous $NaHCO_3$ (100 mL), water (100 mL) and brine (100 mL). The organic layer was dried ($MgSO_4$) and filtered, and the filtrate was concentrated *in vacuo*. The residue was purified via column chromatography on silica gel by eluting with 5% EtOAc-hexane. Pure **81** (46.53 g, 82%) was thereby obtained as a colourless oil; IR (neat): ν_{max} 3075, 2965, 1640, 997, 910 cm^{-1}; ^1H NMR ($CDCl_3$): δ_H 1.46 (*AB*, J_{AB} = 10.2 Hz, 1 H), 1.82 (A*B*, J_{AB} = 10.2 Hz, 1 H), 2.35 (br s, 2 H), 2.45-2.65 (m, 10 H), 5.01 (dd, J = 9.8 & 2.2 Hz, 2 H), 5.07 (dd, J = 15.4 & 1.4 Hz, 2 H), 5.78 (m, 2 H); ^{13}C NMR ($CDCl_3$): δ_C37.5 (t), 41.7 (d), 43.3 (t), 44.5 (d), 47.8 (d), 58.6 (d), 95.1 (s), 116.8 (t), 134.4 (d). CI MS: Calc. for $C_{17}H_{20}O$: $[M + H]^+$ m/z 241.1592. Found: $[M + H]^+$ m/z 241.1601.

5,5-Dicarboxymethyl-4-oxahexacyclo[5.4.1.$0^{2,6}$.$0^{5,10}$.$0^{5,9}$.$0^{8,11}$]dodecane (**82**)

A solution of the diene **81**[1] (3.3 g) in dry methanol (100 mL) was cooled to -78 °C via application of an external dry ice-acetone bath and purged with argon during 20 minutes. Ozone was bubbled into the mixture until a blue-purple colour persisted, thereby indicating the presence of excess ozone and completion of reaction. Excess ozone was flushed from the

reaction vessel with a stream of argon, and the reaction mixture was concentrated in vacuo. Hydrogen peroxide (30 mL, 30%) was added dropwise to a stirred, ice bath cooled mixture of the ozonoide and formic acid (21 mL). The resulting mixture was stirred at ambient temperature during 1 hour and refluxed gently for 12 hours. The reaction mixture was allowed to cool gradually to ambient temperature and was concentrated in vacuo. Pure **82** (2.895 g, 76%) was thereby obtained as a colorless microcrystalline solid: mp 175-175.5 °C; IR (KBr): ν_{max} 3180(s), 2980(s), 1720(vs) cm^{-1}; FAB^+ MS (*m*-Nitrobenzyl alcohol): m/z 408 $[M + H]^+$; ^1H NMR [DMSO, 300 MHz]: δ_H 1.45 (AB, J_{AB}=10 Hz, 1H), 1.83 (AB, J_{AB}=10 Hz, 1H), 2.36-2.80 (m, 12H), 12.15 (br s, 2H, D_2O exchangeable); ^{13}C NMR [DMSO, 50 MHz]: δ_C 37.94 (t), 41.27 (d), 42.81 (t), 44.04 (d), 47.91 (d), 58.55 (d), 92.56 (s) and 171.40 (s); Anal. Calc. for $C_{15}H_{16}O_4$ C, 65.21; H, 5.84. Found C, 65.39; H, 5.71 %

General Procedure for preparing macrocycles **76** and **77**

A suspension of 2,6-pyridine dicarboxylic acid (4 mmol) was refluxed in freshly distilled thionyl chloride (10 mL) under argon overnight. The homogeneous mixture was concentrated in vacuo to afford **88** as a pale brown oil. Mixtures of diamine **86/87** (4 mmol) and NEt_3 (1.5 mL) in toluene (750 mL) and diacyl choride **88** (4 mmol) in toluene (750 mL) were added simultaneously, dropwise with stirring, to toluene (250 mL) during 10 h at 0 °C under argon. The resulting mixture was stirred at ambient temperature for 1 day and concentrated under reduced pressure. The product was purified via column chromatography on silica gel by eluting varying ratios of EtOAc/$CHCl_3$ followed by fractional recrystallisation of the eluate thereby obtained from toluene.

(4*S*,14*S*)-(-)-4,14-Diisopropyl-6,9,12-trioxa-5,15,21-triazabicyclo[15.5.1]henicosa-1(20),17(21),18-triene-2,16-dione (**77**).

Macrocycle **77** was prepared as described above. The crude product was purified by chromatography on silica gel using ethyl acetate/hexane as eluents to give a yellow oil from which the pure product **77** (26 %) was recrystallised from toluene to give white crystals: mp 84-85 °C; $[\alpha]^{22}_D$ -113.64 (c = 0.02, $CHCl_3$); IR (KBr): ν_{max} 3320-3350 (s),2963 (s), 1663 (vs), 1523 (s), 1115 (s) cm^{-1}; FAB^+ MS (*m*-Nitrobenzyl alcohol): m/z 408 $[M+H]^+$; ^1H NMR [$CDCl_3$, 300 MHz]: δ_H 0.90-1.10 (m, 12H), 2.07-2.23 (m, 2H), 3.52-4.00 (m, 12H), 8.00 (t, *J* = 5.5 Hz, 1H), 8.33 (d, *J* = 6 Hz, 2H), 8.45 (d, *J* = 8 Hz, 2H); ^{13}C NMR [$CDCl_3$, 75 MHz]: 19.86(q), 20.11(q), 29.73(d), 55.67(d), 70.30(t), 71.14(t), 72.13(t), 125.08(d), 138.67(d), 149.22(s), 163.38(s); Anal. Calc. for $C_{21}H_{33}N_3O_5$: C, 61.90; H, 8.16; N, 10.31; O, 19.63 Found: C, 62.00; H, 8.19; N, 10.33; O, 19.61 %

General Procedure for preparing macrocycles **78** and **79**

A solution of **82** (4 mmol) in oxalyl chloride (10 mL) was refluxed under argon during 12 h. The resulting homogeneous mixture was concentrated in vacuo to yield **83** as a clear oil. Mixtures of the diamine **86/87** (4 mmol) and NEt_3 (1.5 mL) in toluene (750 mL) and the diacyl chloride **83** (4 mmol) in toluene (750 mL) were added simultaneously, dropwise with stirring to toluene (250 mL) during 10 h at 0 °C under argon. The resulting mixture was stirred at ambient temperature during 1 day and concentrated under reduced pressure. The product was purified via column chromatography on silica gel by eluting with ethyl acetate/dichloromethane followed by fractional recrystallisation of the eluate thereby obtained from toluene.

Macrocycle **78**

Macrocycle **78** was prepared as described above. The crude product was purified by chromatography on silica gel by eluting with ethyl acetate/dichloromethane to give a clear oil from which the pure product **78** (37 %) was recrystallised from toluene to give colorless crystals: mp 94-97 °C; $[\alpha]^{22}_D$ +6.82° (c=0.01, CH_2Cl_2); IR (KBr): ν_{max} 3343(s), 3307(s), 2958(s), 2870(m), 1674(vs), 1517(s), and 1109(s) cm^{-1}; FAB^+ MS (*m*-Nitrobenzylalcohol), m/z 585 $[M+H]^+$. ^1H NMR [$CDCl_3$, 300 MHz]: δ_H 1.49 (AB, J_{AB}=10.5 Hz, 1H), 1.82 (AB, J_{AB}=10.6 Hz, 1H), 2.15-2.80 (m, 10H), 2.89 (AB, J_{AB}=15.5 Hz, 1H), 2.98 (AB, J_{AB}=14.8 Hz, 1H), 3.45-3.95 (m, 12H), 5.09-5.30 (m, 2H), 7.12-7.53 (m, 10H), 7.65 (d, J = 8.1 Hz, 1H), 7.74 (d, J = 8 Hz, 1H); ^{13}C NMR [$CDCl_3$, 75 Hz]: δ_C 39.55 (t), 39.58 (t), 41.00 (d), 41.35 (d), 43.15 (t), 43.68 (d), 43.98 (d), 46.22 (d), 49.76 (d), 52.80 (d), 52.85 (d), 56.36 (d), 60.06 (d), 70.22 (t), 70.89 (t), 70.94 (t), 73.91 (t), 73.94 (t), 93.98 (s), 94.05 (s), 126.62 (d), 127.01 (d), 128.04 (d), 140.25 (s), 140.32 (s), 169.14 (s); Anal. Calc. for $C_{35}H_{40}N_2O_6$: C, 71.90; H, 6.90; N, 4.79; O, 16.42. Found: C, 71.83; H, 7.00; N, 4.72; O, 16.36 %

Macrocycle **79**

Macrocycle **79** was prepared as described above. The crude product was purified via chromatography on silica gel by eluting with ethyl acetate/hexane as eluents to give a clear oil from which the pure product **79** (34 %) was recrystallised from chloroform/hexane to give white crystals: m.p. 103-105 °C; $[\alpha]^{22}_D$ -93.3 (c = 0.0074, $CHCl_3$); IR (KBr): ν_{max} 3305-3350(s), 1670(vs), 1529(s), 1120(s) cm^{-1}; FAB^+ MS (*m*-Nitrobenzylalcohol), m/z 517 $[M+H]^+$. ^1H NMR [$CDCl_3$, 300 MHz]: δ_H 0.78-0.96 (m, 12H), 1.53 (AB, J_{AB}=10.6 Hz, 1H), 1.80-1.95 (m, 3H), 2.40-2.96 (m, 12H), 3.45-3.70 (m, 10 H), 3.71-3.83 (m, 2H), 6.98 (d, J = 8 Hz, 1H), 7.12 (d, J = 8 Hz, 1H). ^{13}C NMR [$CDCl_3$, 50 MHz]: 19.25(q), 19.34(q), 29.50(d), 39.82 (t), 39.88 (t), 41.16 (d), 41.65 (d), 43.46 (t), 43.90 (d), 44.29 (d), 46.33 (d), 50.13 (d),

54.38 (d), 54.44 (d), 56.52 (d), 60.48 (d), 70.66 (t), 71.17 (t), 71.25 (t), 94.09 (s), 94.25 (s), 169.58 (s), 169.61 (s); Calc. for $C_{29}H_{44}N_2O_6$: C, 67.41; H, 8.58; N, 5.42; O, 18.58. Found: C, 67.38; H, 8.47; N, 5.39; O, 18.63 %

U-tube transport experiments

Cation transport experiments were performed in a simple U-tube apparatus by using a previously published procedure.[2] Thus, a solution of optically active macrocycle (27 mmol dm^{-3}) in $CHCl_3$ (10 mL) was placed in a 14 mm i.d. U-tube. The U-tube was designed with a condenser and it was thermostated at 30 °C.(Glenn) Into the source phase of the U-tube was introduced 5.0 mL of a solution that contained the guest ammonium salt (i.e., racemic methyl ester, 1.0 mmol and $LiPF_6$ (0.8 mol dm^{-3}) in aqueous HCl (and 0.08 mol dm^{-3}). Into the receiving phase of the U-tube was placed 0.10 mol dm^{-3} aqueous HCl (5.0 mL, 0.50 mmol). A small magnetic stirring bar was used to mix the $CHCl_3$ and aqueous layers at a constant rate. The UV absorbance of the aqueous receiving was measured at λ_{max} = 286 nm. The optical rotation measured using a 20 cm polarimetry cell (3 mL).

The rate of transport was slowed by using 0.8 mol dm^{-3} HCl in the source phase.

EXPERIMENTAL FOR CHAPTER 4

(*S*)-(+)-Methyl mandelate (**113**)

To a stirred solution of (*S*)-(+)-mandelic acid (1 eq, **112**) in dry methanol was slowly added thionyl chloride (2 eq) at -10 °C. The mixture was stirred at -10 °C for 10 minutes and then at room temperature for a further 4 hours. After evaporation of the solvent, the residue was dissolved in a mixture of ice, water and ether and layers were separated. The organic phase was washed with saturated brine, dried over $MgSO_4$ and filtered. The solvent was removed under reduced pressure.

NMR data identical to an authentic sample.

(*S*)-(+)-Methyl-2-phenyl-2-(tetrahydropyranyloxy)acetate (**114**)

To a mixture of 11.4 g (0.069 mol) of **113** and 8.65 g (0.103 mol) of dihydropyran in dry dichloromethane at 0 °C and under nitrogen was added a catalytic amount of pyridinium *p*-toluenesulphonate (0.8 g). The reaction mixture was stirred at 0 °C for 10 minutes and then at room temperature for 2 hours. The mixture was washed 3 times with ice-cold water, dried over $MgSO_4$ and filtered and the solvent removed under reduced pressure to yield the product (18.98 g).

NMR data identical to an authentic sample.

(*S*)-(+)-2-Phenyl-2-(tetrahydropyranyloxy)ethanol (**109**)

A solution of **114** (18.98 g, 0.076 mol) in THF was added dropwise to a stirred suspension of $LiAlH_4$ (4.33 g, 0.114 mol) in THF at 0°C under nitrogen for 45minutes. The solution was stirred at room temperature for 1 hour, refluxed for 3 hours and left to stir at ambient temperature overnight. The reaction was quenched by dilution with diethyl ether and dropwise addition of saturated Na_2SO_4 solution. The mixture was filtered, dried over $MgSO_4$ and solvent removed under reduced pressure to yield yellowish oil, (17.22 g). The product was purified via column chromatography using silica gel with Hexane/ Ethyl Acetate (70:30). NMR data identical to an authentic sample.

(*S*)-(+)-2-Methyl-2-(tetrahydropyranyloxy)ethanol (**110**)

(*S*)-(+)-Ethyl lactate (15.23 g, 0.13 mol, **115**), dihydropyran (18.9 g, 0.225 mol) and pyridinium *p*-toluenesulphonate (1 g) was stirred at room temperature in dry dichloromethane (300 ml) for 48hours. The solution was washed three times with ice water and once with saturated $NaHCO_3$. The organic layer was separated, dried over $MgSO_4$ and filtered. The solvent was removed under reduced pressure to yield a clear oil residue (25,31 g, 0.125 mol). This residue was dissolved in THF and added dropwise to a stirred solution of $LiAlH_4$ (7.40 g) in THF (200 ml). The mixture was stirred overnight under nitrogen at ambient temperature. Diluting with diethyl ether and dropwise addition of saturated Na_2SO_4 solution quenched the reaction. The mixture was filtered, dried over $MgSO_4$ and filtered again. The solvent was removed under reduced pressure to yield the product (**110**)as a clear oil.
NMR data identical to an authentic sample.

(*S*)-(+)-2-Phenyl-2-(tetrahydropyranyloxy)ethyl tosylate (**122**)

(*S*)-(+)-2-Phenyl-2-(tetrahydropyranyloxy)ethanol (3.54 g, 0.016 mol, **109**), *p*-toluenesulphonyl chloride (4.58 g, 0.024 mol) and triethylamine (10 ml) were stirred in dry dichloromethane (150 ml) overnight. The organic phase was washed with water (3 x 100 ml) and brine (2 x 100 ml), dried over $MgSO_4$ and filtered. The solvent was evaporated under reduced pressure resulting in the product (**122**) as a white solid.
NMR data identical to an authentic sample.

3,5-(2',2"-bis(hydroxyethyl))-4-oxahexacyclo(5.4.1.$0^{2,6}$.$0^{3,10}$.$0^{5,9}$.$0^{8,11}$)dodecane (**73**)

A solution of the diene (**81**, 5 g, 20.3 mmol) in dry methanol (150 mL) was cooled to -78 °C via application of an external dry ice-acetone bath and purged with argon during 20 minutes. Ozone was bubbled into the mixture until a blue-purple colour persisted, thereby indicating the presence of excess ozone and completion of reaction. Excess ozone was flushed from the reaction mixture with a stream of argon, and the reaction mixture was transferred to a 2 l

flask. Sodium borohydride (3 g, 81 mmol) was added over 1 hour to a stirred, ice bath cooled mixture of the ozonoide. The resulting mixture was stirred at ambient temperature for 12 hours and concentrated *in vacuo*. Excess sodium borohydride was quenched with 10 % HCl (200 ml) and extracted with ethyl acetate to give pure product (**73**, 4.4 g, 89 %) as a colourless microcrystalline solid: mp 153-153.5 °C; IR (KBr): ν_{max} 3320(m), 2980(s) cm^{-1}; ^1H NMR [$CDCl_3$, 300 MHz]: δ_H 1.52 (d, J=10.3 Hz, 1H), 1.70-2.05 (m, 4H), 2.28-2.69 (m, 9H), 3.50-3.86 (m, 6H); ^{13}C NMR [$CDCl_3$, 50 MHz]: δ_C 34.3 (t), 41.4 (d), 43.5 (t), 44.1 (d), 47.7 (d), 58.2 (d), 60.0 (t), and 92.4 (s).

Synthesis of PCU ditosylate (**106**)

To a solution of **73** (5 g, 0.0201 mol) and *p*-toluenesulphonyl chloride (11.49 g, 0.0603 mol) in THF (200 ml) was added finely powdered KOH (17 g, 0.3 mol). This mixture was stirred under nitrogen and monitored via TLC (hexane/ethyl acetate; 50:50). When no more diol (rf = 0.5) nor monotosylated product (rf = 0.2) were detected by TLC, water (100 ml) was added to the reaction vessel and the layers are separated. The aqueous phase was extracted with ethyl acetate and the combined organic layers were dried over anhydrous $MgSO_4$. The product was concentrated in *vacuo* and purified via column chromatography (ethyl acetate/hexane; 20:80) to give the product (**106**) as a colourless microcrystalline solid: ; ^1H NMR [$CDCl_3$, 300 MHz]: δ_H 1.43 (AB, J_{AB}=10.5 Hz, 1H), 1.77 (AB, J_{AB}=10.5 Hz, 1H), 2.03 (t, J = 7.0 Hz, 4H), 2.29-2.50 (m, 8H), 2.69 (s, 6H), 4.04 (t, J = 7.0 Hz, 4H), 7.29 (AB, J_{AB}=8.1 Hz, 4H), 7.72 (AB, J_{AB}=8.4 Hz, 4H).

Attempted synthesis of crown ethers **103/104** from **106** and **107/108**

A solution of PCU ditosylate (**106**, 1 eq.) and chiral diol (**107/108**, 1 eq.) in a dry solvent (THF/DMF) was added to a suspension of NaH (3 eq.) in a dry solvent while stirring under inert atmosphere. The reaction was monitored via TLC and when product formation was evident, the temperature was increased (up to 80 °C) *via* application of an external oil bath. Excess base was quenched by the addition of a minimum amount of water and the reaction mixture concentrated under reduced pressure. The residue was taken up in ethyl acetate and washed with water. The organic phase was dried and concentrated.

Attempted synthesis of ligands **120/121** from **106** and **109/110**

A solution of PCU ditosylate (**106**, 1 eq.) and chiral alcohol (**109/110**, 2 eq.) in a dry solvent (THF/DMF) was added to a suspension of NaH (3 eq.) in a dry solvent while stirring under inert atmosphere. The reaction was monitored via TLC and when product formation was evident, the temperature was increased (up to 80 °C) *via* application of an external oil bath.

Excess base was quenched by the addition of a minimum amount of water and the reaction mixture concentrated under reduced pressure. The residue was taken up in ethyl acetate and washed with water. The organic phase was dried and concentrated.

Attempted synthesis of ligands **120/121** from **73** and **122/123**

A solution of PCU diol (**73**, 1 eq.) and chiral monotosylated alcohol (**122/123**, 2 eq.) in a dry solvent (THF/DMF) was added to a suspension of NaH (3 eq.) in a dry solvent while stirring under inert atmosphere. The reaction was monitored via TLC and when product formation was evident, the temperature was increased (up to 80 °C) *via* application of an external oil bath. Excess base was quenched by the addition of a minimum amount of water and the reaction mixture concentrated under reduced pressure. The residue was taken up in ethyl acetate and washed with water. The organic phase was dried and concentrated.

General Procedure for preparing *N*-formyl amino acids **141-144**

Acetic anhydride (30eq) was added dropwise to a stirred solution of the amino acid (1 eq) dissolved in formic acid (approx. 50 ml per 1 g amino acid) at 0 °C. After addition of the acetic anhydride, the solution was stirred at room temperature overnight. The solution was treated with water (half volume of solution). The solvent was removed under reduced pressure to yield a white residue. This residue was recrystallised from water to yield the pure product.

(*R*)-(-)-2-formylamino-butyric acid (141)[3]: yield 63 %, m.p. 153-155 °C; ^{1}H NMR (DMSO) δ_H 0.87 (t, J = 8.1Hz, 3H, 1.50-1.85 (m, 2H), 4.22 (m, 1H), 8.02 (s, 1H, CHO), 8.34 (d, J = 7.1Hz, 1H)

(*S*)-(+)-*N*-formyl valine (142)[4] : yield 72 %, ^{1}H NMR (DMSO) δ_H 1.02 (d, J = 6Hz, 6H), 1.64 (m, 1H), 4.83 (m, 1H), 5.91 (d, J = 8Hz, 1H, NH), 8.25 (s, 1H, CHO)

(*S*)-(+)-*N*-formyl leucine (143)[5] : yield 85 %, ^{1}H NMR (DMSO) δ_H 0.97 (d, J = 6.2Hz, 6H), 1.70-1.92 (m, 3H), 4.10 (m, 1H), 5.95 (d, J = 8Hz, 1H, NH), 8.23 (s, 1H, CHO)

(*S*)-(+)-*N*-formyl phenylglycine (144)[6] : yield 80 %, ^{1}H NMR (DMSO) δ_H 5.37 (d, 1H, J= 8Hz), 7.27-7.43 (m, 5H), 8.07 (s, 1H), 9.01 (d, 1H, J = 9 Hz)

General Procedure for the synthesis of *N*-methyl amino alcohols **145-148**

N-formyl-amino acid (1 eq) was added to a stirred solution of lithium aluminium hydride (4 eq) in dry THF at 0 °C. The solution was allowed to gradually warm up overnight and stirred for a further 12 hours at ambient temperature. The reaction mixture was cooled back to 0°C and an equal volume of diethyl ether was added. The reaction was quenched with saturated Na_2SO_4. The solution was filtered and the solvent removed in *vacuo*.

(*R*)-(-)-2-methylamino-butan-2-ol (145)[7] : 75 %, ^{1}H NMR ($CDCl_3$) δ_H 0.82 (t, J = 7.7 Hz, 3H), 1.25-1.52 (m, 2H), 2.32 (s, 3H), 3.20-3.32 (m, 1H), 3.55 (d, J = 3.9Hz, 1H), 3.51 (d, J = 3.9, 1H)

(*S*)-(+)-*N*-formyl valinol (146)[8] **:** yield 96 %, ^{1}H NMR ($CDCl_3$) δ_H 0.95 (d, J = 7 Hz, 6H), 1.9 (m, 1H), 2.45 (s, 3H), 3.35 (s, 2H), 3.4-3.8 (m, 3H)

S-(+)-N-formyl leucinol **(147)**[9] **:** yield 96 %, ^{1}H NMR ($CDCl_3$) δ_H 0.9 (d, J = 7 Hz, 6H), 1.25 (t, J = 7 Hz, 2H), 1.5-1.9 (m, 1H), 2.4 (s, 3H), 3.3-3.7 (m, 3H), 3.8 (s, 2H)

(*S*)-(+)-*N*-formyl phenylglycinol (148)[6] : yield 90 %, ^{1}H NMR ($CDCl_3$) δ_H 2.32 (s, 2H), 2.68 (br s, 2H), 3.51-3.78 (m, 3H), 7.21-7.42 (m, 5H)

(*S*)-(+)-prolinol (149)[10] : yield 92 %, ^{1}H NMR ($CDCl_3$) δ_H 1.3-1.5 (m, 1H), 1.6-1.9 (m, 4H), 2.8-3.0 (m, 2H), 3.2-3.3 (m, 1H), 3.3-3.4 (m, 1H), 3.4-3.8 (m, 2H)

General Procedure for preparing ligands **132-136**

A mixture of the amino alcohol (2.2 eq.), PCU ditosylate (1 eq.) and Na_2CO_3 in CH_3CN was refluxed for 4 days under argon. The reaction mixture was cooled, filtered and concentrated *in vacuo*. The residue was purified via column chromatography on silica gel (Merck 7734).

Ligand 132 was prepared as described above. The crude product was purified by chromatography on silica gel using $CHCl_3$/MeOH/NH_4OH; 88:10:2 as eluents to give the product as a clear oil (52 %). $[\alpha]^{20}_D$ –7.76 (c = 5, $CHCl_3$); IR (KBr): ν_{max} 3405(br, s), 2961(vs), 1220(m), 798(m) cm^{-1}; FAB$^+$ MS (*m*-Nitrobenzyl alcohol): *m/z* 419 $[M+H]^+$; ^{1}H NMR [$CDCl_3$, 300 MHz]: δ_H 0.2 (t, 6H), 0.98-1.15 (m, 2H), 1.40-1.60 (m, 3H), 1.75-1.98 (m, 5H), 2.15 (s, 6H), 2.25-2.70 (m, 12H), 3.15 (t, 2H), 3.55 (d, J = 4.4Hz, 2H), 3.90 (d, J = 4.4Hz, 2H); ^{13}C NMR [$CDCl_3$, 75 MHz]: δ_C 11.62 (q), 17.74 (t), 17.79 (t), 31.32 (t), 35.59 (q), 35.65 (q), 41.52 (d), 41.59 (d), 43.44 (t), 44.26 (d), 47.76 (d), 47.85 (d), 50.22 (t), 50.28 (t), 58.51 (d), 58.63 (d), 60.47 (t), 66.07 (d), 66.14 (d), 95.03 (s), 95.08 (s); Anal. Calc. for $C_{25}H_{42}N_2O_3$ C, 71.73; H, 10.11; N, 6.69; O, 11.47 Found C, 71.65; H, 10.21; N, 6.72; O, 11.53 %

Ligand 133 was prepared as described above. The crude product was purified by chromatography on silica gel using $CHCl_3$/MeOH/NH_4OH; 93:5:2 as eluents to give the product as a clear oil (64 %). $[\alpha]^{20}_D$ –8.98(c = 2.3, $CHCl_3$); IR (KBr): ν_{max} 3343(br, s), 2952(vs), 1454(m), 1056(m) cm^{-1}; FAB$^+$ MS (*m*-Nitrobenzyl alcohol): *m/z* 446 $[M+H]^+$; ^{1}H NMR [$CDCl_3$, 300 MHz]: δ_H 0.70 (d, J = 6.6Hz, 6H), 0.85 (d, J = 6.6Hz, 6H), 1.48 (AB, J_{AB} = 10.5Hz, 1H), 1.62-1.93 (m, 5H), 2.1-2.9 (m, 22H), 3.0-3.12 (m, 2H), 3.46-3.50 (m, 2H), 4.1 (br s, 2H, deuterium exchangeable); ^{13}C NMR [$CDCl_3$, 75 MHz]: δ_C 19.83 (q), 22.20 (q),

27.87 (q), 31.06 (t), 34.91 (q), 35.07 (q), 41.28 (d), 41.45 (d), 43.39 (t), 44.02 (d), 44.11 (d), 46.83 (d), 48.32 (d), 52.49 (t), 52.63 (t), 57.45 (d), 58.87 (d), 59.31 (t), 71.22 (d), 71.29 (d), 95.08 (s), 95.18 (s); Anal. Calc. for $C_{27}H_{46}N_2O_3$ C, 72.60; H, 10.38; N, 6.27; O, 10.75 Found C, 72, 31; H, 10.35; N, 6.35; O, 10.69 %

Ligand 134 was prepared as described above. The crude product was purified by chromatography on silica gel using $CHCl_3$/MeOH/NH_4OH; 93:5:2 as eluents to give the product as a clear oil (62 %). $[\alpha]^{20}_D$ +23.22(c = 5, $CHCl_3$); IR (KBr): ν_{max} 3411(br, s), 2954(vs), 1464(m), 1057(m), 1032(m) cm^{-1}; FAB^+ MS (*m*-Nitrobenzyl alcohol): *m/z* 475 $[M+H]^+$; ^1H NMR [$CDCl_3$, 300 MHz]: δ_H 0.85 (t, 12H), 0.91-1.05 (m, 2H), 1.19-1.32 (m, 2H), 1.48-1.52 (m, 3H), 1.79-1.98 (m, 5H), 2.15 (s, 6H), 2.25-2.80 (m, 16H), 3.10-3.21 (m, 2H), 3.35-3.45 (m, 2H); ^{13}C NMR [$CDCl_3$, 75 MHz]: δ_C 22.15 (q), 23.74 (q), 25.30 (d), 25.35 (d), 31.31 (t), 33.73 (t), 33.78 (t), 35.64 (q), 35.72 (q), 41.52 (d), 41.58 (d), 43.46 (t), 44.25 (d), 47.88 (d), 49.83 (t), 58.55 (d), 58.59 (d), 61.11 (t), 62.05 (d), 62.09 (d), 95.03 (s), 95.08 (s); Anal. Calc. for $C_{29}H_{50}N_2O_3$ C, 73.37; H, 10.62; N, 5.90; O, 10.11 Found C, 73.25; H, 10.56; N, 6.00; O, 10.15.

Ligand **135**: was prepared as described above. The crude product was purified by chromatography on silica gel using 93 $CHCl_3$:5 MeOH:2 NH_4OH as eluents to give the product as a waxy solid (59%). $[\alpha]^{20}_D$ +28.57(c = 7, $CHCl_3$); IR (KBr): ν_{max} 3393(br, s), 2961(vs), 1458(m), 1026(m), 706(m) cm^{-1}; FAB^+ MS (*m*-Nitrobenzyl alcohol): *m/z* 515 $[M+H]^+$; ^1H NMR [$CDCl_3$, 300 MHz]: δ_H 1.49 (AB, J_{AB} = 10.5Hz, 1H), 1.85 (AB, J_{AB} = 10.5Hz, 1H), 1.89-2.05 (m, 4H), 2.15 (s, 6H), 2.25-2.70 (m, 12H), 3.05 (br s, 2H, deuterium exchangeable), 3.55-3.65 (m, 2H), 3.70-3.82 (m, 2H); 3.86-4.00 (m, 2H), 7.10-7.40 (m, 10H); [$CDCl_3$, 75 MHz]: δ_C 30.28 (t), 36.95 (q), 37.17 (q), 41.53 (d), 41.59 (t), 43.48 (t), 44.25 (d), 44.30 (d), 47.90 (d), 47.99 (d), 50.06 (t), 50.21 (t), 58.53 (d), 58.68 (d), 60.75 (t), 68.77 (d), 68.83 (d), 95.16 (s), 95.20 (s), 127.80 (d), 128.20 (d), 128.96 (d), 135.69 (s), 135.79 (s); Anal. Calc. for $C_{33}H_{42}N_2O_3$ C, 77.01; H, 8.22; N, 5.44; O, 9.33 Found C, 76.90; H, 8.18; N, 5.57, O, 9.27 %

Ligand 136 was prepared as described above. The crude product was purified by chromatography on silica gel using $CHCl_3$/MeOH/NH_4OH; 93:5:2 as eluents to give the product as a waxy solid (60 %). $[\alpha]^{20}_D$ -39.44(c = 5, $CHCl_3$); IR (KBr): ν_{max} 3405(br, m), 3148(br, s), 2954(vs), 1370(m), 1088(m) cm^{-1}; FAB^+ MS (*m*-Nitrobenzyl alcohol): *m/z* 415 $[M+H]^+$; ^1H NMR [$CDCl_3$, 300 MHz]: δ_H 1.49 (AB, J_{AB} = 10.5Hz, 1H), 1.60-2.10 (m, 13H), 2.15-2.62 (m, 16H), 2.74-2.84 (m, 2H), 3.08-3.64 (m, 6H, 2H are deuterium exchangeable);

^{13}C NMR [$CDCl_3$, 75 MHz]: δ_C 23.55 (t), 27.51 (t), 31.38 (t), 41.56 (d), 43.44 (t), 44.22 (d), 44.27 (d), 47.74 (d), 48.09 (d), 50.90 (t), 50.94 (t), 54.24 (t), 54.27 (t), 58.54 (d), 58.87 (d), 62.24 (t), 65.17 (d), 65.21 (d), 95.00 (s), 95.09 (s); $C_{25}H_{38}N_2O_3$ C, 72.43; H, 9.24; N, 6.76; O, 11.58 Found C, 72, 35; H, 9.17; N, 6.70; O, 11.49 %

General Procedure for the enantioselective addition of diethylzinc to benzaldehyde promoted by enantiopure ligands **132-136**

To a solution of the ligand (0.125 mmol) in dry toluene (5 ml) under a nitrogen atmosphere at ambient temperature, was added a solution of $ZnEt_2$ in hexane (1.0 M, 1.25 ml, 1.25 mmol). The mixture was stirred for 30 min, and then benzaldehyde (60 mg, 0.5 mmol) was added. The mixture was monitored by GC analysis until no more benzaldehyde was present and stirred for a further 48 hours. The reaction was quenched by adding 10% HCl and extracted with Et_2O and the organic phase was washed with brine and dried over anhydrous Na_2SO_4. After evaporation of the solvent, the crude oil was purified via prep. TLC (hexane/ethyl acetate) and its enantiomeric excess determined by chiral GC. The *ee* was calculated from the area under the peaks and using the formula: (areaA – areaB)/(areaA + areaB), where areaA is the larger area. The dominant enantiomer was determined by polarimetry.

EXPERIMENTAL FOR CHAPTER 5

General procedure for synthesis of macrocycles **168-171**

To a suspension of NaH (4 eq.) in THF (100ml/0.5 NaH) was added a solution of the diamino diol (**132-135**, 1 eq.) and α,α'-dibromo-o-xylene (1 eq.) dropwise (8 hours) under a nitrogen atmosphere at ambient temperature. The reaction mixture was stirred for a further 12 hours after dropping had been completed. The solution was filtered and concentrated *in vacuo* to give the crude product as a highly viscous oil. This oil was chromatographed on silica gel by eluting with chloroform/methanol/ammonium hydroxide; 96:2:2 to afford the pure macrocycles.

Macrocycle 168: was eluted from the column as a single component (TLC), but NMR spectroscopy revealed the presence of at least two compounds.

Macrocycle 169: clear oil (17 %). $[\alpha]^{20}_D$ +2.124(c = 2, $CHCl_3$); IR (KBr): ν_{max} 2952(vs), 1460(m), 1089(m), 744(m) cm^{-1}; FAB^+ MS (*m*-Nitrobenzyl alcohol): *m/z* 548 $[M+H]^+$; ^1H NMR [$CDCl_3$, 300 MHz]: δ_H 0.90 (d, J = 6.6Hz, 6H), 0.95 (d, J = 6.6Hz, 6H), 1.49 (AB, J_{AB} = 10 Hz, 1H), 1.68-3.13 (m, 27H), 3.35-3.82 (m, 4H), 4.33-4.84 (m, 4H), 7.12-7.54 (m, 4H),

^{13}C NMR [$CDCl_3$, 75 MHz]: δ_C 19.52 (q), 21.09 (q), 28.26 (d), 28.41 (d), 29.67 (t), 38.44 (q), 38.81 (q), 41.24 (d), 41.39 (d), 43.48 (t), 42.79 (d), 43.88 (d), 47.08 (d), 48.61 (d), 50.15 (t), 50.52 (t), 57.89 (d), 59.29 (d), 68.82 (t), 70.79 (t), 70.87 (t), 94.61 (s), 127.58 (d), 127.89 (d), 127.99 (d), 128.19 (d); 136.08 (s), 136.27 (s); Anal. Calc. for $C_{35}H_{52}N_2O_3$ C, 76.60; H, 9.55; N, 5.10; O, 8.75. Found C, 76.52; H, 9.49; N, 5.07; O, 8.80 %

Macrocycle 170: waxy solid (42 %) $[\alpha]^{20}_D$ +17.02(c = 5, $CHCl_3$); IR (KBr): ν_{max} 2954(vs), 1464(m), 1088(m) cm^{-1}; FAB$^+$ MS (*m*-Nitrobenzyl alcohol): *m/z* 576 $[M+H]^+$; ^{1}H NMR [$CDCl_3$, 300 MHz]: δ_H 0.85 (t, 12H), 1.10-1.35 (m, 4H), 1.37-1.51 (AB, J_{AB} 10 Hz, 1H), 1.53-1.68 (m, 2H); 1.71-2.00 (m, 5H), 2.1-2.95 (m, 20H), 3.32-3.48 (m, 2H), 3.5-3.65 (m, 2H); 4.45-4.65 (m, 4H), 7.15-7.45 (m, 4H); ^{13}C NMR [$CDCl_3$, 75 MHz]: δ_C 22.78 (q), 22.98 (q), 25.29 (d), 30.30 (t), 30.47 (t), 37.79 (q), 37.91 (q), 38.06 (t), 38.16 (t), 41.33 (d), 41.41 (d), 43.49 (t), 43.90 (d), 47.59 (d), 48.53 (d), 50.19 (t), 50.51 (t), 58.15 (d), 59.08 (d), 60.49 (d), 60.55 (d), 70.84 (t), 70.97 (t), 71.08 (t), 71.12 (t), 94.78 (s), 127.39 (d), 127.47 (d), 128.21 (d), 128.37 (d), 136.52 (s); Anal. Calc. for $C_{37}H_{56}N_2O_3$ C, 77.04; H, 9.78; N, 4.86; O, 8.32. Found C, 77.92; H, 9.73; N, 4.83; O, 8.40 %

Macrocycle 171: waxy solid (35 %) $[\alpha]^{20}_D$ +11.3(c = 5, $CHCl_3$); IR (KBr): ν_{max} 2923(vs), 1452(m), 1088(m) cm^{-1}; FAB$^+$ MS (*m*-Nitrobenzyl alcohol): *m/z* 617 $[M+H]^+$; ^{1}H NMR [$CDCl_3$, 300 MHz]: δ_H 1.49 (AB, J_{AB} = 10.5Hz, 1H), 1.70-2.73 (m, 25H), 2.80-2.94 (m, 4H), 3.65-4.00 (m, 4H); 4.50-4.65 (m, 4H), 7.15-7.42 (m, 14H), ^{13}C NMR [$CDCl_3$, 75 MHz]: δ_C 30.28 (t), 39.70 (q), 39.79 (q), 41.31 (d), 41.52 (d), 43.53 (t), 43.88 (d), 43.90 (d), 47.34 (d), 48.64 (d), 50.08 (t), 50.24 (t), 57.98 (d), 59.27 (d), 68.31 (d), 70.98 (t), 71.08 (t), 72.28 (t), 94.99 (s), 95.04 (s), 127.18 (d), 127.23 (d), 127.31 (d), 127.57 (d), 128.19 (d), 128.22 (d), 128.25 (d), 128.32 (d), 128.40 (d), 128.43 (d), 128.46 (d), 128.49 (d), 128.52 (d), 128.58 (d), 136.24 (s), 136.43 (s); $C_{41}H_{48}N_2O_3$ C, 79.83; H, 7.84; N, 4.54; O, 7.78. Found C, 79.79; H, 7.82; N, 4.48; O, 7.82 %

General procedure for the Michael addition reaction used to obtain data for tables 8 and 9
A mixture of the macrocycle (0.05 mmol) and base (0.05 mmol) in toluene (2 ml) was stirred for 30 minutes at ambient temperature under a nitrogen atmosphere. The reaction mixture was cooled to –78 °C, methyl phenylacetate (2 mmol) was added and stirred for 10 minutes followed by the addition of methyl acrylate (1 mmol). The reaction was monitored via TLC (Hexane/EtOAc; 9:1) and the spots were detected with UV and anisaldehyde reagent (the product, **174**, orange coloured spot). The reaction was quenched with saturated NH_4Cl (4 ml) and extracted with diethyl ether (4 ml). The solution is concentrated *in vacuo* and product

purified *via* column chromatograph (silica, Hexane/EtOAc; 9:1). The optical purity was determined by dividing the specific rotation of the product by the specific rotation of the literature value and this enabled the calculation of the *ee*.

General procedure for the Michael addition reaction used to obtain data for Table 10
A mixture of methyl phenylacetate (2 mmol) and base (0.05 mmol) in toluene (2 ml) was stirred for 30 minutes at ambient temperature under a nitrogen atmosphere. To this was added the macrocycle (0.05 mmol), cooled to –78 °C and methyl acrylate (1 mmol) was added. The reaction was monitored via TLC (Hexane/EtOAc; 9:1) and the spots were detected with UV and anisaldehyde reagent (**16**, orange coloured spot). The reaction was quenched with saturated NH_4Cl (4 ml) and extracted with diethyl ether (4 ml). The solution was concentrated *in vacuo* and product purified *via* column chromatograph (silica, Hexane/EtOAc; 9:1). The *ee* was monitored by measuring the optical rotation and comparing that to the literature value.

General procedure for the Michael addition reaction used to obtain data for Table 11
The corresponding macrocycle (0.05 mmol) and sodium methoxide (0.05 mmol) was added to a solution of chalcone (1.44 mmol) and 2-nitropropane (3.36 mmol) in dry toluene (3 ml). The mixture was stirred under inert atmosphere at ambient temperature. After the desired reaction time, water (5 ml) and toluene (5 ml) was added. The organic phase was separated and dried over Na_2SO_4. The solvent was evaporated and the crude product purified by column chromatography (silica, Hexane/EtOAc; 9:1)

REFERENCES

1. Marchand, A. P.; Huang, Z.; Chen, Z.; Hariprakasha, H. K.; Namboothiri, I. N. N.; Brodbelt, J. S.; Reyzer, M. L. *J. Heterocyclic Chem.* **2001**, *38*, 1361.
2. Sogah, G.D.Y.; Cram, D.J. *J.Am.Chem.Soc.* **1979**, *101*, 3035.
3. McMeekin; Cohn; Weare *J.Amer.Chem.Soc.* **1936**; 2175.
4. Muramatsu, I. Et al. *Bull.Chem.Soc.Jap.* **1965**; 244.
5 Aizpurua, J.M.; Paloma, C. Synth. Commun. **1983**; *13*, 745.
6. Huszthy, P.; Oue, M.; Bradshaw, J.S.; Zhu, C.Y.; Wang, T. *J.Org.Chem.* **1992**, *57*, 5383.
7. Touet, J.; Baudouin, S.; Brown, E. *J.Chem.Res.Miniprint* **1996**; *5*; 1251.
8. Salvatore, R. N.; Chu, F.; Nagle, A. S.; Kapxhiu, E. A.; Cross, R. M.; Jung, K. W. *Tetrahedron* **2002** *58*, 3329. Karim, A.; Mortreux, A.; Petit, F.; Buono, G.; Pfeiffer, G.; Siv, C.; *J.Organomet.Chem.*; **1986**; 93.
9. Aitali, M.; Allaoud, S.; Karim, A.; Meliet, C.; Mortreux, A. *Tetrahedron:Asymmetry* **2000**, *11*, 1367.
10. Itsuno, S.; Ito, K.; Hirao, A.; Nakahama, S. *J.Chem.Soc.Perkin Trans.1* **1984**; *12*; 2887.

APPENDIX 1

SPECTRA

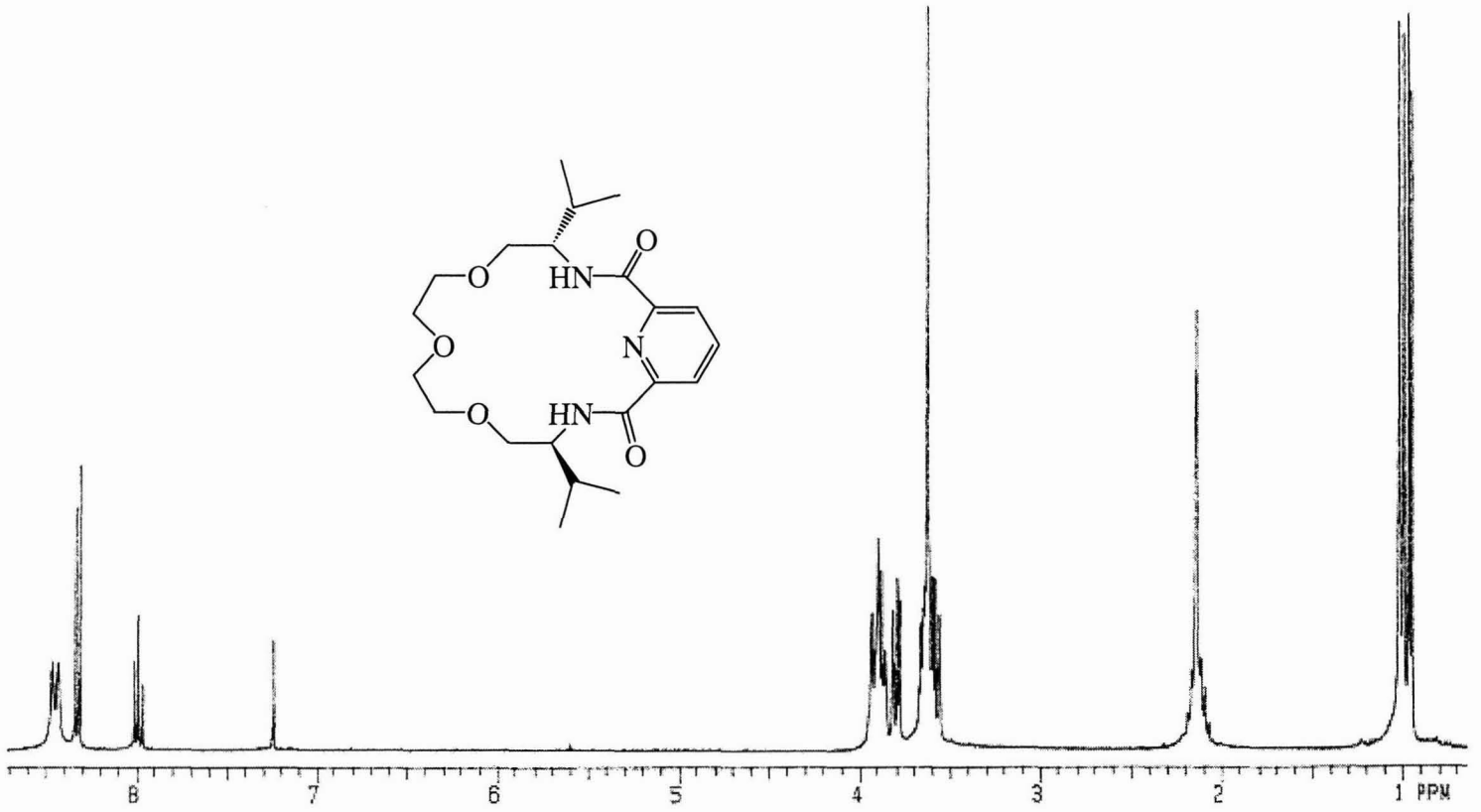

^{1}H nmr ($CDCl_3$) 200 MHz of macrocycle 77

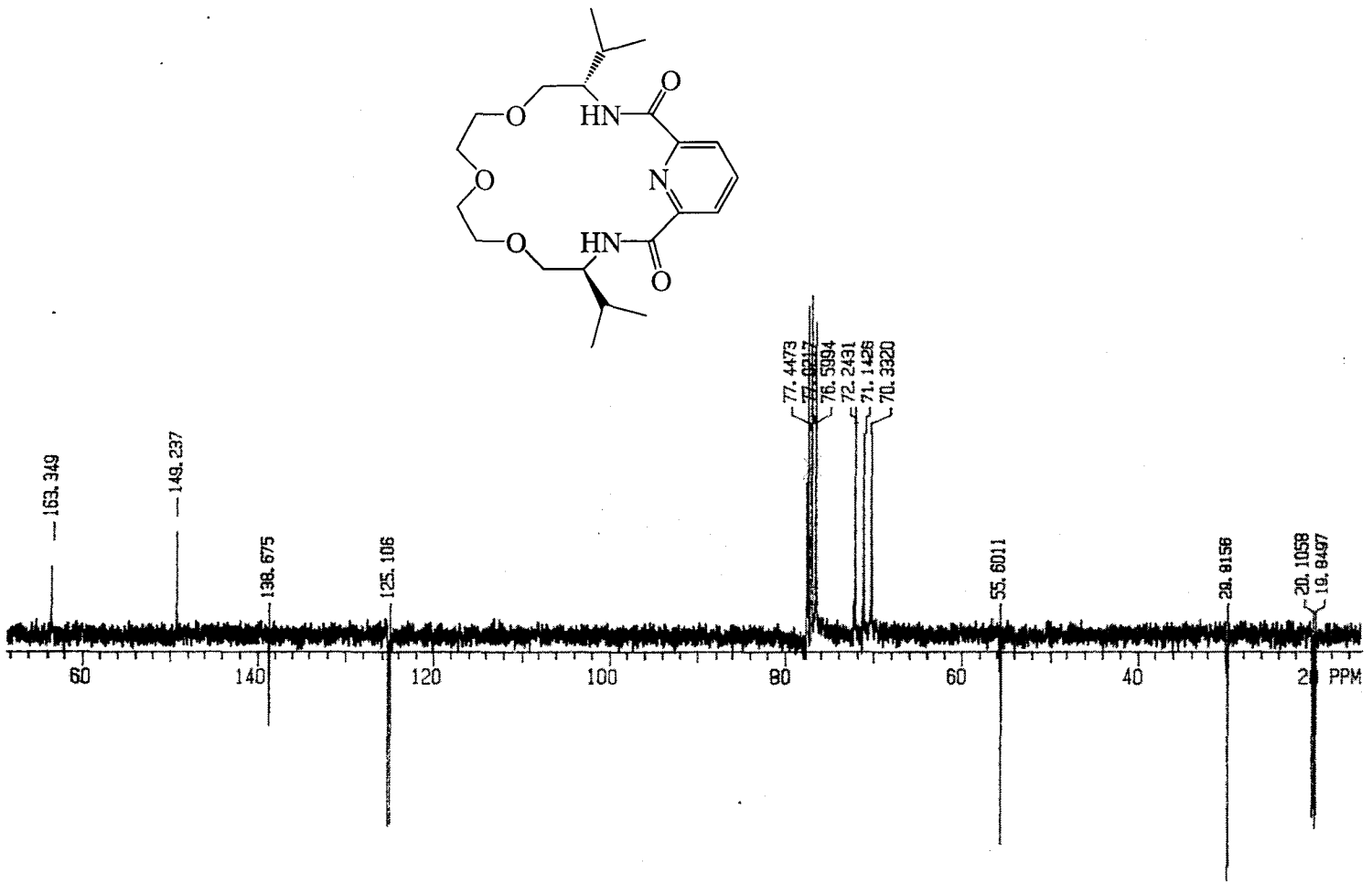

^{13}C APT nmr ($CDCl_3$) 50 MHz of macrocycle 77

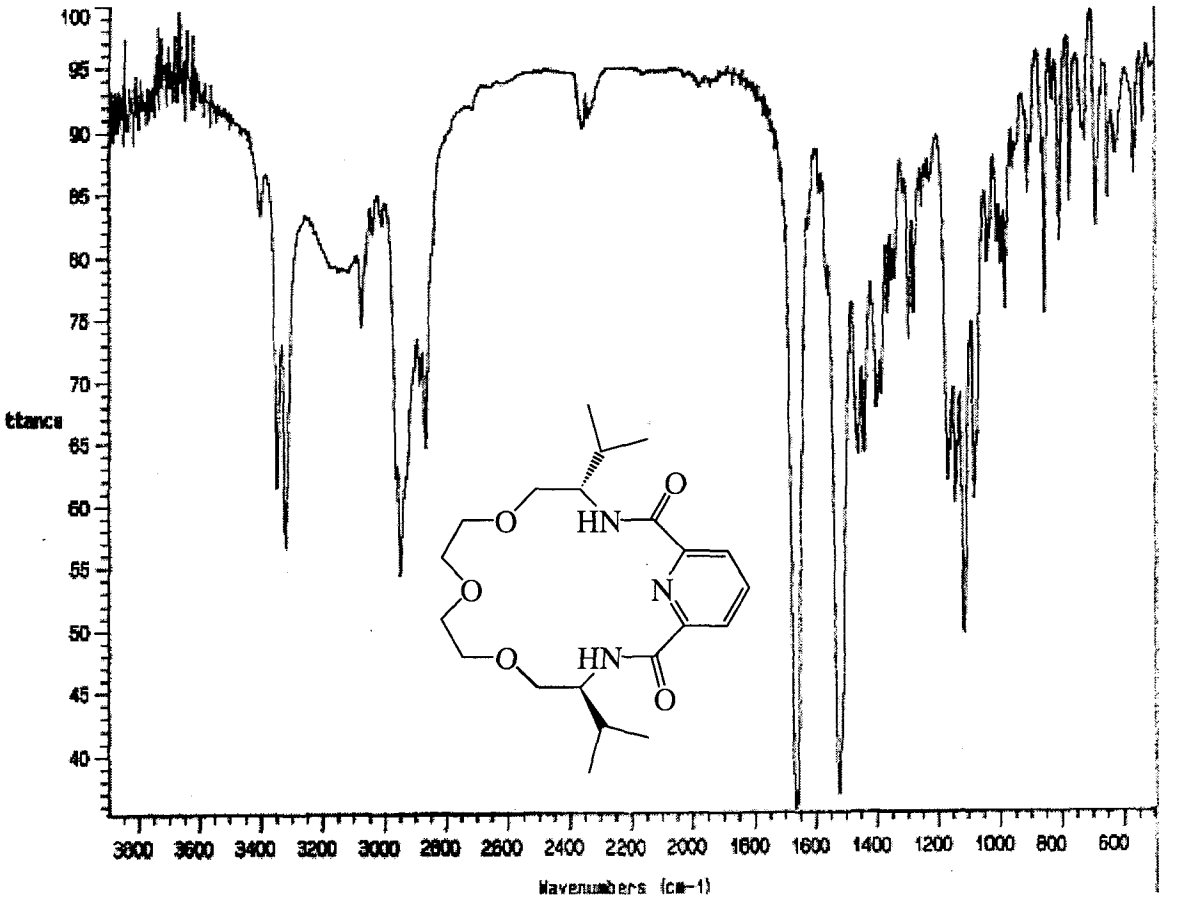

IR spectrum of macrocycle 77

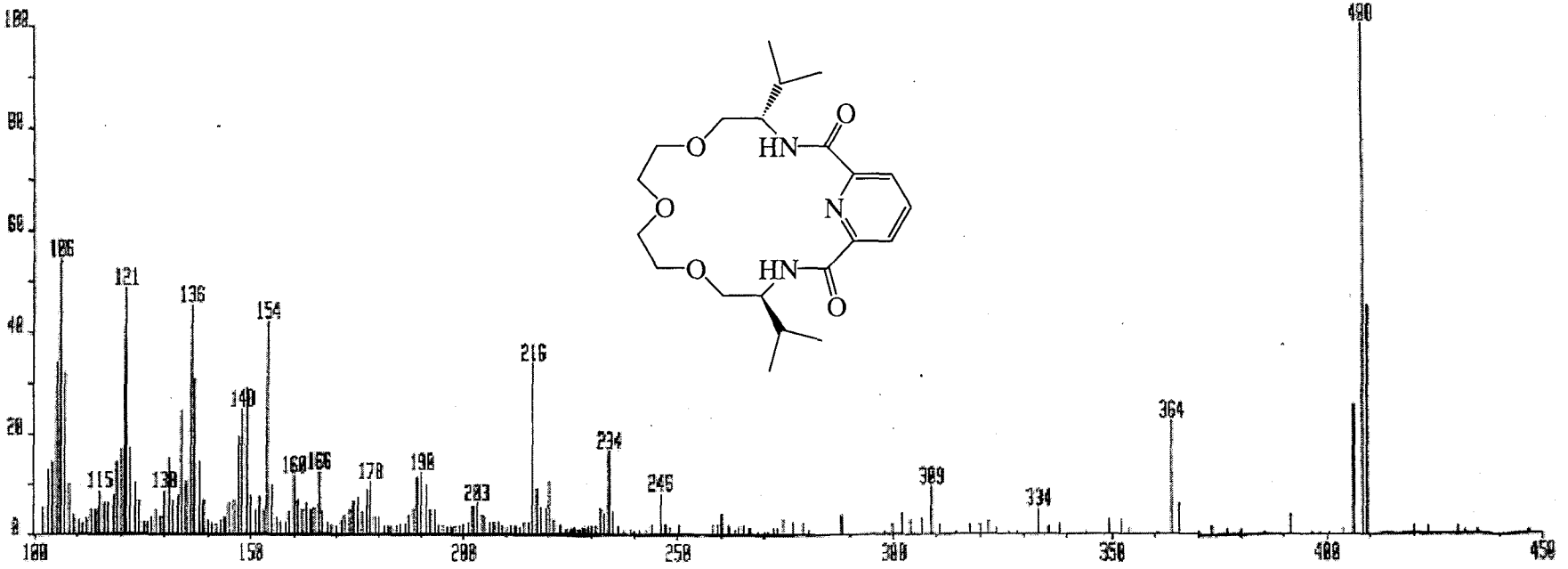

CI MS of macrocycle 77

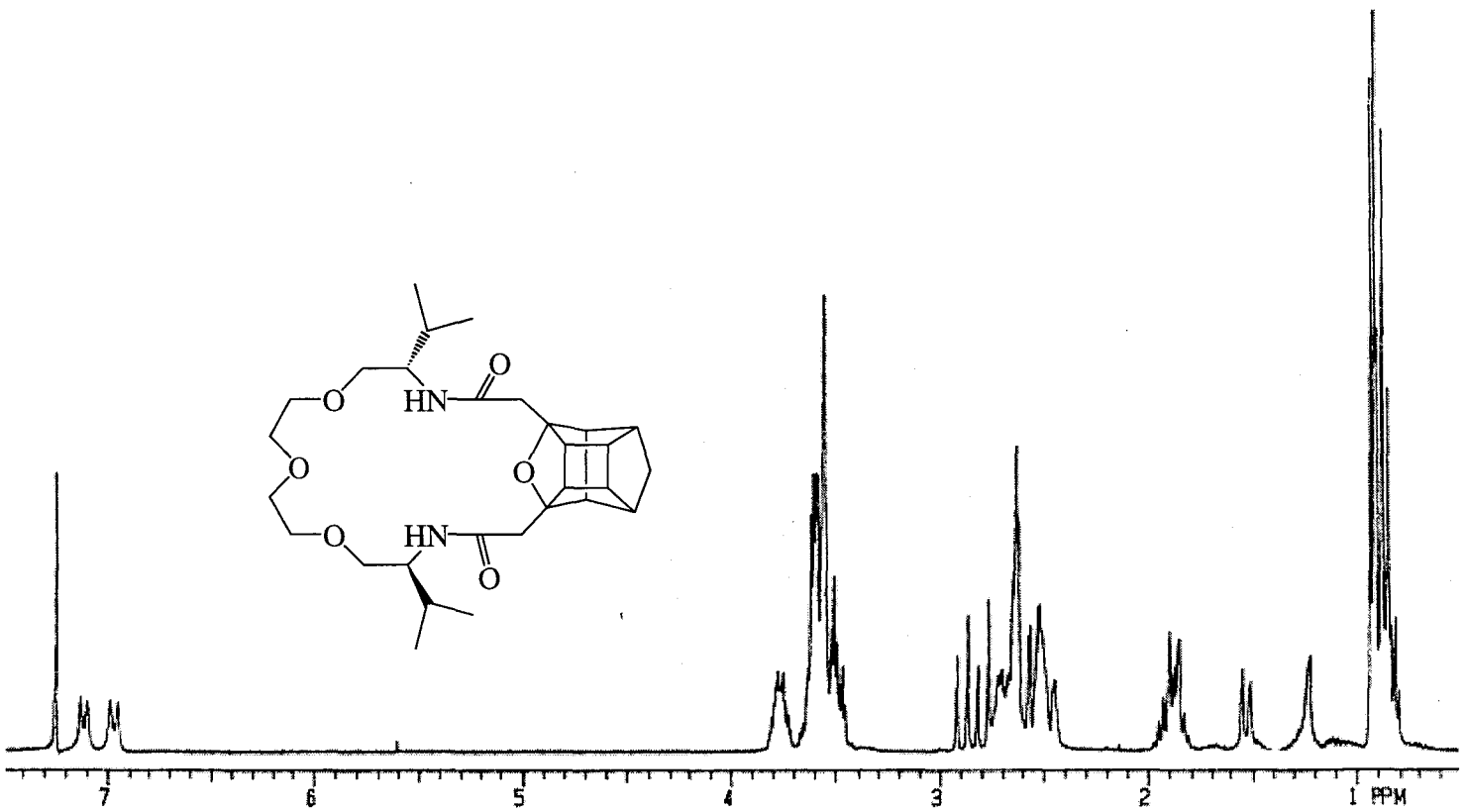

^{1}H nmr ($CDCl_3$) 200 MHz of macrocycle 79

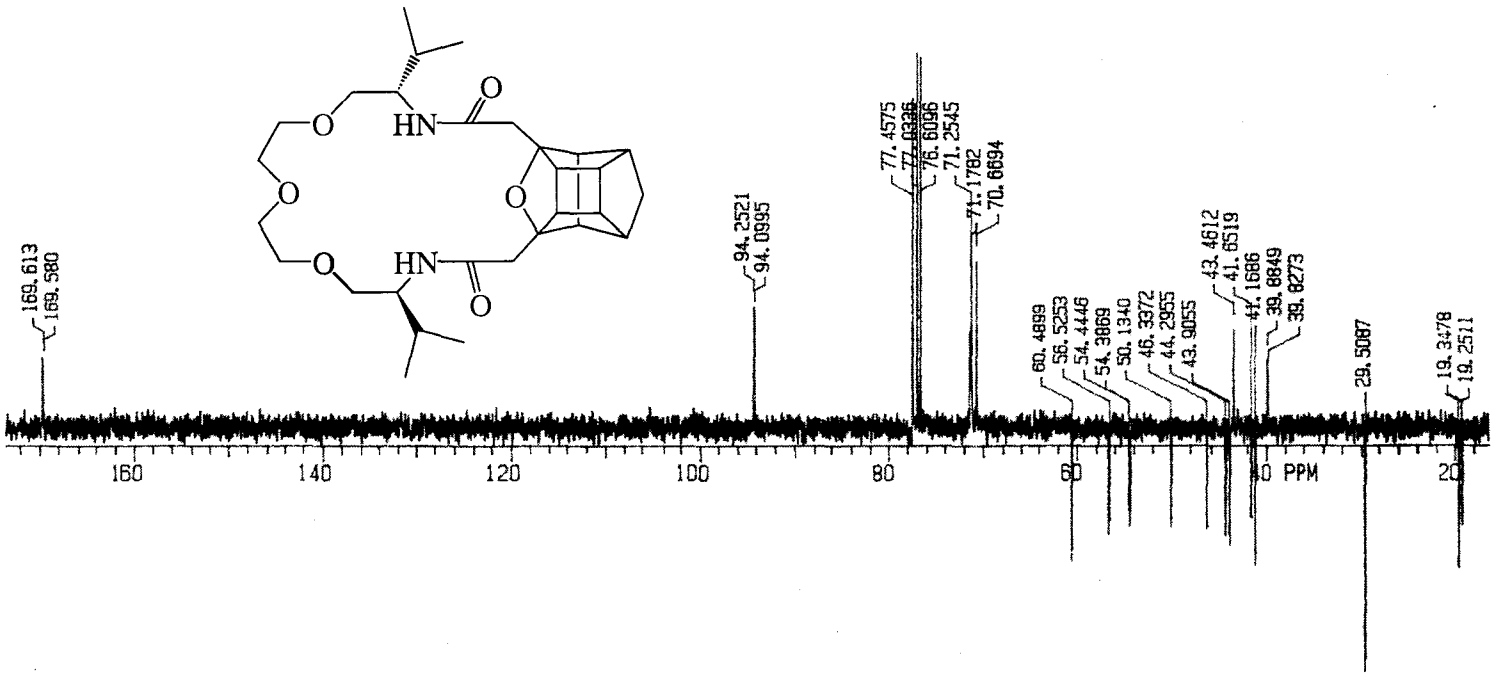

^{13}C APT nmr ($CDCl_3$) 50 MHz of macrocycle 79

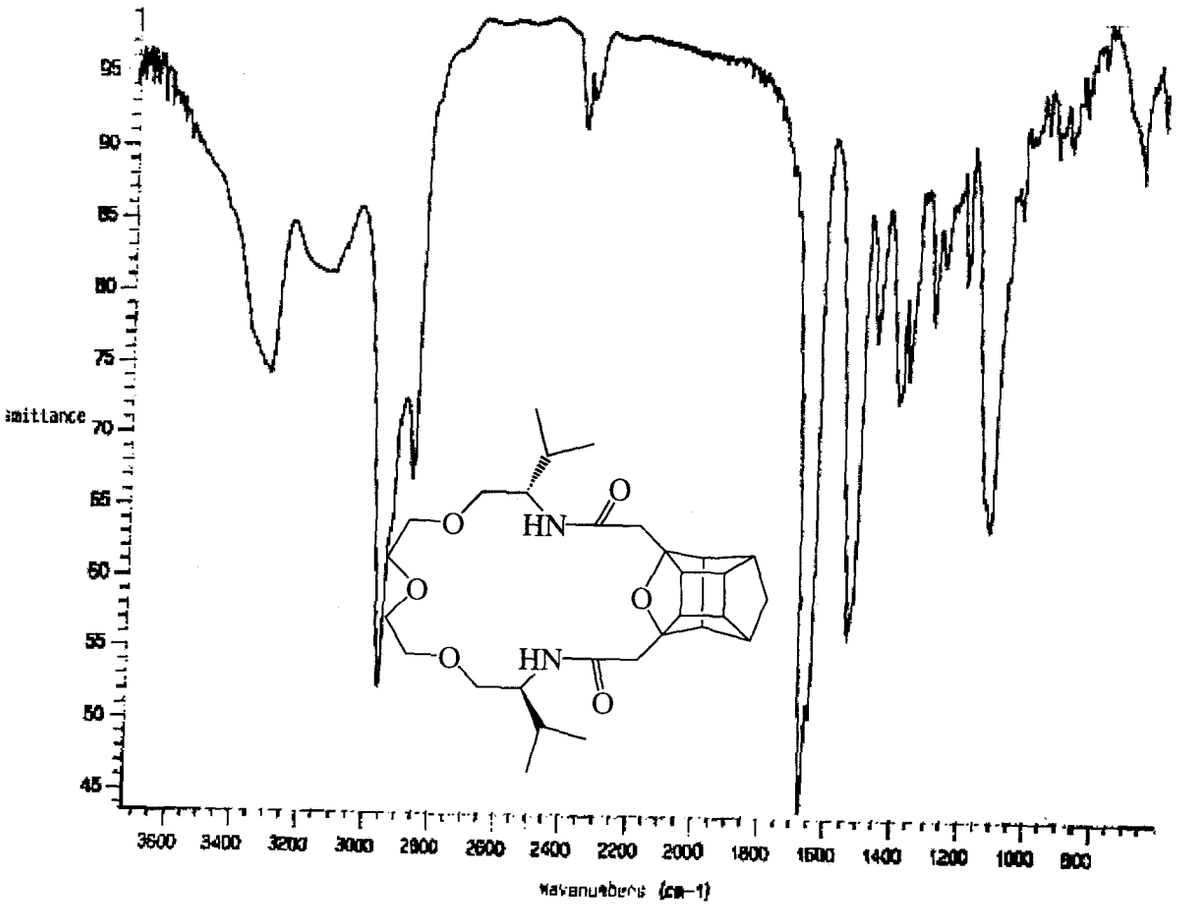

IR spectrum of macrocycle 79

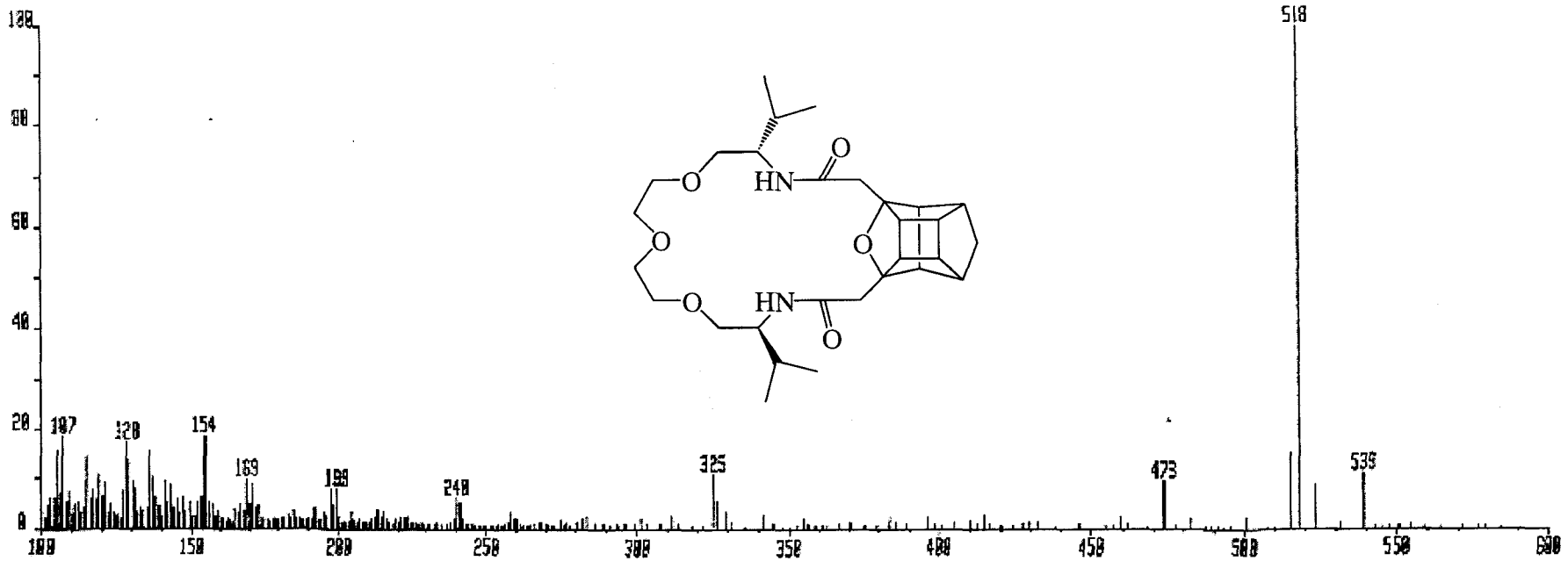

CI MS of macrocycle 77

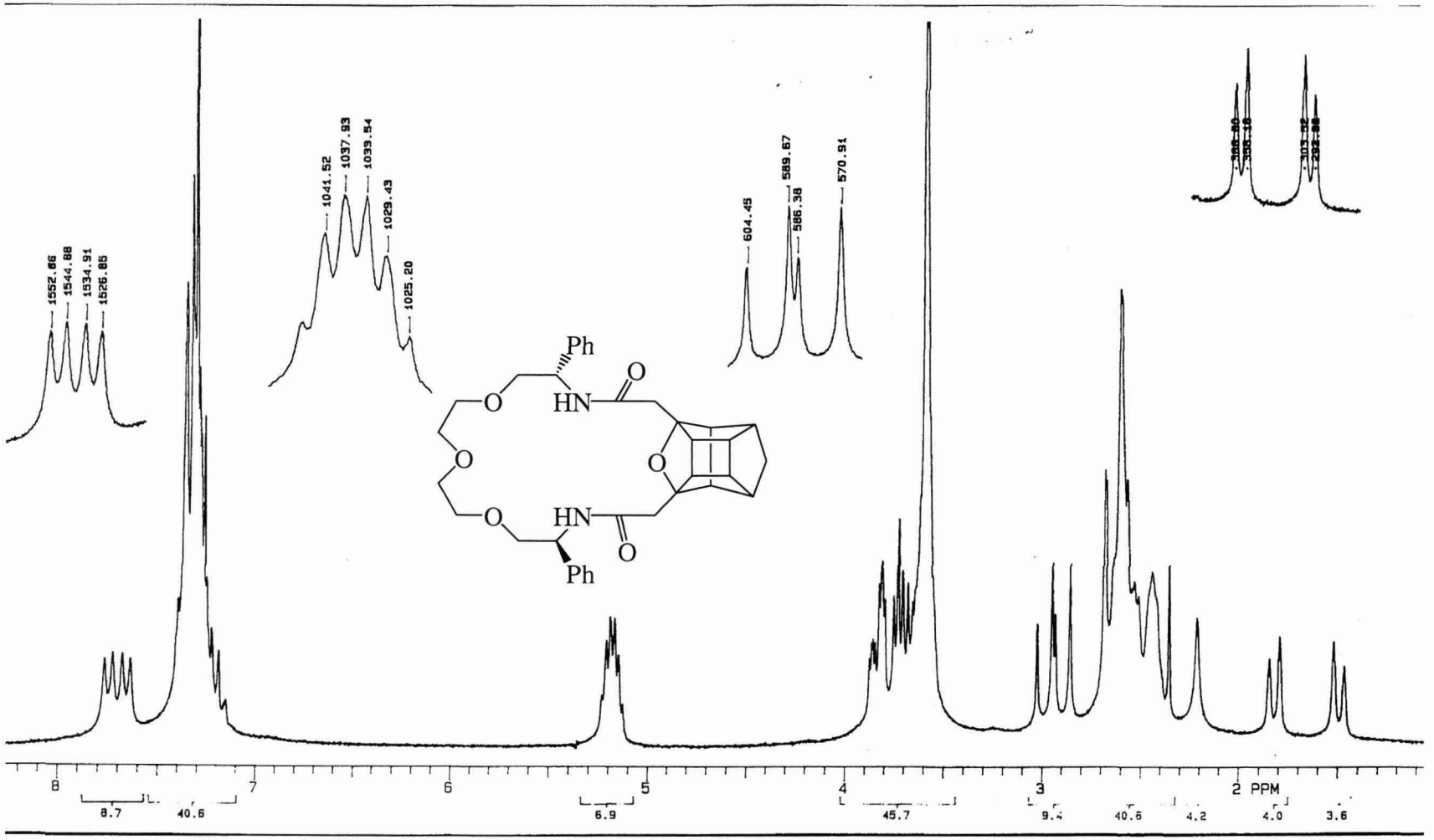

^{1}H nmr ($CDCl_3$) 200 MHz of macrocycle 78

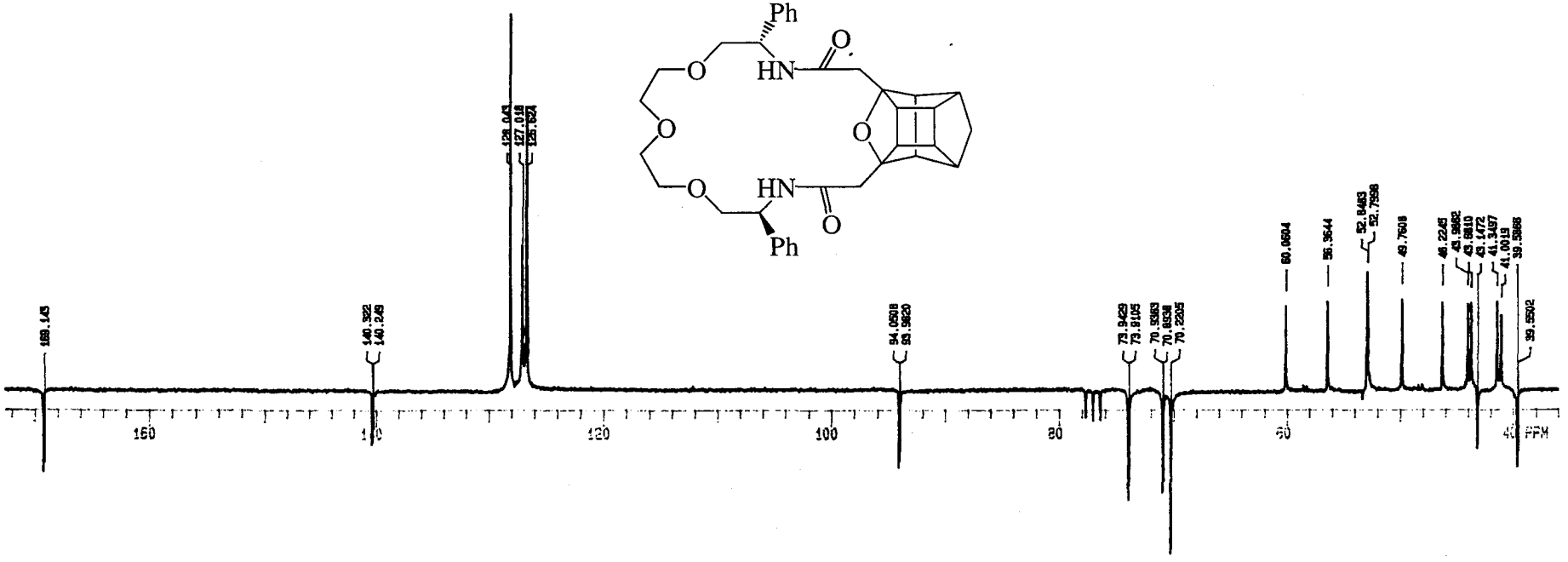

^{13}C APT nmr ($CDCl_3$) 50 MHz of macrocycle 78

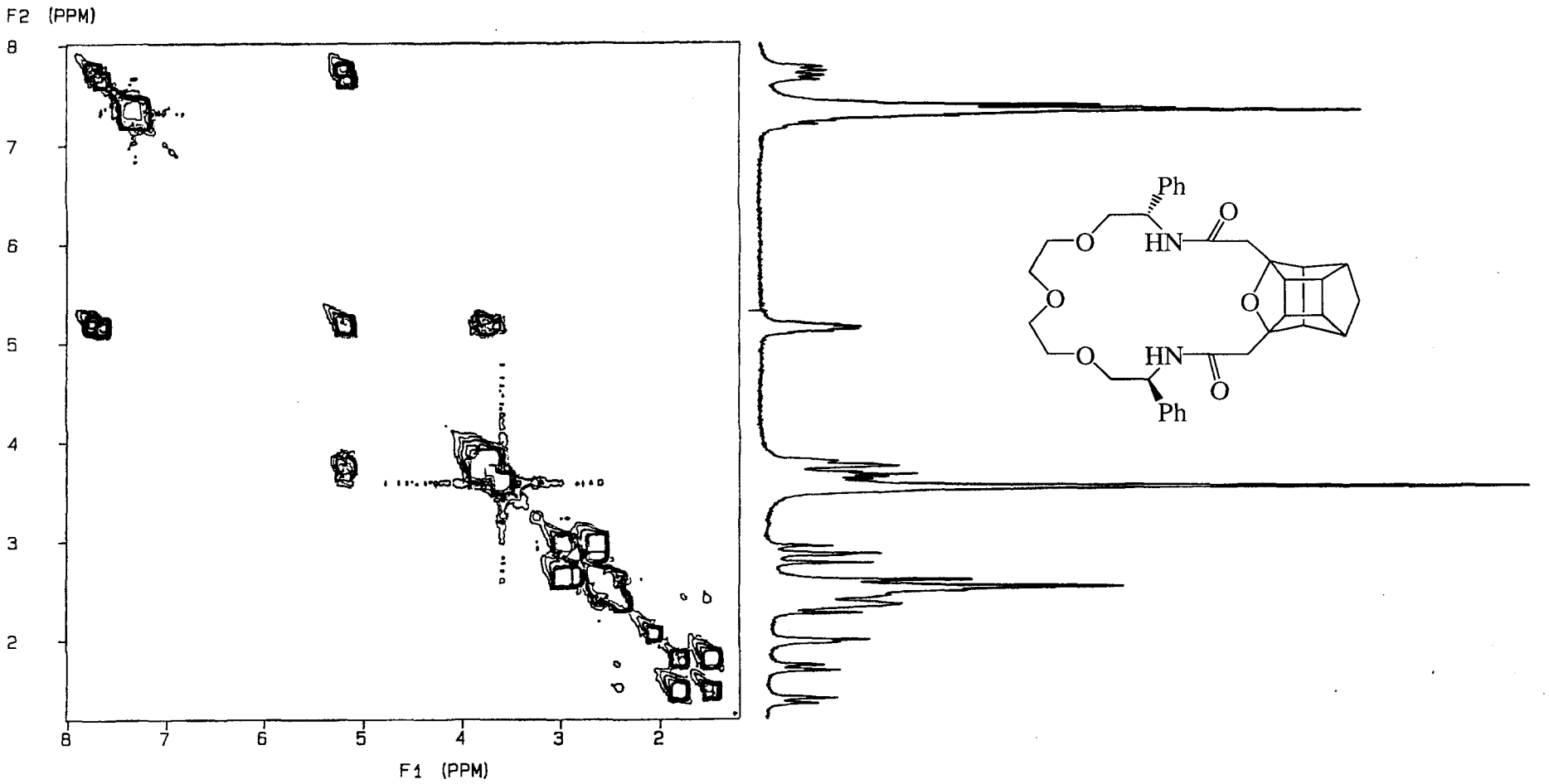

COSY ($CDCl_3$) of macrocycle 78

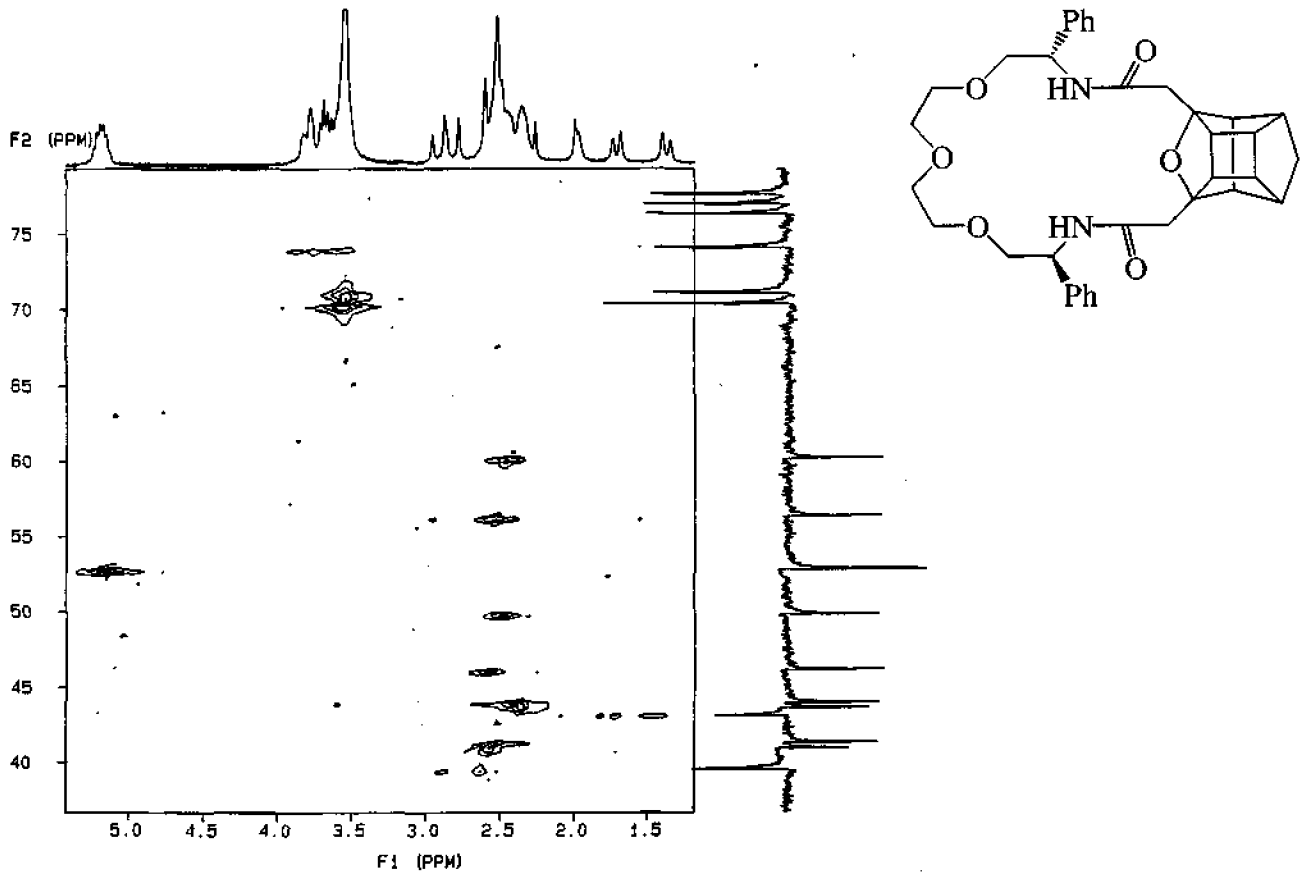

HETCOR ($CDCl_3$) of macrocycle 78

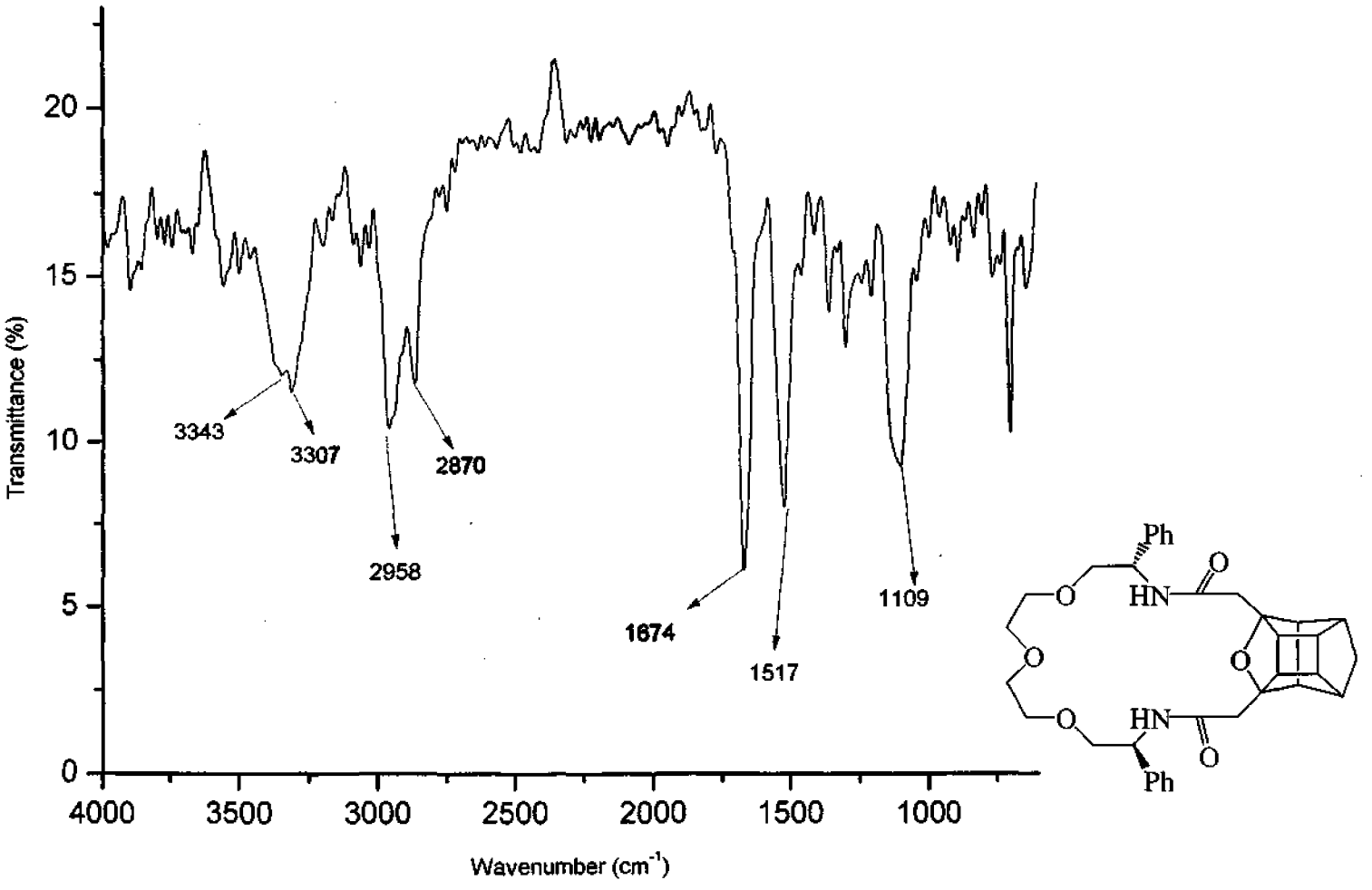

IR spectrum of macrocycle 78

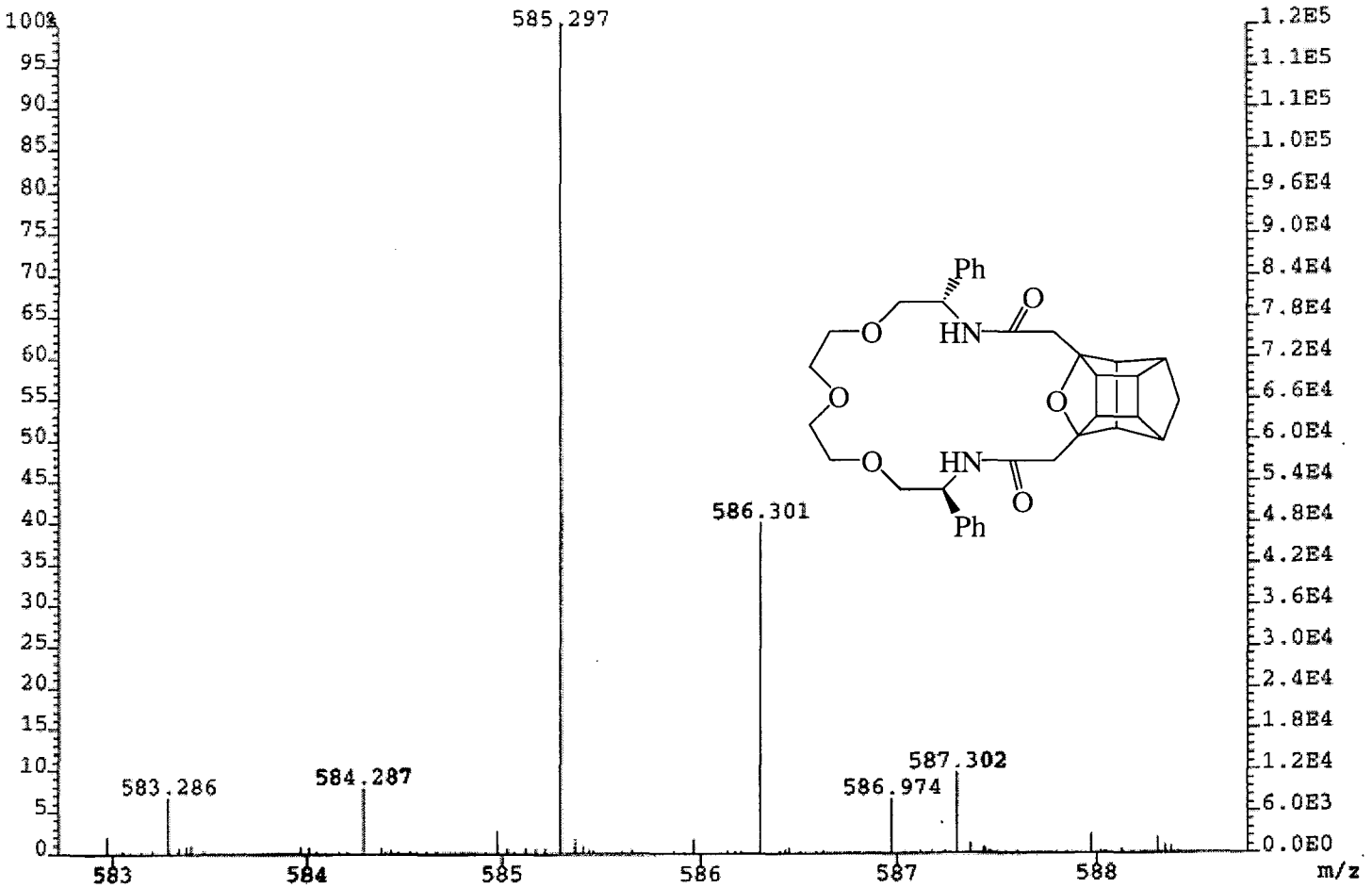

CI MS of macrocycle 78

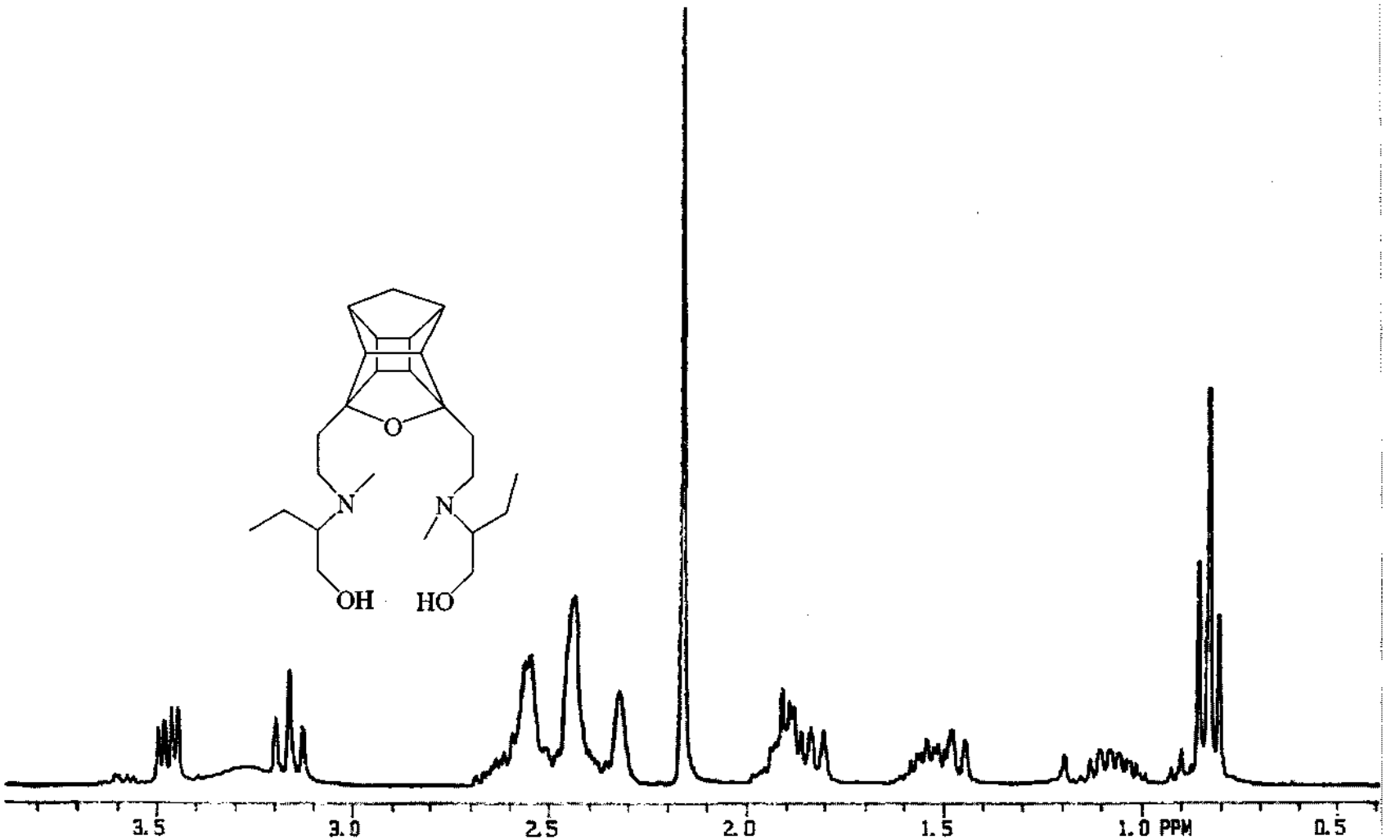

^{1}H nmr ($CDCl_3$) 200 MHz of ligand 133

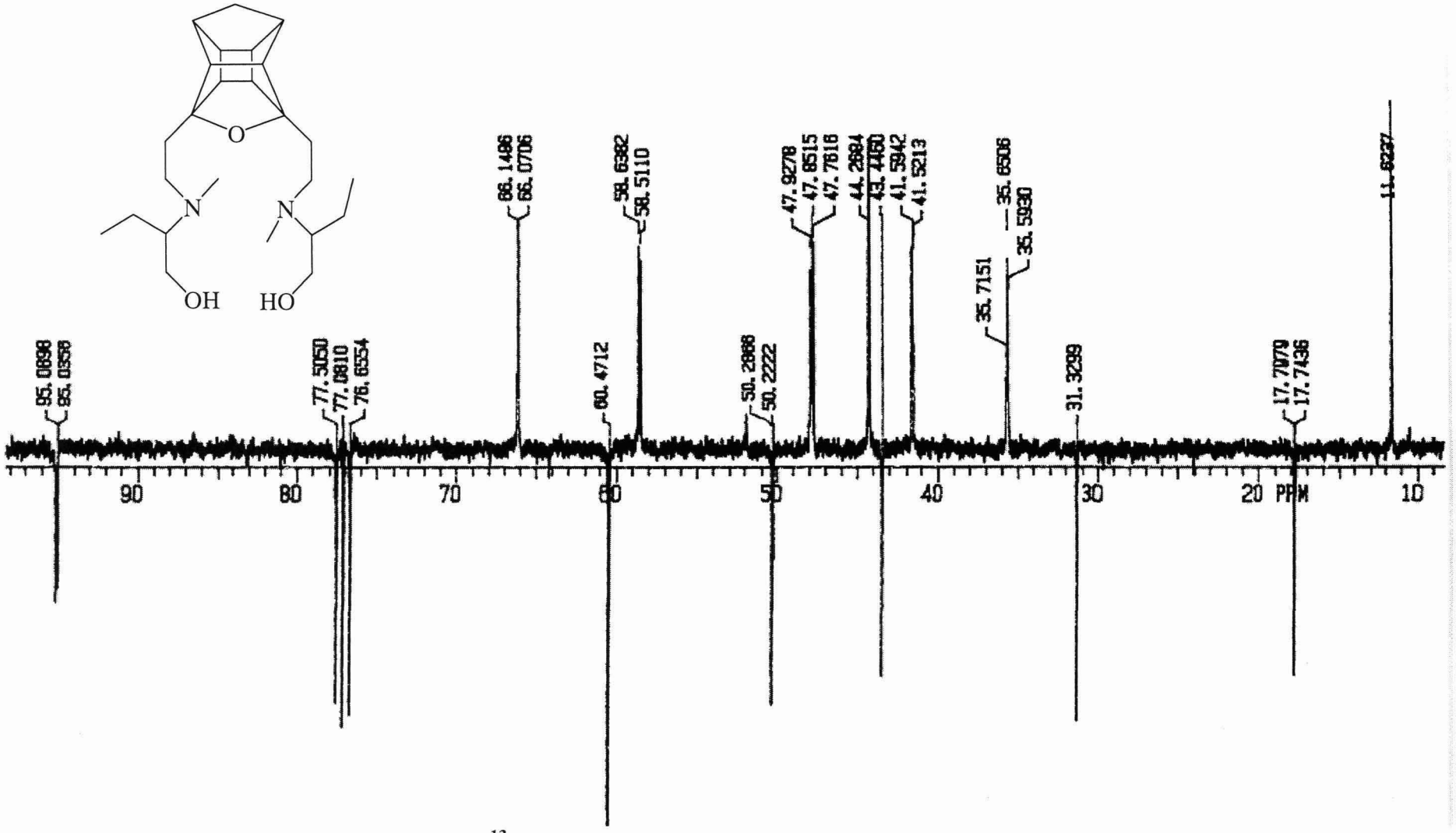

^{13}C APT nmr ($CDCl_3$) 50 MHz of ligand 133

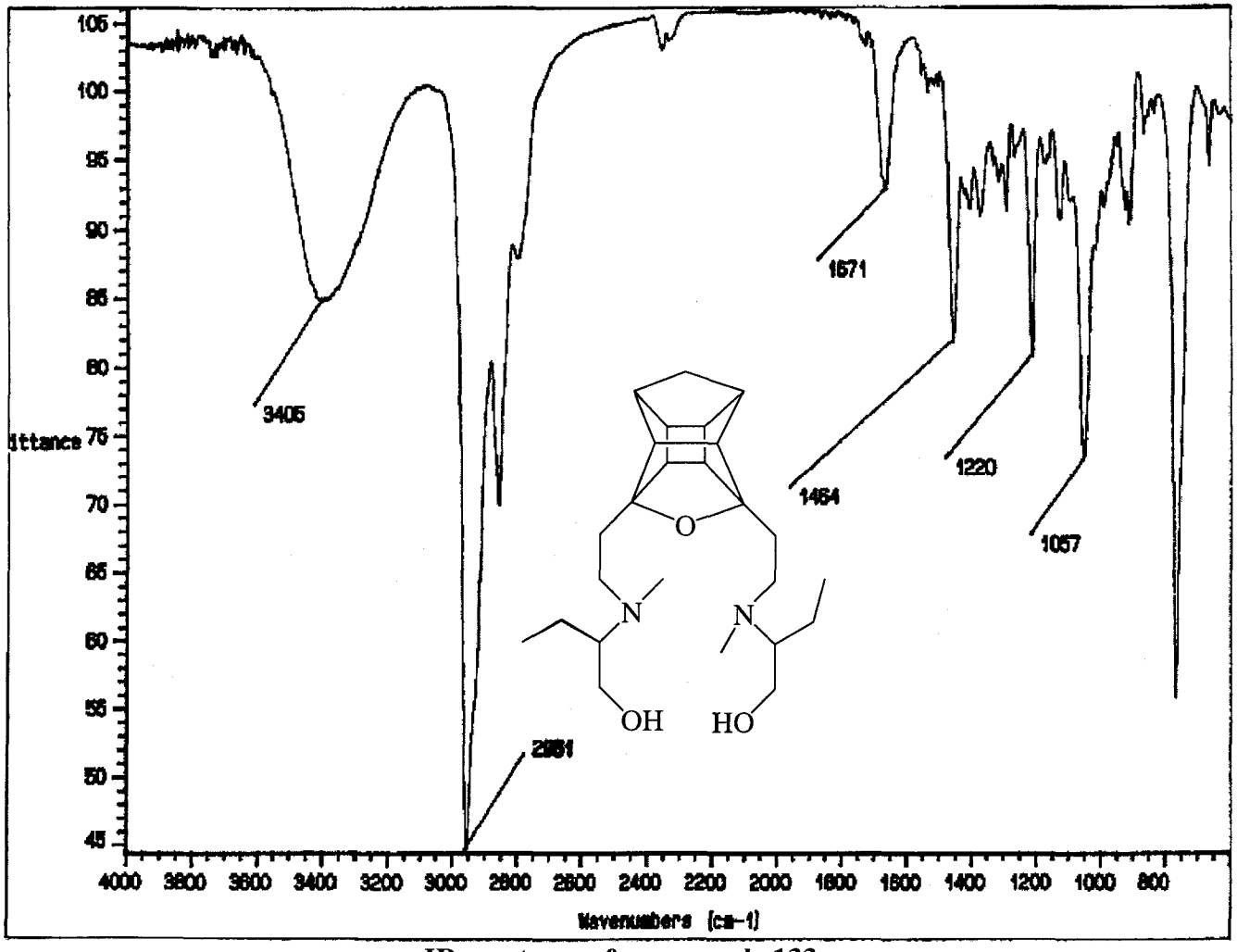

IR spectrum of macrocycle 133

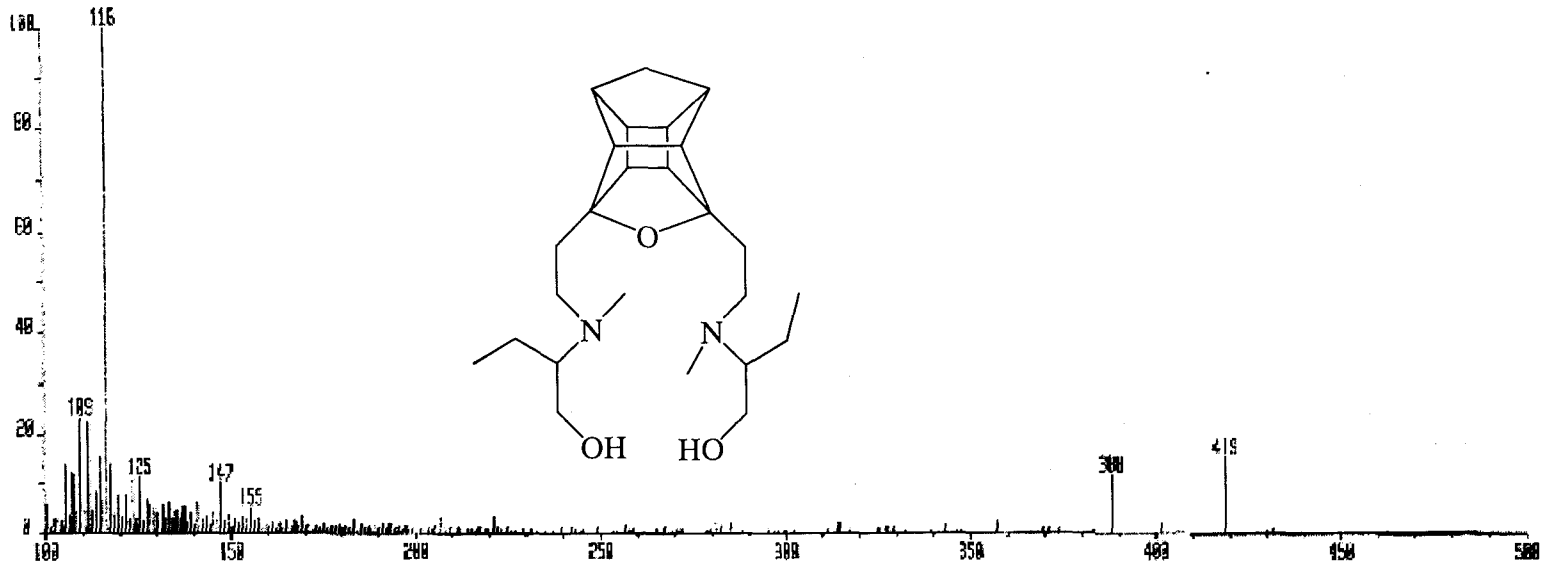

CI MS of macrocycle 133

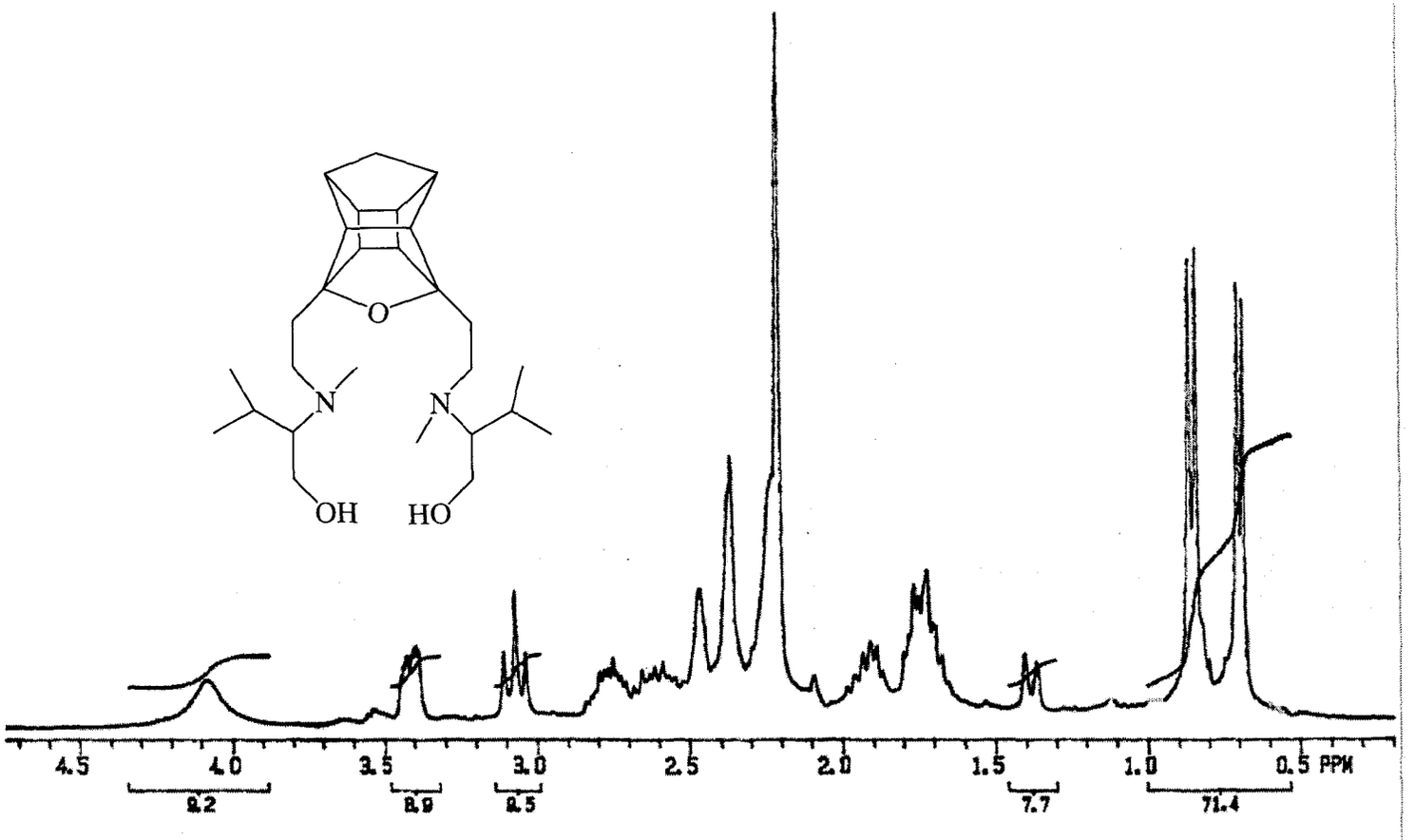

^{1}H nmr ($CDCl_3$) 200 MHz of ligand 134

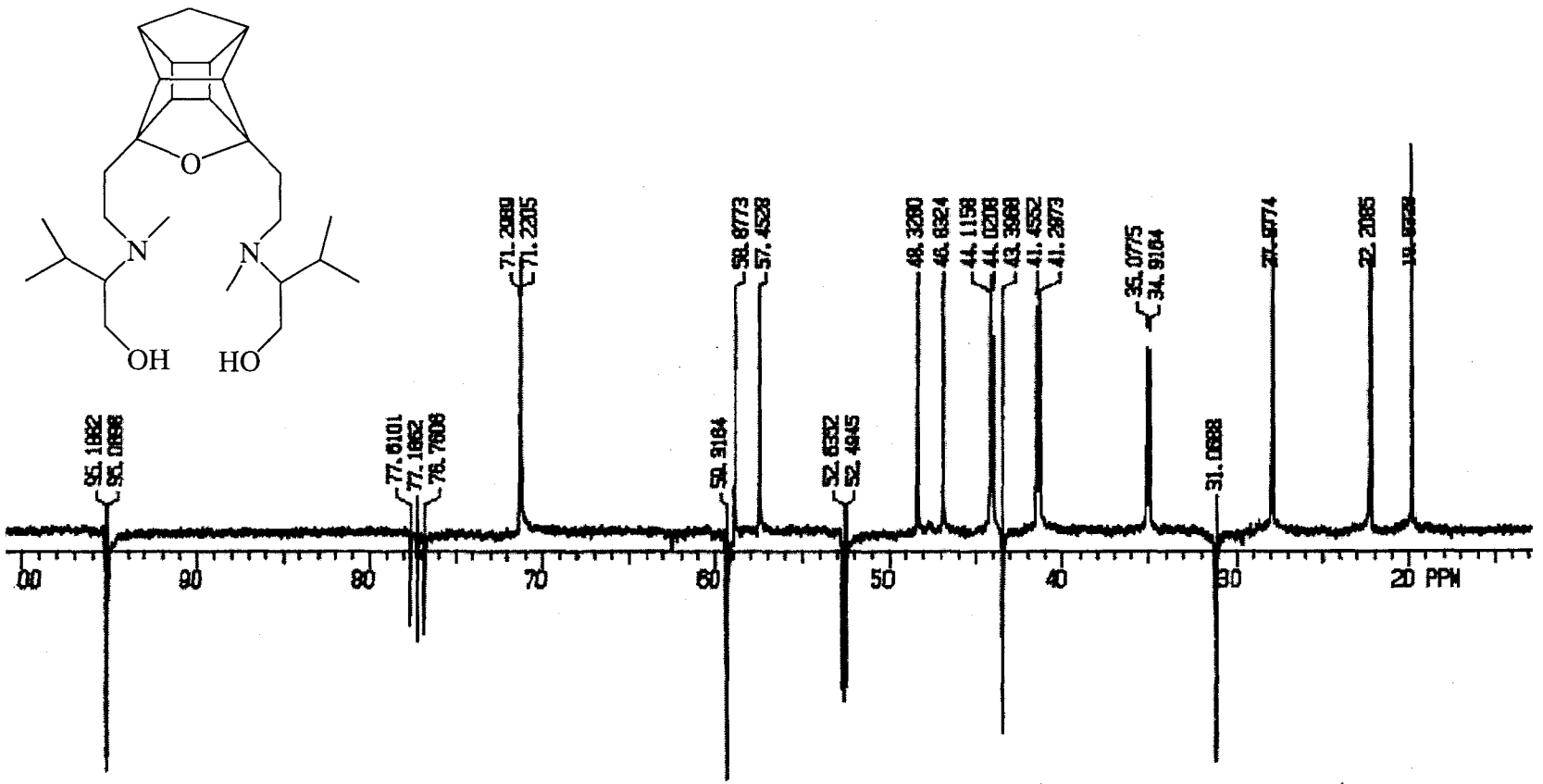

^{13}C APT nmr ($CDCl_3$) 50 MHz of ligand 134

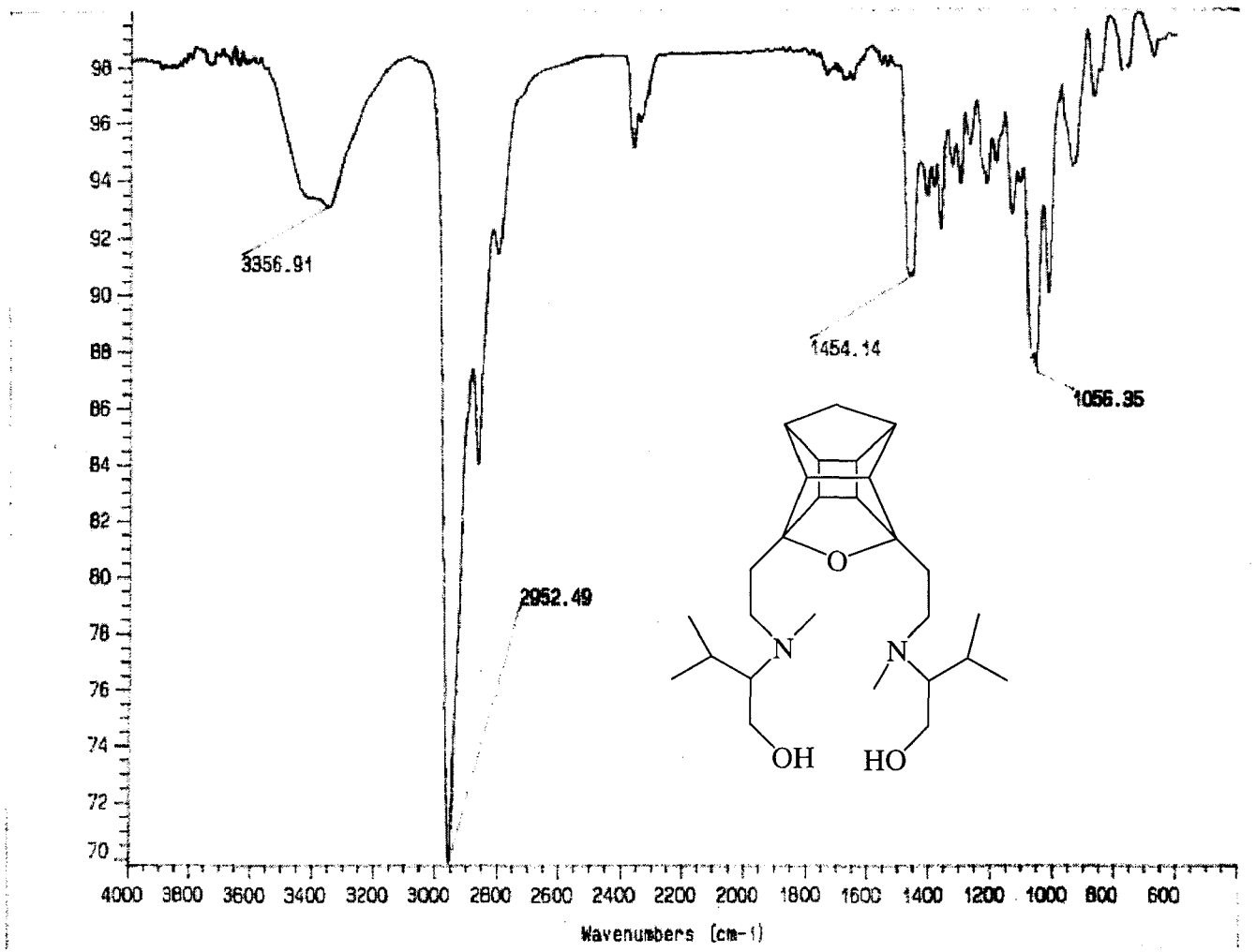

IR spectrum of macrocycle 134

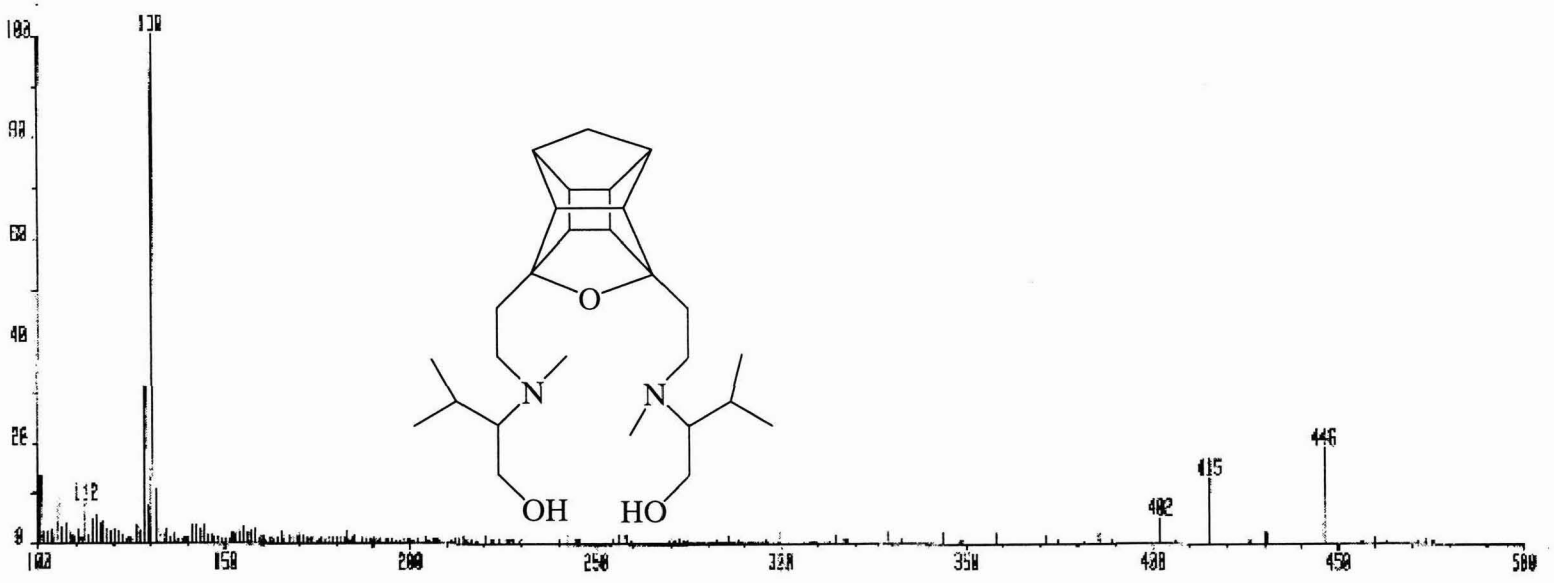

CI MS of macrocycle 134

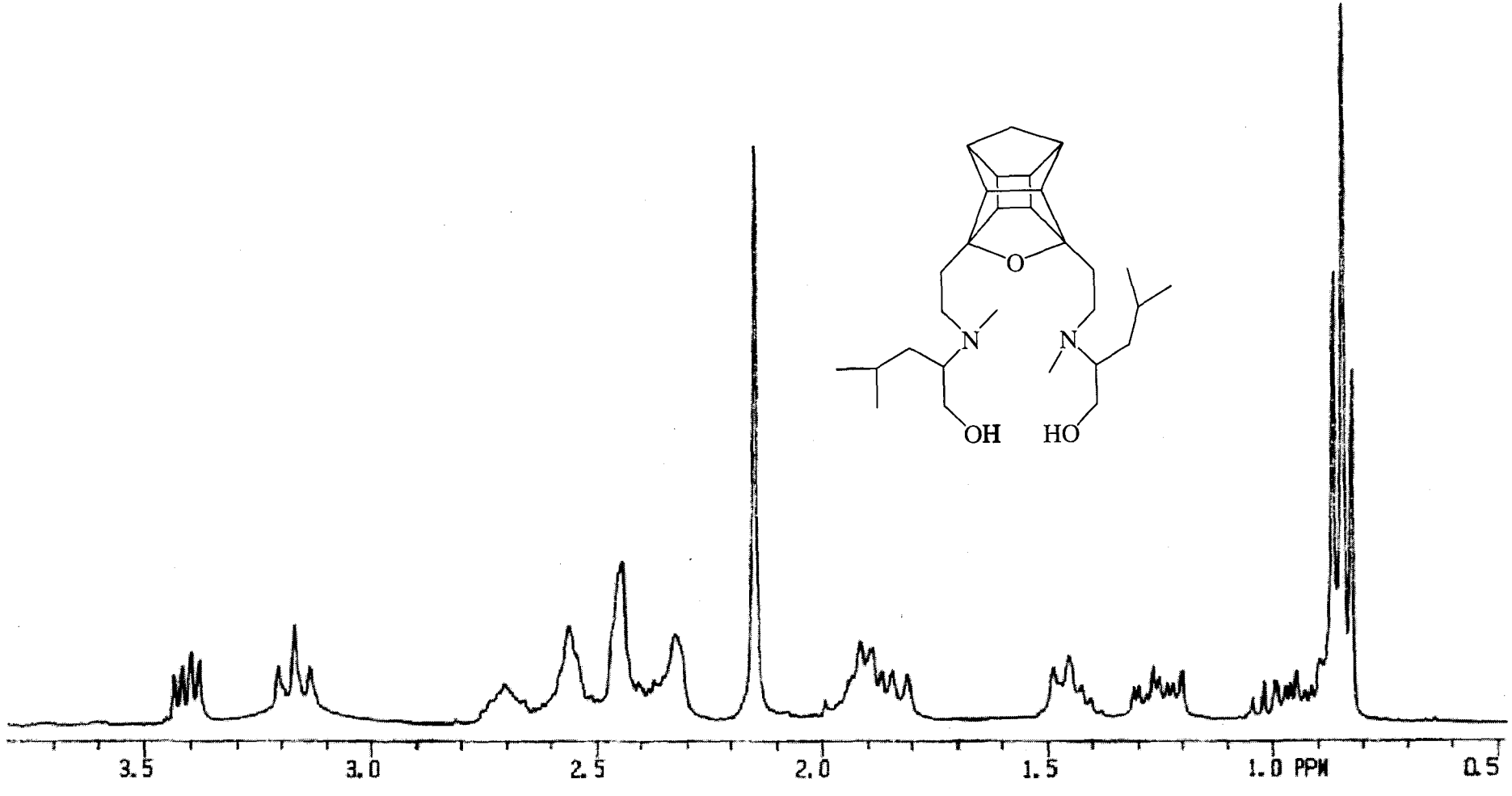

^{1}H nmr ($CDCl_3$) 200 MHz of ligand 135

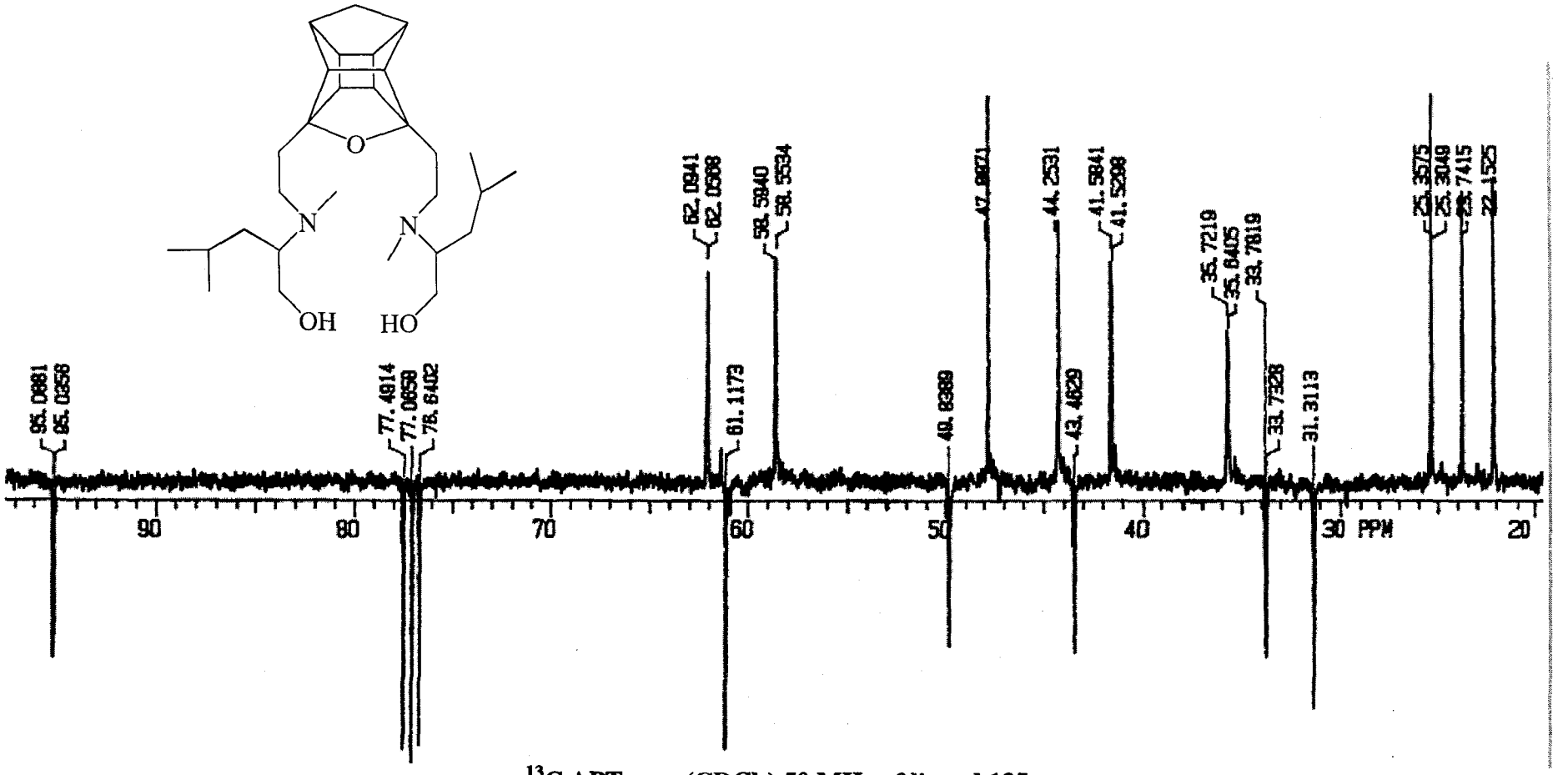

^{13}C APT nmr ($CDCl_3$) 50 MHz of ligand 135

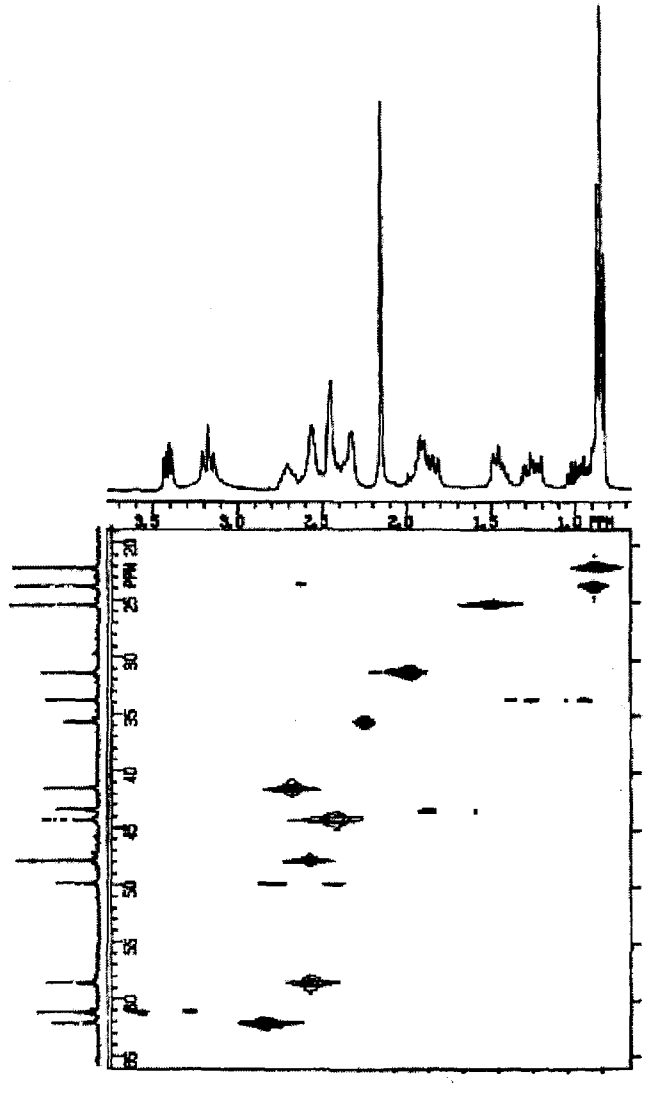

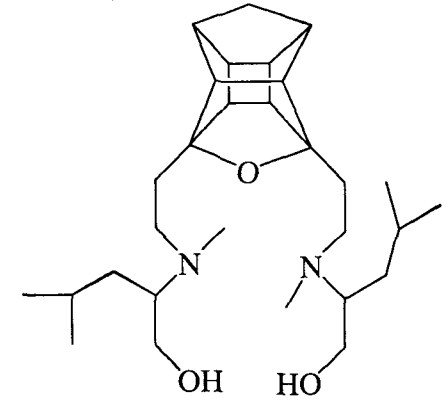

HETCOR of ligand 135

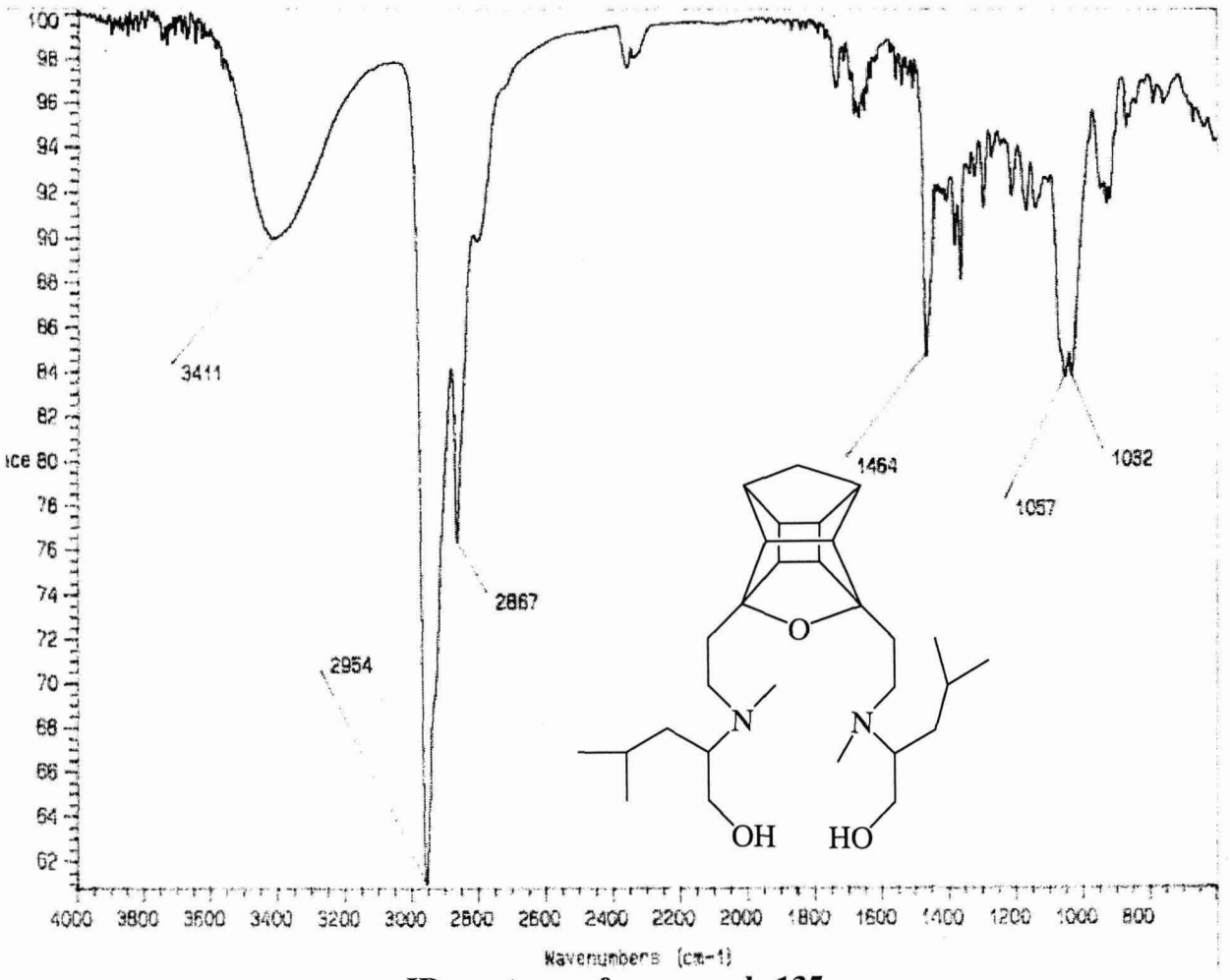

IR spectrum of macrocycle 135

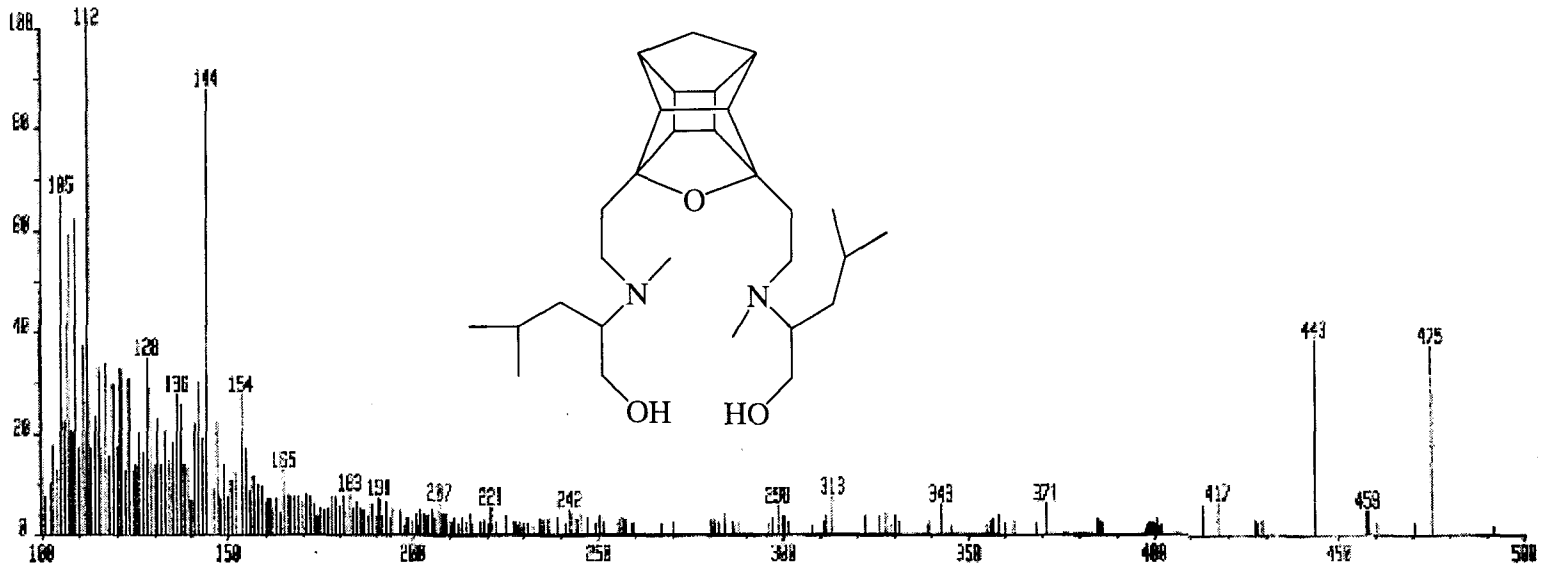

CI MS of macrocycle 135

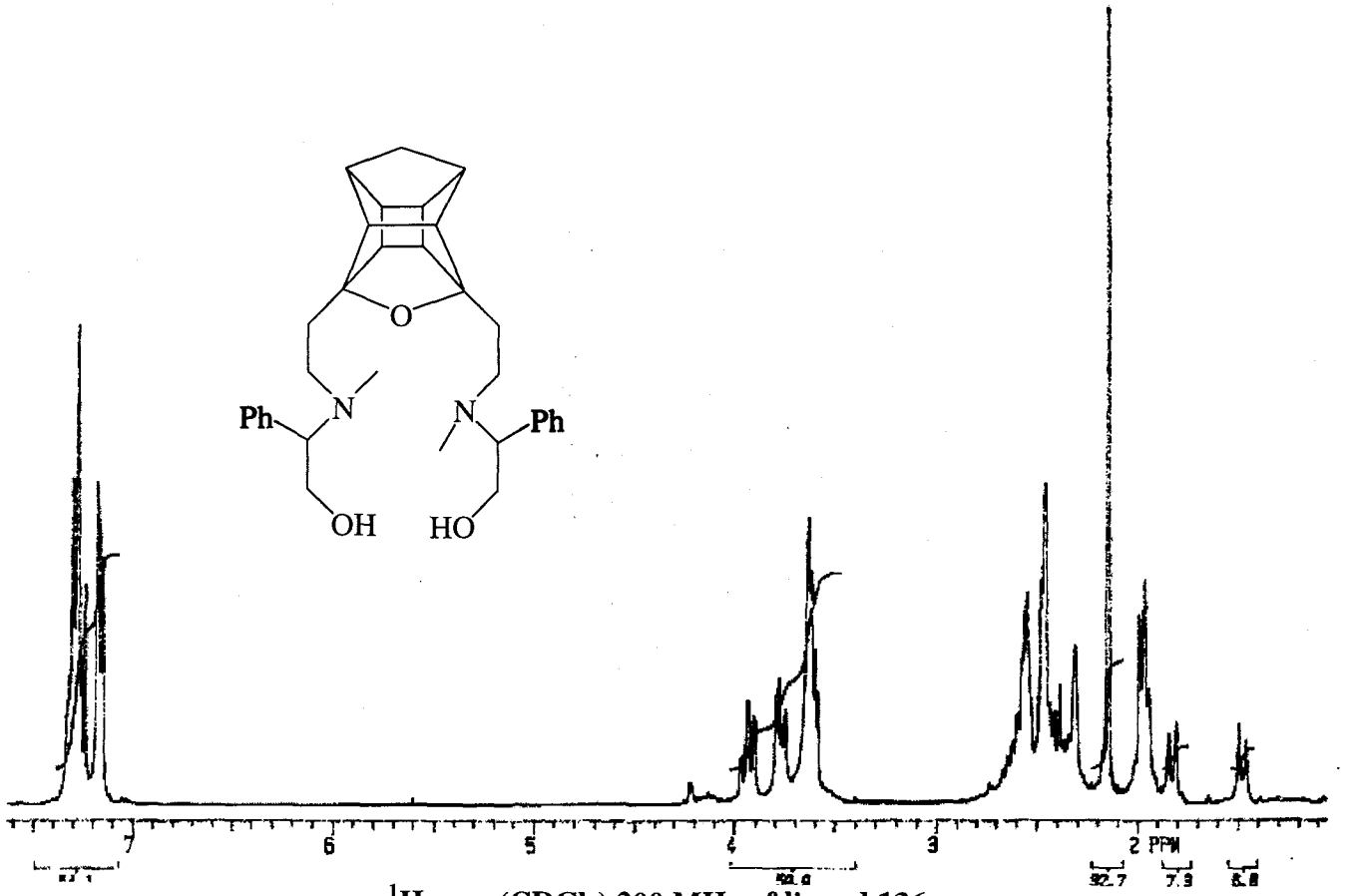

^{1}H nmr ($CDCl_3$) 200 MHz of ligand 136

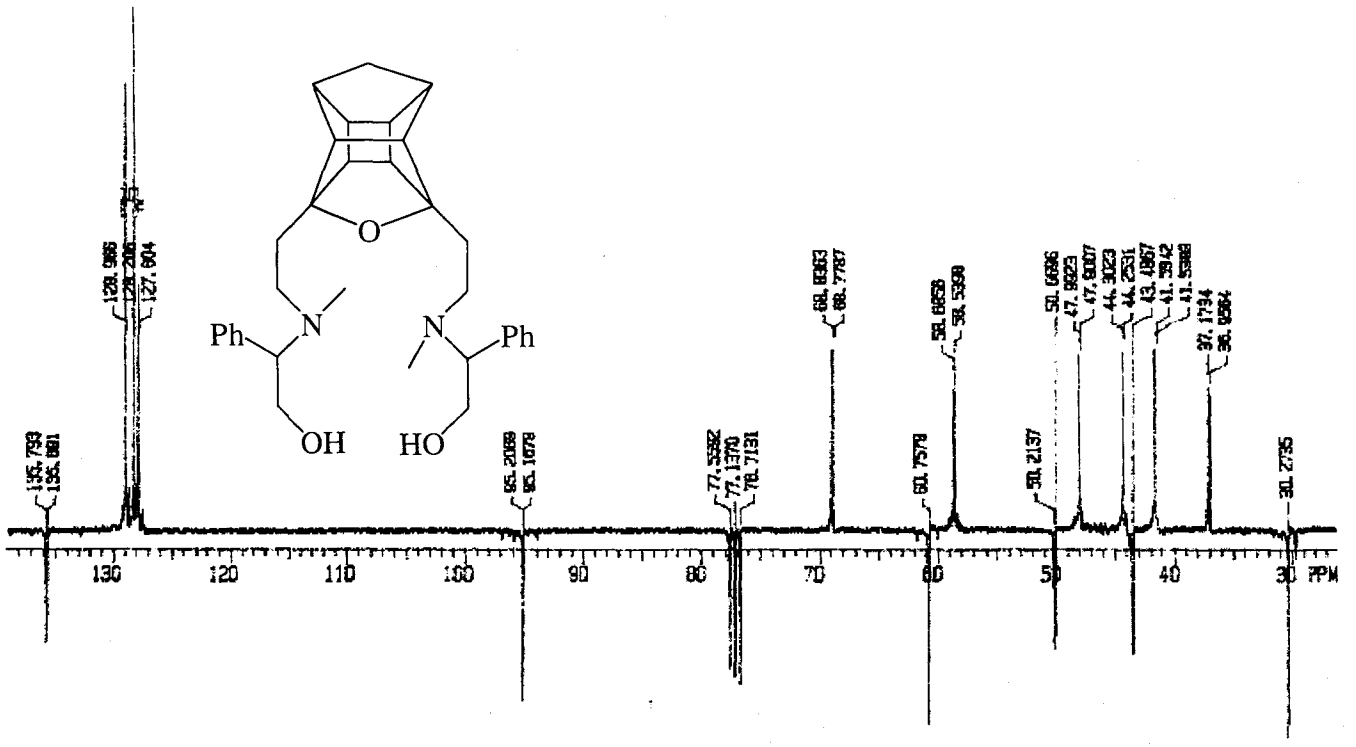

^{13}C APT nmr ($CDCl_3$) 50 MHz of ligand 136

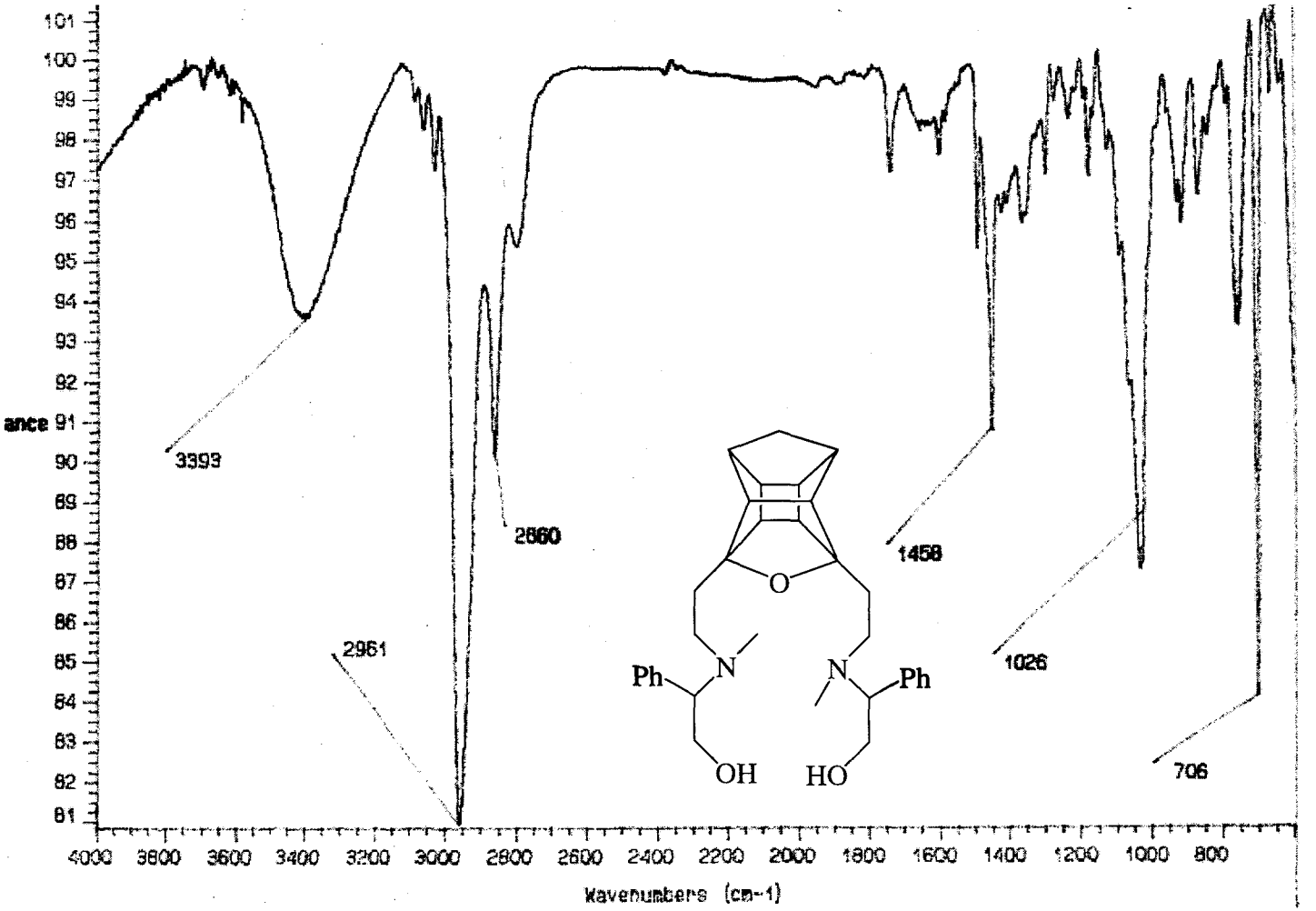

IR spectrum of macrocycle 136

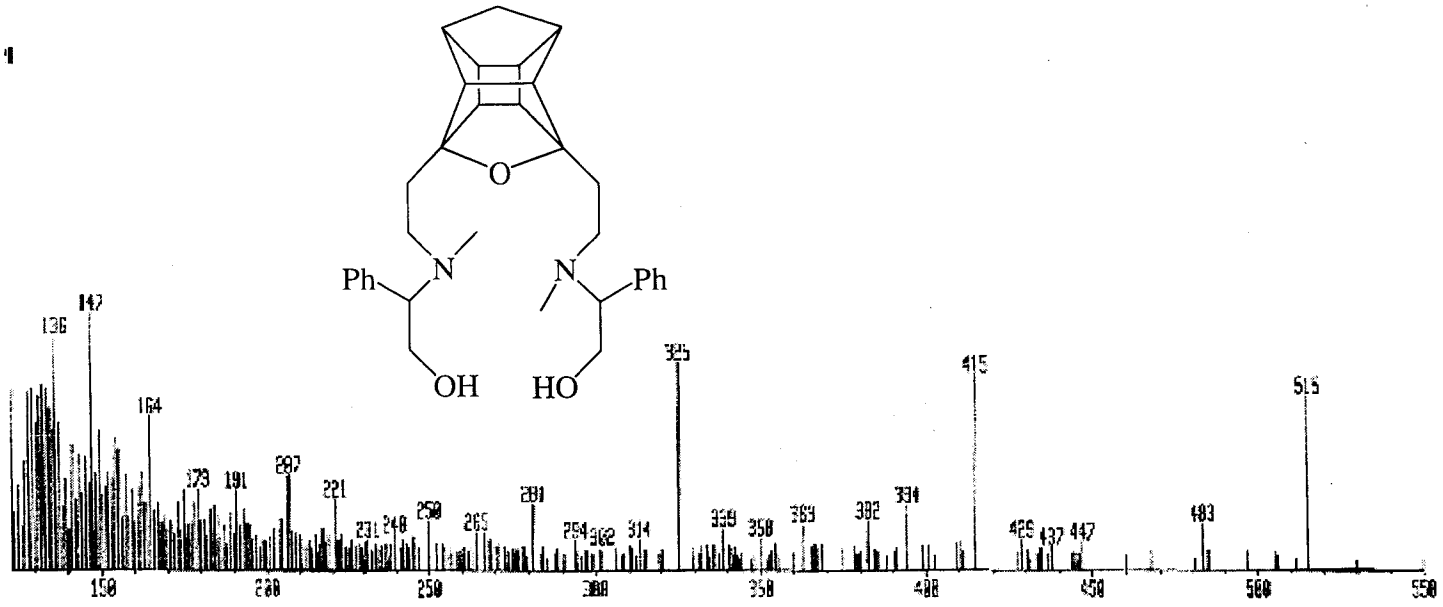

CI MS of macrocycle 136

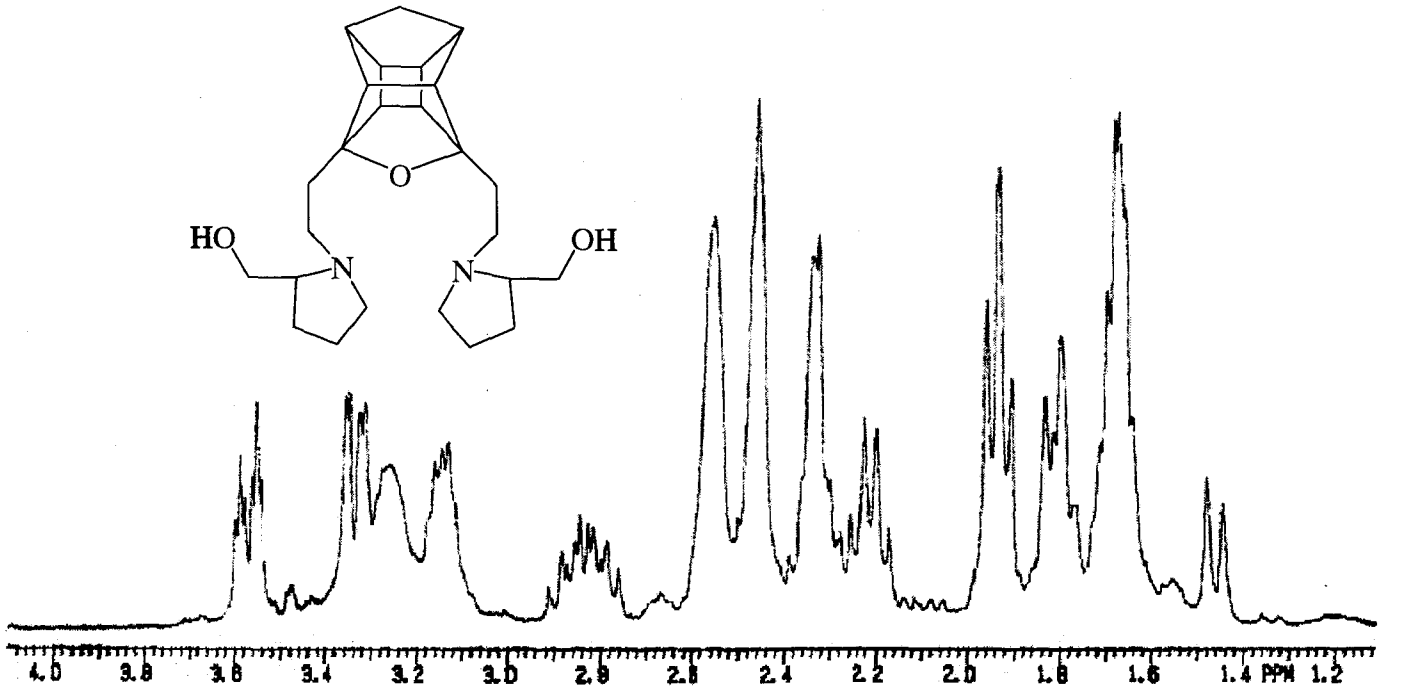

^{1}H nmr ($CDCl_3$) 200 MHz of ligand 137

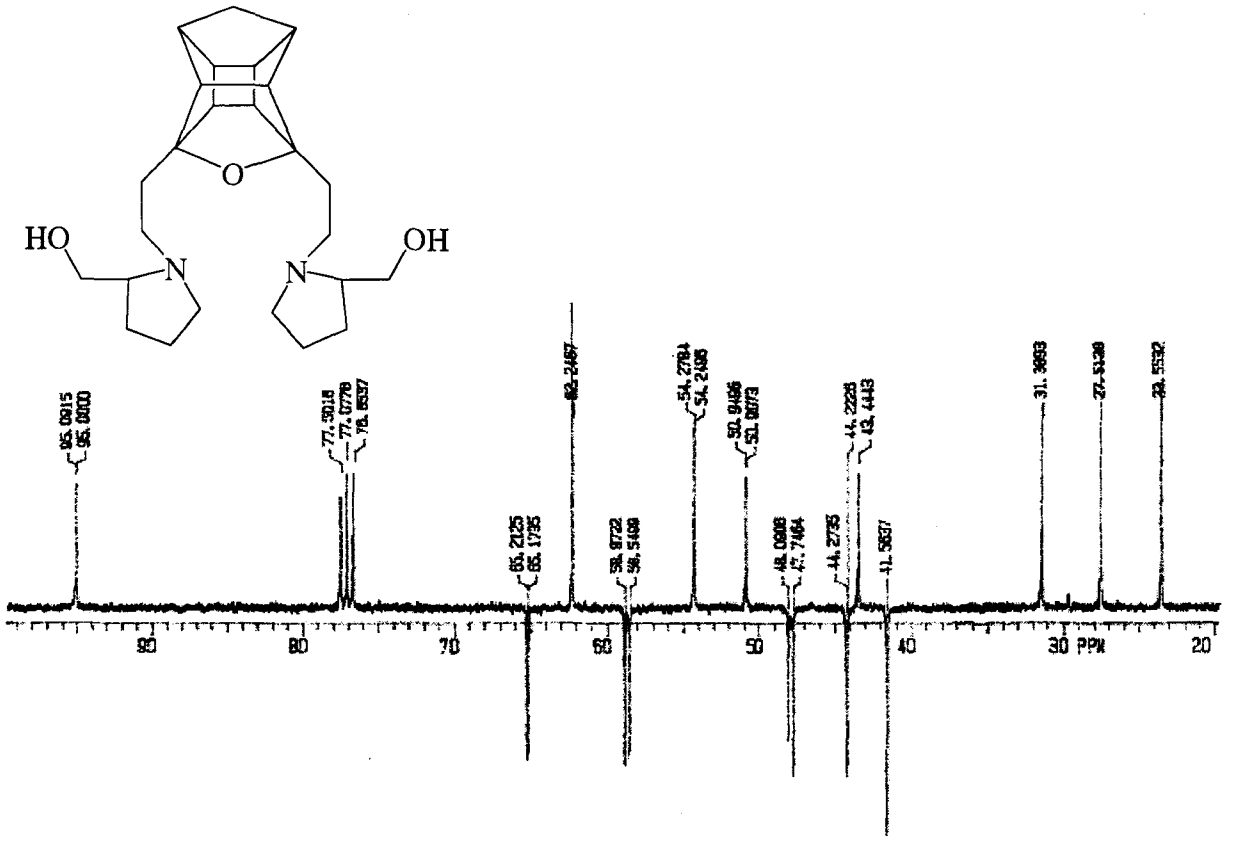

^{13}C APT nmr ($CDCl_3$) 50 MHz of ligand 137

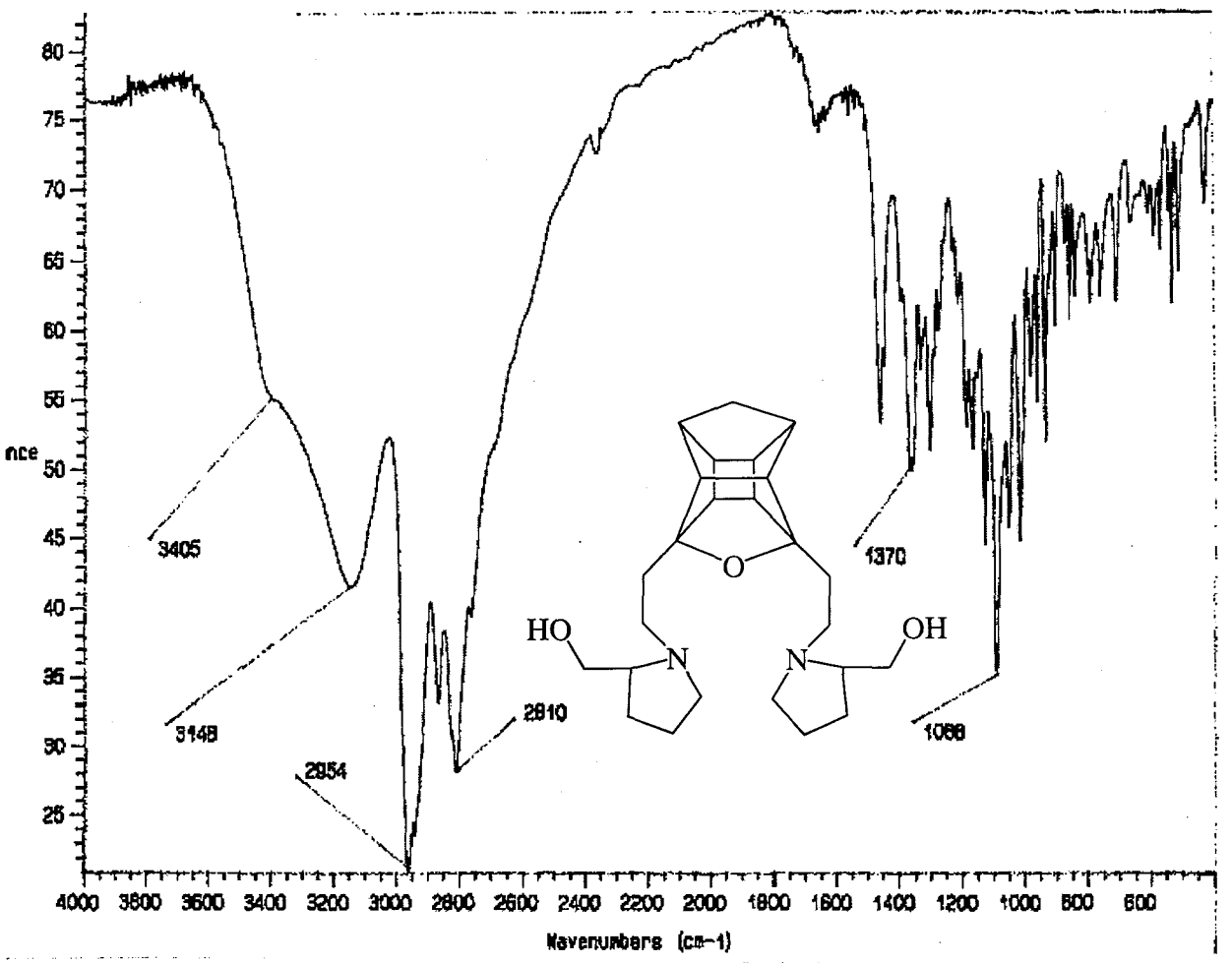

IR spectrum of macrocycle 137

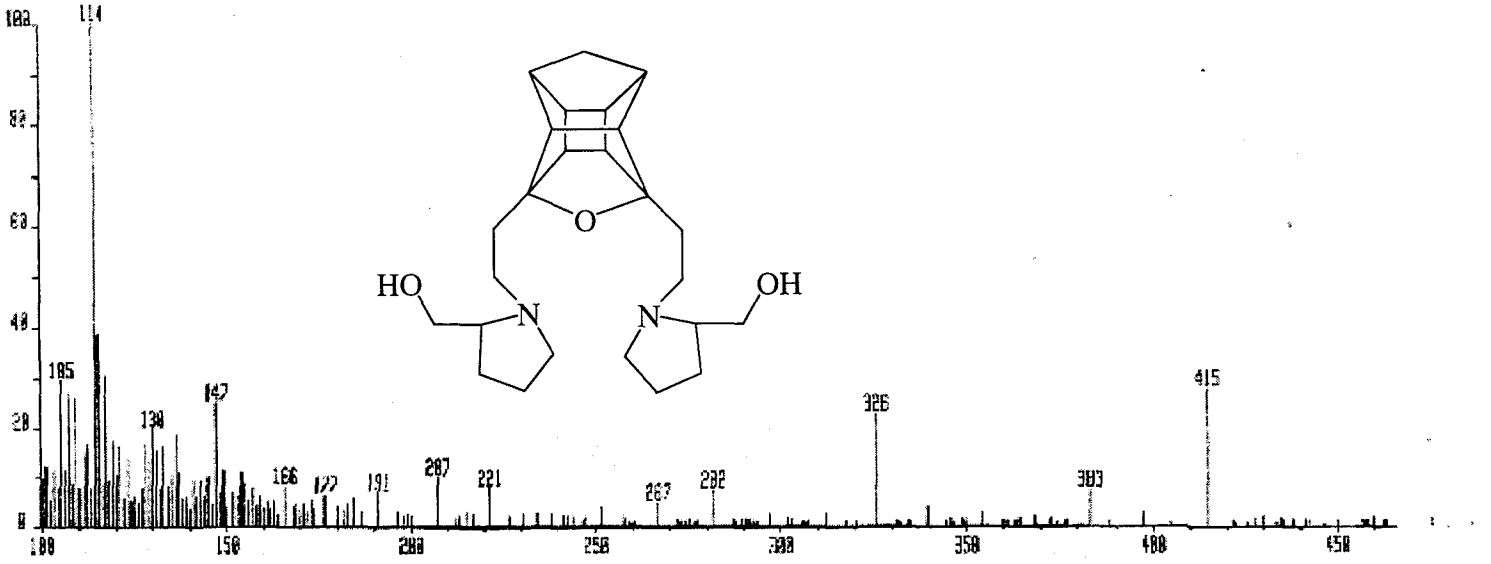

CI MS of macrocycle 137

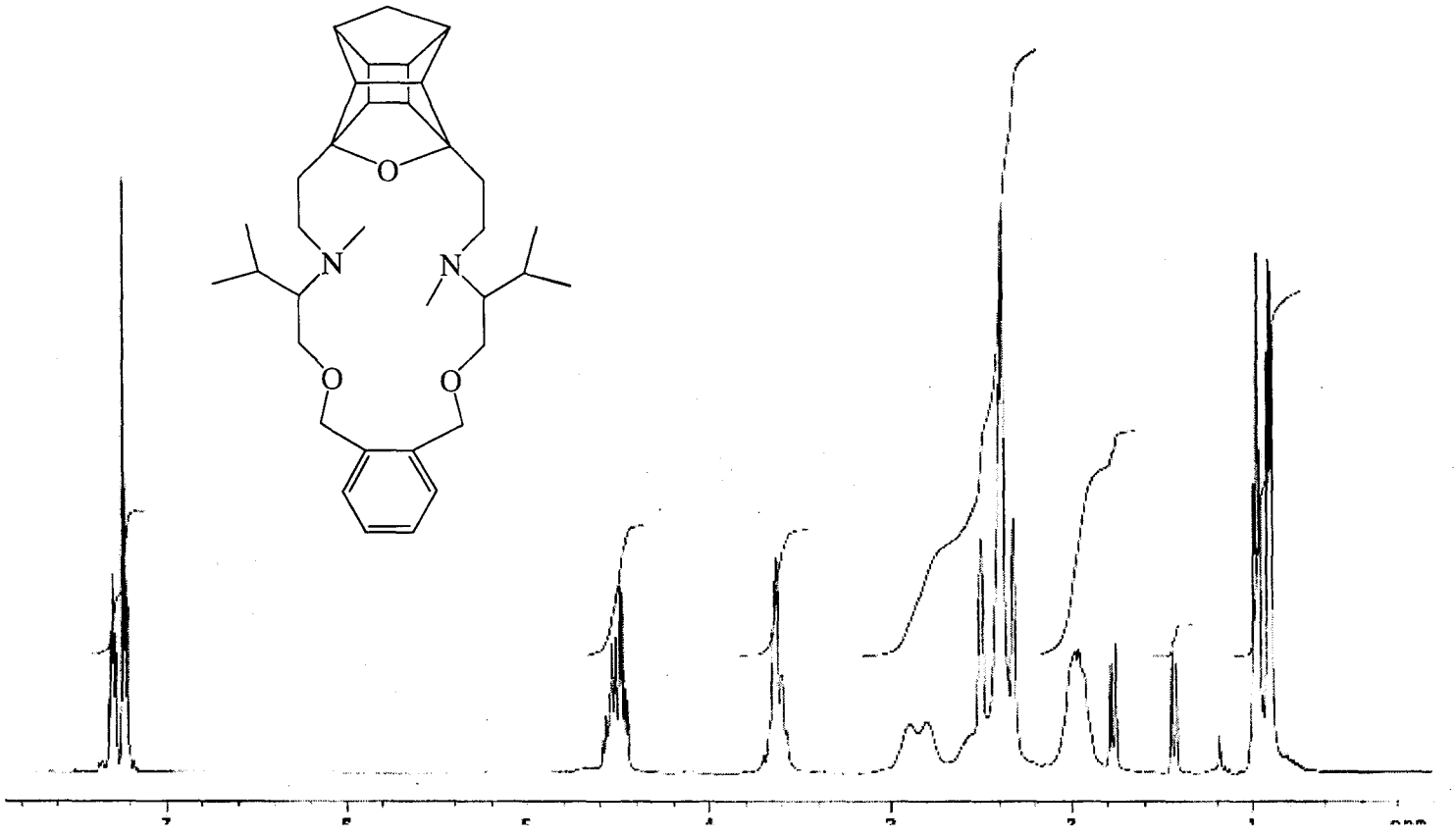

^{1}H nmr ($CDCl_3$) 200 MHz of ligand 169

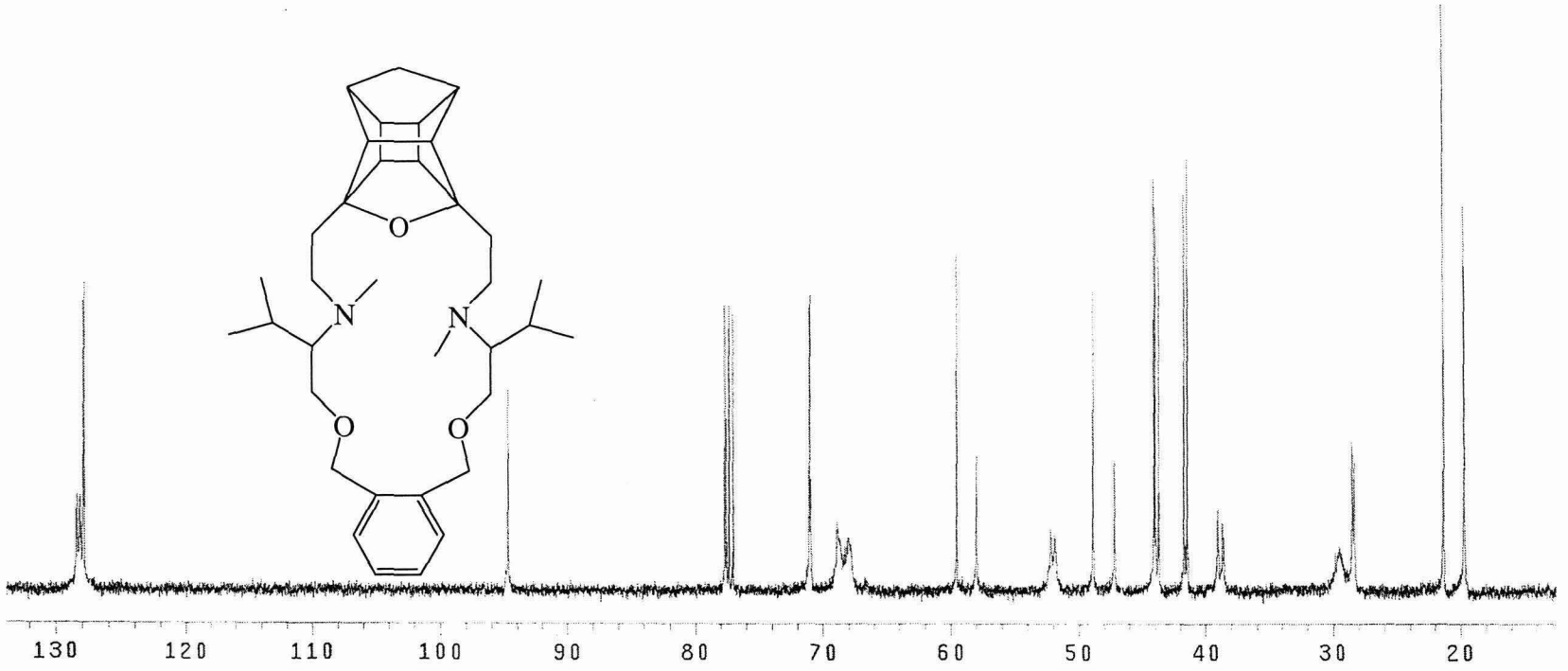

^{13}C nmr ($CDCl_3$) 50 MHz of ligand 169

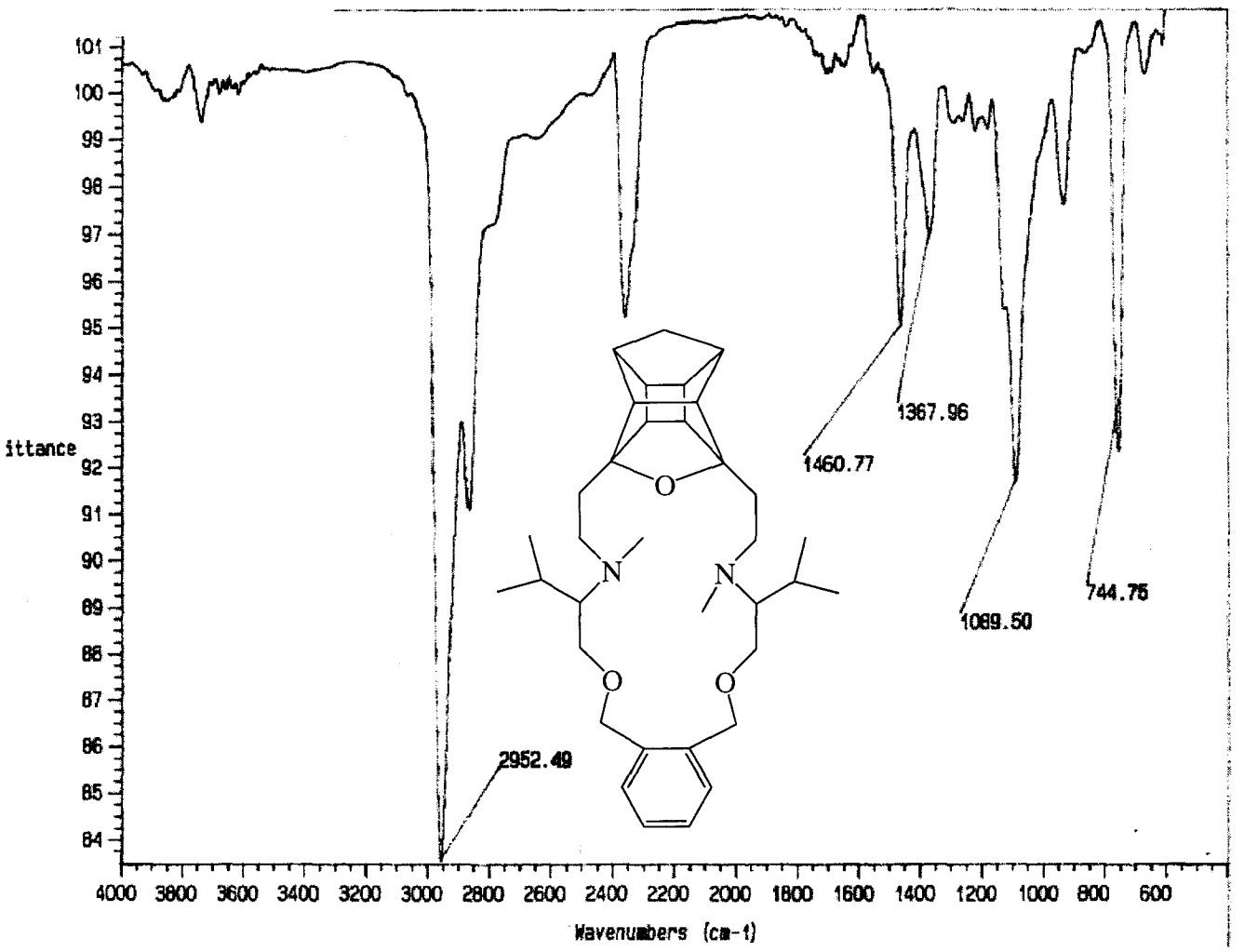

IR spectrum of macrocycle 169

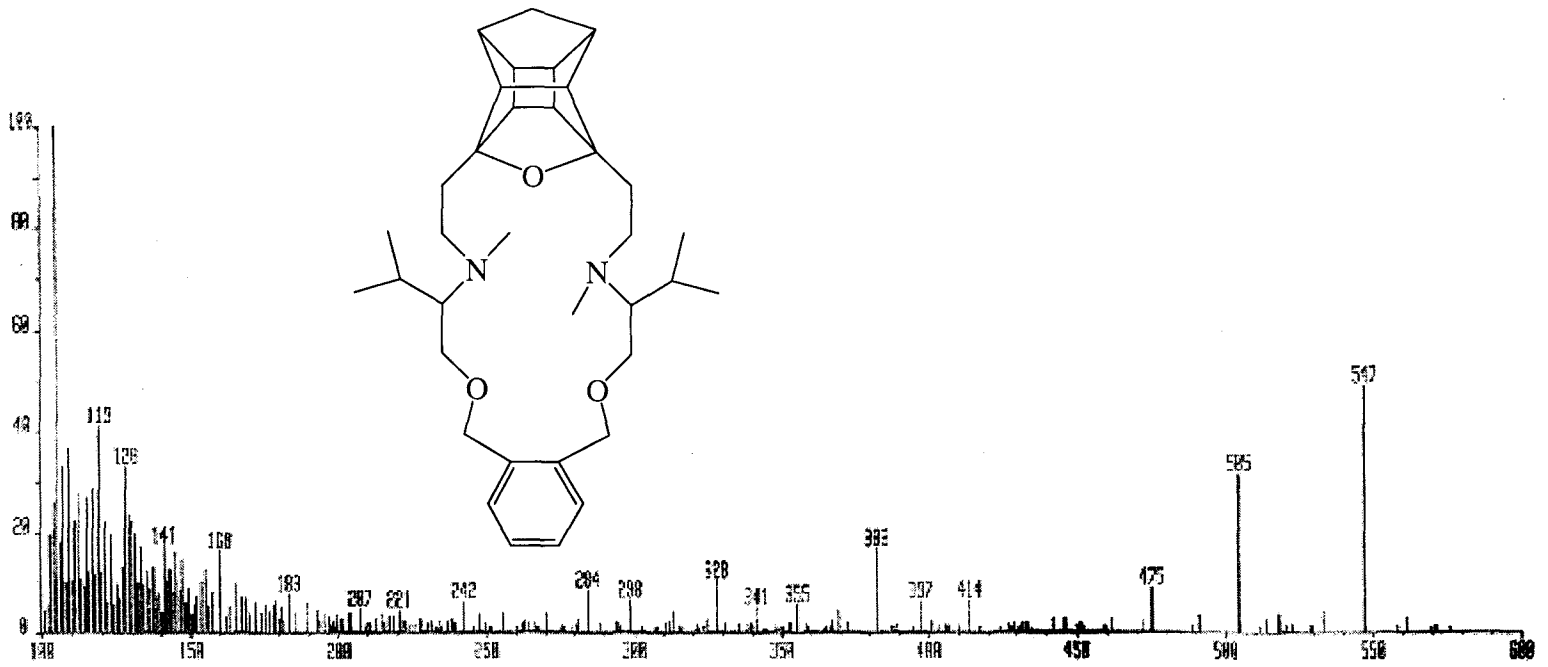

CI MS of macrocycle 169

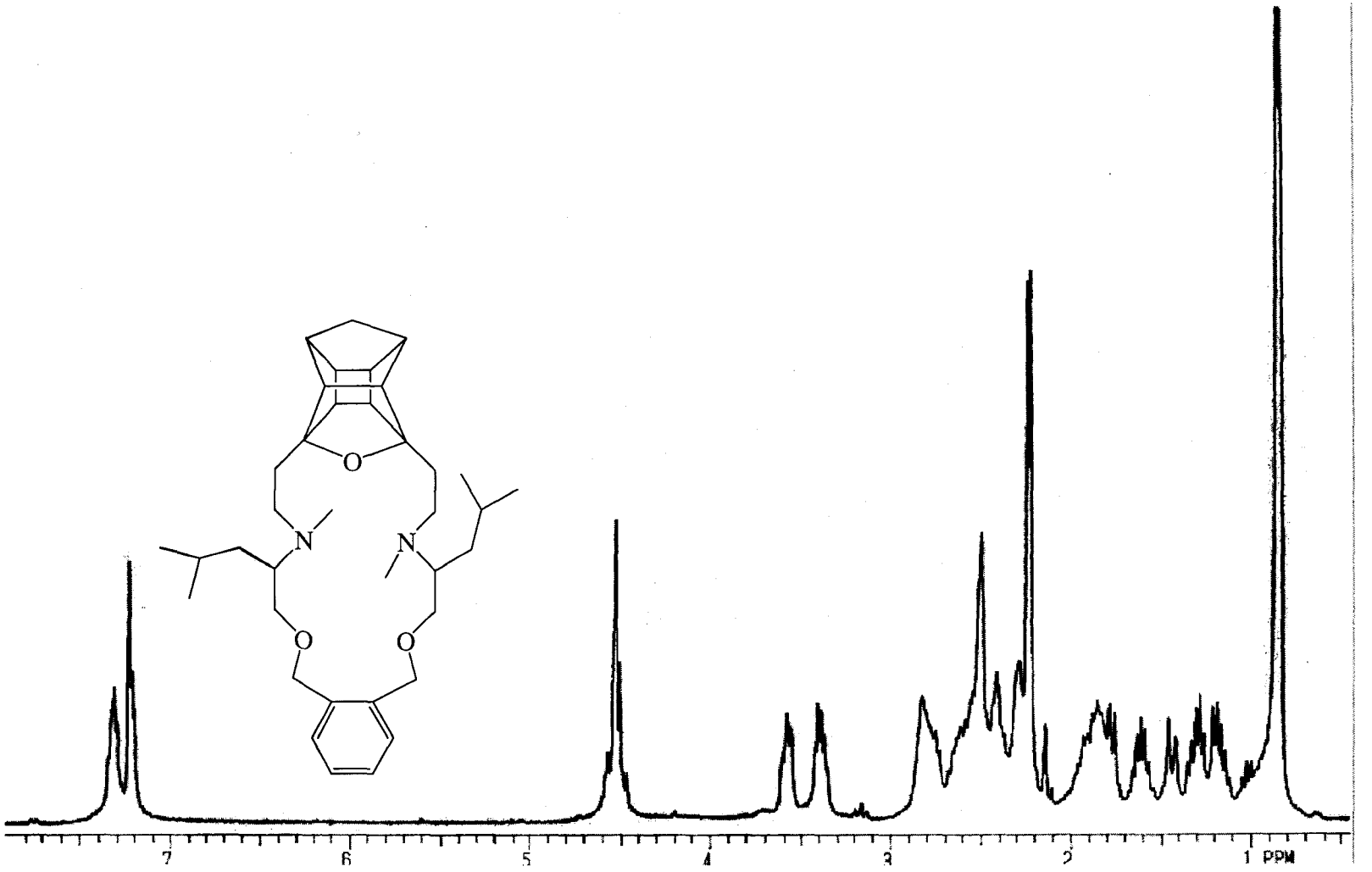

^{1}H nmr ($CDCl_3$) 200 MHz of ligand 170

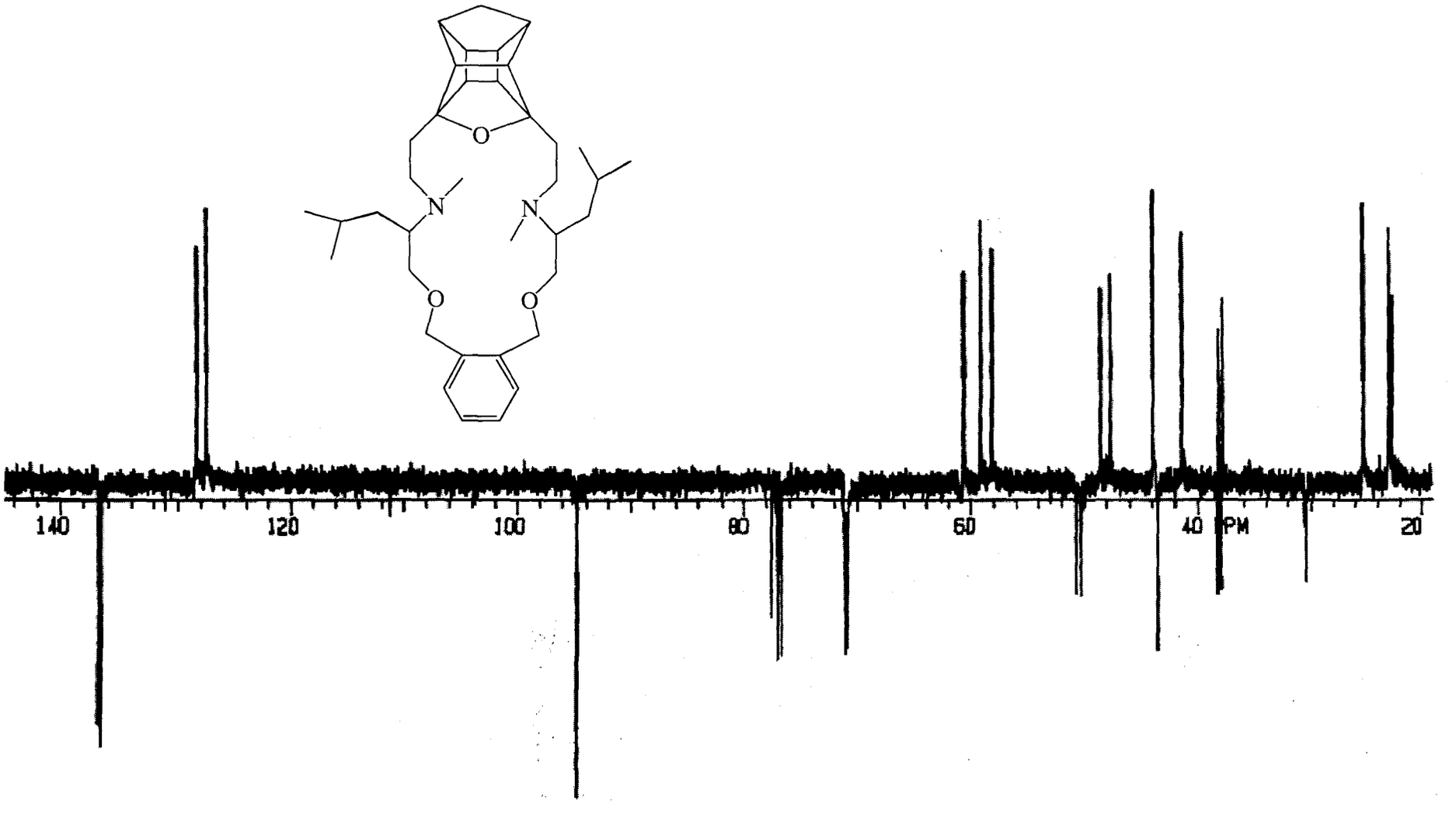

^{13}C APT nmr ($CDCl_3$) 50 MHz of ligand 170

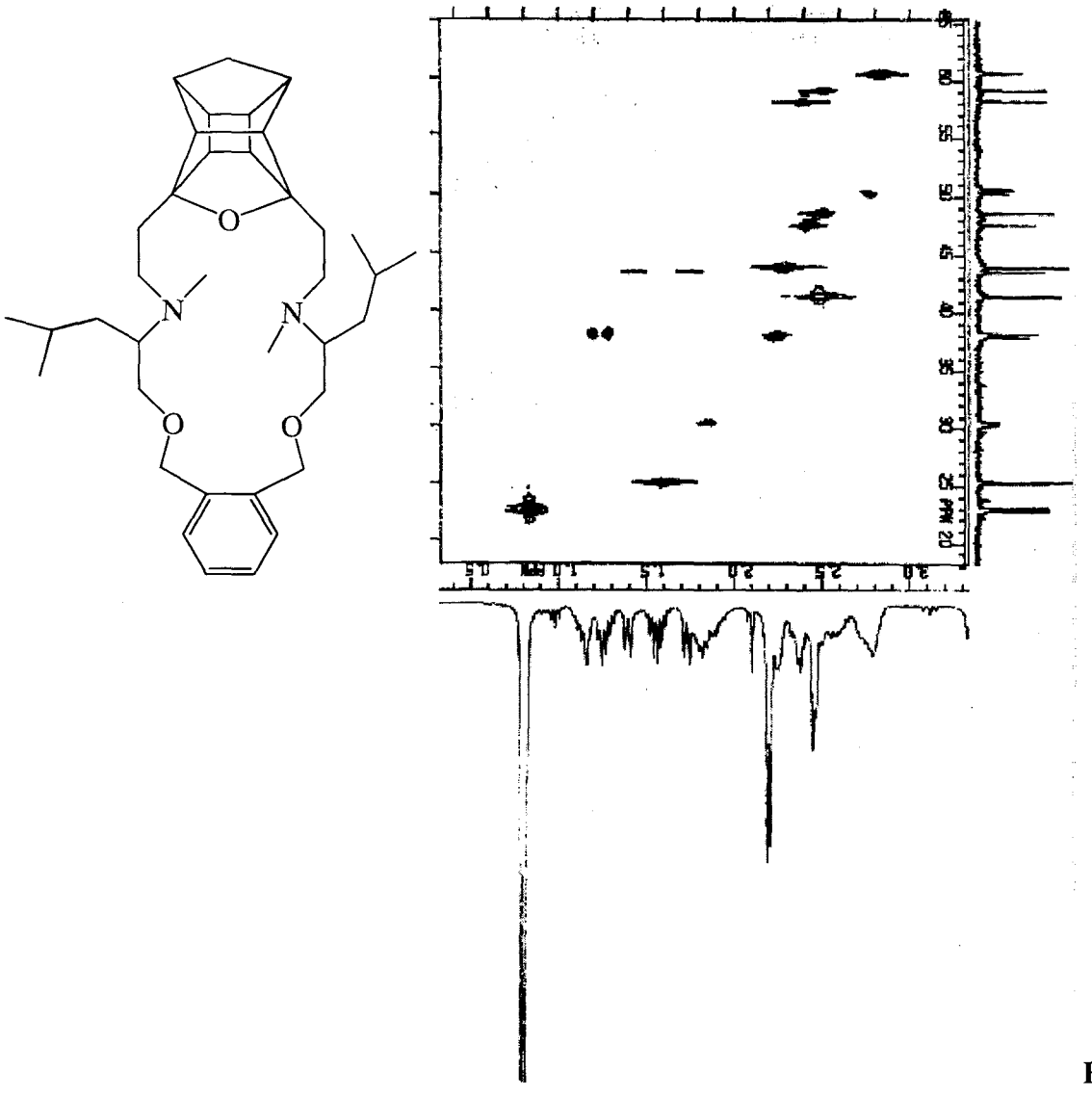

HETCOR of ligand 170

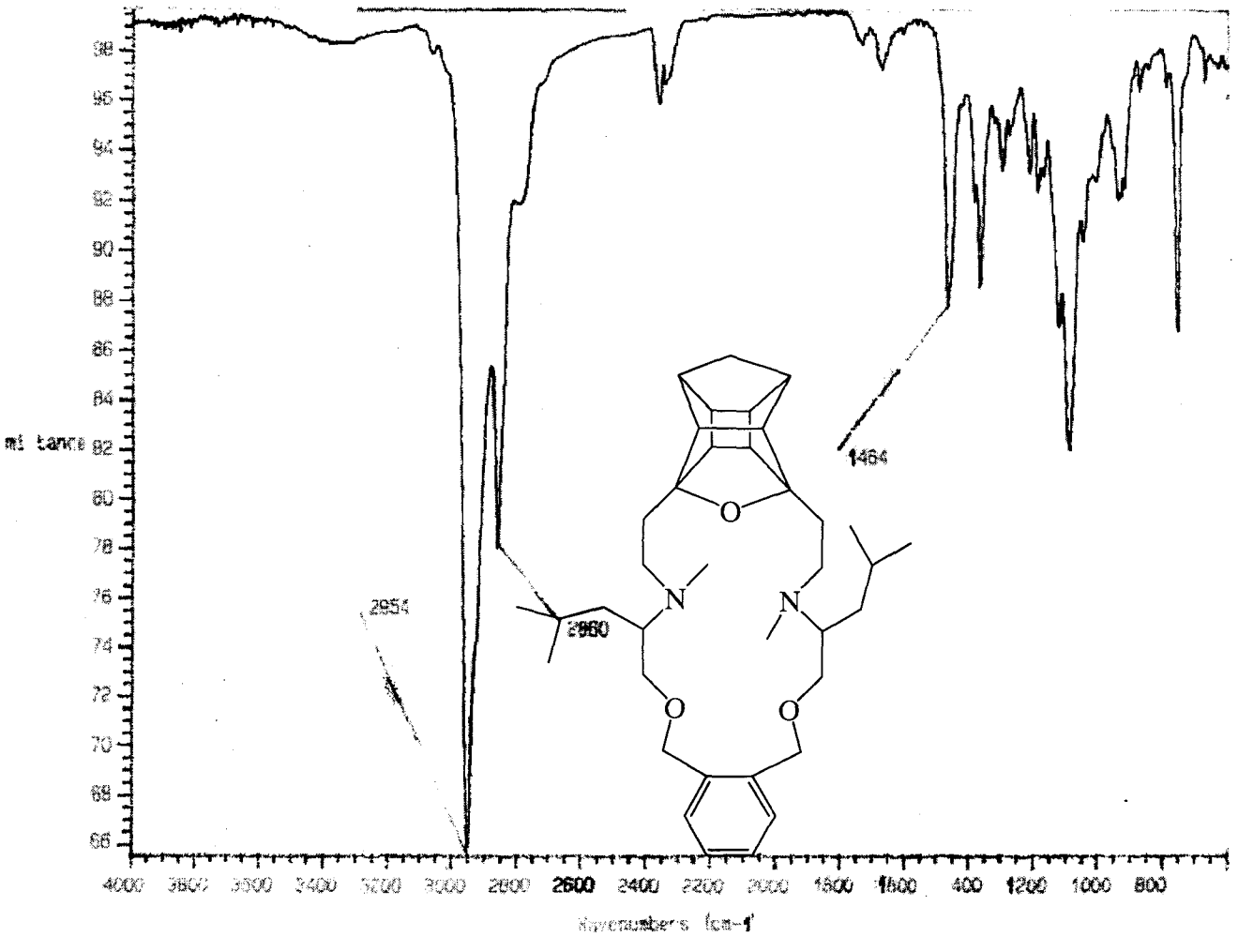

IR spectrum of macrocycle 170

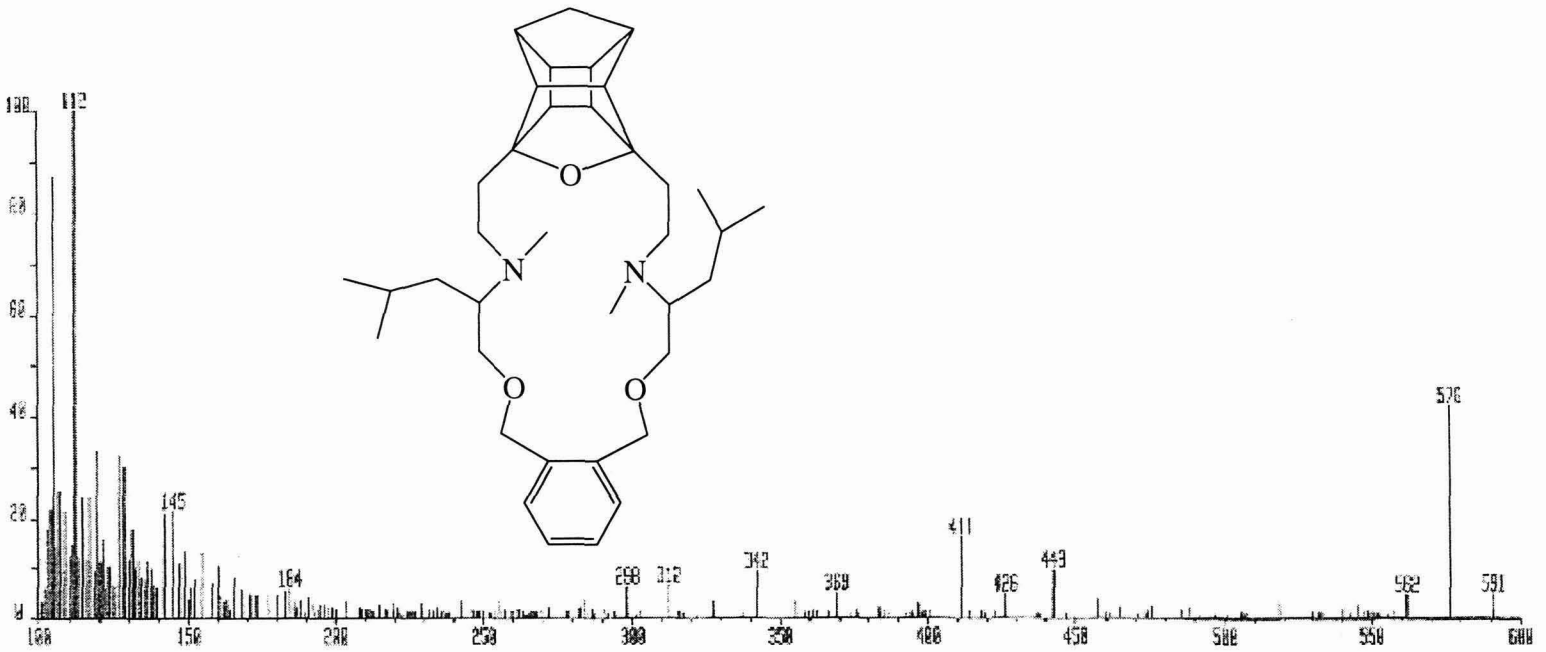

CI MS of macrocycle 170

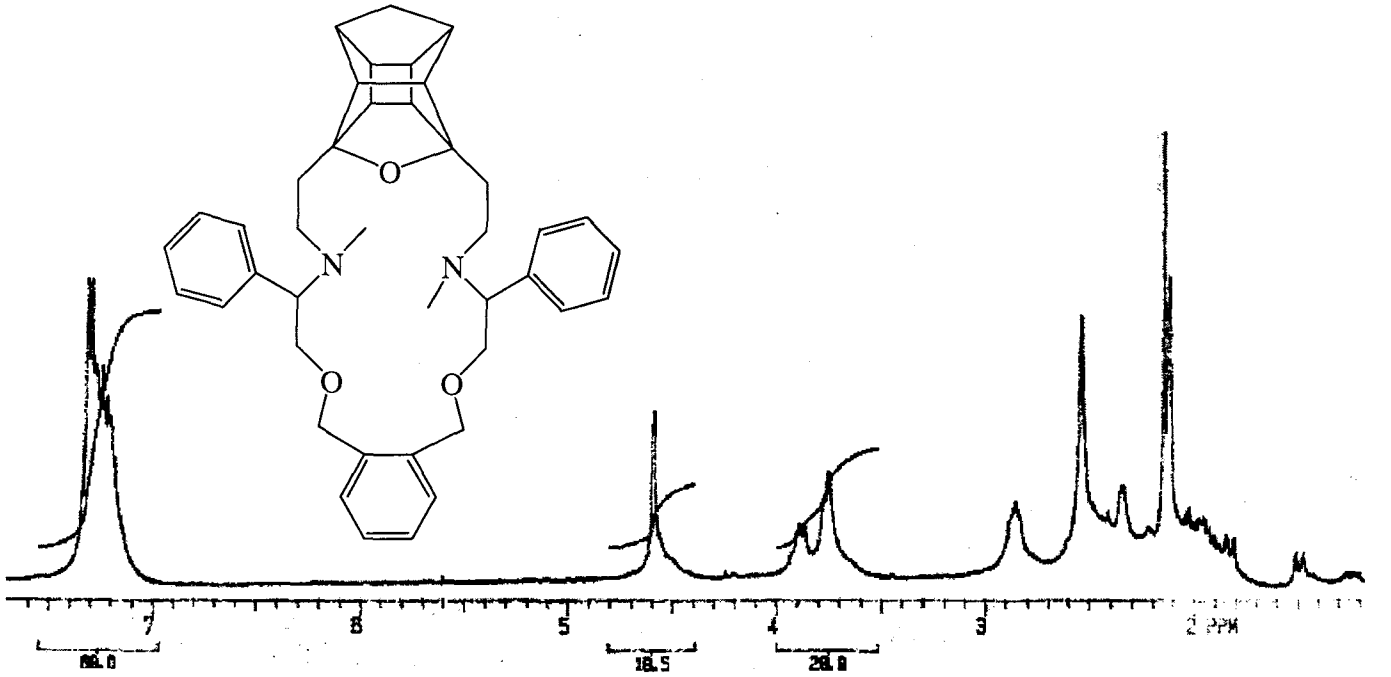

^{1}H nmr ($CDCl_3$) 200 MHz of ligand 171

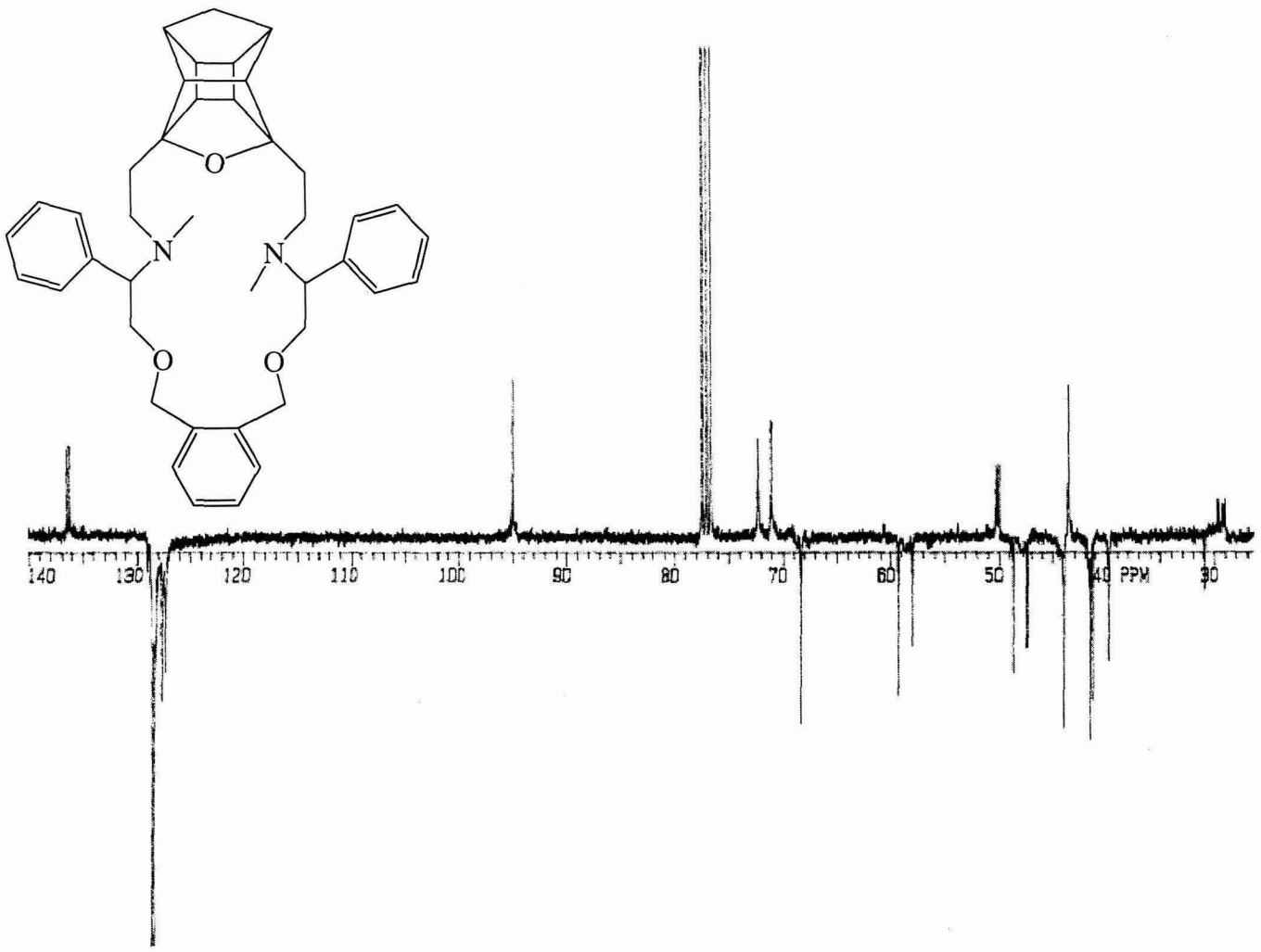

^{13}C APT nmr ($CDCl_3$) 50 MHz of ligand 171

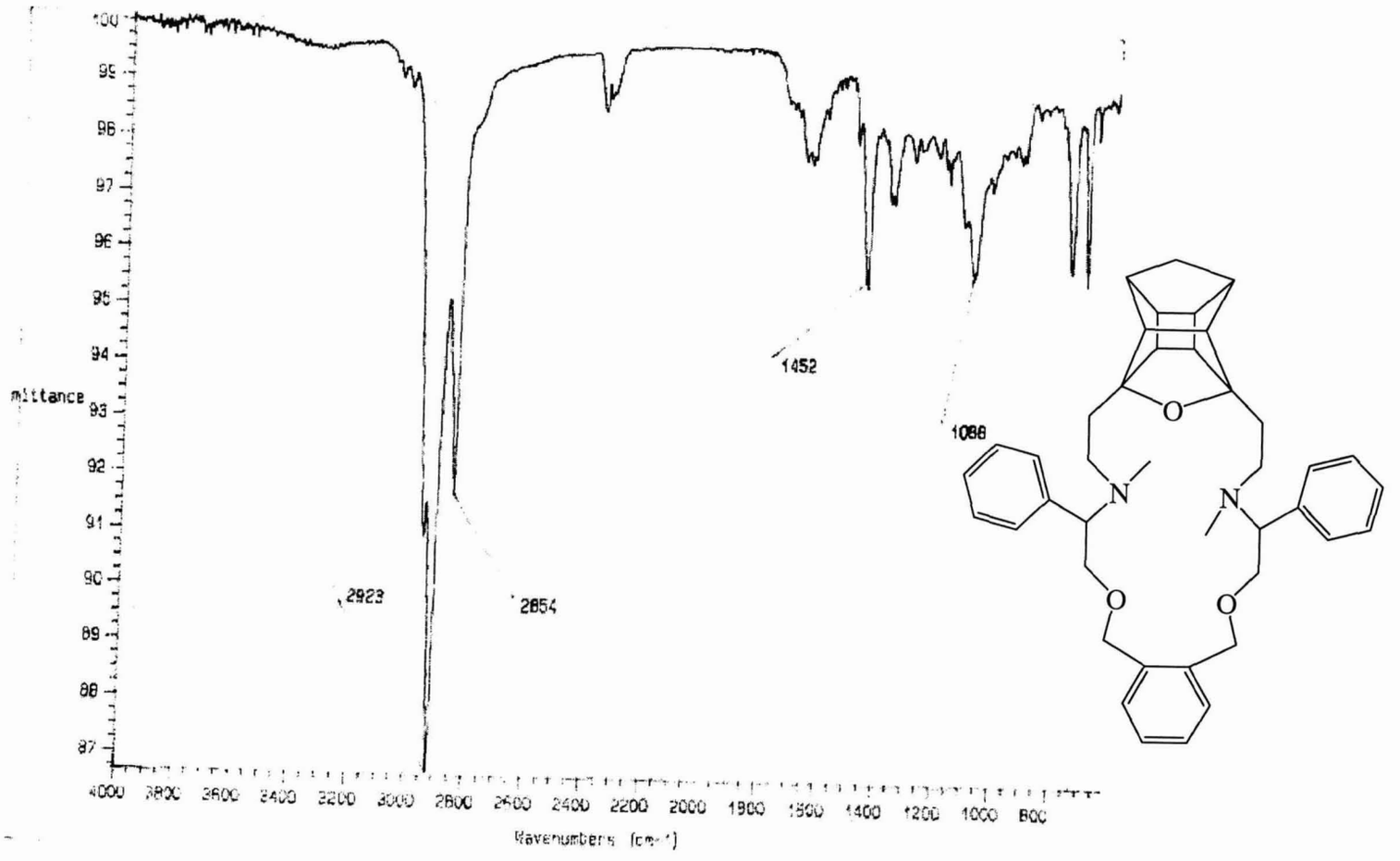

IR spectrum of macrocycle 171

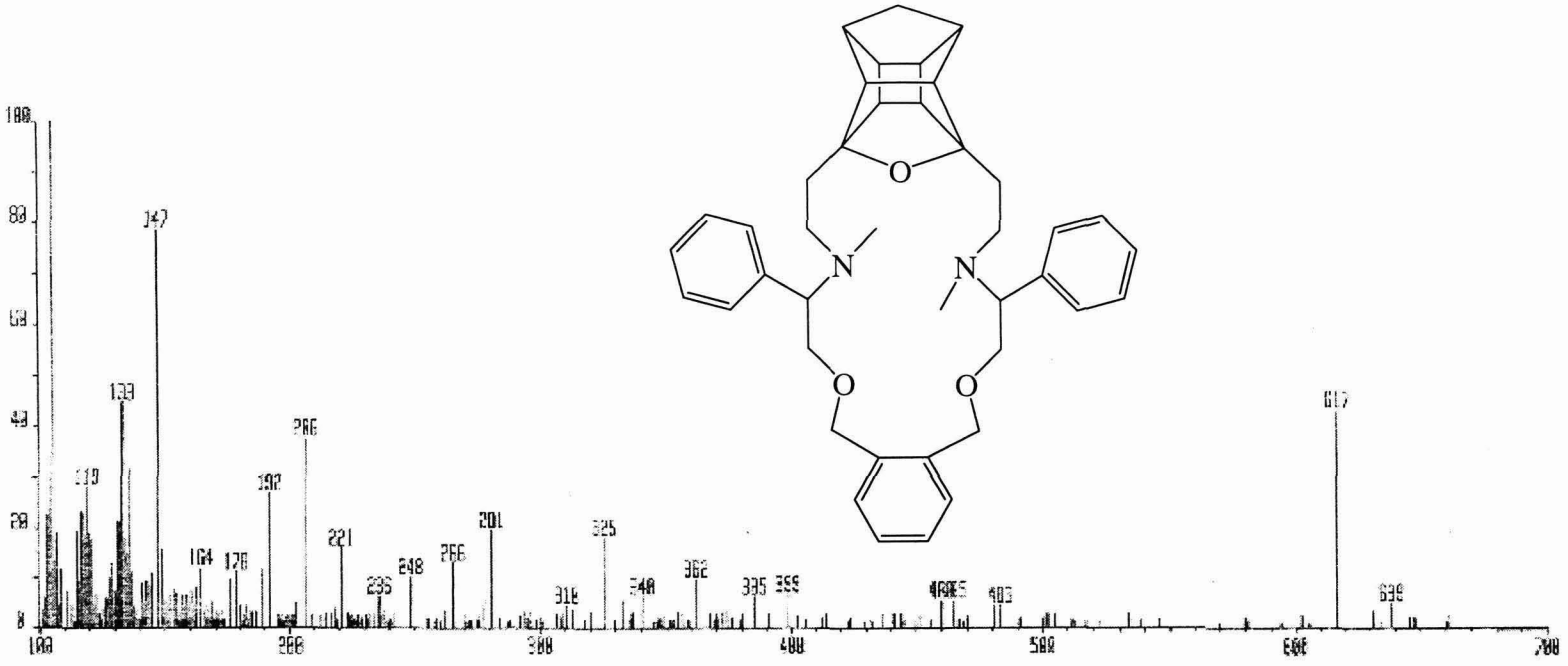

CI MS of macrocycle 171

Appendix 2

Description of the MD model used in Chapter 3

Determining low energy structures of the free host and guest.

Verification of a MM3 method to determine the low energy minima structures of the host systems was achieved using the following procedure: A molecular dynamics (MD) calculation at 600K (to overcome rotational barriers) was performed on the host systems (**89**and **90**) for 5 ps.

The total energy of the system was plotted for 500 snapshots (see Figure A2.1). Twenty structures corresponding to the lowest minima on the plot of the total energy of the system against time (see Figure A2.1) were manually chosen and optimised with MM3. The twenty structures were rank ordered by energy and the five lowest structures were then optimised using DFT. The order by energy remained unchanged upon optimisation with DFT. This result indicates that MM3 calculations can be used for determining the conformational preference of macrocycles (host systems).

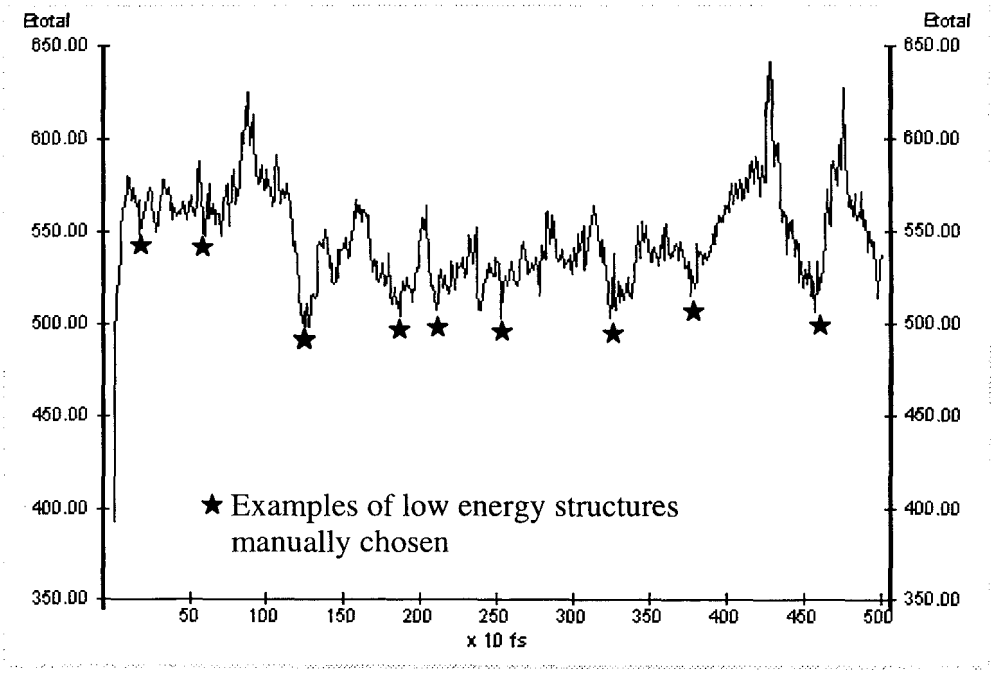

Figure A2.1: Plot of energy vs time during a typical MD calculation

The low energy minima structures for all other host systems were determined, as described above, using MM3 exclusively.

The lowest energy found (E_{host}) is used to determine the approximate binding energy (BE) as described in equation 1.

A similar MD calculation (600K) is performed on the free guest to obtain a number (3-5) of low energy guest structures. Each of the low energy guest structures were optimised using MM3 and the lowest structure/energy (E_{guest}) was used in equation 1.

Determining low energy structures of the host-guest complex

In a number of cases the lowest energy host structure obtained above was completely bent. Since effective host-guest complexation requires a relative flat host, a number (between 4 and 6) of minimum structures (see Figure A2.1) with flatter geometries at higher energy were manually chosen for the docking experiment described below. As the MD calculations used for the docking procedure, described below, normally induce dramatic movement of the host-guest complex, the degree of flatness is not critical, as long as the heavy atoms of the guest system is not shielded from the guest by side chains or other atoms.

Docking procedure to find the host-guest starting structures

The following MM3 MD docking procedure was applied in an attempt to obtain a complex structure with a high degree of interaction between the host and guest:

The ammonium group of the chiral guest is placed approximately 4 Å away from the center of the host macrocycle ("flat" structure obtained as described above). The N-C bond of the guest is placed perpendicular to the plane of the heavy atoms of the macrocycle (see Figure 5). This is done for each of the 4-6 "flat" host structures.

Each of the 4-6 starting "complexes" is subjected to a sequence of MM3 MD calculations as described below. MD for 5 ps at 1K, 3 ps at 50K, 3 ps at 100k, 3 ps at 200K, 5 ps at 300K and lastly 3 ps again at 100K.

The total energy of the system is plotted against time and a typical graph normally exhibits an initial maximum, followed by one or more minima (See Figure A2.2). The structure corresponding to the lowest minimum after the initial maximum is used in the next MD run. The same procedure is followed to obtain a low energy structure after the initial maximum of the second MD run (at 50K), followed by the next MD sequences (3 ps at 100k, 3 ps at 200K, 5 ps at 300K and lastly 3 ps again at 100K).

Some of these starting complexes would produce an optimised complex of lower energy, and other would fall apart during the MD procedure. In some cases the host guest complex will undergo dissociation as result of weak interaction between the ammonium ion and the heavy atoms of the macrocycle, or unfavourable steric influences. In such cases the last successful structure obtained is used as described in the subsequent routine.

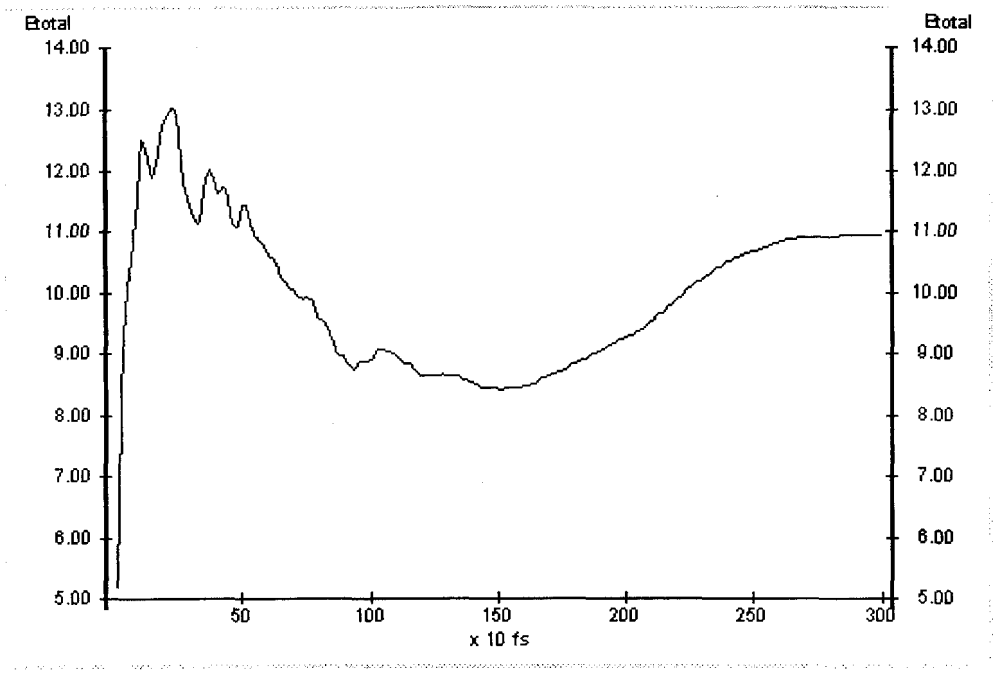

Figure A2.2: A typical MD plot of Total Energy of the host-guest system against time.

The lowest energy complex geometry obtained from this docking procedure is optimised using the full MM3 matrix minimization to produce a low energy structure. The same MD sequences are performed on each of the 4-6 starting structures. The corresponding host-guest structures are ranked ordered, and the lowest energy complex used in the conformational search described below.

In most cases, approximately the same host-guest complex will be obtained for the 4-6 different starting structures. The step-size during the MD procedure can be quite large and, as a result, the guest molecule is able to rotate, relative to the host, by as much as 40 - 180° during the complete MD procedure. The initial host framework also undergoes remarkable movement and bending during the whole procedure.

Note that in a few cases the reaction profile does not exhibit a minimum after 3 ps (50K), but the energies kept rising with time for the duration of the MD run. This is presumably the result of an unfavourable host-guest starting complex with a relative high-energy barrier. The last structure of the MD run is then used for a next MD run at the same temperature, but for 5 ps. In a few cases the prolonged MD run would also not produce a minimum on the reaction profile, whereupon MD at a higher temperature is performed on the last structure of the MD. At higher temperature (100K or 200K), the energy barrier is either overcome, or the host-guest structure starts to fall apart during the MD run.

In a few cases one is able to find a host-guest complex with considerably stronger interaction between hosts and guest, resulting in a much lower energy. Although it is preferred to find this lower energy host-guest complex, the rest of the procedure depends on relative energies

using the same host guest framework and it was found that where a host-guest with higher energy is in fact used in the conformational search described next, essentially the same magnitude of chiral preference is observed. Note that the same host-guest framework is used for the conformational search described next, the guest is only rotated with respect to the host.

Conformational search to find the lowest energy host guest complex

In order to ensure a reasonable chance to obtain the lowest energy host-guest structure, the following conformational search is performed:

The lowest energy host-guest structure obtained above is taken and the guest successively rotated manually by approximately 70° to produce five new starting conformations. Side chains are also manually rotated to avoid excessive steric hinderance caused by the rotation of the guest. The chirality of the guest is manually changed for each of the five starting complex structures to produce five starting host-guest structures with a guest of opposite chirality.

The ten starting host-guest conformations [five with *(S)*-guest and five with *(R)*-guest] are then subjected to a similar MD procedure as described as above:

3-5 ps at 1K, 3 ps at 50K and then 5ps at 100K, followed by a MM3 optimization of the minimum energy structure obtained at 100K. The minimum energy structure is taken as the lowest minimum structure after the initial maximum on the energy profile plot (see Figure A2.2).

The ten complex structures [five with *(S)*-guest and five with *(R)*-guest] are ranked ordered by energy and the lowest energy ($E_{(S)\text{-complex}}$ and $E_{(R)\text{-complex}}$) is used to determine the approximate binding energy as described in equation 1.

The lowest energy structure for each system *(S)* or *(R)*-guest is determined and chiral thermodynamic preference determined ($E_{ctp} = | E_{(S)\text{-complex}} - E_{(R)\text{-complex}}|$) in kcal mol^{-1}.

Some pictures of the optimised complexes

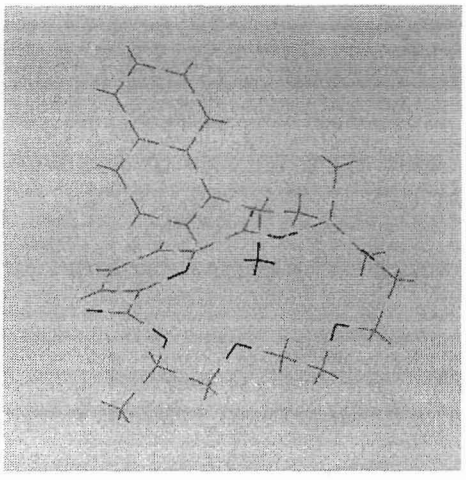

AM1 optimised structure of **89**

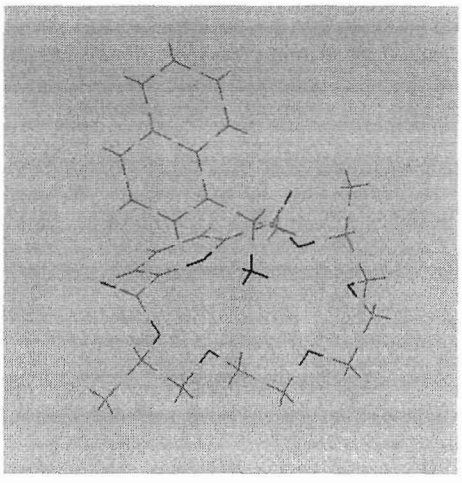

PM3 optimised structure of **89**

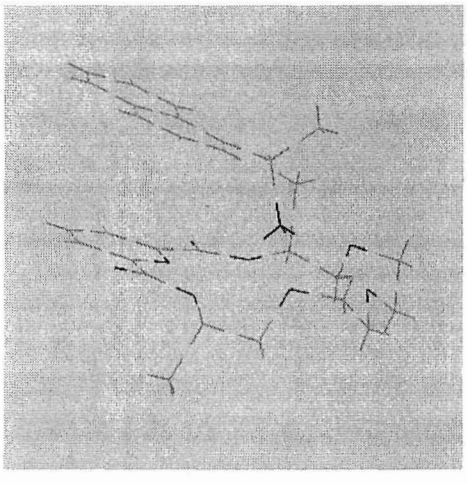

MM3 optimised structure of **89**

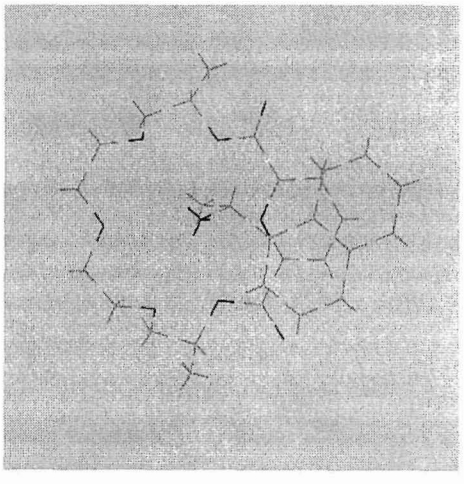

B3lyp optimised structure of **89**

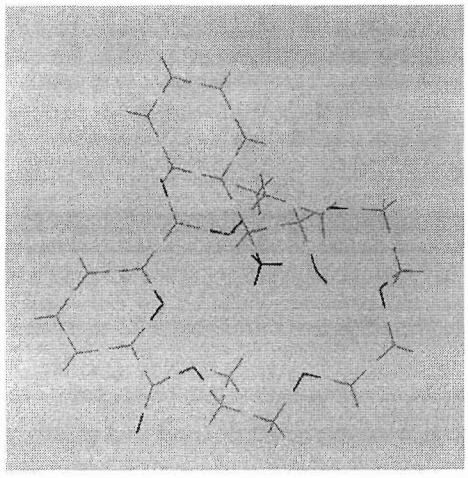

AM1 optimised structure of **90**

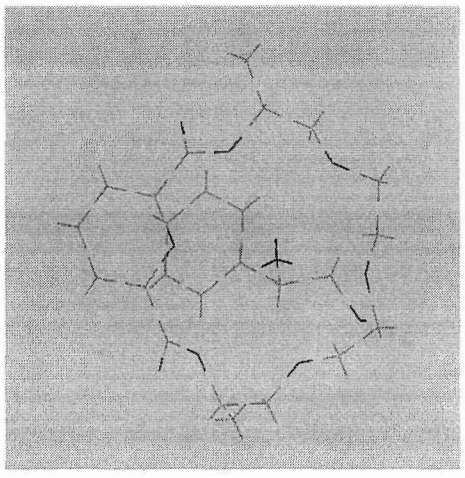

PM3 optimised structure of **90**

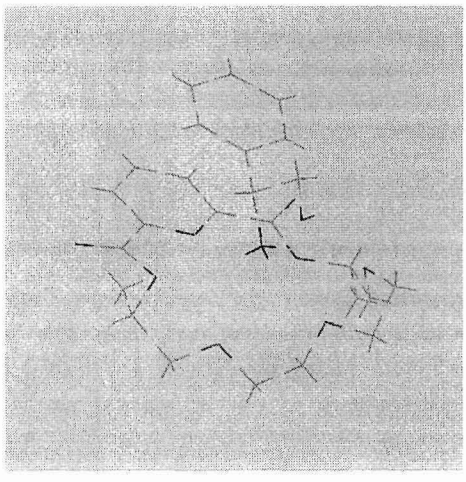

MM3 optimised structure of **90**

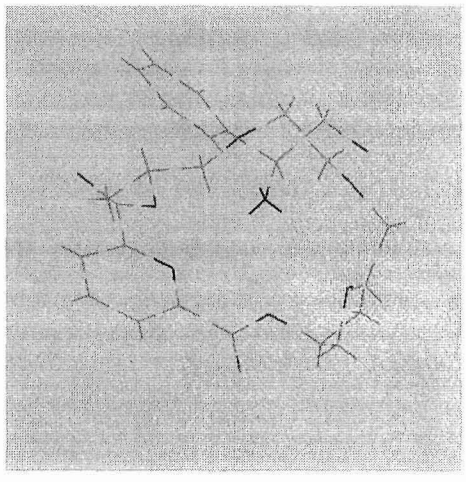

B3lyp optimised structure of **90**

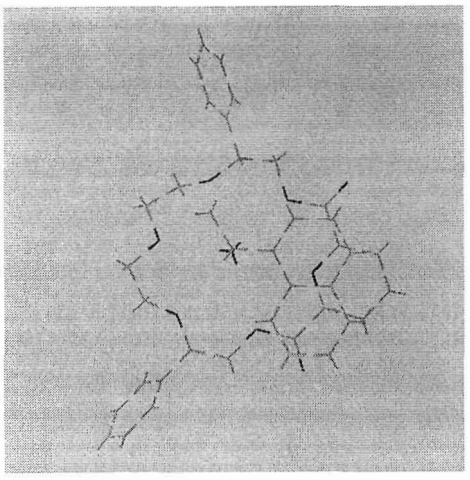

(S,S)-**91** and *(R)*-(**96**)

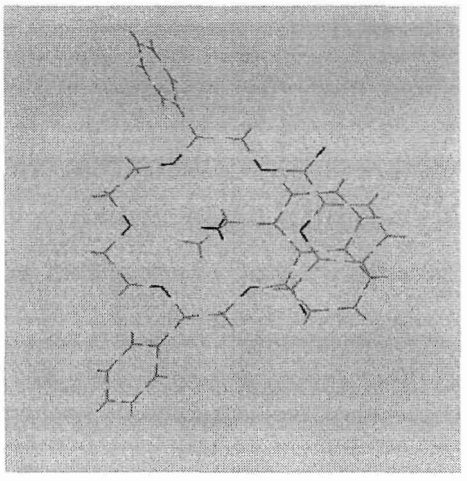

(S,S)-**91** and *(S)*-(**96**)

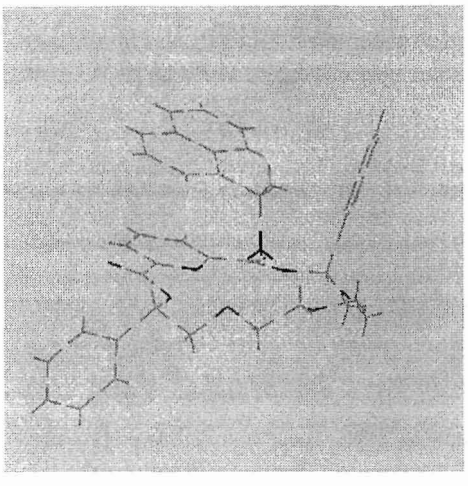

(S,S)-**92** and *(R)*-(**96**)

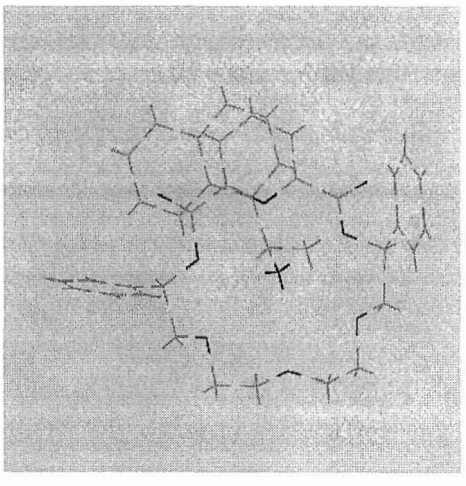

(S,S)-**92** and *(S)*-(**96**)

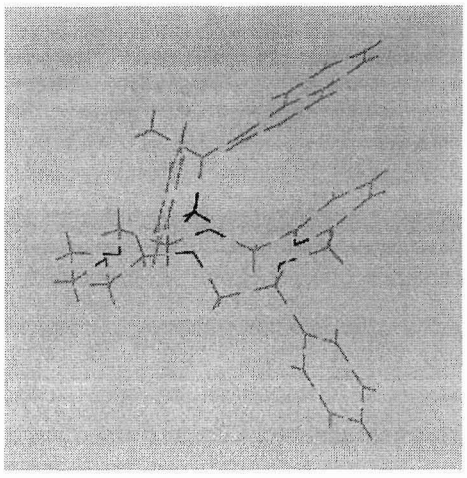

(R,R)-**93** and *(S)*-(**96**)

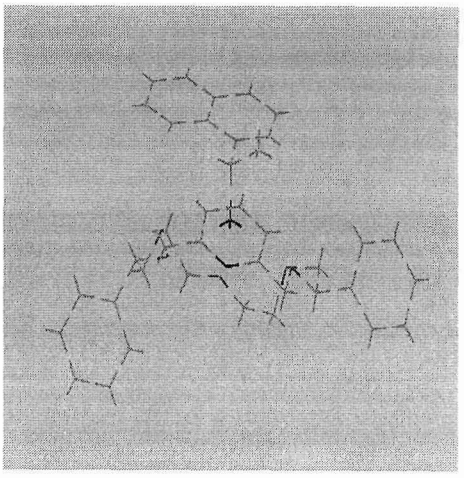

(R,R)-**93** and *(R)*-(**96**)

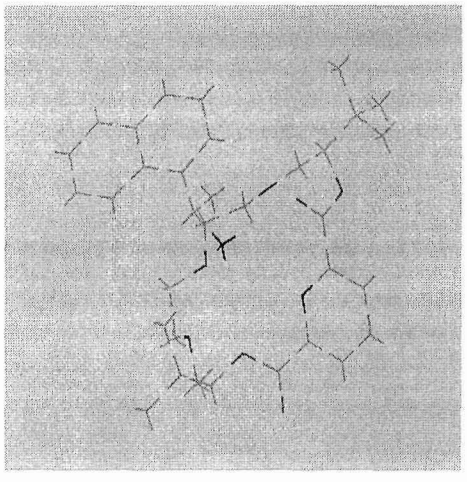

(S,S)-**94** and *(S)*-(**96**)

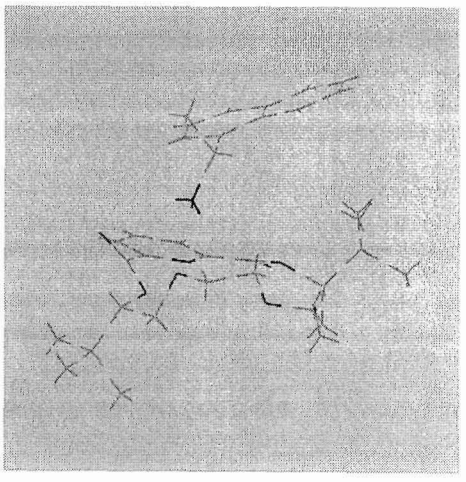

(S,S)-**94** and *(R)*-(**96**)

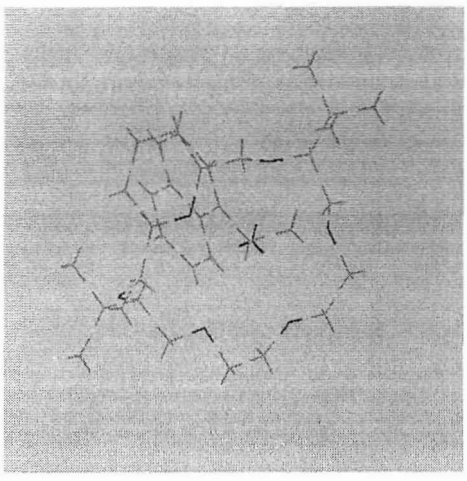

(S,S)-**95** and *(S)*-(**96**)

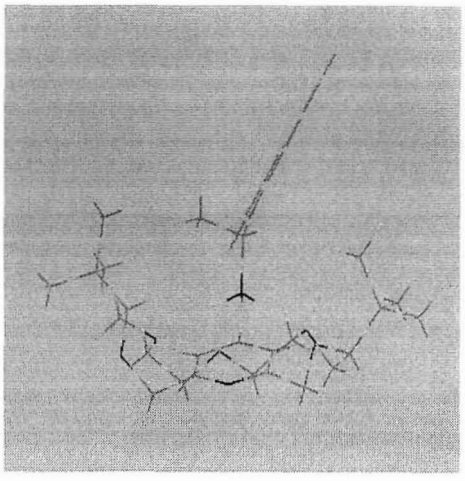

(S,S)-**95** and *(R)*-(**96**)

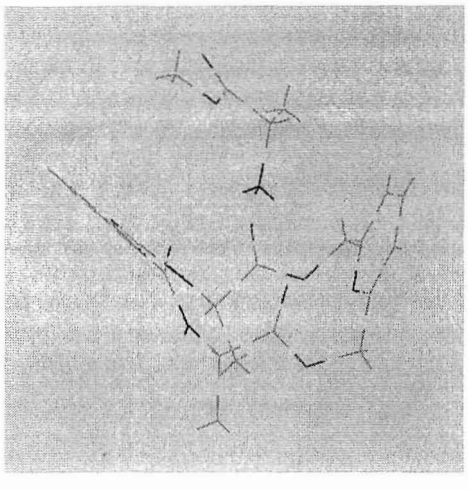

(S,S)-**97** and *(R)*-(**99**)

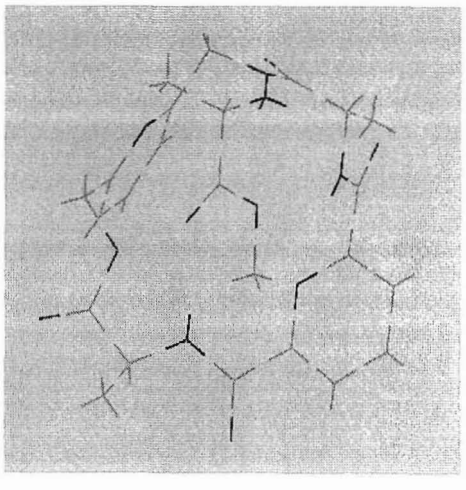

(S,S)-**97** and *(S)*-(**99**)

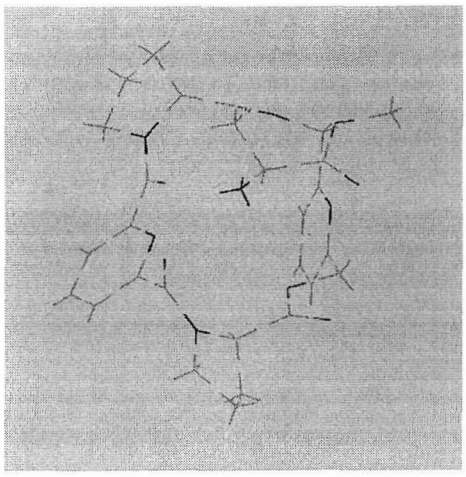

(S,S)-**98** and *(R)*-(**99**)

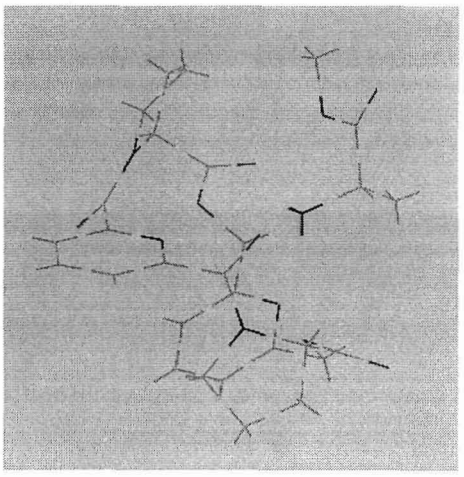

(S,S)-**98** and *(S)*-(**99**)

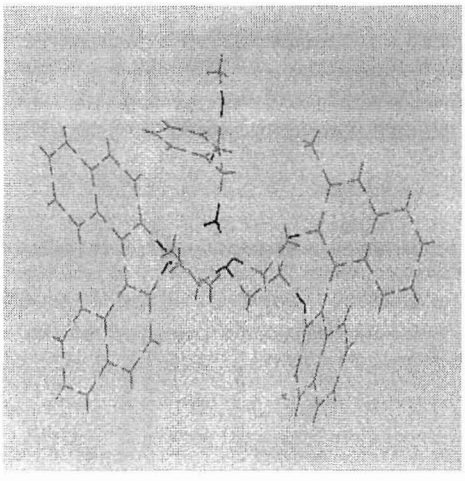

(R,R)-**51** and *(S)*-(**88**)

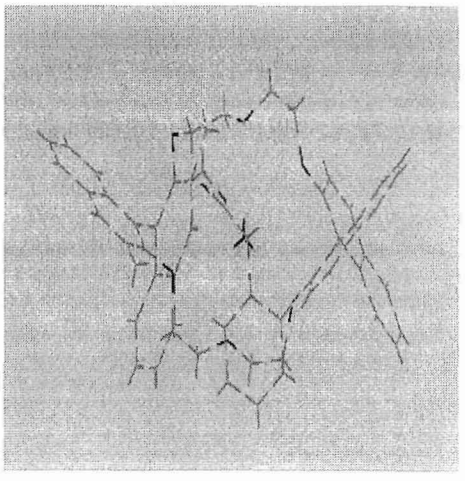

(R,R)-**51** and *(R)*-(**88**)

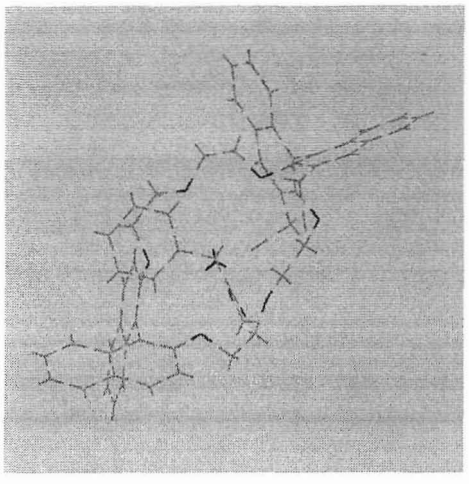

(R,R)-**75** and *(S)*-(**88**)

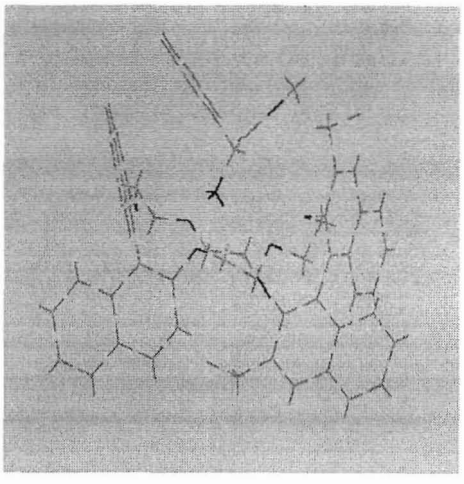

(R,R)-**75** and *(R)*-(**88**)

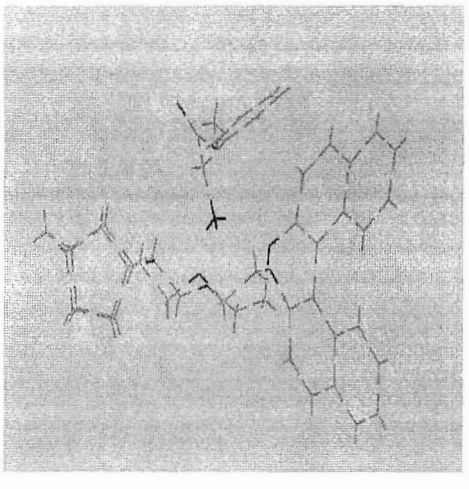

(R,R)- **57** and *(S)*-(**88**)

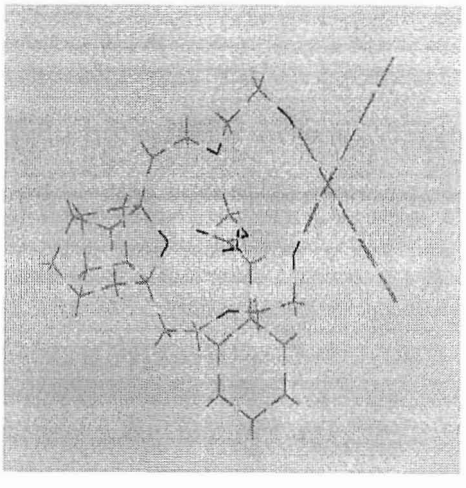

(R,R)-**57** and *(R)*-(**88**)

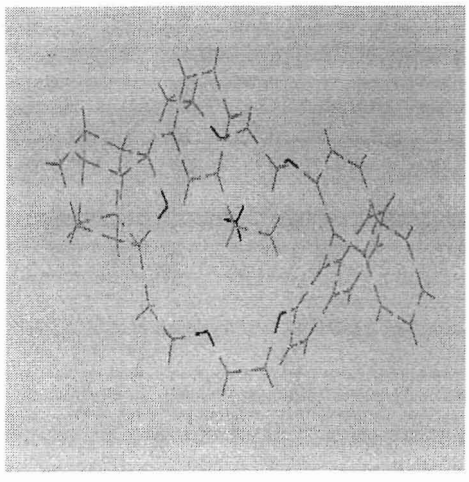

(R,R)-**57** *(S)*-(**87**)

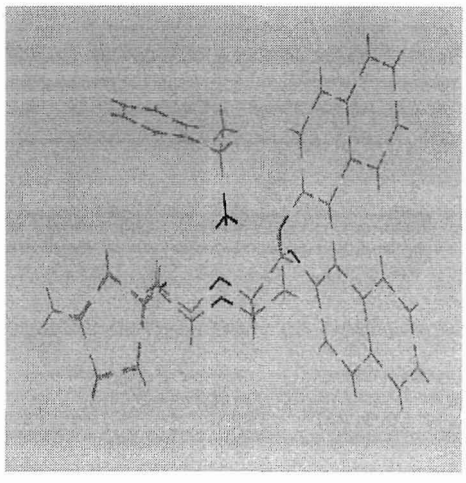

(R,R)-**57** and *(R)*-(**87**)

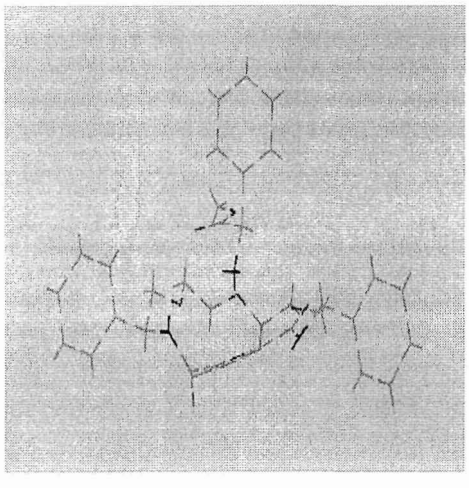

(S,S)-**76** and *(S)*-(**88**)

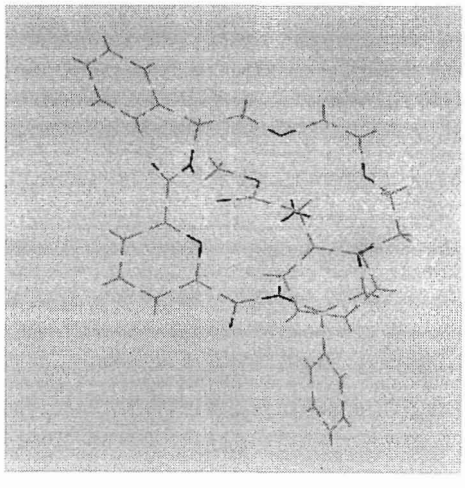

(S,S)-**76** and *(R)*-(**88**)

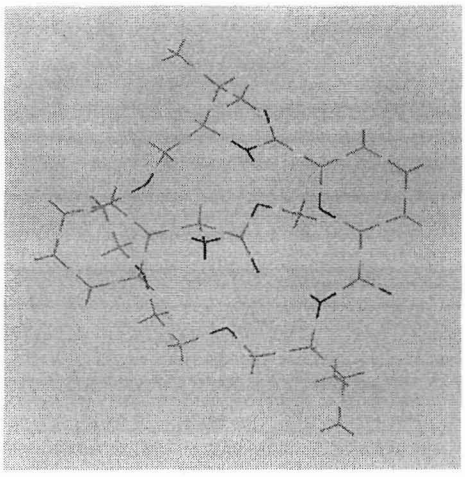

(S,S)-**77** and *(S)*-(**88**)

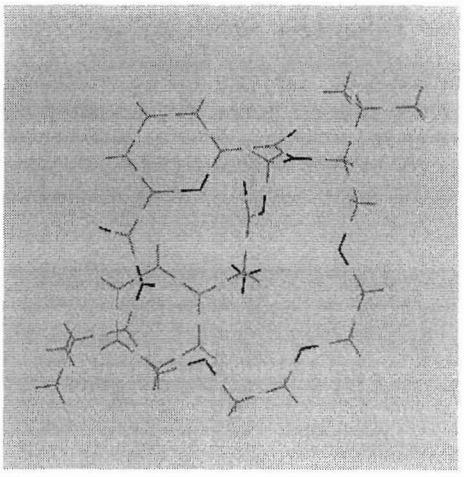

(S,S)-**77** and *(R)*-(**88**)

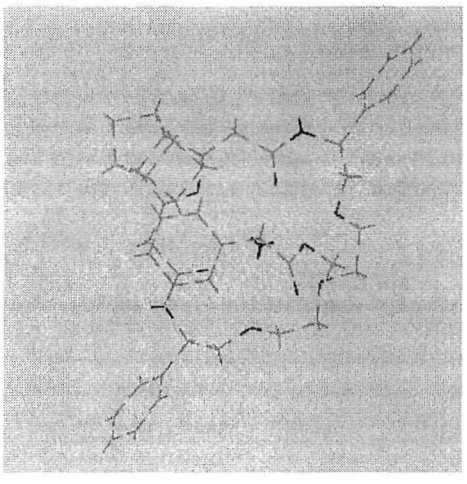

(S,S)-**78** and *(S)*-(**88**)

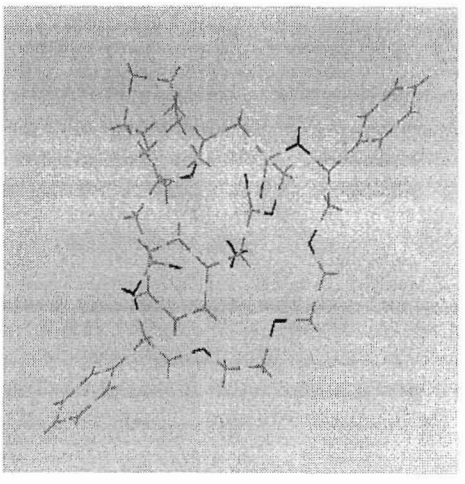

(S,S)-**78** and *(R)*-(**88**)

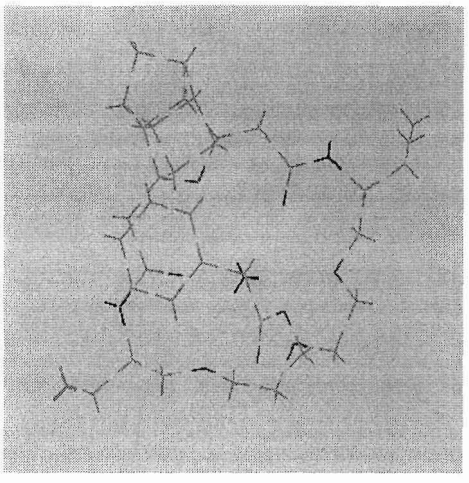

(S,S)-**79** and *(S)*-(**88**)

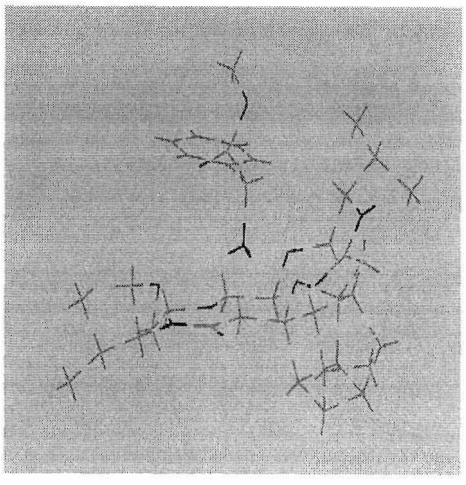

(S,S)-**79** and *(R)*-(**88**)